

AWARD NUMBER: W81 XWH-11-1-0498

TITLE: Engineered Herpes Simplex Viruses for the Treatment of Malignant Peripheral Nerve Sheath Tumors

PRINCIPAL INVESTIGATOR: James M. Markert, MD

CONTRACTING ORGANIZATION: University of Alabama at Birmingham
Birmingham, AL 35294-3410

REPORT DATE: November 2015

TYPE OF REPORT: Final

PREPARED FOR: U.S. Army Medical Research and Materiel Command
Fort Detrick, Maryland 21702-5012

DISTRIBUTION STATEMENT: Approved for Public Release;
Distribution Unlimited

The views, opinions and/or findings contained in this report are those of the author(s) and should not be construed as an official Department of the Army position, policy or decision unless so designated by other documentation.

REPORT DOCUMENTATION PAGE

Form Approved
OMB No. 0704-0188

Public reporting burden for this collection of information is estimated to average 1 hour per response, including the time for reviewing instructions, searching existing data sources, gathering and maintaining the data needed, and completing and reviewing this collection of information. Send comments regarding this burden estimate or any other aspect of this collection of information, including suggestions for reducing this burden to Department of Defense, Washington Headquarters Services, Directorate for Information Operations and Reports (0704-0188), 1215 Jefferson Davis Highway, Suite 1204, Arlington, VA 22202-4302. Respondents should be aware that notwithstanding any other provision of law, no person shall be subject to any penalty for failing to comply with a collection of information if it does not display a currently valid OMB control number. **PLEASE DO NOT RETURN YOUR FORM TO THE ABOVE ADDRESS.**

1. REPORT DATE November 2015		2. REPORT TYPE Final		3. DATES COVERED 1Sep2011 - 31Aug2015	
4. TITLE AND SUBTITLE Engineered Herpes Simplex Viruses for the Treatment of Malignant Peripheral Nerve Sheath Tumors				5a. CONTRACT NUMBER W81XWH-11-1-0498	
				5b. GRANT NUMBER	
				5c. PROGRAM ELEMENT NUMBER	
6. AUTHOR(S) James M. Markert, MD; G. Yancey Gillespie, PhD; Stephanie J. Byer; Steven L. Carroll, MD; Jennifer M. Coleman; Joshua D. Jackson; Catherine P. Lankford E-Mail: JMarkert@uabmc.edu				5d. PROJECT NUMBER	
				5e. TASK NUMBER	
				5f. WORK UNIT NUMBER	
7. PERFORMING ORGANIZATION NAME(S) AND ADDRESS(ES) University of Alabama at Birmingham FOT 1060 1720 2 nd Avenue South Birmingham, AL 35294-3410				8. PERFORMING ORGANIZATION REPORT NUMBER	
9. SPONSORING / MONITORING AGENCY NAME(S) AND ADDRESS(ES) U.S. Army Medical Research and Materiel Command Fort Detrick, Maryland 21702-5012				11. SPONSOR/MONITOR'S REPORT NUMBER(S)	
13. SUPPLEMENTARY NOTES					
14. ABSTRACT Many patients with neurofibromatosis type I (NF-1) will develop tumors in their peripheral nerves that progress to a cancer called a malignant peripheral nerve sheath tumor or MPNST. These tumors grow progressively and if they cannot be completely removed surgically, they are eventually fatal. Radiation provides some benefit but is mostly ineffective and there are no proven chemotherapies or medicines that will prevent the progressive growth of these tumors. We have been working with genetically engineered human herpes simplex virus (HSV) as a means of treating nervous system tumors. We have genetically modified these viruses to make them safe and unable to grow in normal cells, but that can grow in tumor cells causing them to die, a process called oncolysis (tumor lysis). In addition, we have inserted genes in these viruses that allow them to overcome different mechanisms that tumor cells have to prevent virus growth. Our objective is to determine how effectively MPNST cells can be infected and killed by our engineered HSVs. We will test our panel of viruses against a panel of MPNST-derived cells. We will examine the molecular features of the tumor cells to identify similarities which reflect a tumor cell's response to oHSV.					
15. SUBJECT TERMS Oncolytic Herpes Viruses; Malignant Peripheral Nerve Sheath Tumors; Mouse; Human					
16. SECURITY CLASSIFICATION OF:			17. LIMITATION OF ABSTRACT	18. NUMBER OF PAGES	19a. NAME OF RESPONSIBLE PERSON USAMRMC
a. REPORT U	b. ABSTRACT U	c. THIS PAGE U			19b. TELEPHONE NUMBER (include area code)
			UU	205	

Table of Contents

	<u>Page</u>
1. Introduction	1
2. Keywords	1
3. Overall Project Summary	1
4. Key Research Accomplishments	24
5. Conclusions	26
6. Publications, Abstracts, and Presentations	29
7. Inventions, Patents and Licenses	29
8. Reportable Outcomes	29
9. Other Achievements	30
10. References	30
11. Appendices	
Appendix I: Year 1 Report	
Appendix II: Year 2 Appendices and Supporting Data	
Appendix III: Year 3 Appendices and Supporting Data	
Appendix IV: Year 4 Appendices and Supporting Data	

Introduction

The following final report summarizes the results obtained during our four years of research support from the DOD. During this time we obtained several significant findings regarding MPNST tumor cell biology which contribute to the explanation of the disparate responses to oncolytic HSV therapy in these tumors. The novel findings regarding our most recent work include: (1) association of STAT1 activation with resistance to oncolytic HSV; (2) basal expression of ISGs in MPNST cells; and (3) NFκB dependent expression of ISGs. We are excited about the implications this work has for the field of oncolytic HSV. Furthermore, we believe this work is relevant to conventional MPNST therapy since it has been established that activation of STAT1 and ISG expression is associated with resistance to radiation and chemotherapy, modalities which are generally ineffective in MPNSTs. These discoveries would not have been possible apart from the support provided by the DOD during this time. Our most recent work described has been assembled into a manuscript and is in preparation for submission to the journal *Molecular Cancer Research* and is attached in the appendix of this report.

Keywords

Oncolytic HSV, nectin-1, MPNST, STAT1, ISGF3, ISG, interferon, NFκB

Overall Project Summary

Our goals for this grant are summarized below and include:

- 1) To determine the molecular basis for the sporadic susceptibility or resistance to infection of MPNST cells to genetically engineered, oncolytic herpes simplex viruses (oHSVs) in our repository;
- 2) To examine inherent mechanisms expressed in MPNSTs that inhibit the replication of oHSVs and abrogate the ability of these viruses to kill infected cells and spread to neighboring tumor cells; and
- 3) To test the relative ability of our oHSVs to produce an anti-tumor effect alone and if this anti-tumor effect can be significantly enhanced by a low dose of radiation administered to the tumor.

Our progress is summarized below and has been organized within the 4 major milestones listed in our Statement of work and addressed with regard to each of the Tasks and SubTasks.

Milestone 1: We will identify at least 2 oHSV-sensitive and 2 oHSV-resistant MPNST cell lines by completing the *in vitro* characterization of both human and mouse MPNST cell lines with respect to oHSV infection and killing. We have preliminary analysis of 2 human and two murine MPNST lines. They range from sensitive to resistant to oHSV infection and killing. This milestone will provide the prototypic MPNST cell lines that will be studied more extensively in all three aims.

Milestone 2: We will characterize each of the 9 human MPNST cell line and at least 18 of the 100+ mouse MPNST cell lines with regard to expression of HSV entry molecules expressed on the cell surface. This milestone will enable us to determine whether prevention of entry by down-regulation of appropriate receptors is the reason for oHSV resistance and, if so, whether we should define alternative receptors to which new oHSVs could be targeted.

Milestone 3: We will characterize the replication of oHSVs in each of the oHSV-sensitive and oHSV resistant MPNST cells identified in Milestone 1 by FACS and by titrating virus at regular post-infection intervals. Within this context, we will establish the extent to which replication is enhanced in infected MPNST cells by oHSVs engineered to express proteins that directly promote virus replication. This milestone will allow us to select either the HCMV IRS-1 or the constitutively activated MEK gene as the most appropriate insert to overcome replication resistance.

Milestone 4: We will determine which of the oHSVs identified as “effective” in the first two aims of this proposal actually produce the expected anti-MPNST effect in oHSV-sensitive and oHSV-resistant tumors of human or mouse origin placed orthotopically in the appropriate strain of mouse (see below). Efficacy alone or in combination with enhancing adjunctive therapies will be defined. This milestone will serve to validate (or refute) the process for selection of effective oHSVs that could be advanced to clinical trials in patients with MPNSTs and identify which modality is most likely to have an impact on the natural history of this disease.

Task 1: Characterize the *in vitro* sensitivity of a panel of human and mouse MPNST cell lines to a panel of available oncolytic HSVs.

SubTask 1a. Using methods that we have described in Preliminary Findings in the Proposal, we will complete the screening of all 9 human MPNST cell lines and at least 18 of the 100+ mouse MPNST cell lines using FACS for detection of expression and modulation of HSV entry molecules (nectin-1, nectin-2) and alternative entry molecules (HVEM, IL13R α 2, uPAR, Her2/neu) recognized by fluorochrome-labeled antibodies.

Status: Year 1: During the first year of funding, we examined whether the expression levels of the three principal HSV entry receptors (CD111, CD112, HVEM) correlated with viral recovery in the human MPNST tumor cell lines. Receptor expression levels were measured using antibodies against these major HSV entry molecules nectin-1 (CD111), nectin-2 (CD112) and HVEM by immunofluorescence microscopy and by flow cytometry. The MPNST cell lines demonstrated greater nectin-2 surface expression than nectin-1 surface protein. While a peripheral blood leukocyte positive control sample stained with the antibody against HVEM, none of the human MPNST tested lines expressed HVEM based upon flow cytometry and immunofluorescence. The relative surface expression of Nectin 1 and Nectin 2 was then compared with viral recovery data as represented in Appendix I, Figure 1. The results show that surface expression of nectin 1 and 2 did not correlate directly with viral replication in these cells.

This suggests that entry molecule surface expression is not a rate-limiting step in viral infection in the MPNST cell lines. To further test this hypothesis, however, we created a lentivirus that expressed the human nectin-1 gene and have transduced

both murine and human cell lines to test this hypothesis. The lentivirus was created by PCR amplifying the human Nectin-1 coding domain (including the signal sequence) from a validated cDNA clone (Open Biosystems) and inserting it into a lentiviral targeting vector, pCK2015. This targeting vector contains the nectin-1 coding domain followed by an internal ribosomal entry sequence and the puromycin resistance gene. We created the nectin-1 lentivirus by co-transforming pCK2015 with plasmids encoding the VSV envelope and accessory vector in 293-T cells and collecting the supernatants 48h post-transfection. The MPNST cells were incubated with these supernatants and as demonstrated in Figure 2, the level of lentiviral-transduced cell lines express abundant immunoreactive nectin-1 on their surface. Studies are currently ongoing to determine: 1) if increasing nectin-1 surface expression improves viral entry, 2) if increasing nectin-1 surface expression improves oHSV replication in MPNST cells, and 3) if oHSV entry and gene expression downmodulates lentiviral nectin-1 surface expression similar to that shown for native nectin-1 during infection.

Year 2: During the second year of funding, we have extended our studies from the first year and have identified that for the 8 human lines tested, entry molecule expression is largely limited to nectin-1. There is one exception and that is the newly tested 2XSB line which exhibits both nectin-1 and HVEM entry receptor expression by flow cytometry. In addition to native expression, we have transduced cells and over-expressed the HSV entry molecule nectin-1 in two human MPNST cell lines (STS26T-luc and T265-luc). We have also measured the relative absorbance to quantify receptor expression and have examined if this correlates with viral replication for wild-type and each of the clinical grade oHSVs and wild-type HSV (shown in Appendix II, Figure 1). The results show that nectin-1 expression correlates with improved viral recovery for wild-type HSV ($R=0.75$, $P<0.05$) and for one of the second generation viruses (C134, $R=0.63$, $P=ns$) whereas other viruses (R7020, M002, M032, C101, G207) derived no benefit from the increased nectin expression (Appendix II, Figure 2). Until recently, reagents for examining mouse nectin-1 have been lacking for flow cytometry-based assays. We have identified two potential antibodies (from Santa Cruz and Alomone) that will permit these studies in year 3. Based upon the fact that all MPNST tumors tested express the nectin 1 entry molecule and support HSV replication, we no longer intend to look at alternative entry receptors (IL13R α 2, uPAR, Her2/neu) as the oHSVs do not require re-targeting to these receptors.

Year 3: Due to contamination of a number of the MPNST cell lines with mycoplasma which was discussed in the previous report, we changed the number of cell lines for all subsequent studies to 8

human and 14 mouse MPNST cell lines that have been confirmed to be free of mycoplasma.

For a complete description of methodology used in Sub-Task 1a, we refer the reader to the attached publication (Appendix III, Jackson, *et al.*). In summary, all human MPNST cell lines were found to express detectable levels of nectin-1, the major HSV-1 entry receptor by FACS analysis (Publication Figure 1f). One cell line expressed significant levels of the alternative entry receptor HVEM (Publication Supplemental Figure 1d). We overexpressed nectin-1 in oHSV resistant cell lines to determine the effect of increased entry receptor expression on the productive capacity of each cell for oHSV replication and cell-to-cell spread. This did not result in a substantial improvement for the oHSVs by *in vitro* or *in vivo* measurements (Publication Figures 2 and 3) but did yield a benefit to the wild-type virus by *in vitro* assays (Publication Figure 2 and Publication Supplemental Figure 4). We therefore conclude that entry receptor expression is not the primary mechanism of resistance to our attenuated oHSVs. Furthermore, basal levels of nectin-1 expression in MPNST cell lines appear sufficient to mediate entry for wild-type HSV-1 and by extension oHSVs.

Although we did not conduct these experiments in mouse cell lines, the data from human cell lines indicates that the means of resistance to oHSVs lies elsewhere and that entry receptor expression is sufficient, at least in MPNST-derived cell lines. We therefore do not plan to expend any additional resources into the investigation of HSV entry receptors.

Year 4: Completed. No updates from previous report (2014).

SubTask 1b. Using methods that we have described in Preliminary Findings in the Proposal, we will complete the screening of the human and mouse MPNST cell lines using oHSVs that express eGFP for detection of infection and cell death using FACS.

Status: Year 1: We are starting these studies and have examined some of the cell lines as shown later in the progress report in Subtask 1.

Year 2: We screened and identified resistant and sensitive cell lines based upon viral replication and cytotoxicity as described below in Sub Task 1c. This was determined to be sufficient for identifying sensitive and resistant cell lines. We have since examined these lines based upon viral GFP expression utilizing multistep replication assays and extended the spread assay to assess the effects of increased nectin-1 expression on spread. These studies have been completed for the following cell lines (STS26T-luc, T265-luc, S462-luc, NMS2-PC, STS26T-N1MED, STS26T-N1HI, and T265-N1HI) as shown in Appendix II, Figures

3 and 4. Cell lines STS26T-N1MED, STS26T-N1HI, and T265-N1HI are cell lines that stably overexpress nectin-1 via a lentiviral construct (Appendix II, Figure 5) and have been confirmed to overexpress nectin-1 that is functional for HSV-1 entry (Appendix II, Figure 6). These cell lines have been used to more comprehensively address the tasks regarding entry receptor expression and replication as described in other areas of Sub Task 1. When we designed these studies, we anticipated that viral GFP would provide a surrogate measurement for viral replication and sensitivity to oHSV therapy. What we have discovered is that, at least in the context of the parent and nectin-1 transduced MPNST lines available, the assay provides a sensitive measure of viral spread but is not always indicative of replication or cytotoxicity. For example, we have identified that while nectin-1 overexpression may lead to marginal improvement (<1/2 log change) in viral replication, it does benefit spread of virus *in vitro* (Appendix II, Figure 8) (based upon % GFP positive cells) as discussed in later sections; therefore the original assumptions have been qualified with respect to this discovery—namely, that replication, spread and cytotoxicity are not explicitly dependent phenotypes in all cell lines.

Year 3: We have completed the screening of the 8 human and 14 mouse MPNST cell lines using representative viruses with eGFP expression. In this assay we infected each cell line at a multiplicity of infection (MOI) of 0.1 and then subjected the cells to FACS detection of viral GFP at 48 hours post infection (hpi). We have simultaneously measured the absolute cell killing of each virus using FACS counting beads. Both second generation viruses C154 and M201 demonstrated significantly higher GFP positive cells (Appendix III, Figure 1a) and reduction in relative cell counts (Appendix III, Figure 1b) as compared to C101. As expected the wild-type virus also demonstrated these increases (Appendix III, Figure 1a-b). We expect that cell lines which support viral productivity will show an increased number of cells positive for GFP and a simultaneous decrease in the number of cells as compared to an uninfected control. As demonstrated in Figure 1 c-e, the percentage of cells expressing viral GFP is significantly correlated with the relative decrease in cell numbers for viruses C101 ($\Delta\gamma_{134.5}$), C154 ($\Delta\gamma_{134.5}$, IRS-1), and M201 ($\Delta\gamma_{134.5}$, IL-12) but not for the representative wild-type virus M2001 (Appendix III, Figure 1 f). The fact wild-type HSV-1 infected have low cell counts but no correlative in GFP expression is likely due to the rapid course of infection for the wild-type HSV-1 compared to $\Delta\gamma_{134.5}$ oHSVs, such that by 48 hpi wild-type infected cells are likely no longer actively expressing GFP due to cell death in certain cell lines.

This data suggests that this FACS based assay is a valid measurement of oHSV productivity. It effectively divides oHSV resistant cells (low number of GFP positive cells, high relative

cell counts) from oHSV permissive cell lines (high number of GFP positive cells, low relative cell counts). This experiment also confirms that both C154 and M201 (and by extension the non-GFP expressing viruses C134 and M002) are more effective than a first-generation $\Delta\gamma_134.5$ oHSV (C101, based on R3616). All MPNST cell lines are susceptible to wild-type HSV-1 (M2001).

Year 4: Completed. No updates from previous report (2014).

SubTask 1c. Screen each of the 9 human and 18 mouse MPNST cell lines for sensitivity to infection and killing by clinical candidate viruses G207, NV1020, M032 and C134 using classical virology techniques to measure cytopathic effect on monolayers, single step and multi-step replication assays.

Status: Year 1: Over the past year, we focused on the in vitro characterization of the MPNST cell lines. We have tested 7 recombinant HSVs (4 of which are available as clinical grade virus), in 7 of the 9 human MPNST cell lines and 16 of the 18 murine MPNST cell lines proposed. The results of these studies are based upon increasing susceptibility/support for replication in the MPNST cell line (Appendix I, Figures 1 and 2). In order to finalize this milestone, we will test 2 additional human and 2 additional murine MPNST cell lines that Dr. Carrol's laboratory will supply to us.

Thus far we have detected a 100,000 fold (5 log) difference in viral replication between the least and the most susceptible cell lines with our recombinant viruses (Figure 3). Of the murine MPNST cell lines, the A382 cell line is the least hospitable to viral replication. The oHSVs generate only 10^3 (plaque forming units) pfu in single step replication assays in this cell line. Following the A382 cell line, the B91 cells are the second most restrictive cell line for three of the GLP quality oHSVs (G207, M032, and C134) whereas the A387 cell line is more restrictive to R7020 replication. With regard to murine MPNST cell lines that support viral replication, the 231 Trig and the A18 cell lines produced the highest overall viral recovery (10^8 PFU/ml).

For the Human MPNST cell lines, the choices for cell lines are more limited (7 cell lines tested). Most of the cell lines have been transduced to stably express luciferase (Luc). The most restrictive human MPNST cell lines to date are the T265T-LUC and S26T. These cell lines limited viral replication such that only 10^1 - 10^5 PFU of virus is produced following single step replication assays. The most susceptible human cell line was S462 cell line which generated $\sim 10^7$ - 10^8 PFU for all of the viruses tested. Identification of the second most susceptible cell line was more complex. Depending upon the virus used, certain cell lines were

more permissive than others in these assays (Appendix I, Figure 4). For two of the clinical grade oHSVs (R7020 and C134), the YST-1 cell line produced the greatest amount of virus (7.7×10^5 and 9.3×10^5 pfu). For the G207 and M032 oHSVs, NMS2PC was the next most susceptible cell line producing 4.33×10^5 pfu and 2.07×10^8 pfu respectively.

Composites of the viral recovery results for all of the cell lines are provided in Appendix I, Figures 3 and 4. These allow comparison between the cell lines. In addition to this broad overview of all of the results, we have also included the results from viral replication (multistep replication studies with CPE images, single step replication results with CPE images, cytotoxicity studies, and western blot data for the cell lines) for each of the cell lines in Appendix I, Figures 5-41.

Year 2: We focused and completed the majority of this task in Year 1: During Year 2 we were forced to repeat some of these studies for select cell lines after identifying Mycoplasma infection in some of the cell lines obtained from the originating lab (human: S462, 90-8, 2XSB, HS-PSS; murine: A18, A390, B97, and B76). Mycoplasma is a cellular pathogen that can potentially impact viral replication. We therefore repeated the viral replication for the cell lines that were capable of being cleared of Mycoplasma infection (human: S462, 90-8, 2XSB; murine: A18) to insure that the Year 1 data was valid. Cell lines S462 and 90-8 were updated to luciferase versions (S462-luc and 90-8-luc) which were confirmed to be free of Mycoplasma.

Comparison of viral recovery before and after decontamination allowed us to clarify that the Mycoplasma infection did not change oHSV susceptibility in our representative sensitive and resistant cell lines (summarized in Appendix II, Table 1). We have updated these data and are pleased to report that the overall trend remains unchanged from our prior data although the absolute viral recovery studies differs from the prior report for certain viruses. We have included updated viral recovery data (Appendix II, Figures 9 and 10) and provide specific examples of the differences in our results in the presence and absence of Mycoplasma infection (Appendix II, Figure 11). Following clearance of the Mycoplasma from cell cultures, these cell lines were validated to remain free of Mycoplasma infection (after two months of passaging without antibiotic pressure), we repeated the viral recovery and cytotoxicity assays. The cells are now monitored regularly (once monthly) by mass PCR screening and without cell culture antibiotics and they remain free of Mycoplasma infection.

We also identified that the puromycin used to maintain the luciferase transduced cell lines was affecting viral recovery in some instances (e.g. STS26T-luc, T265-luc, 88-14-luc). These

data were also repeated with puromycin-free media and confirm that virus recovery was suppressed in the presence of puromycin. When the puromycin was discontinued, viral recovery of these cell lines increased greater than 1 log for a majority of the viruses. The data is summarized in Appendix II, Figure 12. The most restrictive human MPNST cell lines to date remain T265-luc and STS26T-luc even after reevaluation of this data.

At the present time we have completed the viral recovery for nine of the nine human MPNST cell lines and 15 of the 18 murine MPNST cell lines. Data from cell lines in which Mycoplasma was unable to be cleared (human: HS-PSS; murine: A390, B97, and B76) has been excluded and these cell lines will not be used in future studies. We have been able to identify sufficient sensitive and resistant cell lines in both murine and human systems to advance them to *in vivo* testing. Should we determine that the tumor lines are not tumorigenic in mice, we have alternative lines as back-up that we can further validate if necessary. After clearing Mycoplasma infection and removing puromycin, there is still a significant difference in viral replication between the least and most susceptible cell lines with our recombinant viruses (4 log) (Appendix II, Figure 9). The most susceptible human cell line remains the S462-luc cell line which generated $\sim 10^7$ - 10^8 pfu for all of the viruses tested. As shown in Appendix II, Figures 3 and 4, we have continued to use this as one of our prototype "oHSV sensitive cell lines." However, S462-luc does not appear to be tumorigenic in mice, limiting its utility for *in vivo* studies. We are currently investigating the possibility of using Matrigel to assist with tumorigenesis. We are also identifying additional sensitive cell lines. Identification of the additional susceptible cell line was more complex. Depending upon the virus used, certain cell lines were more permissive than others in cytotoxicity assays (Appendix II, Figures 13-16). Potential lines for study include YST-1, which is sensitive to R7020 and C134 and is amenable to *in vivo* tumor formation (Appendix II, Table 1). 2XSB is a second tumor line we intend to investigate, because it is susceptible to viruses containing $\gamma_{134.5}$ or equivalent IFN evasion genes (IRS1) but resistant to viruses lacking $\gamma_{134.5}$. Its ability to establish *in vivo* tumors is currently being investigated.

As described in Sub Task 1b, we have used the identified resistant and permissive cell lines to test additional hypotheses. These hypotheses are: 1) that nectin-1 expression is a rate limiting restriction to viral replication; and 2) IFN acts as a greater rate limiting restriction for viral replication and spread disproportionately in first generation oHSV. These hypotheses have been addressed in part and the subsequent data assembled into a manuscript for submission to the journal Neuro-Oncology (Appendix II, Appendix A).

We have also provided a summary of the MPNST susceptibility to oHSV anti-tumor activity based upon alamar blue cytotoxicity assays. The metabolically sensitive alamar blue assays however, were affected by the puromycin and Mycoplasma infection and these updated studies have been provided for the two resistant and two sensitive cell lines that will be subjected to further study (Appendix II, Figures 13-16)

Year 3: This task has been previously addressed (Appendix III, Figures 2 and 3). In summary, there is variation in the ability of each cell line to support replication of oHSVs. All cell lines support higher levels of wild-type HSV-1 (M2001). However, some cell lines (i.e. S462-luc) support replication of all oHSVs including fully attenuated first-generation oHSVs (C101, G207) and second-generation oHSVs (M002, M032, C134), while other cell lines tend to only support replication of the wild-type virus and viruses such as C134 which are engineered to counteract the anti-viral response. This is concordant with other assays and gives support to the hypothesis that the loss of the $\gamma_{134.5}$ gene is irrelevant in some cell lines but its function may be necessary in others to support a productive infection.

Year 4: Completed. No updates from previous report (2014).

SubTask 1d. Correlate the data in the described experiments to identify oHSV-sensitive and oHSV-resistant MPNSTs and select 2 of each to study in the subsequent experiments.

Status: Year 1: We have chosen representative HSV sensitive and resistant human and murine cell lines and are proceeding with studies involving these:

- Human HSV Sensitive cell lines: (S462 and NMS2PC)
- Human HSV-Resistant cell lines (T265-luc and S26T-luc)
- Murine HSV Sensitive cell lines (A18 and 231 Trig)
- Murine HSV Resistant cell lines (A382 and A202)

Based upon our preliminary analysis summarized for Appendix I, Figures 5-42, we have numerous MPNST cell lines (murine and human) available that will provide us with interesting scientific question. In the event that we experience unanticipated pitfalls with the above cell lines, we have other candidate cell lines that we can use as a substitute for future studies.

Year 2: These results were completed in Year 1 when we chose representative HSV sensitive and resistant human and murine cell lines based upon viral replication (Sub Tasks 1a-c).

Human HSV-Sensitive cell lines: (S462-luc and NMS2-PC)
Human HSV-Resistant cell lines (T265-luc and STS26T-luc)
Murine HSV-Sensitive cell lines (A18 and 231 Trig)
Murine HSV-Resistant cell lines (A382 and A202)

As indicated in our prior report, we are fortunate to have numerous MPNST cell lines (murine and human) available and this has turned out to be critical. Having started our *in vivo* analysis of these tumor lines in Year 2, we have made several unanticipated discoveries that have led to new research avenues for the project.

First, we have identified in our ongoing preliminary analysis that the initial “oHSV sensitive” human MPNST cell lines tested (S462-luc and NMS2-PC) do not establish *in vivo* tumors in the sub-cutaneous flank model. We are currently repeating these studies. Dr. Carroll has also identified similar results in their laboratory. Of the human cell lines tested thus far, STS26T-luc, YST-1 and 88-14-luc are capable of engraftment in athymic nude immunocompromised mice. As discussed above, we may have to reselect our prototypical sensitive and resistant cell lines based upon capability of engraftment.

Second, we have also discovered that for one of the cell lines (STS26T-luc) transduction with nectin-1 improved the establishment of the cell line *in vivo* (Appendix II, Figure 17) demonstrating a statistically significant shift of approximately 21 days in the initial growth of the tumor. This is an exciting discovery which we are currently investigating and testing if this holds true for the other cell lines, particularly those oHSV-sensitive cell lines for which we were unable to establish an *in vivo* model. Our *in vitro* studies show that the nectin-1 transduction does not change the mitotic activity of the STS26T-luc cell line in cell culture and only affects the tumor growth and implantation success in the *in vivo* model.

Third, our *in vitro* GFP spread studies suggest that second generation viruses (e.g. C134) capable of IFN evasion benefit the greatest from tumors which have relatively greater amounts of nectin-1 (Appendix II, Figure 3 and 4). *In vivo* studies are currently ongoing to identify oHSV treatment effect upon STS26T-luc and STS26T-nectin-1 anti-tumor activity. These studies are also specifically designed to investigate the mechanism by which nectin-1 overexpression influences the MPNST tumor biology and the effect of overexpression upon viral spread and replication in the tumor. Our *in vitro* results suggest that the nectin-1 expression increases oHSV spread. We are excited to determine if this holds true in the more complex tumor architecture and microenvironment present *in*

vivo, and these initial studies will be completed in the near future. Of note, should we experience unanticipated pitfalls with the above cell lines, we have other candidate cell lines that we can use as a substitute for future studies.

Year 3: These results were completed in year 1 when we chose representative HSV sensitive and resistant human and murine cell lines based upon viral replication (Subtasks 1a-c). For the correlation of receptor expression (nectin-1) with viral titers, we refer the reader to the Publication Figure 1 a-e in the attached manuscript. For correlation with GFP and cell count data please refer to SubTask 1b.

Human HSV Sensitive cell lines: (S462-luc and NMS2-PC)

Human HSV-Resistant cell lines (T265-luc and STS26T-luc)

Murine HSV Sensitive cell lines (A18 and 231 Trig)

Murine HSV Resistant cell lines (A382 and A202)

We will use the cell lines identified above to further test hypotheses regarding signaling pathways described in Aim 2.

Year 4: Completed. No updates from previous report (2014).

SubTask 1e. Correlate the expression of alternative molecules on oHSV-resistant MPNSTs with the potential to engineer oHSVs that can utilize these receptors to enter cells that resist HSV entry.

Status: Year 1: Our data show that even in HSV-resistant lines, the virus is capable of entry and replication. We are currently examining (as described in Subtask 1b) if the abundance of the HSV-entry molecule (nectin 1) alters viral entry and replication. These studies will identify if viral cell entry is the principal impediment to efficient viral replication or whether other viral functions (gene expression, protein synthesis, DNA replication, virus assembly, or egress) occurring after viral entry are suppressed by cellular antiviral responses leading to lowerviral replication. Preliminary results suggest that the overexpression of nectin 1 can produce a small but reproducible improvement in viral recovery in one cell line but has no effect in the other cell line tested thus far (Figure 43).

Year 2: Our data show that even in relatively HSV-resistant lines, the virus is still capable of entry and replication. We have examined (as described in Sub Task 1b) if the abundance of the HSV-entry molecule (nectin-1) alters viral entry and replication. These studies have assessed if viral cell entry is the principal impediment to efficient viral replication or whether other viral functions (gene expression, protein synthesis, DNA replication, virus assembly, or egress) occurring after viral

entry are suppressed by cellular antiviral responses leading to lower viral replication. We have concluded that overexpression of nectin-1 produces a small but reproducible improvement in viral recovery in one cell line (STS26T-luc) but has no effect in the other cell line tested (T265-luc) Appendix II, Figure 7). Thus, retargeting to alternative entry molecules has been determined to be unnecessary to improve HSV entry. This task is completed as the oHSVs do not require retargeting to improve their replication.

Year 3: We have published the results of this correlation in the attached article (Appendix III, Jackson *et al.*) (Appendix III, Figure 1 a-e). In summary, no oHSV (G207, C101, R7020, M002, M032, or C134) had a significant correlation with the capacity to support viral replication. Although not statistically significant, the second generation virus C134 showed a trend toward increased replication with increased nectin-1 expression. The wild-type virus did in fact show a strong and significant correlation with viral titers and entry-receptor expression. We refer the reader to the attached article and to the comments in SubTask 1a for further detail.

Year 4: Completed. No updates from previous report (2014).

Task 2: Establish the most effective means of enhancing virus replication by modifying a HSV-resistant phenotype.

SubTask 2a. In Aim 2, we will test two different engineering solutions to enhance the expression of HSV “late genes” in both oHSV-sensitive and –resistant MPNST cell lines. We will use a combination of classical virology methods (plaque-titering at 24hr-intervals boost infection; single-step & multi-step replication assays) and FACS monitoring the extent and time course of oHSV infection based on expression of eGFP and other fluorescent markers by FACS assays

Status: Year 1: These studies are commencing. We are focusing on the prototypical resistant and sensitive cell lines chosen for future studies. We are also investigating if the abundance of HSV entry receptor expression alters infection and spread in these cell lines (Appendix I, Figure 44).

Year 2: We have shown that viruses capable of evading IFN mediated antiviral mechanisms are superior to those containing uncompensated $\gamma_134.5$ deletions in MPNST lines suggesting that IFN activation is the principal impediment of oHSV replication and spread in the MPNST cells. Year 3 of the grant we will specifically test this hypothesis and the IFN mediated mechanisms limiting viral replication and spread. We are focusing on the prototypical resistant and sensitive cell lines chosen for these studies. In conclusion, our data indicates that entry is not the principal limitation although increased

expression of nectin can benefit a virus capable of IFN evasion. This conclusion is more comprehensively addressed in the attached manuscript being readied for publication (Appendix I, Appendix i).

Year 3: We have shown that viruses capable of evading IFN mediated antiviral mechanisms are superior to those containing uncompensated $\gamma_134.5$ deletions in MPNST lines suggesting that IFN activation is the principal impediment of oHSV replication and spread in the MPNST cells. We are in the process of testing this hypothesis and the IFN mediated mechanisms limiting viral replication and spread.

Our studies to date have established that all MPNST cell lines are susceptible to the wild-type virus, however only certain cell lines are permissive to $\Delta\gamma_134.5$ oHSVs. This has led us to hypothesize that the functions of the $\gamma_134.5$ gene product ICP34.5 may be necessary in resistant cell lines but dispensable in permissive cell lines. We will discuss briefly the known functions of ICP34.5 to establish our recent work which has yielded significant results and a more promising line of research than what was originally proposed.

The $\gamma_134.5$ gene product ICP34.5 has several documented functions. ICP34.5 recruits the protein phosphatase 1-alpha (PP1 α) to protein kinase R (PKR) in order to reverse the phosphorylation of PKR. PKR is normally phosphorylated following detection of double-stranded RNA, such as that produced upon viral transcription. This phosphorylation event activates PKR to phosphorylate its target eukaryotic translation initiation factor 2A (eIF2a). Phosphorylation of eIF2a inhibits translation of messenger transcripts including those produced by the virus. The dephosphorylation of PKR by ICP34.5 therefore reverses this translational arrest and permits viral protein translation to continue. We have demonstrated that both permissive and resistant MPNST cell lines phosphorylate eIF2a in response to R3616, a representative $\Delta\gamma_134.5$ oHSV (Appendix III, Figure 4). Furthermore, PKR is phosphorylated in the majority of human MPNST cell lines including the previously established permissive cell lines (e.g. S462-luc and NMS2PC). A mouse compatible p-PKR antibody has not yet been acquired. Therefore the lack of PKR/eIF2a phosphorylation in permissive cell lines does not explain the difference observed between the permissive and resistant cell lines.

A second known function of ICP34.5 is the inhibition of TANK binding kinase-1 (TBK-1) activation¹. TBK-1 is a downstream target of pattern recognition receptors (PRRs) which detect pathogen associated molecular patterns (PAMPs, e.g. viral dsRNA). The normal consequence of TBK-1 activation is the phosphorylation of interferon regulator factor-3 (IRF-3) and the

subsequent binding of IRF-3 to interferon promoter elements which increases transcription of Type-I interferons (IFNs) which include the cytokines IFN- α and IFN- β ². Autocrine and paracrine interaction of extracellular Type-I IFN with its cognate receptor stimulates Janus kinases (JAK) to phosphorylate the signal transducer and activator of transcription-1 and 2 (STAT1/2). STAT dimers then enter the nucleus and promote transcription of a host of interferon stimulated genes (ISGs)³. These ISGs are primarily involved in amplifying and promoting viral resistance³. Therefore, ICP34.5 inhibition of TBK-1 results in the loss of Type-I interferon expression and thus subsequent activation of the associated STATs and target ISGs.

To test the hypothesis that permissive cell lines did not respond to $\Delta\gamma_134.5$ oHSV infection by activating STAT1, we performed western blot analysis of mock or R3616 infected cell lysates to look at the phosphorylation of STAT1. Cells were infected at an MOI of 1 and lysates collected at 6 hpi. The timepoint 6 hpi was confirmed in our assays to represent the peak of STAT1 phosphorylation with subsequent reduction in phosphorylation at subsequent timepoints. STAT1 phosphorylation was observed in 2 of 8 human MPNST cell lines (STS26T-luc and 88-14-luc) and 7 of 14 mouse cell lines (Figure 5). STAT1 was expressed in all cell lines (Figure 5) and all human MPNST cell lines responded to exogenously applied IFN- β with STAT1 phosphorylation (Figure 6) (murine cell lines are in the process of being tested) indicating that all (human) cell lines have functional IFN receptors and JAKs. We then separated the quantitative data of viral productivity acquired from our previous experiments into pSTAT1+ and pSTAT1- groups and tested whether there was a statistically significant difference between the groups. We found significant inverse associations ($P < 0.05$) between the ability of a cell line to activate STAT1 and the capacity to support productive viral infection. The percentage of cells positive for viral GFP at 48 hpi was significantly increased for C101, C154, and M201 in cells which did not activate STAT1 (Appendix III, Figure 7 A-C). In addition there was a significant decrease in the relative cell counts for C154 and M201 in cell lines which did not activate STAT1 (Appendix III, Figure 7 F-G). There was no difference observed between the STAT1 phosphorylation status with the wild-type virus as both pSTAT1+ and pSTAT1- cell lines were statistically indistinguishable by percentage GFP positive and relative cell loss measurements (Appendix III, Figure 7 D and H). Titers of R3616 infected cells (MOI=1, 24 hpi) were also significantly increased in pSTAT1- cell lines (Appendix III, Figure 8).

These findings have led us to conclude that all $\Delta\gamma_134.5$ oHSVs, including the second-generation M002 and C134 viruses, are significantly inhibited in cell lines which are competent in their ability to respond to HSV infection by activating the antiviral

cascade involving STAT1. The association of pSTAT1 with resistance leads us to question whether pSTAT1 mediates this resistance or whether STAT1 phosphorylation occurs as a consequence of, or in parallel with the actual mediators of resistance. We are currently testing the first hypothesis, that pSTAT1 mediates this resistance, by stably expressing a dominant-negative STAT1 (dnSTAT1) which will result in a loss of function for STAT1 transcriptional activation. We will further test the role of Type I IFNs in inducing pSTAT1 by using neutralizing antibodies to IFN α and IFN β and observe the effect upon $\Delta\gamma_134.5$ oHSV infection in resistant cells. We will perform the reciprocal experiment in permissive cell lines by observing the extent to which exogenously applied IFN β inhibits productive $\Delta\gamma_134.5$ oHSV infection in normally permissive MPNST cell lines.

Finally, cell lines which are capable of responding to infection with oHSVs by activating the IFN/STAT1 cascade may be primed to resist the virus prior to infection. We have observed that basal levels of interferon stimulated genes (ISGs), the transcriptional targets of pSTAT1, are elevated at baseline in pSTAT1+ human MPNSTs (Figure 9). Both pSTAT1+ cell lines STS26T-luc and 88-14-luc show elevated expression of the ISGs myxovirus resistance-1 (MX1) and interferon-induced protein with tetratricopeptide repeats 3 (IFIT3) as compared to pSTAT1- cell lines. This may indicate aberrant low-level expression of IFN in these cell lines which elevates the endogenous levels of ISGs that mediate resistance to oHSV and primes them for oHSV resistance. We will test this by exposing these cell lines to neutralizing IFN antibodies and observe any transient decrease in ISG expression. Basal expression of ISGs will also be tested in our dominant-negative STAT1 cell lines and compared to the parent cell lines.

Year 4: Following the characterization of 8 human and 13 mouse MPNST-derived cell lines (21 in total) and their response to our engineered oHSVs in the first years of this research, our primary focus has been to determine the molecular basis of the oHSV responsive and non-responsive phenotypes. Our initial studies established that expression of the entry receptors which enable HSV-1 cellular entry was not a “resistance factor” for oHSV inasmuch as the oHSV was attenuated by deletion of the $\gamma_134.5$ neurovirulence gene ($\Delta\gamma_134.5$). Overexpression of entry receptors in resistant cell lines enhanced cell-to-cell spread for wild-type HSV-1 and a 2nd generation oHSV (C134) capable of PKR evasion, but fully attenuated $\Delta\gamma_134.5$ oHSV was not substantially affected. This data was published last year in the journal *Gene Therapy* (Appendix IV, Jackson 2014).

Because the major function of the $\gamma_134.5$ gene product is to reverse intrinsic cellular immune responses within the infected cell, we subsequently hypothesized that the capacity of a cell to

activate such responses may be the primary determinant of a productive infection. The activation of the pattern recognition receptor (PRR) protein kinase R (PKR) is believed to be a primary mechanism by which cells detect and resist productive infection by HSV. Activation of PKR results in the phosphorylation of the eukaryotic translation initiation factor 2 α (eIF2 α) resulting in translational arrest, and expression of the $\gamma_134.5$ gene in wild-type HSV is known to reverse this effect. We proposed that the ability of a cell to activate PKR could be a determinant of productive infection for $\Delta\gamma_134.5$ oHSVs, however, we discovered that cells of both resistant and permissive phenotypes respond to $\Delta\gamma_134.5$ oHSV infection with activation of PKR and eIF2 α phosphorylation (Manuscript Figs. 1C-D). In addition to PKR, cells express a broad system of PRRs which induce expression of the anti-viral cytokine interferon (IFN) in response to pathogen associated molecular patterns (PAMPs). IFN in turn activates, in an autocrine and paracrine manner, signal transducer and activator of transcription 1 (STAT1). As a transcription factor, STAT1 induces the expression of several hundred anti-viral genes, termed interferon stimulated genes (ISGs), with diverse anti-viral functions. We hypothesized that activation of STAT1 in response to oHSV was predictive of oHSV resistance. We discovered that unlike PKR, STAT1 was activated in only a subset of the 21 MPNST cell lines and was associated with diminished oHSV productivity (Manuscript Figs. 2A-D). Perhaps most intriguing was the finding that many of these cell lines constitutively expressed ISGs prior to infection (Manuscript Fig. 5A), suggesting potential markers of oHSV resistance. ISG expression could be down-modulated prior to infection by treatment with inhibitors of Janus kinase 1 (JAK1), the kinase responsible for the signal transduction between IFN and STAT1, with benefits to viral replication and spread (Manuscript Fig. 4). Additionally we report a putative link between the basal expression of ISGs and basal NF κ B signaling (Manuscript Fig. 6).

We refer to the appended draft-manuscript for a complete description of this data, conclusions, discussion, and the associated methods.

SubTask 2b. Determine the ability of HSV-mediated expression of constitutively activated-MAP kinase (MEK) will result in an increase in HSV late gene expression, higher HSV particle production and cytotoxicity.

Status: Year 1: We have discovered two new and unexpected findings that will be pursued in follow up studies. The first novel discovery is that both of the IL-12 expressing $\Delta\gamma_134.5$ viruses, M002, and M032, are capable of late viral protein synthesis that surpasses that of other $\Delta\gamma_134.5$ viruses tested (C101 and G207) and can replicate as well as wild-type HSV in the MPNST tumor cells tested.

However, unlike wild-type HSV or the two recombinants, R7020 and C134, the IL-12 expressing $\Delta\gamma_{134.5}$ viruses do not contain PKR-evasion genes. This is shown in Figure 45 Panel A, that M002 and M032 are unable to block PKR-mediated phosphorylation of eIF-2 α . (Appendix I, Figure 45 Panel A p- eIF-2 α immunostaining panel). This suggests that in the MPNST tumor cells the M002 and M032 oHSVs encode an alternative mechanism to allow late viral protein synthesis that differs from that of the C134 and R7020. There are two possible explanations: (i) that the M002 and M032 recombinants contain secondary mutations that enhance viral protein translation independent of eIF-2 regulation of translation initiation. Efforts are currently underway to identify genetic differences between the M002/M032 recombinants and the parent $\Delta\gamma_{134.5}$ recombinant used to construct the IL-12 expressing viruses.

The second novel finding is that certain MPNST cell lines restrict C134 late viral protein synthesis and replication. Preliminary studies show that in most of the MPNST cell lines, C134 is capable of PKR-evasion and replicates similar to the $\Delta\gamma_{134.5}$ containing viruses (R7020 and M2001). This is consistent with our prior studies in glioma tumors (Shah 2007). However, in select MPNST cell lines, C134 is unable to evade PKR-mediated translational arrest and its replication is restricted similarly to that seen with $\Delta\gamma_{134.5}$ virus (G207 and C101). This divergent late protein synthesis phenotype is summarized using 2 of the MPNST cell lines shown in Figure 45. In the Human MPNST 90-8 cell line, C134 is capable of evading translational arrest based upon decrease in eIF-2 α phosphorylation and increase in glycoprotein D expression in the C134 infected cells. In this cell line the $\Delta\gamma_{134.5}$ cell lines, G207, M002, and M032 induce phosphorylation of eIF-2 α and produce less glycoprotein D (a late HSV gene) than the recombinants expressing PKR-evasion genes (M2001, R2070, and C134). This ability to synthesize late viral proteins also correlates with improved viral replication for the C134 recombinant. In contrast to the 90-8 cell line, the mouse B76 MPNST cell line activated eIF-2 α after infection by $\Delta\gamma_{134.5}$ oHSVs. These cell lines will provide valuable tools for further characterization of the mechanism by which C134 and specifically the IRS1 gene targets PKR and the translational machinery. This work may in turn allow improved efficacy of C134 when ultimately tested in clinical trials.

Year 2: Preliminary examination of MEK activity assessed by immunoblots of phosphorylated ERK 1/2 (the established target of MEK) indicated that MEK is active at basal levels as well as following viral infection in many MPNST cell lines (data not shown). Most significantly in oHSV resistant cell lines T265-luc and STS26T-luc demonstrate basal and sustained ERK 1/2 phosphorylation suggesting that activated MEK is not sufficient to impart nor does it correlate with an oHSV permissive

phenotype. For example basal activity of MEK is not apparent in the permissive cell line YST-1 and yet this cell line yields consistently higher titers of virus as compared to the resistant cell lines.

Year 3: Preliminary examination of MEK activity assessed by immunoblots of phosphorylated ERK 1/2 (the established target of MEK) indicated that MEK is active at basal levels as well as following viral infection in many MPNST cell lines (Figure 10). Most significantly in oHSV resistant cell lines T265-luc and STS26T-luc demonstrate basal and sustained ERK 1/2 phosphorylation suggesting that activated MEK is not sufficient to impart nor does it correlate with an oHSV permissive phenotype. For example basal activity of MEK is not apparent in the permissive cell line YST-1 and yet this cell line yields consistently higher titers of virus as compared to the resistant cell lines.

Due to the findings regarding the activation of the STAT1 pathway discussed in SubTask 2a, we believe that our efforts will be more fruitful by further investigating the STAT1 signaling pathway as opposed to the MEK/ERK pathway which has not shown promise in preliminary work. Thus, the focus of this subtask has been changed as a result of data generated during the performance of our work related to this grant.

Year 4: We determined the basal status of MEK and ERK phosphorylation by western blot in the 8 human MPNST cell lines (Manuscript Supplemental Fig. S4). We identified that elevated MEK/ERK phosphorylation was present in both permissive (NMS2PC) and resistant (T265-luc) cell lines suggesting that the capacity to activate this pathway does not benefit $\Delta\gamma_{134.5}$ oHSV infection. These findings follow similar data and conclusions reached by Mahller (Mahller, 2006) regarding the benefits of Ras signaling for oHSV productivity in MPNSTs.

SubTask 2c. Determine the ability of HSV-mediated expression of a human cytomegalovirus gene, IRS-1, that promotes late gene expression in CMV, to increase oHSV late gene expression, higher HSV particle production and MPNST cytotoxicity.

Status: Year 1: These studies are near completion and as shown Appendix I, Figures 5-42, we have tested if HCMV

Year 2: These studies are complete. The chimeric oHSV C134 which expresses CMV IRS-1 yields consistently higher titers of virus compared to the parent virus C101 (Appendix II, Figures 9 and 10) and approaches the replicative capacity, cytotoxicity, and spread of the representative wild-type virus M2001.

Year 3: We have determined that the IRS-1 expressing oHSV C134 (and the eGFP variant C154) significantly improves the productive capacity of $\Delta\gamma_134.5$ oHSVs. This is evident by an increase in viral titer (Publication Supplementary Figure 1b) as well as by increased cell-to-cell spread (Appendix IV, Figures 1a and Publication Figure 3 d-e) and a reduction in relative cell counts as compared to the unmodified $\Delta\gamma_134.5$ oHSVs C101 and R3616 (Figure 1b). Although C134 approaches the replicative capacity, spread, and cell killing that the wild-type virus does in a number of cell lines, there are still cell lines which resist this virus. This indicates that the expression of IRS-1 and consequent inhibition of PKR activation may not be sufficient to reverse the $\Delta\gamma_134.5$ oHSV resistant phenotype. We further show in SubTask 2a that cell lines which are capable of activating the antiviral signaling pathway mediated by STAT1 have significantly diminished capacity to support the productive infection of $\Delta\gamma_134.5$ oHSVs including C134.

Year 4: We have determined that the IRS-1 expressing oHSV C134 (and the eGFP variant C154) significantly improves the productive capacity of $\Delta\gamma_134.5$ oHSVs in MPNSTs. This is evident by an increase in viral titer as well as by increased cell-to-cell spread (Appendix IV, Jackson, 2014) and a reduction in relative cell counts as compared to the unmodified $\Delta\gamma_134.5$ oHSVs C101 and R3616 (Appendix IV, Figure 1b). Although C134 approaches the replicative capacity, spread, and cell killing that the wild-type virus does in a number of cell lines, there are still cell lines which resist this virus. This indicates that the expression of IRS-1 and consequent inhibition of PKR activation may not be sufficient to reverse the $\Delta\gamma_134.5$ oHSV resistant phenotype. We further show in the appended manuscript that cell lines which are capable of activating the antiviral signaling pathway mediated by STAT1 have significantly diminished capacity to support the productive infection of $\Delta\gamma_134.5$ oHSVs including C134 (Manuscript Fig. 3).

SubTask 2d. Examine the impact of p38MAPK activation in MPNST tumors to have a positive or negative impact on the ability of these engineered oHSVs to display greater replication and oncolysis.

Status: Year 1: See explanation in SubTask 2e. Based on our observations, these two tasks do not seem to be critical to the development of more effective oHSVs for treatment of MPNSTs and consequently will be deleted.

Year 2: See explanation in Sub Task 2e. Preliminary western blots suggest that there is p38 activation in both resistant and sensitive cell lines (data not shown). These studies are being actively pursued as we enter Year 3.

Year 3: Preliminary western blots suggest that there is p38 activation in both resistant and sensitive cell lines (Appendix III, Figure 10). These studies were being actively pursued as we entered year 3.

Similar to our discussion in SubTask 2b, due to the findings regarding the activation of the STAT1 pathway discussed in SubTask 2a, we believe that our efforts will be more fruitful by further investigating the STAT1 signaling pathway as opposed to the p38 pathway which has not shown promise in preliminary work.

Year 4: No updates from previous report (2014).

SubTask 2e. Correlate and compare the data sets obtained from the studies in oHSV-sensitive and –resistant MPNSTs using the caMEK viruses (R2660, R2636) and the IRS-1 viruses (C134, C154).

Status: Year 1: One of the possible solution to the issue of poor replication is the level of Mitogen-Activated Protein Kinase activation (phosphorylation), which is perceived as important for optimum late virus gene expression and optimum downregulation of PKR activation preventing eIF2 α activation which would shut-off protein synthesis. A strategy has been to consider exogenous expression of an upstream mediator, mitogen-activated protein kinase kinase (MEK $\frac{1}{2}$). oHSVs expression constitutively activated MEK (ca-MEK) or dominant negative MEK are available to study this. However, our studies show that most MPNSTs already have high levels of activated p38 MAPK and phosphorylated Erk1/Erk2, immediate downstream targets of MEK. Thus, a strategy of trying to coordinately upregulate MEK activation to achieve greater virus replication is likely not to be a worthwhile study. Based on our observations of elevated MEK with several MPNSTs, we are no longer considering that ca-MEK oHSV would be an effective strategy, unless we discover MPNSTs that would not already have phosphorylation of MEK.

Year 2: Based upon our past review and findings from an unrelated grant, we are re-opening these studies and have commenced testing the MPNST tumor lines for p38MAPK activity. It is possible that the *in vivo* environment and relative hypoxia in this environment may impact upon p38MAPK activity *in vivo*. We are therefore investigating this possibility and whether this could impact upon oHSV replication and spread *in vivo*. We are currently completing preliminary studies and if they suggest that this could limit viral anti-tumor activity, we will re-investigate this using *in vitro* methods that can reproduce the relative hypoxia present *in vivo* as well as using the *in vivo* systems (1).

Year 3: Correlate and compare the data sets obtained from the studies in oHSV-sensitive and –resistant MPNSTs using the caMEK viruses (R2660, R2636) and the IRS-1 viruses (C134, C154).

See explanation in SubTask 2d. While we do not anticipate further exploring the p38 or MEK/ERK pathways, we will have correlated the STAT1 status with the panel of oHSVs as described in SubTask 2a.

Year 4: No updates from previous report (2014).

SubTask 2f. Select the most appropriate (set of) oHSV virus(es) to advance to preclinical *in vivo* studies with human and mouse MPNSTs.

Status: Year 1: Several studies remain to be completed before the candidate oHSVs can be appropriately selected. Preliminarily, we believe both M032 and C134 will prove to be the most attractive candidates. Once we have completed our evaluation of our panels of MPNSTs with regard to virus infectivity, virus replication and capacity of our experimental and clinical candidate HSVs to produce an oncolytic effect *in vitro*, we will be able to select the most appropriate MPNST lines to use in our heterotropic and orthotropic models to evaluate the *in vivo* effects. In essence, the xenogenic models with human tumors in immunocompromised mice will permit evaluation of the 3 clinical candidate viruses. In our syngeneic mouse models in immunocompromised mice, we will also be able to assess anti-tumor efficacy as it is affected by the host immune response. These studies are the basis of Milestone 4.

Year 2: For the human cell lines, we have discovered that the IFN evasion virus holds a distinct advantage (spread by GFP assay) over first generation viruses and second generation viruses incapable of IFN evasion (M201, M002, M032). Because the cytokine expressing virus would provide less advantage as a therapeutic in the athymic models, we chose to limit our analysis in preliminary studies to C134 and its parent virus C101. In our later studies we have also begun to investigate the viruses for which clinical grade product is available. Now that we have identified that the human tumor experience is limited in the *in vivo* model, we are beginning to investigate the syngeneic models but have not begun these implantations. For the syngeneic studies, we hypothesize (as stated in our previous progress report) that in addition to the C134 based virus, the M032 virus will also be an especially attractive virus to test because of its ability to enhance an immune-mediated anti-tumor response. We have followed the path outlined in our most recent progress report. The xenogeneic models with human tumors in immunocompromised mice have permitted evaluation of the three clinical candidate

viruses as well as differences in C101 and C154. We are now initiating studies in the syngeneic mouse models and will assess anti-tumor efficacy and how the host immune response impacts efficacy. Initial pilot studies in the tumors derived from STS26T-luc show promising efficacy of clinical grade oHSVs (Appendix II, Figure 18). These studies are the basis of Milestone 4.

Year 3: For the human cell lines, we have discovered that the IFN evasion virus holds a distinct advantage (spread by GFP assay) over first generation viruses and second generation viruses incapable of IFN evasion (M201, M002, M032). Because the cytokine expressing virus would provide less advantage as a therapeutic in the athymic models, we chose to limit our analysis in preliminary studies to C134 and its parent virus C101. In our later studies we have also begun to investigate the viruses for which clinical grade product is available. Now that we have identified that the human tumor experience is limited in the *in vivo* model, we are beginning to investigate the syngeneic models but have not begun these implantations. For the syngeneic studies, we hypothesize (as stated in our previous progress report) that in addition to the C134 based virus, the M032 virus will also be an especially attractive virus to test because of its ability to enhance an immune-mediated anti-tumor response. The xenogeneic models with human tumors in immunocompromised mice have permitted evaluation of the 3 clinical candidate viruses as well as differences in C101 and C154. We are now initiating studies in the syngeneic mouse models and will assess anti-tumor efficacy and how the host immune response impacts efficacy. These studies are the basis of Milestone 4.

Year 4: We propose to advance the second generation oHSVs C134 and M002/M032 to *in vivo* MPNST studies. We believe this is justified based on our prior use of these viruses in *in vivo* models of glioblastoma, and the *in vitro* data obtained with these viruses in MPNST would suggest a similar advancement of these studies.

Task 3: Validate the ability of selected oHSV to produce an oncolytic anti-MPNST effect in established tumors in mouse models and quantify the capacity of a low dose of radiation to enhance this anti-tumor effect.

SubTask 3a. Tumor cells growing *in vivo* often display significant biologic differences from those growing *in vitro*. The first subtask will be to establish a baseline of the ability of oHSVs to infect and kill human or mouse MPNST cell lines transplanted into appropriate host mouse strains. The ability of generic $\Delta\gamma_{134.5}$ HSV (G207, NV1070) to produce an antitumor effect as observed in Task 1c *in vitro* will be determined by direct injection of bioluminescence-enabled human or mouse MPNSTs placed

in an orthotopic location (sciatic nerve). Both oHSV-sensitive and oHSV-resistant MPNSTs will be compared.

Status:

Year 1: We have not initiated these experiments.

Year 2: These studies are ongoing and will continue in Year 3.

Year 3: We have completed training of sciatic nerve tumor grafting and plan to advance in vivo studies within the next year.

Year 4: These studies remain incomplete.

SubTask 3b.

Compare the abilities of selected oHSVs (e.g., M002, C134, R2660, etc) from previous studies to produce an enhanced anti-MPNST effect compared to that of the generic viruses. Oncolysis of orthotopically-placed oHSV-sensitive and oHSV-resistant MPNSTs will be compared.

Year 1: We have not initiated these experiments.

Year 2: We have initiated these studies and will continue these in year 3.

Year 3: We have completed training of sciatic nerve tumor grafting and plan to advance in vivo studies within the next year.

Year 4: These studies remain incomplete.

SubTask 3c.

Determine whether or not a single low dose of radiation (2-5Gy) delivered to the tumor within 24 hrs of injection of selected oHSVs enhances the replication and spread of the virus yielding an enhanced anti-MPNST effect. Irradiation has a more pronounced and sometimes paradoxical effect in vivo than it does in vitro and thus, irradiation effects will not be explored in vitro.

Status:

Year 1: We have not initiated these experiments.

Year 2: We have not initiated these experiments as we are waiting on the *in vivo* oHSV results.

Year 3: We have completed training of sciatic nerve tumor grafting and plan to advance in vivo studies within the next year.

Year 4: These studies remain incomplete.

SubTask 3d.

Compare and correlate the findings from these sub-tasks to select the most likely combination of oHSV and adjunctive therapy that will be most effective oncolytic, anti-MPNST modality for human or mouse MPNSTs transplanted orthotopically and test this combination in the P₀-GGFβ3 x

Elux mouse against MPNST tumors that arise sporadically and spontaneously.

Year 1: We have not obtained sufficient data to be able to complete this subtask.

Year 2: We have not obtained sufficient data to be able to complete this subtask.

Year 3: We have not obtained sufficient data to be able to complete this subtask.

Year 4: These studies remain incomplete.

SubTask 3e. Review the entire data set to design studies that will be able to validate the selected oHSV with or without adjunctive therapy that can be advanced to a Phase I/II clinical trial to test the safety, identify unanticipated toxicities and establish preliminary evidence of efficacy in patients with MPNST.

Year 1: We have not obtained sufficient data to be able to complete this subtask.

Year 2: We have not obtained sufficient data to be able to complete this subtask.

Year 3: We have not obtained sufficient data to be able to complete this subtask.

Year 4: These studies remain incomplete.

Key Research Accomplishments

Year 1:

- See Appendix I

Year 2:

- Nectin-1 is expressed in all of our MPNST cell lines; Bayesian analysis suggests that this is the probable state for MPNST tumors in general.
- HVEM expression is present in at least one of our cell lines, however its limited or non-existent expression in the remaining cell lines would not suggest its role as a significant player in HSV entry in MPNSTs.
- Even low levels of nectin-1 expression, as determinable by current techniques, appear sufficient to permit viral entry and subsequent replication in our MPNST cell lines.
- However, these low levels of nectin-1 expression may negatively impact first generation $\Delta\gamma 134.5$ oHSV cell-to-cell spread.

- Key mediator of MPNST host cell resistance to oHSV is not entry molecule expression, but interferon evasion, as confirmed by C134 vs. C101 experiments, above.
- Other non-entry related mechanisms of resistance likely exist.
- Nectin-1 overexpression can increase MPNST tumorigenicity and growth rate in at least one MPNST model.
- The increased tumorigenicity produced by nectin-1 overexpression may abrogate the potential gains for tumor oHSV mediated therapy as the resultant increases in viral replication, spread, and tumor cytolysis are relatively small in comparison especially for first generation $\Delta\gamma_134.5$ viruses; however, the increase in syncytia formation provided by such overexpression may produce an advantage in evasion of the cellular immune response for the virus.
- *In vitro* models demonstrate that oHSV replication, spread, and cytolysis can be independent variables and efficient therapy should maximize each variable.
- Late HSV viral protein expression can be upregulated in $\gamma_134.5$ -deleted viruses via a PKR-independent mechanism as seen in M002 and M032.

Year 3:

- Peer-reviewed publication documenting our studies of entry receptor expression in the context of different viral genotypes
- Nectin-1 is expressed in all of our MPNST cell lines; Bayesian analysis suggests that this is the probable state for MPNST tumors in general
- HVEM expression is present in at least one of our cell lines, however its limited or non-existent expression in the remaining cell lines would not suggest its role as a significant player in HSV entry in MPNSTs
- Even low levels of Nectin-1 expression, as determinable by current techniques, appear sufficient to permit viral entry and subsequent replication in our MPNST cell lines
- All MPNST cell lines are competent in their ability to phosphorylate eIF2a in response to infection with oHSV
- No correlation exists between the PKR/eIF2a activation status and permissive/resistant phenotypes
- The ability of a cell line to activate the antiviral cascade involving STAT1 in response to oHSV infection is significantly and negatively correlated with the productive capacity of $\gamma_134.5$ -deleted viruses, including second-generation viruses
- Wild-type HSV-1 demonstrates productive infection in all cell lines regardless of their capacity to activate STAT1
- Cell lines which demonstrate STAT1 activation also have greater expression of ISGs prior to infection
- Multistep assays using $\gamma_134.5$ -deleted viruses demonstrate significant correlation between the ability of the virus to spread from cell-to-cell and the relative loss of cells.

Year 4:

In addition to the key research accomplishments reported in prior funding years, we report these as relevant to the most recent year of funding:

- Activation of STAT1 in MPNST cells is associated with increased resistance to $\Delta\gamma_134.5$ oHSVs, including a $\Delta\gamma_134.5$ oHSV capable of PKR evasion.
- Elevated basal levels of interferon stimulated genes (ISGs), common to numerous MPNST cell lines, are associated with increased resistance to $\Delta\gamma_134.5$ oHSVs.
- The use of JAK1 inhibitors can reduce the basal expression of ISGs in MPNSTs resulting in improved $\Delta\gamma_134.5$ oHSV productivity.
- Inhibiting the activity of the NF κ B transcription factor by overexpression of its negative regulator inhibitor of κ B (I κ B) results in the diminished basal expression of ISGs. This is the first report of cancer-associated NF κ B signaling and the induction of ISG expression.

Conclusions:

- Year 1:**
- A382:** This is one of the more resistant mouse cell lines tested and we intend to use this as one of the two resistant mouse cell lines for future studies.
- A202:** The A202 cell line is considered resistant to HSV replication and cytopathic effect. We intend to further study this line as one of the 2 resistant murine cell lines. We have chosen it because there is differential replication of the $\Delta\gamma_134.5$ viruses in this cell line.
- B91:** This is another resistant murine cell line (similar to A202) where the clinical grade viruses exhibit differential replication profiles and may be of interest in future studies.
- U231-Trig:** The 231-Trig MPNST cells are a sensitive cell line. We intend to include this as one of the 2 oHSV sensitive MPNST cell lines in future studies as described in Subaim 1d.
- A18:** The A18 cell line will be one of the 2 sensitive murine MPNST cell lines that we will use in future studies because it shows a greater differential effect on $\Delta\gamma_134.5$ replication. The C134 recombinant differs from its parent virus (C101) in this cell line and is capable of maintaining late viral protein synthesis and precludes PKR mediated shutoff similar to that shown in other human tumor cell lines tested (Shah, 2007).
- T265-luc:** This is an interesting cell line that we intend to include in future studies as a representative resistant human cell line for future studies as described in Subaim 1d.
- S26-T-luc:** The 26-T-luc is an interesting cell line that we intend to include in future studies as a representative resistant human cell line Subaim 1d.
- YST-1:** YST-1 represents a human MPNST cell line that allows the replication of all of our viral mutants under study and is sensitive to the virus as a cytotoxic agent.
- NMS2PC:** NMS2PC represents a human MPNST cell line that both allows the replication of all of our viral mutants under study and is more sensitive to the virus as a cytotoxic agent than most other human lines.
- S462:** S462 represents a human MPNST cell line that both highly supports the replication of all of our viral mutants under study and is uniformly sensitive to the virus as a cytotoxic agent. Viral mutants M002 and M032, and to lesser degree, C134, replicated particularly well in this line.

HS-PSS: SH-PSS represents a human MPNST cell line that both highly supports the replication of all our viral mutants under study and is uniformly sensitive to the virus as a cytotoxic agent. Viral mutants M002, M032, and C134 replicated particularly well in this line.

Year 2: There are additional restrictions to oHSV replication independent of HSV entry in MPNSTs. The fact that viruses with genes that can substitute for $\gamma 134.5$ functions (e.g. late viral protein synthesis) suggest that restricted viral growth within the infected cell is the principal limitation to oHSV efficacy.

Contrary to prior assumptions nectin-1 expression even at minimal levels (detected by flow cytometry) are sufficient for viral entry and efficient replication as evidenced by the lowest nectin-1 expression in the cell line 90-8-luc however with many instances of greater titers of virus in this cell line compared to other cell lines with higher expression of nectin-1. Higher nectin-1 levels correlate with improved spread in vitro of second generation vectors (e.g. C134) and wild-type HSV. Supra-biologic nectin-1 expression levels are not sufficient to increase spread of first generation viruses to that seen with second generation viruses (Figures 3 and 4). Additionally increased nectin-1 does not permit first generation viruses (C101, M201) to spread at the rate observed in permissive cell lines (S462-luc, NMS2-PC).

Based upon our preliminary in vivo studies using the STS26T-luc nectin over-expressing cell lines, nectin-1 overexpression may increase tumor growth rate (Figure 17). Nectin-1 overexpressing tumors, because of their hypothetical improved growth and the limited spread seen with first generation viruses, may diminish any benefits conferred by increased nectin-1 levels. The net effect of increased nectin-1 expression may limit the efficacy of first generation $\Delta\gamma 134.5$ oHSV therapy in vivo rather than a benefit as previously assumed.

Previously we equated oHSV replication, spread, and cytotoxic effects as dependent variables. Based upon our work over the last year, we now recognize that these are actually independent variables. While they often correlate in sensitive cell lines, the nectin-1 expression studies have shown that one phenotype can be altered (spread) without significantly changing the viral recovery or replication phenotype.

We have identified using a stably expressing nectin-1 cell line that overexpression of this adhesion molecule also enhances syncytial formation during oHSV infection.

We have also shown evidence of nectin-1 expression in nine human MPNST cell lines. All are positive but the levels are lower than reported for other tumors (carcinomas).

2XSB cell line expresses HVEM (unlike any of the other MPNST tumor lines). This is an entry receptor usually limited to lymphoid cells has not been previously identified in neuroectodermal tissue.

Year 3: As a first approach to distinguish between permissive and resistant phenotypes, we hypothesized that the expression of the entry receptors which the virus uses to gain access into the cell was limited in cells which were resistant to oHSV. We tested this hypothesis by overexpressing the major HSV-1 entry receptor nectin-1 in cells which we had previously identified as resistant. By several measures, this increase in nectin-1 did

little to improve the productive capacity of our oHSVs and did not reproduce the permissive phenotype observed in other cell lines. We have therefore concluded that differences in HSV-1 entry receptor expression do not explain the disparate phenotypes observed in MPNSTs.

These conclusions are counter to those reported for oHSVs in other cancer types. These other studies demonstrate that the level of entry receptor expression is directly related to oncolytic efficacy. One major difference between these studies is the use of oHSVs which contain a functional copy of the HSV neurovirulence gene γ 134.5. The viruses used in our lab are all based upon the deletion of both copies of γ 134.5. Indeed, these viruses did not demonstrate a correlation with entry receptor expression nor did they substantially benefit from increased entry receptor expression. However, in our studies the wild-type virus did show dramatic benefit and showed significant correlation with entry receptor expression. We have also shown that all MPNST cell lines are susceptible to productive infection by the wild-type virus. This has led us to conclude that entry receptor expression is not the primary mode of resistance.

The results regarding the involvement of the STAT1 signaling pathway have provided us with a promising new approach to determine the source of resistance to our oHSVs. Although we have not yet performed the studies which look into the function role of STAT1 activation (using a dnSTAT1), early data indicates that there is a significant association with a cell's ability to activate this pathway and the outcome of the infection. Interestingly, this association holds for the second-generation $\Delta\gamma$ 134.5 oHSVs (C134 and M201) despite the fact that these viruses perform much better than the first-generation $\Delta\gamma$ 134.5 oHSV C101. The virus C134 expresses the chimeric transgene HCMV IRS-1 which has been shown to inhibit the activation of PKR thereby preventing translational arrest. This would presumably compensate for one function of ICP34.5. The STAT1 data however suggests that prevention of PKR activation may not be sufficient to allow a productive infection in cells which are STAT1 responsive. This observation may be due to the other roles that ICP34.5 provides during infection, including the prevention of TBK-1 induced expression of IFN and the subsequent activation of STAT1. We are excited to further pursue these studies as they have not yet been explored in the context of oHSV virotherapy. Furthermore, pharmacologic modulators exist for the STAT1 signaling cascade which may suggest a potential avenue for adjuvant therapies which overcome resistance attributable to STAT1 activation.

Year 4: As a first approach to distinguish between permissive and resistant phenotypes, we hypothesized that the expression of the entry receptors which the virus uses to gain access into the cell was limited in cells which were resistant to oHSV. We tested this hypothesis by overexpressing the major HSV-1 entry receptor nectin-1 in cells which we had previously identified as resistant. By several measures, this increase in nectin-1 did little to improve the productive capacity of our oHSVs and did not reproduce the permissive phenotype observed in other cell lines. We have therefore concluded that differences in HSV-1 entry receptor expression do not explain the disparate phenotypes observed in MPNSTs.

The results regarding the involvement of the STAT1 signaling pathway have provided us with a promising new approach to determine the source of resistance to our oHSVs. Our data indicates that there is a significant association with a cell's ability to activate this pathway and the outcome of the infection. Interestingly, this association holds for the second-generation $\Delta\gamma$ 134.5 oHSVs (C134 and M201) despite the fact that these viruses

perform much better than the first-generation $\Delta\gamma_{134.5}$ oHSV C101. The virus C134 expresses the chimeric transgene HCMV IRS-1 which has been shown to inhibit the activation of PKR thereby preventing translational arrest. This would presumably compensate for one function of ICP34.5. The STAT1 data however suggests that prevention of PKR activation may not be sufficient to allow a productive infection in cells which are STAT1 responsive or which have basally stimulated STAT1 pathways. The JAK1 inhibitor ruxolitinib was able to down-modulate the basal expression of ISGs and improve oHSV productivity *in vitro* and may be a potential avenue for adjuvant therapies which overcome resistance attributable to STAT1 activation.

Publications, Abstracts, and Presentations

Manuscripts

Jackson, J. D., Markert, J. M., Li, L., Carroll, S. L., and Cassady, K. A, "Assessment of oncolytic HSV efficacy following increased entry-receptor expression in malignant peripheral nerve sheath tumor cell lines." *in preparation for Molecular Cancer Research*

Presentations

Joshua D. Jackson, Adrienne M. McMorris, Jennifer M. Coleman, Justin C. Roth, Steven L. Carroll, Kevin A. Cassady, and James M. Markert, "Assessment of oncolytic HSV efficacy following increased entry receptor expression in malignant peripheral nerve sheath tumor cell lines", Comprehensive Cancer Center Retreat, Graduate Student Poster Session, Oct. 6 2014

Jackson, J., McMorris, A., Roth, J., Coleman, J., Whitley, R., Gillespie, Y., Carroll, S., Markert, J., Cassady, K., "High nectin-1 expression in malignant peripheral nerve sheath tumor cell lines benefits oncolytic herpes simplex viruses which compensate for $\gamma_{134.5}$ deletion" UAB Graduate Student Research Symposium (2014)

Jackson, J., McMorris, A., Roth, J., Coleman, J., Whitley, R., Gillespie, Y., Carroll, S., Markert, J., Cassady, K., "High nectin-1 expression in malignant peripheral nerve sheath tumor cell lines benefits oncolytic herpes simplex viruses which compensate for $\gamma_{134.5}$ deletion" UAB Comprehensive Cancer Center Retreat (2013)

Jackson, J., McMorris, A., Roth, J., Coleman, J., Whitley, R., Gillespie, Y., Carroll, S., Markert, J., Cassady, K., "Effect of Oncolytic Herpes Simplex Virus Replication in MPNST Cell Lines Over-Expressing Nectin-1" UAB Comprehensive Cancer Center Retreat (2012)

Inventions, Patents and Licenses

Nothing to report.

Reportable Outcomes

- Previous reports have suggested that expression of the HSV-1 entry receptors, specifically nectin-1, is a limiting factor to the productive infection of oHSVs. Our publication (Jackson 2014) establishes that the ability of increased nectin-1 expression to benefit oHSV is related to the genotype of the oHSV, specifically whether it possess the capacity to alter the intrinsic antiviral response. While increased entry receptor expression in resistant cell lines benefits oHSVs which can first address intrinsic antiviral responses, oHSVs fully attenuated in this

response do not benefit, suggesting that evasion of the intrinsic antiviral response is a primary source of resistance to such viruses while entry receptor expression is of secondary importance.

- PKR activation has long been described as the major intrinsic antiviral pathway responsible for resistance to HSV-1 and especially $\Delta\gamma_134.5$ oHSVs which lack the capacity to reverse the effects of PKR. While reversing PKR effects is beneficial to the virus, as evident by expressing the transgene IRS-1 in the chimeric oHSV C134, PKR activation does not appear to fully explain resistance to $\Delta\gamma_134.5$ oHSVs including C134. Furthermore, PKR activation (or eIF2 α phosphorylation) is observed in response to $\Delta\gamma_134.5$ oHSV in cell lines with permissive and those with resistant phenotypes, suggesting PKR activation is not exclusive to resistant phenotypes.
- The major reportable outcome from this research is the identification of an intrinsic anti-viral signaling pathway (STAT1 and subsequent expression of ISGs) which is basally active in a number of MPNST-derived cell lines. Activation of this pathway and basal expression of ISGs is associated with resistance to oHSVs. Although similar reports have been made for other oncolytic viruses, this is the first report describing the contribution of this pathway to the resistance of oncolytic HSV. Because STAT1/ISG expression has been frequently observed in patient-tissue samples, and because STAT1/ISG expression has been implicated in resistance conventional therapies such as chemotherapy and radiation, we believe our findings may have significant impact in the broader field of MPNST research.

Other Achievements

Degree received: Joshua D. Jackson, Ph.D, Aug. 8 2015

References

Year 1:

See Appendix I

Year 2:

1. G. K. Friedman, M. C. Haas, V. M. Kelly, J. M. Markert, G. Y. Gillespie, K. A. Cassady, Hypoxia Moderates gamma $\gamma_134.5$ -Deleted Herpes Simplex Virus Oncolytic Activity in Human Glioma Xenoline Primary Cultures. *Translational oncology* 5, 200-207 (2012)

Year 3:

1. Verpooten D, Ma Y, Hou S, Yan Z, He B. Control of TANK-binding kinase 1-mediated signaling by the $\gamma_134.5$ protein of herpes simplex virus 1. *Journal of biological chemistry* 2009; 284(2): 1097-1105.
2. Randall RE, Goodbourn S. Interferons and viruses: an interplay between induction, signalling, antiviral responses and virus countermeasures. *Journal of General Virology* 2008; 89(1): 1-47.
3. Liu S-Y, Sanchez DJ, Aliyari R, Lu S, Cheng G. Systematic identification of type I and type II interferon-induced antiviral factors. *Proceedings of the National Academy of Sciences* 2012; 109(11): 4239-4244.

4. Khodarev NN, Beckett M, Labay E, Darga T, Roizman B, Weichselbaum RR. STAT1 is overexpressed in tumors selected for radioresistance and confers protection from radiation in transduced sensitive cells. *Proceedings of the National Academy of Sciences of the United States of America* 2004; 101(6): 1714-1719.
5. Liu Y-P, Suksanpaisan L, Steele MB, Russell SJ, Peng K-W. Induction of antiviral genes by the tumor microenvironment confers resistance to virotherapy. *Scientific reports* 2013; 3.
6. Escobar-Zarate D, Liu Y, Suksanpaisan L, Russell S, Peng K. Overcoming cancer cell resistance to VSV oncolysis with JAK1/2 inhibitors. *Cancer gene therapy* 2013.
7. Frank DA, Mahajan S, Ritz J. Fludarabine-induced immunosuppression is associated with inhibition of STAT1 signaling. *Nature medicine* 1999; 5(4): 444-447.
8. Spurrell E, Gangeswaran R, Wang P, Cao F, Gao D, Feng B et al. STAT1 interaction with E3-14.7 K in monocytes affects the efficacy of oncolytic adenovirus. *Journal of virology* 2014; 88(4): 2291-2300.

Year 4:

1. Jackson, J. D., A. M. McMorris, J. C. Roth, J. M. Coleman, R. J. Whitley, G. Y. Gillespie, S. L. Carroll, J. M. Markert, and K. A. Cassady. "Assessment of oncolytic HSV efficacy following increased entry-receptor expression in malignant peripheral nerve sheath tumor cell lines." *Gene Therapy* 21, No. 11 (2014): 984-990.
2. Mahller, Yonatan Y., Fatima Rangwala, Nancy Ratner, and Timothy P. Cripe. "Malignant peripheral nerve sheath tumors with high and low Ras-GTP are permissive for oncolytic herpes simplex virus mutants." *Pediatric blood & cancer* 46, no. 7 (2006): 745-754.

UAB SCHOOL OF MEDICINE
Department of Surgery
Division of Neurosurgery
James M. Markert, M.D.

March 11, 2013

Iddil Bekirov, Ph.D.
Science Officer
1053 Patchel Street
Fort Detrick, MD 21702
Iddil.bekirov@us.army.mil

RE: DOD Award (11-1-0498) Annual Report

Dear Dr. Bekirov:

Thank you for your instructions and critique of our previously submitted annual report. We appreciated the guidance you have given us on the desired presentation of the annual reports. Since this is our first such report, we were not familiar with many of these and have made the adjustments as requested.

Specifically, to address the requests in our critique, we have cited the figures within the text to support key research findings. The results of the anti-tumor activity assays are now described in the body of the report, and legends have been provided to the figures. All placeholder figures for data that have not yet been collected have been removed. Figures now include descriptive legends.

A request for a description of statistical analyses was previously absent and now has been included with indicators of significance.

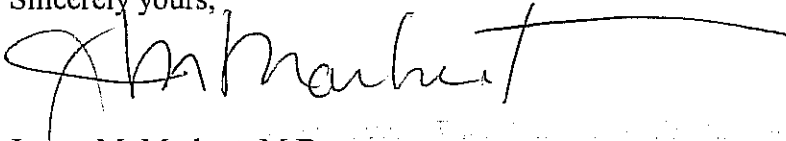
The western blots utilized in this study were for qualitative purposes only and not quantitative. Specifically, we felt it important for the purposes of this assay to include data utilizing the same number of cells for each blot. Glyco-protein D is produced at extraordinarily high levels by our herpes simplex virus, and thus, it is quite common in herpes simplex virology to have relative over-expression of this protein while other proteins are

expressed at much lower levels. This should explain the appearance of the blots as presented.

Finally, the research report has been rewritten against project tasks in the statement of work (SOW) and we have included additional analyses and descriptions of the data obtained for each task.

Thank you very much for your understanding in this, our first attempt at providing such a report for our DOD grant. Best wishes.

Sincerely yours,

A handwritten signature in black ink, appearing to read "J. Markert", with a long horizontal flourish extending to the right.

James M. Markert, M.D.
Division Director, Neurosurgery
James Garber Galbraith Professor
Neurosurgery, Physiology and Pediatrics, and Cell Biology

Award Number: W81 XWH-11-1-0498

TITLE: Engineered Herpes Simplex Viruses for the Treatment of Malignant Peripheral Nerve Sheath Tumors

PRINCIPAL INVESTIGATOR: James M. Markert, MD

CONTRACTING ORGANIZATION: University of Alabama at Birmingham
FOT 1060
1720 2nd Avenue South
Birmingham, AL 35294-3410

REPORT DATE: Original 9/28/12
Resubmitted 3/11/13

TYPE OF REPORT: Annual

PREPARED FOR: U.S. Army Medical Research and Materiel Command
Fort Detrick, Maryland 21702-5012

DISTRIBUTION STATEMENT: Approved for public release;
Distribution Unlimited

The views, opinions and/or findings contained in this report are those of the author(s) and should not be construed as an official Department of the Army position, policy or decision unless so designated by other documentation.

REPORT DOCUMENTATION PAGE

Form Approved
OMB No. 0704-0188

Public reporting burden for this collection of information is estimated to average 1 hour per response, including the time for reviewing instructions, searching existing data sources, gathering and maintaining the data needed, and completing and reviewing this collection of information. Send comments regarding this burden estimate or any other aspect of this collection of information, including suggestions for reducing this burden to Department of Defense, Washington Headquarters Services, Directorate for Information Operations and Reports (0704-0188), 1215 Jefferson Davis Highway, Suite 1204, Arlington, VA 22202-4302. Respondents should be aware that notwithstanding any other provision of law, no person shall be subject to any penalty for failing to comply with a collection of information if it does not display a currently valid OMB control number. PLEASE DO NOT RETURN YOUR FORM TO THE ABOVE ADDRESS.

1. REPORT DATE 28-09-2012/Resub 11-03-2013	2. REPORT TYPE Annual	3. DATES COVERED 01SEP2011 thru 31AUG12
--	---------------------------------	---

4. TITLE AND SUBTITLE Engineered Herpes Simplex Viruses for the Treatment of Malignant Peripheral Nerve Sheath Tumors	5a. CONTRACT NUMBER W81XWH-11-1-0498
	5b. GRANT NUMBER
	5c. PROGRAM ELEMENT NUMBER

6. AUTHOR(S) James M. Markert, MD; G. Yancey Gillespie, MD; Kevin Cassady, MD; Steve L. Carroll, MD; Jacqueline N. Parker, PhD E-Mail: JMarkert@uabmc.edu	5d. PROJECT NUMBER
	5e. TASK NUMBER
	5f. WORK UNIT NUMBER

7. PERFORMING ORGANIZATION NAME(S) AND ADDRESS(ES) University of Alabama at Birmingham FOT 1060 1720 2 nd Avenue South Birmingham, AL 35294-3410	8. PERFORMING ORGANIZATION REPORT NUMBER
--	---

9. SPONSORING / MONITORING AGENCY NAME(S) AND ADDRESS(ES) U.S. Army Medical Research and Materiel Command Fort Detrick, Maryland 21702-5012	10. SPONSOR/MONITOR'S ACRONYM(S)
--	---

	11. SPONSOR/MONITOR'S REPORT NUMBER(S)
--	---

12. DISTRIBUTION / AVAILABILITY STATEMENT
Approved for Public Release; Distribution Unlimited

13. SUPPLEMENTARY NOTES

14. ABSTRACT

The first year of our funding has been very productive and has led to new information regarding the susceptibility of Malignant peripheral nerve sheath tumors (MPNST), which occur in patients with neurofibromatosis type-1, to oncolytic HSV (oHSVs). We have demonstrated that many of the MPNSTs that we have tested are indeed sensitive to our oHSV, but that some are resistant (both murine and human). It is apparent from our data that ability to replicate in these tumor cells is related to additional factors besides simply status of HSV-1 receptors nectin-1 and nectin-2. We are examining further the mechanisms that may be responsible for sensitivity and resistance in these lines which we hope to exploit in the future. We are currently testing 2 new hypotheses developed based upon the first year of data and are pursuing a surprising observation regarding the C134 and the M032 viruses and their ability to maintain late viral protein synthesis in the infected MPNST cells. This is an unanticipated finding that could only have been discovered empirically. These advances would not have been possible without these DOD funded studies.

15. SUBJECT TERMS
Oncolytic Herpes Viruses; Malignant Peripheral Nerve Sheath Tumors; Mouse; Human

16. SECURITY CLASSIFICATION OF:			17. LIMITATION OF ABSTRACT	18. NUMBER OF PAGES	19a. NAME OF RESPONSIBLE PERSON
a. REPORT	b. ABSTRACT	c. THIS PAGE			USAMRMC
U	U	U	UU	32	19b. TELEPHONE NUMBER (Include area code)

Table of Contents

	Page
Introduction.....	4
Body.....	4
Key Research Accomplishments.....	7-46

The first year of our funding has been very productive and has led to new information regarding the susceptibility of MPNST to oHSVs. We are currently testing 2 new hypotheses developed based upon the first year of data and are pursuing a surprising observation regarding the C134 and the M032 viruses and their ability to maintain late viral protein synthesis in the infected MPNST cells. This is an unanticipated finding that could only have been discovered empirically. These advances would not have been possible without these DOD funded studies.

Our goals for this grant are summarized below and include:

- 1) To determine the molecular basis for the sporadic susceptibility or resistance to infection of MPNST cells to genetically engineered, oncolytic herpes simplex viruses (oHSVs) in our repository;
- 2) To examine inherent mechanisms expressed in MPNSTs that inhibit the replication of oHSVs and abrogate the ability of these viruses to kill infected cells and spread to neighboring tumor cells; and
- 3) To test the relative ability of our oHSVs to produce an anti-tumor effect alone and if this anti-tumor effect can be significantly enhanced by a low dose of radiation administered to the tumor.

Thus far our work during the initial year of funding has focused upon the first 2 aims listed. Our progress is summarized below and has been organized within the 4 major milestones listed in our Statement of work and addressed with regard to each of the Tasks and SubTasks.

Milestone 1: We will identify at least 2 oHSV-sensitive and 2 oHSV-resistant MPNST cell lines by completing the *in vitro* characterization of both human and mouse MPNST cell lines with respect to oHSV infection and killing. We have preliminary analysis of 2 human and two murine MPNST lines. They range from sensitive to resistant to oHSV infection and killing. This milestone will provide the prototypic MPNST cell lines that will be studied more extensively in all three aims.

Milestone 2: We will characterize each of the 9 human MPNST cell line and at least 18 of the 100+ mouse MPNST cell lines with regard to expression of HSV entry molecules expressed on the cell surface. This milestone will enable us to determine whether prevention of entry by down-regulation of appropriate receptors is the reason for oHSV resistance and, if so, whether we should define alternative receptors to which new oHSVs could be targeted.

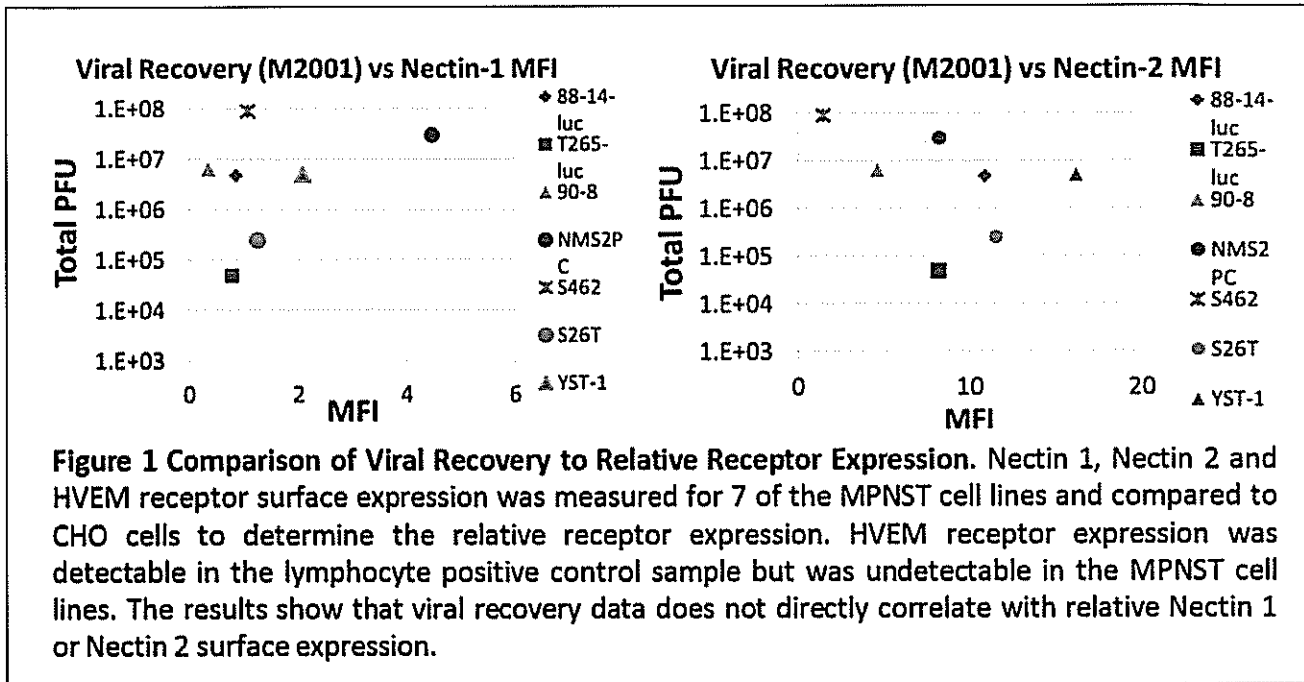
Milestone 3: We will characterize the replication of oHSVs in each of the oHSV-sensitive and oHSV resistant MPNST cells identified in Milestone 1 by FACS and by titring virus at regular post-infection intervals. Within this context, we will establish the extent to which replication is enhanced in infected MPNST cells by oHSVs engineered to express proteins that directly promote virus replication. This milestone will allow us to select either the HCMV IRS-1 or the constitutively activated MEK gene as the most appropriate insert to overcome replication resistance.

Milestone 4: We will determine which of the oHSVs identified as “effective” in the first two aims of this proposal actually produce the expected anti-MPNST effect in oHSV-sensitive and oHSV-resistant tumors of human or mouse origin placed orthotopically in the appropriate strain of mouse (see below). Efficacy alone or in combination with enhancing adjunctive therapies will be defined. This milestone will serve to validate (or refute) the process for selection of effective oHSVs that could be advanced to clinical trials in patients with MPNSTs and identify which modality is most likely to have an impact on the natural history of this disease.

Task 1: Characterize the *in vitro* sensitivity of a panel of human and mouse MPNST cell lines to a panel of available oncolytic HSVs.

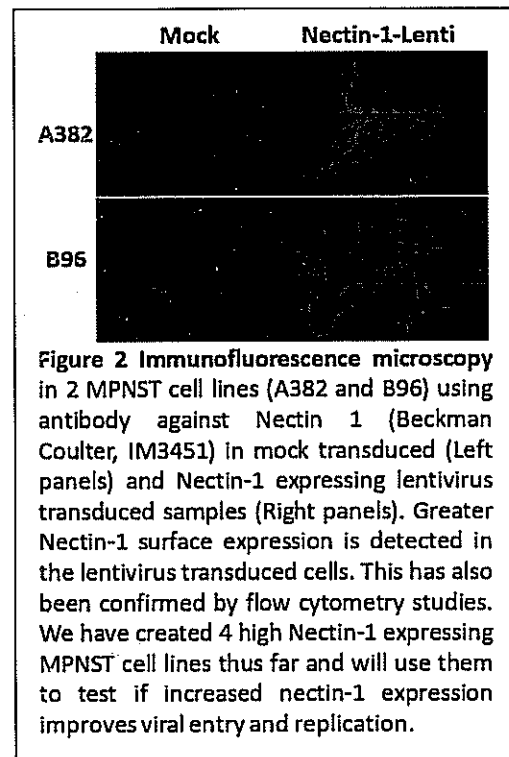
SubTask 1a. Using methods that we have described in Preliminary Findings in the Proposal, we will complete the screening of all 9 human MPNST cell lines and at least 18 of the 100+ mouse MPNST cell lines using FACS for detection of expression and modulation of HSV entry molecules (nectin-1, nectin-2) and alternative entry molecules (HVEM, IL13R α 2, uPAR, Her2/neu) recognized by fluorochrome-labeled antibodies.

Status: During the first year of funding, we examined whether the expression levels of the three principal HSV entry receptors (CD111, CD112, HVEM) correlated with viral recovery in the human MPNST tumor cell lines. Receptor expression levels were measured using antibodies against these major HSV entry molecules nectin-1 (CD111), nectin2 (CD112) and HVEM by immunofluorescence microscopy and by flow cytometry. The MPNST cell lines demonstrated greater nectin-2 surface expression than nectin-1 surface protein. While a peripheral blood leukocyte positive control sample stained with the antibody against HVEM, none of the human MPNST tested lines expressed HVEM based upon flow cytometry and immunofluorescence. The relative surface expression of Nectin 1 and Nectin 2 was then compared with viral recovery data as represented in **Figure 1**. The results show that surface expression of nectin 1 and 2



did not correlate directly with viral replication in these cell lines.

This suggests that entry molecule surface expression is not a rate-limiting step in viral infection in the MPNST cell lines. To further test this hypothesis, however, we created a lentivirus that expresses the human nectin-1 gene and have transduced both murine and human cell lines to test this hypothesis. The Lentivirus was created by PCR amplifying the human Nectin-1 coding domain (including the signal sequence) from a validated cDNA clone (Open Biosystems) and inserting it into a lentiviral targeting vector, pCK2015. This targeting vector contains the Nectin-1 coding domain followed by an internal ribosomal entry sequence and the puromycin resistance gene. We created the Nectin-1 Lentivirus by co-transforming pCK2015 with plasmids encoding the VSV envelope and accessory vector in 293-T cells and collecting the supernatants 48h post-transfection. The MPNST cells were incubated with these supernatants and as demonstrated in **Figure 2**, the lentiviral-transduced cell lines express abundant immunoreactive nectin-1 on their surface. Studies are currently ongoing to determine: 1) if increasing nectin-1 surface expression improves viral entry, 2) if increasing nectin-1 surface expression improves oHSV replication in MPNST cells, and 3) if oHSV entry and gene expression downmodulates lentiviral nectin-1 surface



expression similar to that shown for native nectin-1 during infection.

SubTask 1b Using methods that we have described in Preliminary Findings in the Proposal, we will complete the screening of all 9 human MPNST cell lines and at least 18 of the 100+ mouse MPNST cell lines using oHSVs that express eGFP for detection of infection and cell death using FACS.

Status: We are starting these studies and have examined some of the cell lines as shown later in the progress report in Subtask 1

SubTask 1c. Screen each of the 9 human and 18 mouse MPNST cell lines for sensitivity to infection and killing by clinical candidate viruses G207, NV1020, M032 and C134 using classical virology techniques to measure cytopathic effect on monolayers, single step and multi-step replication assays .

Status: Over the past year, we focused on the in vitro characterization of the MPNST cell lines. We have tested 7 recombinant HSVs (4 of which are available as clinical grade virus), in 7 of the 9 human MPNST cell lines and 16 of the 18 murine MPNST cell lines proposed. The results of these studies are based upon increasing susceptibility / support for replication in the MPNST cell line (Figures 1 and 2). In order to finalize this milestone, we will test 2 additional human and 2 additional murine MPNST cell lines that Dr. Carroll's laboratory will supply to us.

Thus far we have detected a 100,000 fold (5 log) difference in viral replication between the least and most susceptible cell lines with our recombinant viruses (**Figure 3**). Of the murine MPNST cell lines, the A382 cell line is the least hospitable to viral replication. The oHSVs generate only $\sim 10^3$ (plaque forming units) pfu in single step replication assays in this cell line. Following the A382 cell line, the B91 cells are the second most restrictive cell line for three of the GLP quality oHSVs (G207, M032, and C134) whereas the A387 cell line is more restrictive to R7020 replication. With regard to murine MPNST cell lines that support viral replication, the 231 Trig and the A18 cell lines produced the highest overall viral recovery (10^8 PFU/ml).

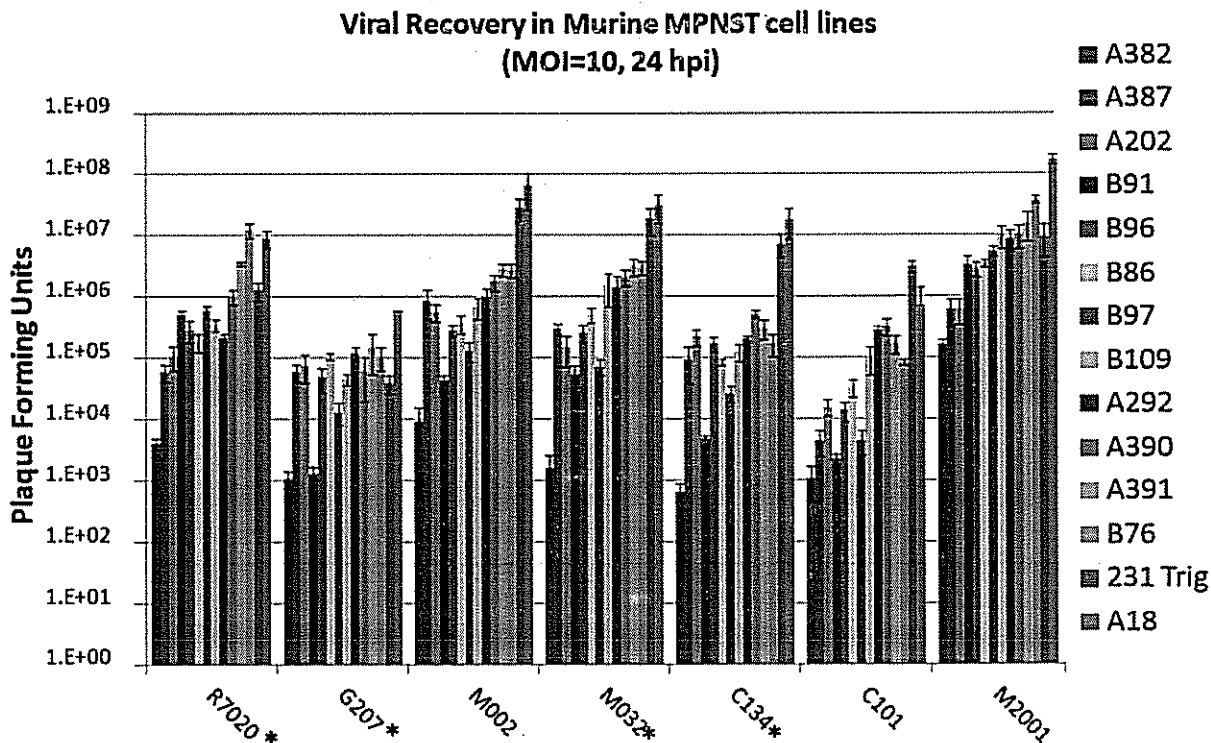


Figure 3: Summary of viral recovery studies in murine MPNST cell lines in order of least to greatest viral recovery. * denotes oHSVs with clinical grade virus available

For the Human MPNST cell lines, the choices for cell lines are more limited (7 cell lines tested). Most of the cell lines have been transduced to stably express luciferase (Luc). The most restrictive human MPNST cell lines to date are the T265T-LUC and S26T. These cell lines limited viral replication such that only 10^1 - 10^5 PFU of virus is produced following single step replication assays. The most susceptible human cell line was the S462 cell line which generated $\sim 10^7$ - 10^8 pfu for all of the viruses tested. Identification of the second most susceptible cell line was more complex. Depending upon the virus used, certain cell lines were more permissive than others in these assays (**Figure 4**). For two of the clinical grade oHSVs (R7020 and C134), the YST-1 cell line produced the greatest amount of virus (7.7×10^5 and 9.3×10^6 pfu). For the G207 and M032 oHSVs, NMS2PC was the next most susceptible cell line producing 4.33×10^5 pfu and 2.07×10^6 pfu, respectively.

We have also provided a summary of the MPNST susceptibility to oHSV anti-tumor activity based upon two independent assays (alamar blue and virus induced cytopathic effect [CPE]) These studies are ongoing and show that late viral protein synthesis and regulation of protein synthesis initiation limits some of the oHSVs to replicate in the tumor cells. Viruses that are capable of enhanced late viral protein synthesis, as demonstrated by gD protein production in infected cells on the whole replicate better than those that undergo translational arrest, which is a common antiviral response in infected cells. It has been well described (Mohr, 1995, Cassady 1998, Cassady 2005, Shah 2006) that viruses capable of evading this host translation shutoff response synthesize greater amounts of late viral proteins and replicate better than $\Delta\gamma_134.5$ recombinant viruses incapable of blocking this anti-viral response. It is therefore not surprising that the R7020 and C134 recombinant, both of which contain PKR evasion genes (R7020 a single copy of the $\gamma_134.5$ gene, and C134 the HCMV IRS1 gene), synthesized late viral proteins and replicated better than two of the $\Delta\gamma_134.5$ viruses tested (C101 and G207) in MPNST cell lines. Immunostaining studies show that the R7020 and C134 recombinants evaded this host antiviral response whereas the two $\Delta\gamma_134.5$ recombinants (C101 and G207) without PKR-evasion genes were incapable of blocking translational arrest as indicated by phosphorylation of eIF2 α .

Composites of the viral recovery results for all of the cell lines are provided in Figures 3 and 4. These allow comparison between the cell lines. In addition to this broad overview of all of the results, we

have also included the results from viral replication (multistep replication studies with CPE images, single step replication results with CPE images, cytotoxicity studies, and western blot data for the cell lines) for each of the cell lines in Figures 5-41.

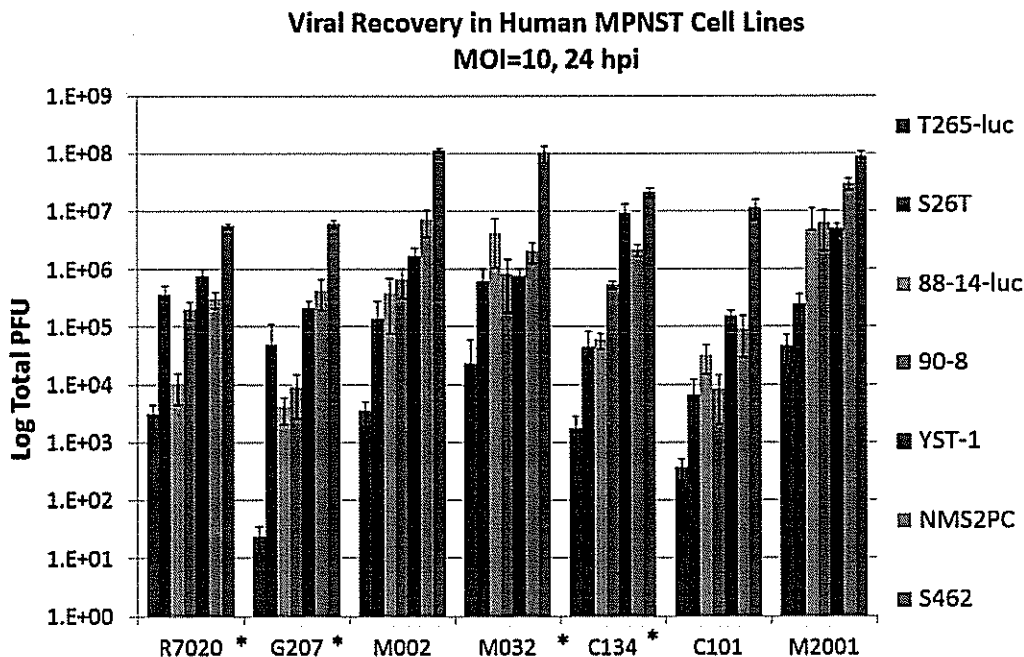


Figure 4: Summary of viral recovery studies in human MPNST cell lines in order of least to greatest viral recovery. * denotes oHSVs with clinical grade virus available

Summary and Analysis (A382)

The A382 line is one of the more restrictive cell lines to HSV replication. Even wild-type HSV encoding the GFP gene replicates poorly in this MPNST generating only 10^4 PFU on D1-3 post infection. The clinical grade viruses (C134, M032, G207, R7020) produce 10-100x less virus than wild-type in single step replication assays. (Figure 5A) At high MOI the cells exhibit early CPE (Figure 5B, D). C134 exhibits no replication advantage over its $\Delta\gamma_134.5$ parent virus (C101) in this cell line. The multistep replication studies are incomplete but based upon the single step replication studies, the cell line is highly restrictive to the clinical grade viruses (Figure 5D). As discussed below, this cell line is restrictive to HSV replication and we intend to further investigate this cell line as one of the two restrictive murine cell lines in future studies (as discussed in sub-task 1d)

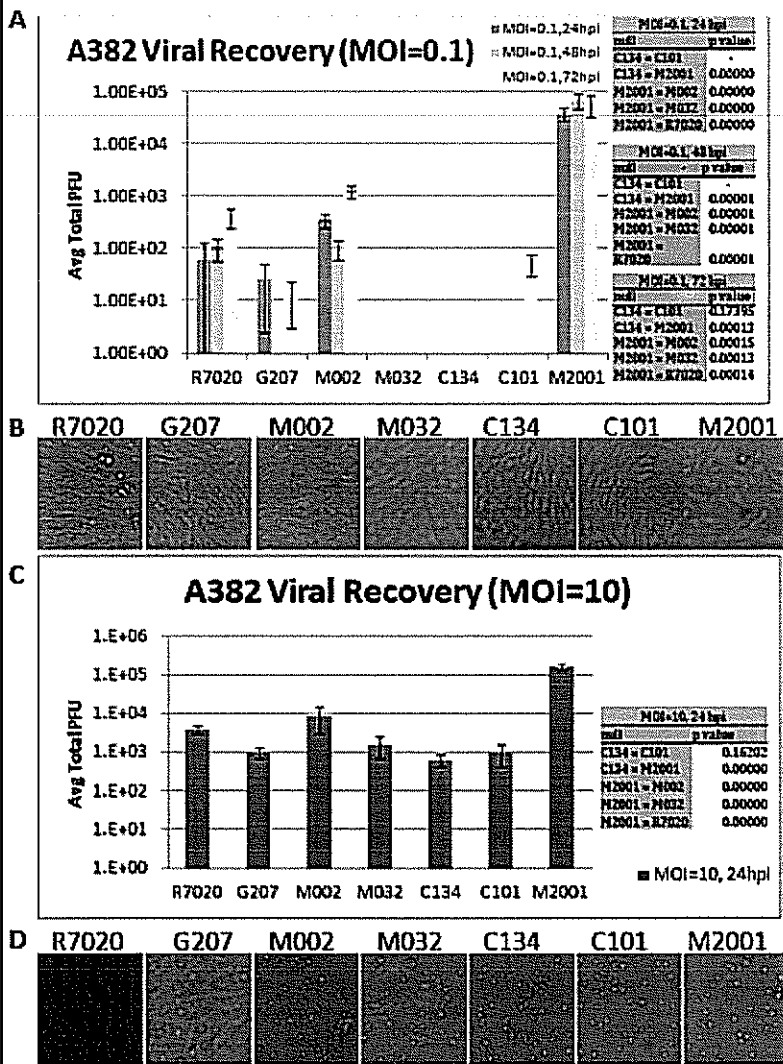


Figure 5: Composite of A382 murine MPNST cell line *in vitro* studies. A. Multistep Replication Study using a low multiplicity of infection (MOI: 0.1 plaque forming unit/cell) (PFU/cell). Viral recovery data shown at 24/ 48/ 72hpi with standard deviation (SD). **B.** Photomicrographs demonstrate cytopathic effect (CPE) in multistep replication study (24hpi) for all oHSVs tested on A382 cells (100X mag). **C.** Single-step replication study using a high MOI (10 PFU/cell). viral recovery data (24hpi) shown with SD. **D.** Photomicrographs of cytopathic effect at high MOI for all oHSVs tested on A382 cells (density of 1.5×10^5 cells/well; 100X magnification).

Summary and Analysis (A382 cont'd.)

Consistent with the CPE images shown in the prior figure, there is evidence of cell killing by Alamar blue assay. There is no difference in A382 cell killing between R7020, C134, M002 or M032). Alamar blue assay, however, shows that M2001 (wild-type HSV expressing EGFP) is more effective than $\Delta\gamma_134.5$ viruses at killing the A382 cell line(Figure 6A,B).

Western blot images (Figure 6C) show that viruses that in other cell lines are capable of PKR evasion (R7020, M2001, C134) at 12hpi synthesize greater gD at 24hpi. In addition the M002 virus also accumulates gD. M032 is incomplete based upon less protein loading as shown by actin staining. While eIF2 α staining is interpretable in the 12h samples, by 24hpi there is no staining detected in any of the virus infected samples (total or phosphorylated). At this time, we do not know if this is a technical limitation with sample preparation or if this is a due to loss of eIF2 α in infected cells. The presence of eIF2 α in the mock sample suggests that this is due to loss of the protein in infected cells.

Conclusion: This is one of the more resistant mouse cell lines tested and we intend to use this as one of the two resistant

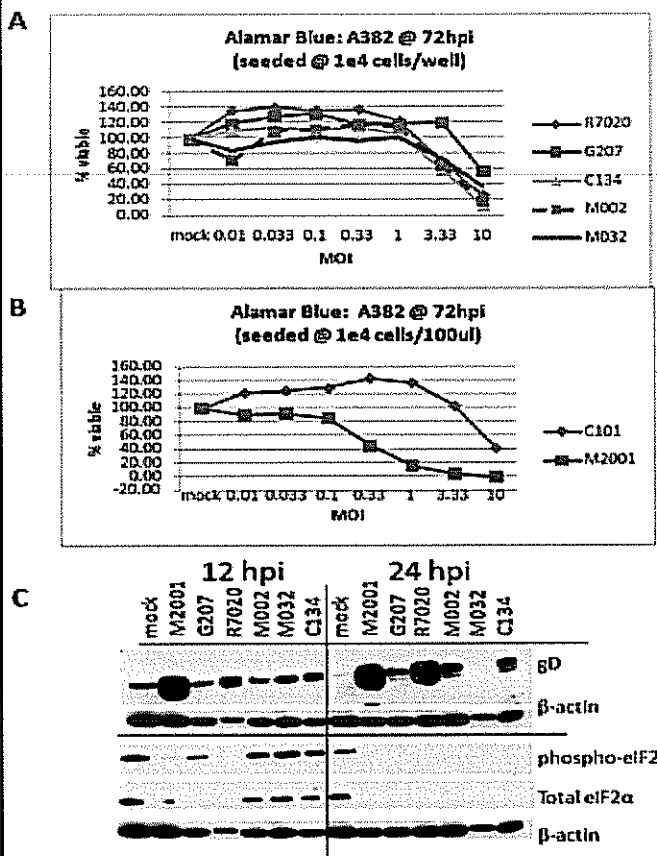


Figure 6: Composite of A382 murine MPNST cell line *in vitro* studies. A. Alamar Blue cell viability assay comparing clinical grade oHSVs (and the non-clinical grade oHSV M002) antitumor effect at 72hpi. B. Alamar Blue cell viability assay comparing nonclinical grade oHSVs C101 ($\Delta\gamma_1 34.5$) vs. M2001 (wt) at 72hpi. C. Immunostaining studies demonstrating synthesis of late gene product (glycoprotein D), phosphorylated and total eIF-2 α along with β -actin protein loading controls at 12hpi (left panel) and 24hpi (right panel).

mouse cell lines for future studies. Of particular interest is the change in the protein synthesis phenotype and the eIF2 α changes in infected cells.

Summary and Analysis (A387)

A387 does not support efficient HSV replication. In contrast to the previous cell line however, M002 replicates as well as M2001 and exhibits a similar replication kinetic as M2001 (Figure 7A,C). The cells round lose contractility and form clumped spheroid forms during HSV infection as shown in the early CPE images (Figure 7B). Of note the cells also form these rounded structures during growth in cell culture making it difficult to establish a uniform and reproducible infection results in vitro and test-retest reliability. This may limit the interpretation of subsequent studies such as western blotting and alamar blue

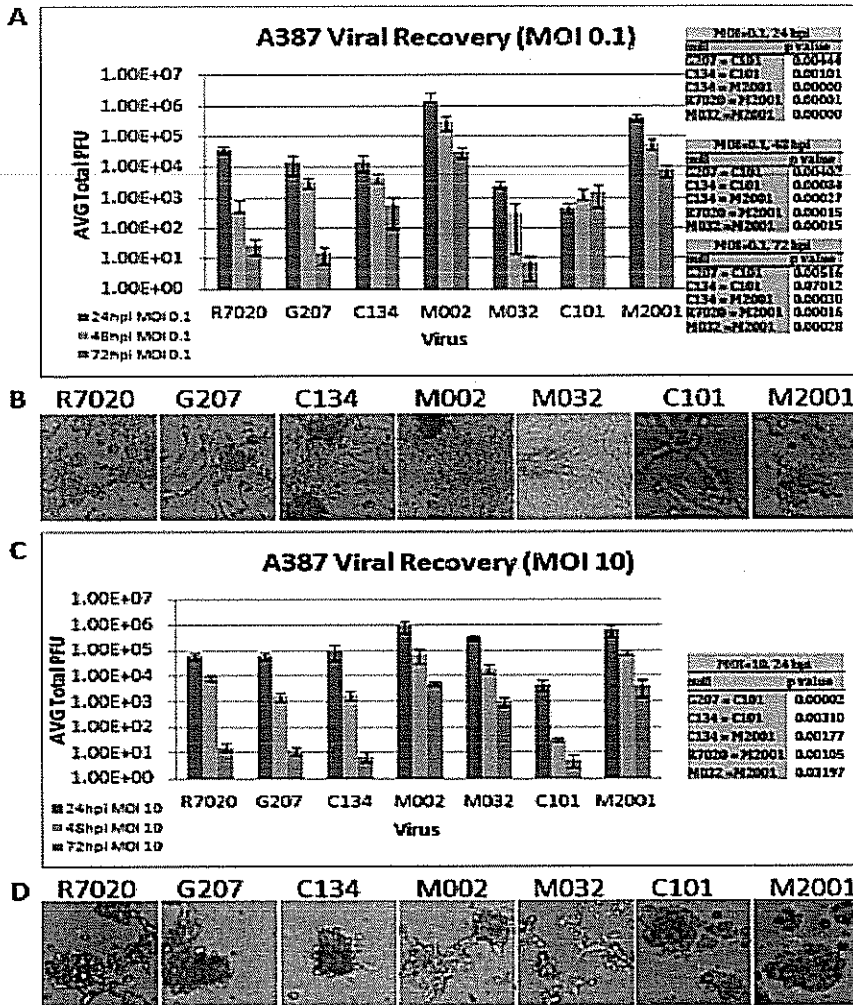


Figure 7: Composite of A387 murine MPNST cell line *in vitro* studies. A. Multistep Replication Study using a low multiplicity of infection (MOI: 0.1 plaque forming unit/cell) (PFU/cell). Viral recovery data shown at 24/ 48/ 72hpi with standard deviation (SD). **B.** Photomicrographs demonstrate cytopathic effect (CPE) in multistep replication study (24hpi) for all oHSVs tested on A387 cells (100X mag). **C.** Single-step replication study using a high MOI (10 PFU/cell). viral recovery data (24hpi) shown with SD. **D.** Photomicrographs of cytopathic effect at high MOI for all oHSVs tested on A387 cells (density of 1.5e5 cells/well:100X magnification).

Summary and Analysis (A387 cont'd.)

In alamar blue studies the M002 and M032 (murine and human IL-12 expressing viruses) produced paradoxical results (Figure 8A,B). Whereas M002 (along with R7020) produced the greatest cell killing in alamar blue cell killing assays, M032 performed the worst.

Immunostaining studies show that the $\gamma_{134.5}$ containing viruses (R7020 and M2001) are capable of producing appreciable gD after high MOI infection (Figure 8C). It is also interesting that in the M2001 and R7020 infected samples there is loss of actin staining over the initial 24hpi. C134 infected cells also exhibit loss of actin staining.

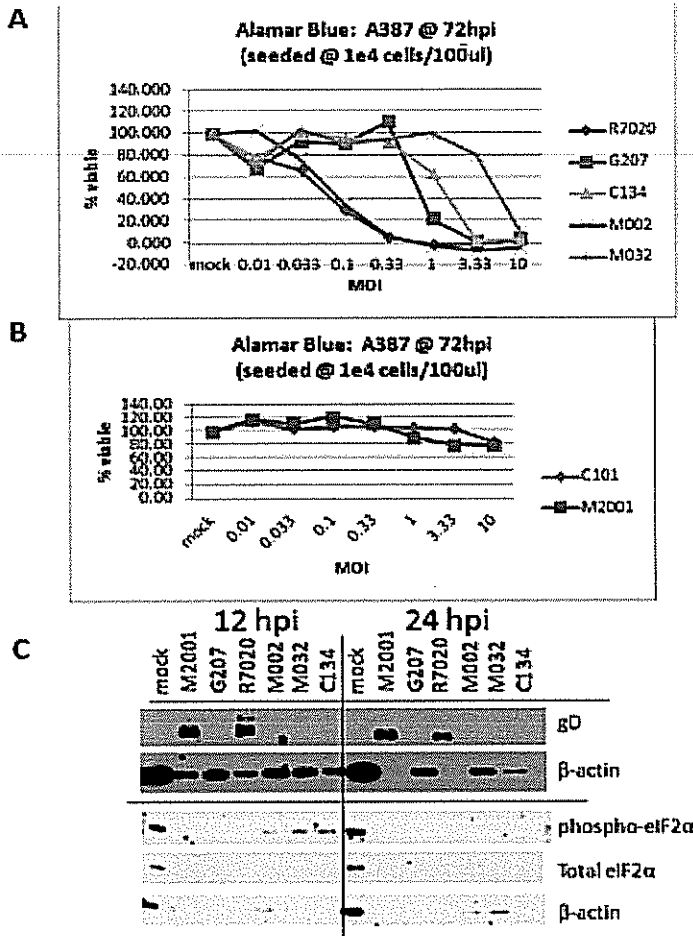


Figure 8: Composite of A387 murine MPNST cell line *in vitro* studies. **A.** Alamar Blue cell viability assay comparing clinical grade oHSVs (and the non-clinical grade oHSV M002) antitumor effect at 72hpi. **B.** Alamar Blue cell viability assay comparing nondinical grade oHSVs C101 ($\Delta\gamma_{134.5}$) vs. M2001 (wt) at 72hpi. **C.** Immunostaining studies demonstrating synthesis of late gene product (glycoprotein D), phosphorylated and total eIF-2 α along with β -actin protein loading controls at 12hpi (left panel) and 24hpi (right panel).

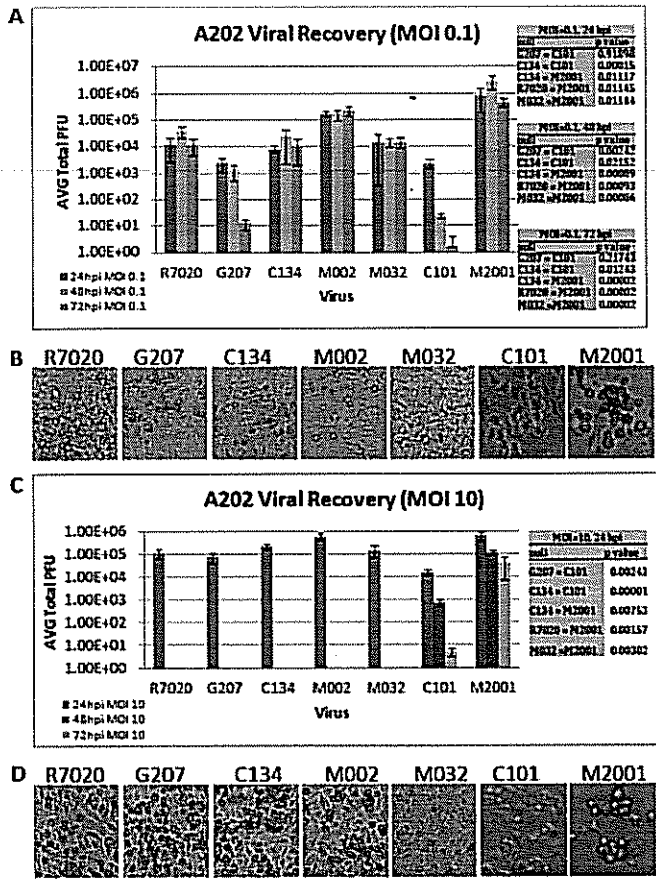


Figure 9: Composite of A202 murine MPNST cell line *in vitro* studies. A. Multistep Replication Study using a low multiplicity of infection (MOI: 0.1 plaque forming unit/cell) (PFU/cell). Viral recovery data shown at 24/ 48/ 72hpi with standard deviation (SD). **B.** Photomicrographs demonstrate cytopathic effect (CPE) in multistep replication study (24hpi) for all oHSVs tested on A202 cells (100X mag). **C.** Single-step replication study using a high MOI (10 PFU/cell). viral recovery data (24hpi) shown with SD. **D.** Photomicrographs of cytopathic effect at high MOI for all oHSVs tested on A202 cells (density of 1.5e5 cells/well; 100X magnification).

Summary and Analysis (A202)

Most of the viruses tested were capable of sustained replication over the initial 72h of infection. The two viruses incapable of sustained replication (C101 and G207) were the prototypical $\Delta\gamma_134.5$ viruses. M2001 replicated the best followed by M002. The M032, C134 and R7020 viruses exhibited similar replication patterns (Figure 9A,C)

CPE images reveal that M2001 produced the greatest early CPE. While C134, M002, G207, and R7020 also induced cytopathic changes. In contrast, M032 and C101 infection did not elicit significant cytopathic effect (Figure 9B,D).

Conclusion: the A202 cell line is considered resistant to HSV replication and cytopathic effect. We intend to further study this line as one of the 2 resistant murine cell lines. We have chosen it because there is differential replication of the $\Delta\gamma_134.5$ viruses in this cell line.

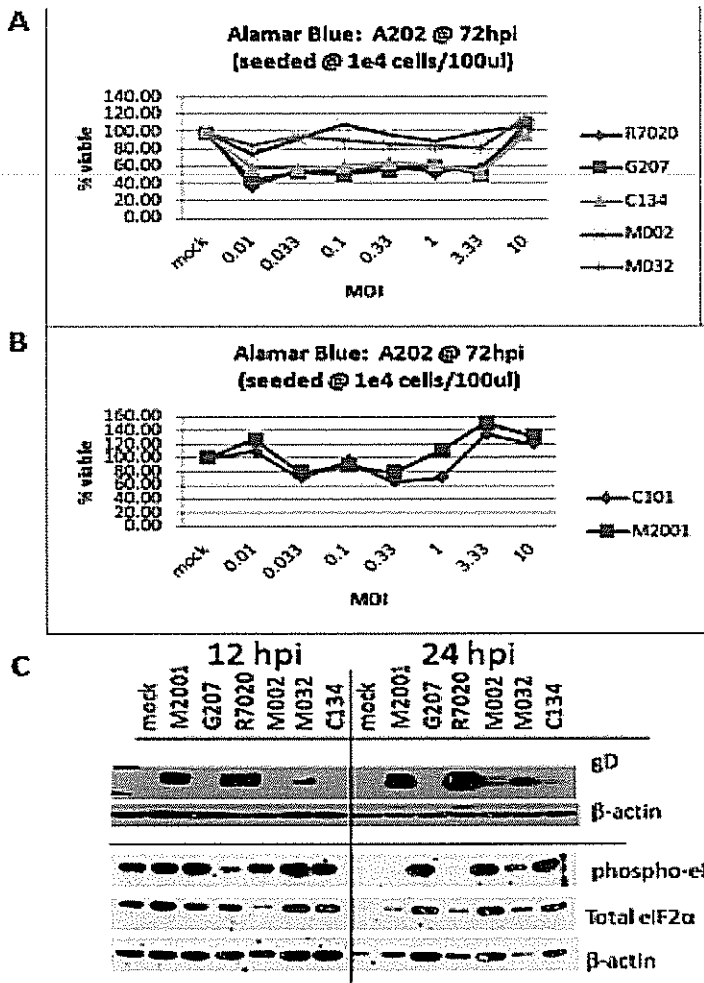


Figure 10: Composite of A202 murine MPNST cell line *in vitro* studies. **A.** Alamar Blue cell viability assay comparing clinical grade oHSVs (and the non-clinical grade oHSV M002) antitumor effect at 72hpi. **B.** Alamar Blue cell viability assay comparing nondclinical grade oHSVs C101 ($\Delta\gamma 1$ 34.5) vs. M2001 (wt) at 72hpi. **C.** Immunostaining studies demonstrating synthesis of late gene product (glycoprotein D), phosphorylated and total eIF-2 α along with β -actin protein loading controls at 12hpi (left panel) and 24hpi (right panel).

Summary and Analysis (A202 cont'd.)

Alamar Blue studies are difficult to interpret. No killing is seen by M002 and M032 (Figure 10A,B). The remaining viruses shows some killing at low to moderate MOI, but none at high MOI. Our working hypothesis is that the this MPNST cell line has aberrant redox properties that limit the alamar blue assay and render it uninterpretable.

Immunostaining studies (Figure 10C) show that the $\gamma 1$ 34.5 containing viruses (R7020 and M2001) accumulate the greatest gD. In the revised image, the actin staining shows similar loading between samples, The p-eIF2 α studies show that C134 is incapable of PKR evasion in this cell line based upon limited gD production and the presence of p-eIF2 α .

As discussed previously (Figure 9), we intend to further study the A202 cell line as one of the two resistant murine MPNST cell lines. Of particular interest is its metabolic profile and whether this may alter interpretation of the alamar blue cytotoxicity assay. The cell line is also interests us because of the C134 virus phenotype in this cell line. Preliminary results show that C134 acts similar to its parent virus (C101) in certain assays (p-eIF2 α and gD immunostaining studies) but is capable

of sustained replication in the multistep replication studies unlike C101.

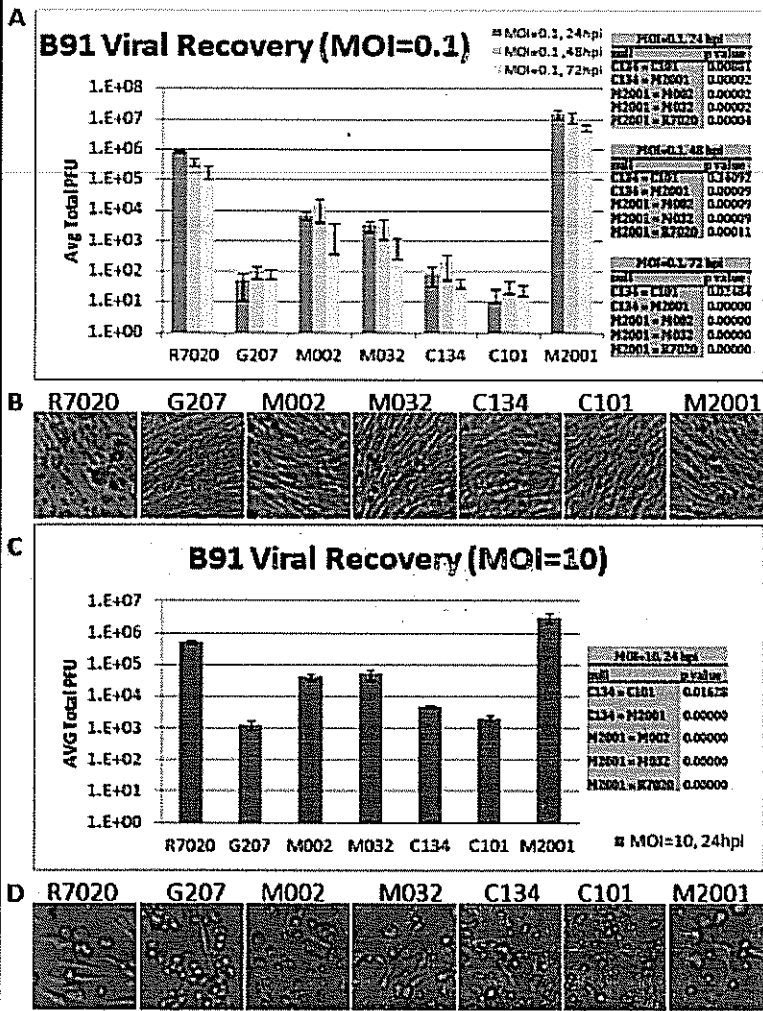


Figure 11: Composite of B91 murine MPNST cell line *in vitro* studies. A. Multistep Replication Study using a low multiplicity of infection (MOI: 0.1 plaque forming unit/cell) (PFU/cell). Viral recovery data shown at 24/ 48/ 72hpi with standard deviation (SD). **B.** Photomicrographs demonstrate cytopathic effect (CPE) in multistep replication study (24hpi) for all oHSVs tested on B91 cells (100X mag). **C.** Single-step replication study using a high MOI (10 PFU/cell), viral recovery data (24hpi) shown with SD. **D.** Photomicrographs of cytopathic effect at high MOI for all oHSVs tested on B91 cells (density of 1.5e5 cells/well;100X magnification).

Summary and Analysis (B91)

The $\gamma_134.5$ containing viruses (R7020 and M2001) replicate best in B91 cells (Figure 11A,B). Of the $\Delta\gamma_134.5$ viruses (M032 and M002) replicate better than G207, C101 or C134. The chimeric HSV replicates only marginally better than its $\Delta\gamma_134.5$ parent virus C101. This cell line is considered resistant to HSV replication and to early viral cytopathic effect (Figure 11C) based upon the multistep replication studies. In high MOI infection there is evidence of early CPE indicating that it is possible to overcome this resistance.

Conclusion: This is another resistant murine cell line (similar to A202) where the clinical grade viruses exhibit differential replication profiles and may be of interest in future studies.

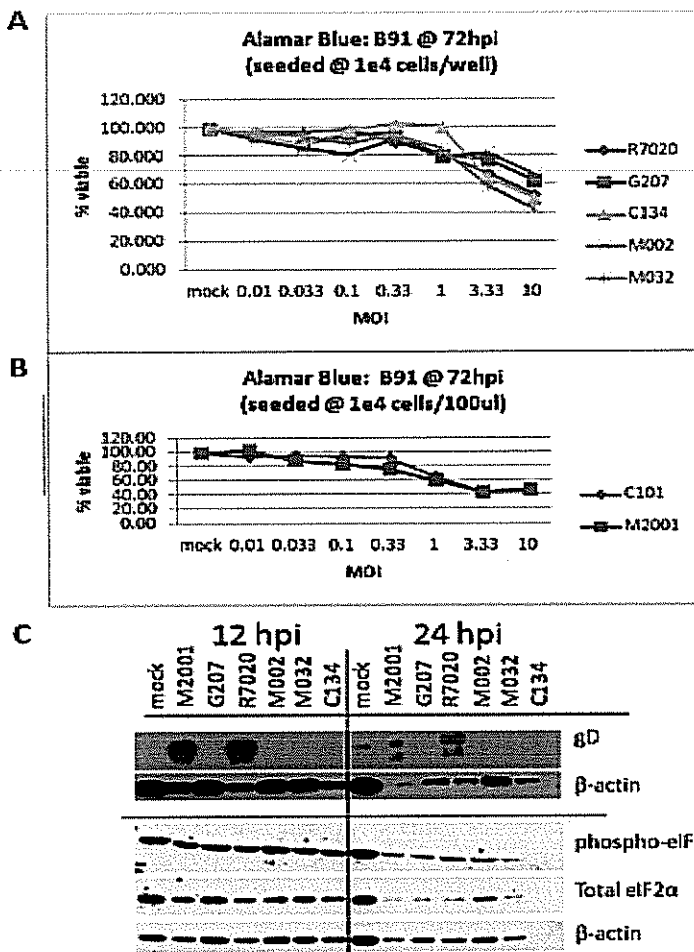


Figure 12: Composite of B91 murine MPNST cell line *in vitro* studies. **A.** Alamar Blue cell viability assay comparing clinical grade oHSVs (and the non-clinical grade oHSV M002) antitumor effect at 72hpi. **B.** Alamar Blue cell viability assay comparing nonclinical grade oHSVs C101 ($\Delta\gamma_1 34.5$) vs. M2001 (wt) at 72hpi. **C.** Immunostaining studies demonstrating synthesis of late gene product (glycoprotein D), phosphorylated and total eIF-2 α along with β -actin protein loading controls at 12hpi (left panel) and 24hpi (right panel).

Summary and Analysis (B91 cont'd.)

Despite significant differences in viral replication and CPE, Alamar blue measurement of cell viability showed no difference between the recombinants tested (Figure 12A). Even more surprising there was no difference detected between wild-type and $\Delta\gamma_1 34.5$ virus (Figure 12B).

Western blots (Figure 12C) show gD accumulation only in the $\gamma_1 34.5$ containing viruses (M2001 and R7020). Also surprising was presence of p-eIF2 α in infected and uninfected B91 cells (12hpi). This suggests that the $\gamma_1 34.5$ containing viruses were still capable of late viral protein synthesis. The 24hpi images are difficult to interpret and show differential loss of actin staining suggestive of loss of viable cells in some samples. This is especially evident in the M2001 samples where there is loss of gD staining and actin suggestive of overall cell loss secondary to cytopathic effect. The C134 virus acts similar to the C101 parent virus in this cell line with limited gD accumulation and lower viral replication.

Summary and Analysis (B96)

The B96 murine MPNST line, provides an intermediate replication environment for HSV (in single step replication studies) (Figure 13A). The $\gamma_134.5$ containing viruses (M2001, R7020) replicate the best in these cells with M2001 replicating the best. The M002, M032, and C134 recombinants replicate similarly in this cell line with G207 and C101 replicating the poorest.

Early cytopathic effects are seen in all cell lines at high MOI (Figure 13B).

Immunostaining studies (Figure 13C) show inconsistent gD, actin staining at 12-24h likely related to cell loss and CPE (as shown above in figure 13b).

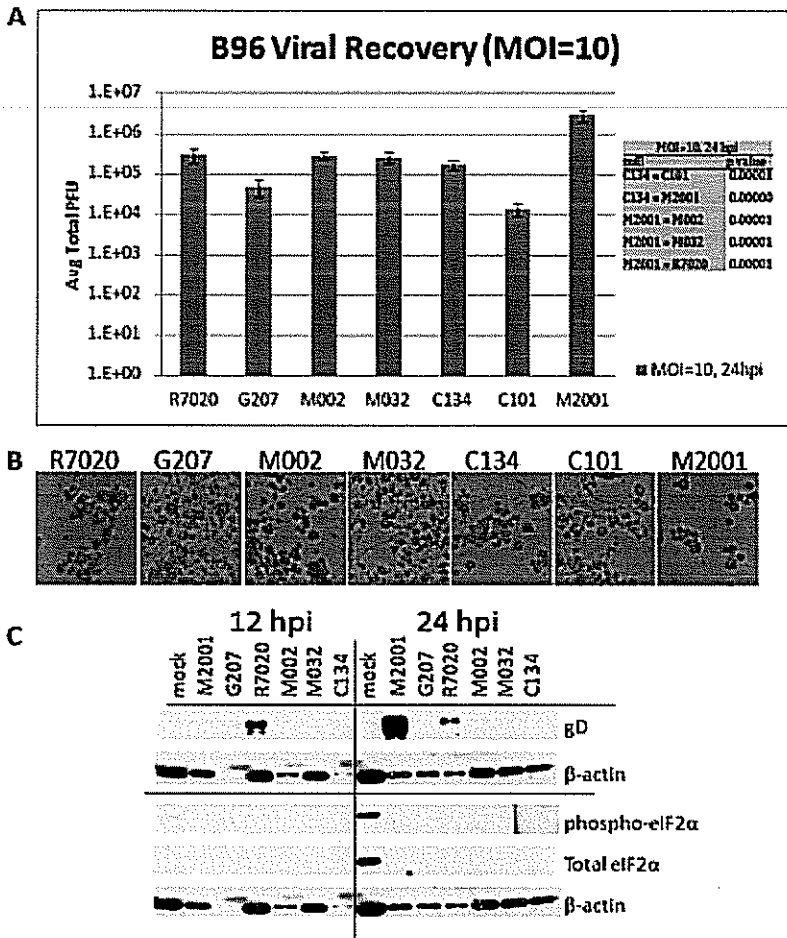
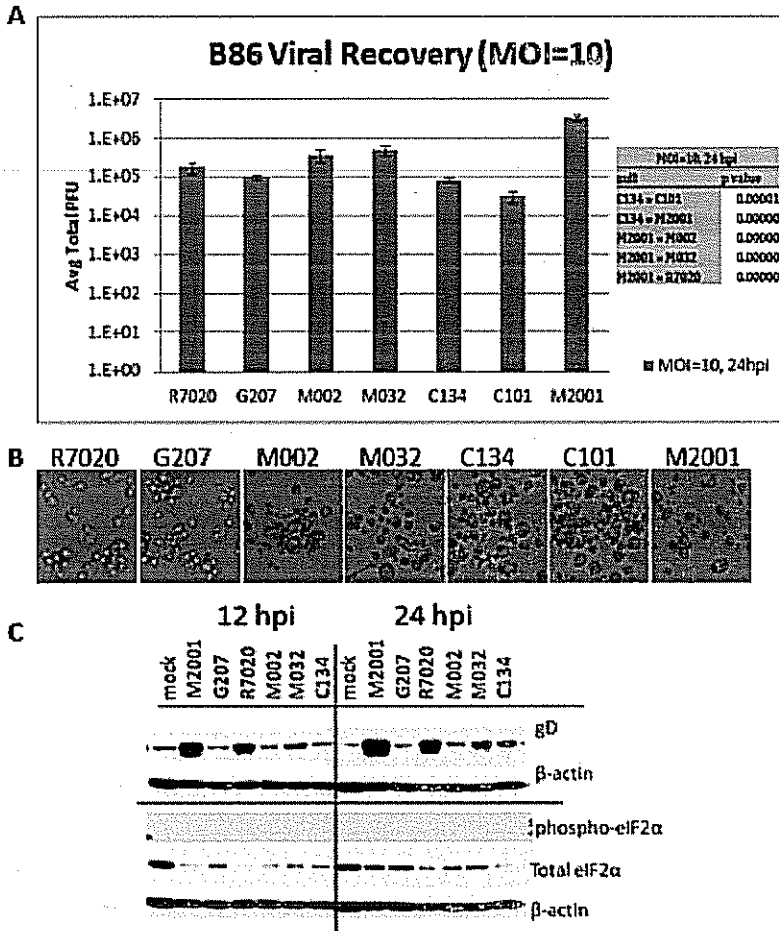


Figure 13: Composite of B96 murine MPNST cell line *in vitro* studies. A. Single-step replication study using a high MOI (10 PFU/cell), viral recovery data (24hpi) shown with SD. **B.** Photomicrographs of cytopathic effect at high MOI for all oHSVs tested on B96 cells (density of 1.5e5 cells/well; 100X magnification). **C.** Immunostaining studies demonstrating synthesis of late gene product (glycoprotein D), phosphorylated and total eIF-2α along with β-actin protein loading controls at 12hpi (left panel) and 24hpi (right panel).

Summary and Analysis (B86)



The B86 MPNST cell line similar to B96 provides an intermediate replication environment for HSV (Figure 14A). Again, M2001 replicates the best in this tumor line. In contrast with the B96 cell line discussed above (Figure 13), M002 and M032 replicate better than the R7020 ($\gamma_{134.5}$ single copy) recombinant. C134 and C101 exhibit the lowest replication of the viruses tested in spite of its ability to synthesize similar levels of gD as M032 at 24hpi (Figure 14C). Again, early cytopathic effect is seen with all viruses at high MOI (Figure 14B).

Figure 14: Composite of B86 murine MPNST cell line *in vitro* studies. A. Single-step replication study using a high MOI (10 PFU/cell), viral recovery data (24hpi) shown with SD. **B.** Photomicrographs of cytopathic effect at high MOI for all oHSVs tested on B86 cells (density of 1.5×10^5 cells/well; 100X magnification). **C.** Immunostaining studies demonstrating synthesis of late gene product (glycoprotein D), phosphorylated and total eIF-2 α along with β -actin protein loading controls at 12hpi (left panel) and 24hpi (right panel).

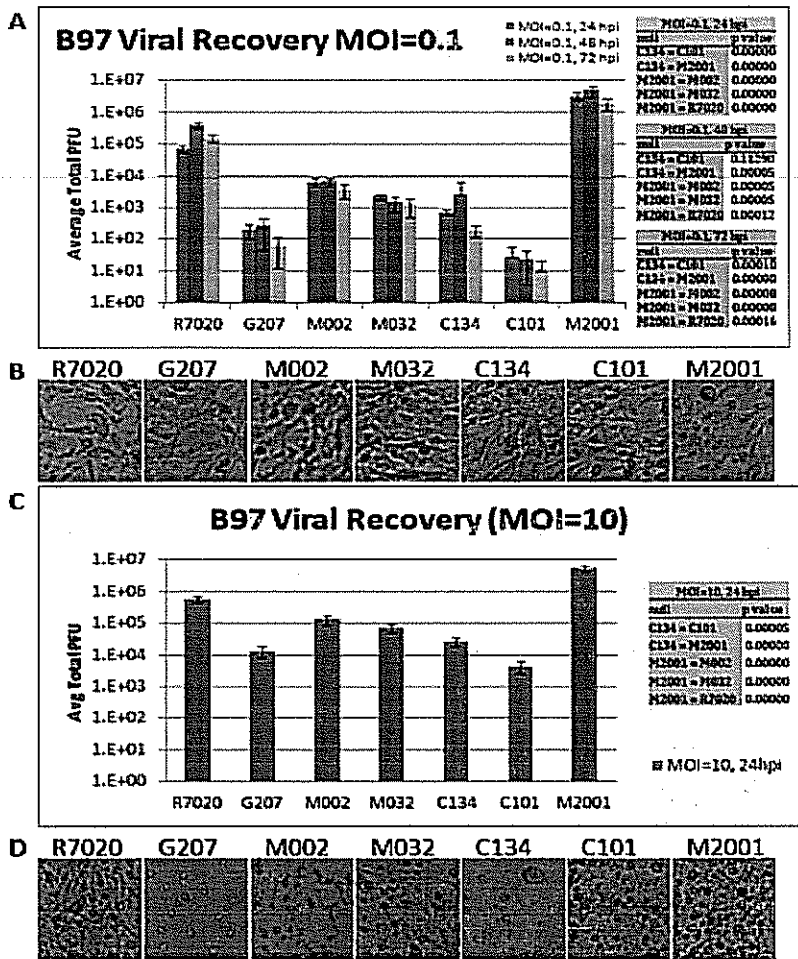


Figure 15: Composite of B97 murine MPNST cell line *in vitro* studies. A. Multistep Replication Study using a low multiplicity of infection (MOI: 0.1 plaque forming unit/cell) (PFU/cell). Viral recovery data shown at 24/ 48/ 72hpi with standard deviation (SD). **B.** Photomicrographs demonstrate cytopathic effect (CPE) in multistep replication study (24hpi) for all oHSVs tested on B97 cells (100X mag). **C.** Single-step replication study using a high MOI (10 PFU/cell). viral recovery data (24hpi) shown with SD. **D.** Photomicrographs of cytopathic effect at high MOI for all oHSVs tested on B97 cells (density of 1.5e5 cells/well;100X magnification).

Summary and Analysis (B97.)
 The B97 MPNST cell line produces the highest differential replication rates between the γ_1 34.5 and $\Delta\gamma_1$ 34.5 viruses tested (100,000x fold difference between C101 and M2001 in multistep replication assays) (Figure 15A,C). The γ_1 34.5 containing viruses (R7020 and M2001) produce early CPE at low and high MOI (Figure 15B,D). The $\Delta\gamma_1$ 34.5 recombinants only produced significant CPE at high MOI in this cell line. C134 replicates better than its parent virus C101 in this cell line but the M032 and M002 virus replicate better than C134.

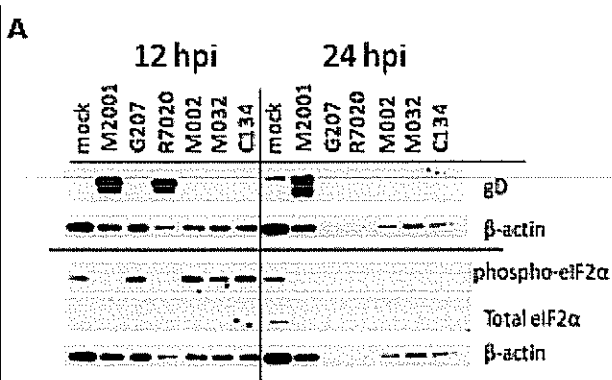


Figure 16: Composite of B97 murine MPNST cell line *in vitro* studies. A. Immunostaining studies demonstrating synthesis of late gene product (glycoprotein D), phosphorylated and total eIF-2α along with β-actin protein loading controls at 12hpi (left panel) and 24hpi (right panel).

Summary and Analysis (B97 cont'd.)

Immunostaining studies (Figure 16A) are interpretable for the 12h timepoint and show gD accumulation only in the M2001 and R7020 samples. Despite their improved replication over C101, the M002, M032, and C134 samples show no significant accumulation of gD suggestive of protein shutoff. The p-eIF2α staining also suggests this. The total eIF-2α staining is uninterpretable. There is differential actin staining which when combined with the replication data in Figure 15 suggests that there is greater cell loss in the R7020 and M2001 samples than in the mock and Δγ_{134.5} infected cells.

Summary and Analysis (B109)

The murine B109 MPNST cell line supports HSV replication. As is true for all the cell lines, M2001 replicated best. The IL-12 expressing viruses (M002, M032) and the single $\gamma_134.5$ copy virus (R7020) were the next best replicating recombinants (Figure 17A). C134 replicates similar to its parent virus C101 in this cell line suggesting that it is restricts the IRS1 PKR evasion (as shown by p-eIF2 α staining and the lack of appreciable gD accumulation in panel C, (Figure 17C)). All viruses exhibited early CPE at high MOI (Figure 17B).

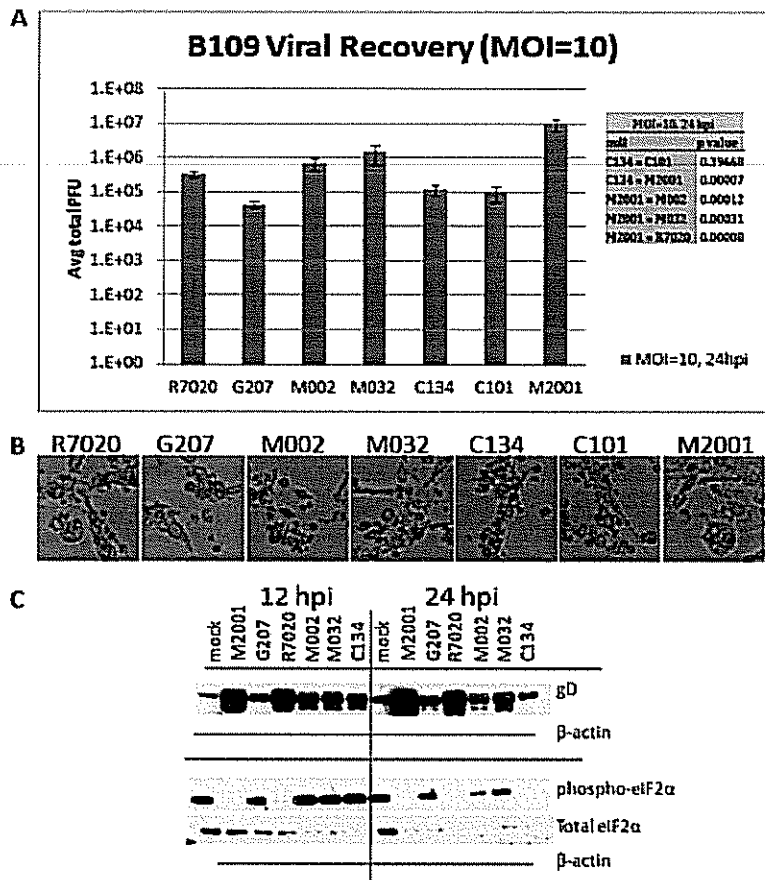
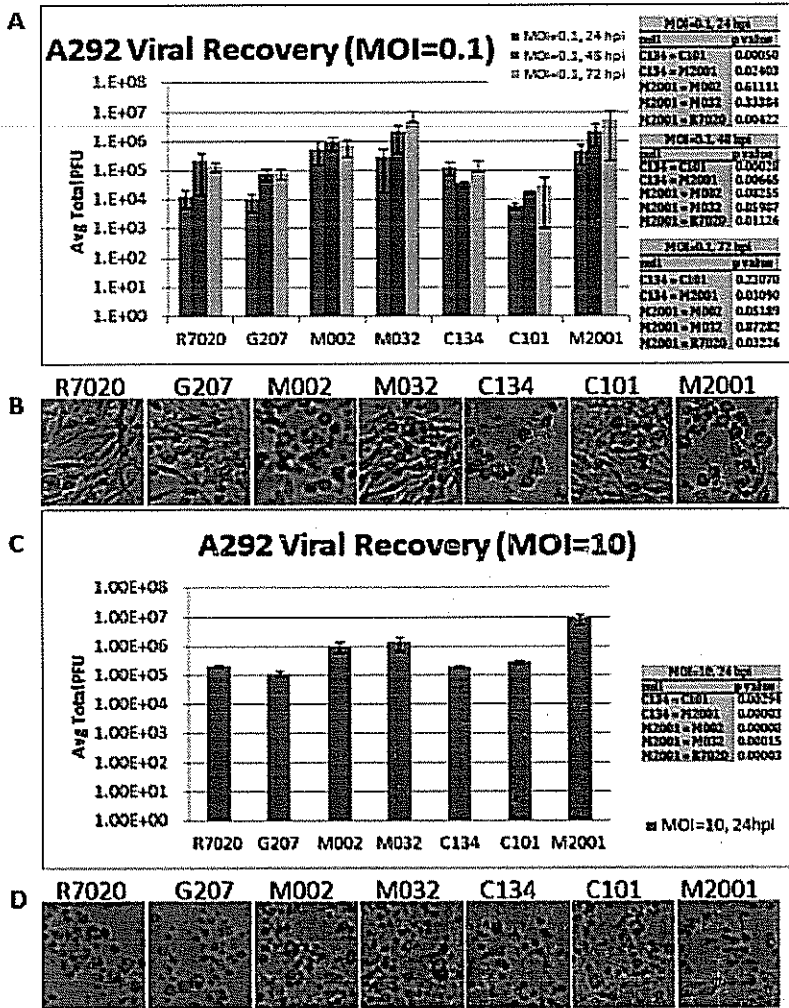


Figure 17: Composite of B109 murine MPNST cell line *in vitro* studies.
A. Single-step replication study using a high MOI (10 PFU/cell). viral recovery data (24hpi) shown with SD. **B.** Photomicrographs of cytopathic effect at high MOI for all oHSVs tested on B109 cells (density of 1.5e5 cells/well; 100X magnification). **C.** Immunostaining studies demonstrating synthesis of late gene product (glycoprotein D), phosphorylated and total eIF-2 α at 12hpi (left panel) and 24hpi (right panel).

Summary and Analysis (A292.)



The A292 murine MPNST cell line supports HSV replication. Recombinant viral replication approaches that of the wild-type-GFP virus M2001. The M032 virus replicates better than the single copy γ_1 34.5 virus R7020 and C134 (Figure 18A,B). In the early CPE images, the C134 infected cells show the greatest CPE of the non-M2001 samples. It is interesting that in multistep replication studies, in contrast to the other viruses tested, it is the only recombinant incapable of increasing virus recovery over time (Figure 18A)

Figure 18: Composite of A292 murine MPNST cell line *in vitro* studies.
A. Multistep Replication Study using a low multiplicity of infection (MOI: 0.1 plaque forming unit/cell) (PFU/cell). Viral recovery data shown at 24/ 48/ 72hpi with standard deviation (SD). **B.** Photomicrographs demonstrate cytopathic effect (CPE) in multistep replication study (24hpi) for all oHSVs tested on A292 cells (100X mag). **C.** Single-step replication study using a high MOI (10 PFU/cell), viral recovery data (24hpi) shown with SD. **D.** Photomicrographs of cytopathic effect at high MOI for all oHSVs tested on A292 cells (density of 1.5e5 cells/well;100X magnification).

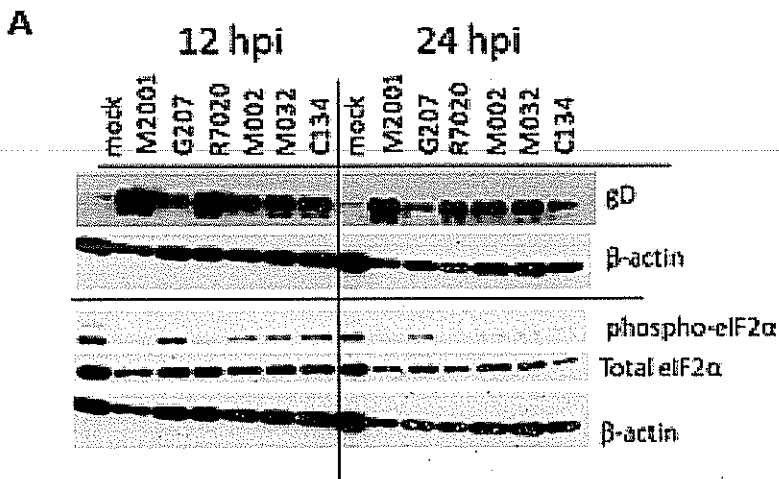
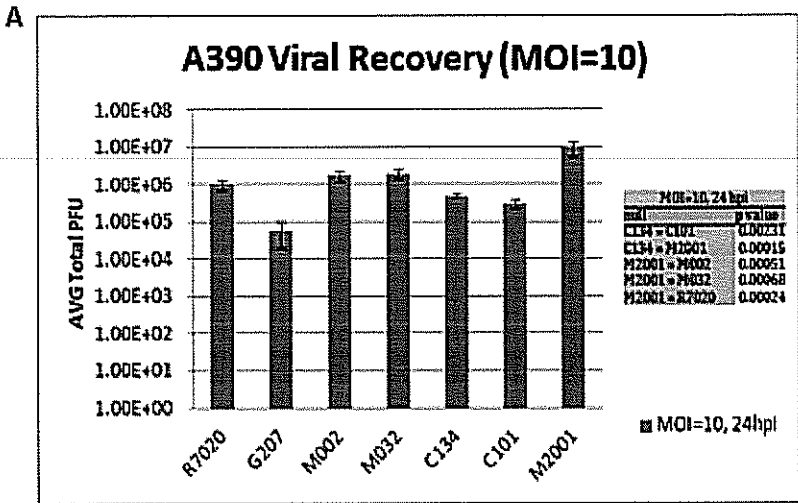


Figure 19: Composite of A292 murine MPNST cell line *in vitro* studies. A. Immunostaining studies demonstrating synthesis of late gene product (glycoprotein D), phosphorylated and total eIF-2 α along with β -actin protein loading controls at 12hpi (left panel) and 24hpi (right panel).

In immunostaining studies (Figure 19A) the viruses initially synthesize gD (of note, G207 produces the least of the viruses in the 12h samples). By 24h however, the C134 virus produces less gD, similar to G207. Immunostaining for p-eIF2 α at 12hpi shows that there is baseline phosphorylation in uninfected A292 cells but that the $\gamma_{134.5}$ containing virus infected cells (R7020 and M2001) there is less p-eIF-2 α detected.

Summary and Analysis (A390)



In preliminary single step replication studies, the viruses tested replicated within 100x of one another (Figure 20A). The M2001 produced a significantly greater amount of virus followed by M032, M002 and R7020. G207 produced the least amount of virus. C134 and C101 produced virus at an intermediate level between G207 and R7020). All of the viruses produced early cytopathic effect at high MOI.



Figure 20: Composite of A390 murine MPNST cell line *in vitro* studies.
A. Single-step replication study using a high MOI (10 PFU/cell), viral recovery data (24hpi) shown with SD. **D.** Photomicrographs of cytopathic effect at high MOI for all oHSVs tested on A390 cells (density of 1.5e5 cells/well; 100X magnification).

Summary and Analysis (A390 cont'd.)

Alamar blue cytotoxicity studies were inconsistent with the CPE analysis and replication based studies, showing viability in the 60-90% range at 72 hpi. C101 showed early CPE exceeding M2001, which is an uninterpretable result. (Figure 21A,B).

The immunostaining studies (Figure 21C) showed the greatest gD accumulation in the M2001 and R7020 infected cells. There was baseline eIF2 α phosphorylation detected in A390 MPNST cells. HSV infection did not appear to alter the accumulation of eIF2 α accumulation.

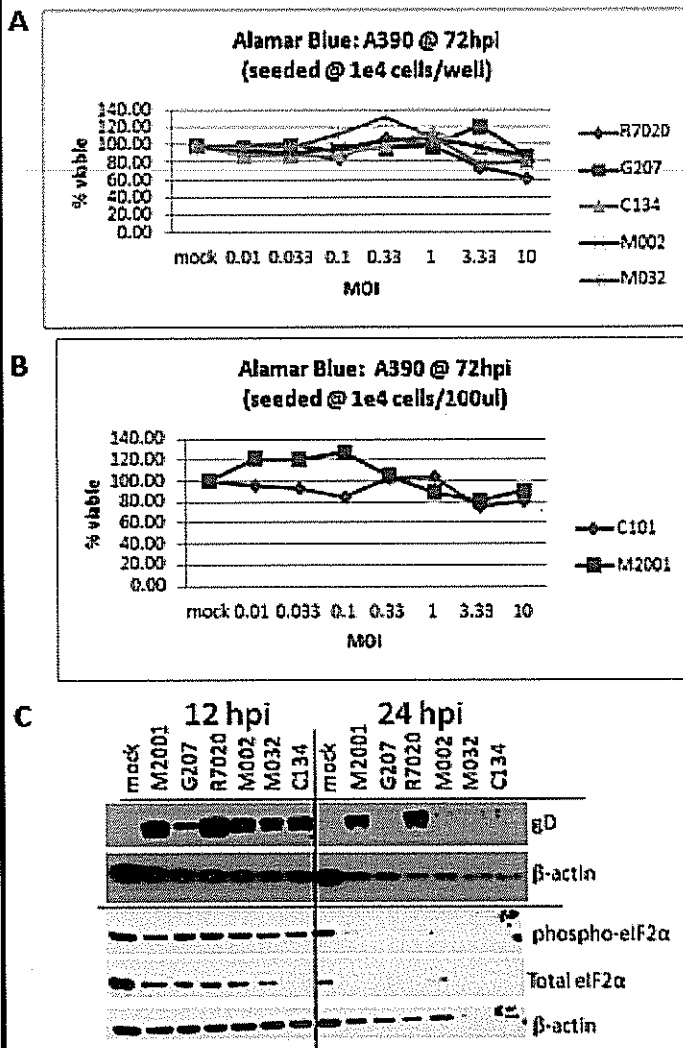


Figure 21: Composite of A390 murine MPNST cell line *in vitro* studies. A. Alamar Blue cell viability assay comparing clinical grade oHSVs (and the non-clinical grade oHSV M002) antitumor effect at 72hpi. **B.** Alamar Blue cell viability assay comparing nondinical grade oHSVs C101 ($\Delta\gamma$ 1 34.5) vs. M2001 (wt) at 72hpi. **C.** Immunostaining studies demonstrating synthesis of late gene product (glycoprotein D), phosphorylated and total eIF-2 α along with β -actin protein loading controls at 12hpi (left panel) and 24hpi (right panel).

Summary and Analysis (A391)

The A391 MPNST cell line is sensitive and supports HSV replication. All of the viruses tested were capable of generating $>10^5$ PFU in single step replication assays (Figure 22A) with CPE at 24 hpi (Figure 22B) at high MOI.

Immunostaining studies (Figure 22C) showed greater gD accumulation in the M2001 and R7020 infected cells (consistent with the replication data), and p-eIF-2 α in the $\Delta\gamma 134.5$ viruses, particularly at 12h.

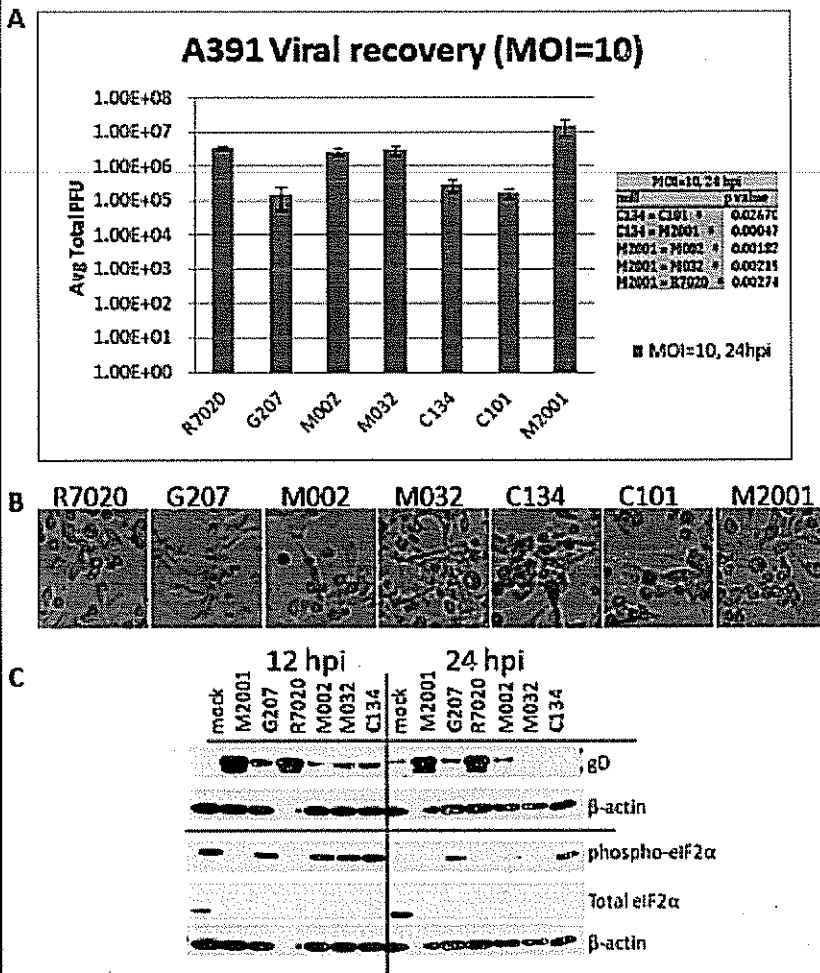


Figure 22: Composite of A391 murine MPNST cell line *in vitro* studies.
A. Single-step replication study using a high MOI (10 PFU/cell). viral recovery data (24hpi) shown with SD. **B.** Photomicrographs of cytopathic effect at high MOI for all oHSVs tested on A391 cells (density of 1.5×10^5 cells/well; 100X magnification). **C.** Immunostaining studies demonstrating synthesis of late gene product (glycoprotein D), phosphorylated and total eIF-2 α along with β -actin protein loading controls at 12hpi (left panel) and 24hpi (right panel).

Summary and Analysis (B76)

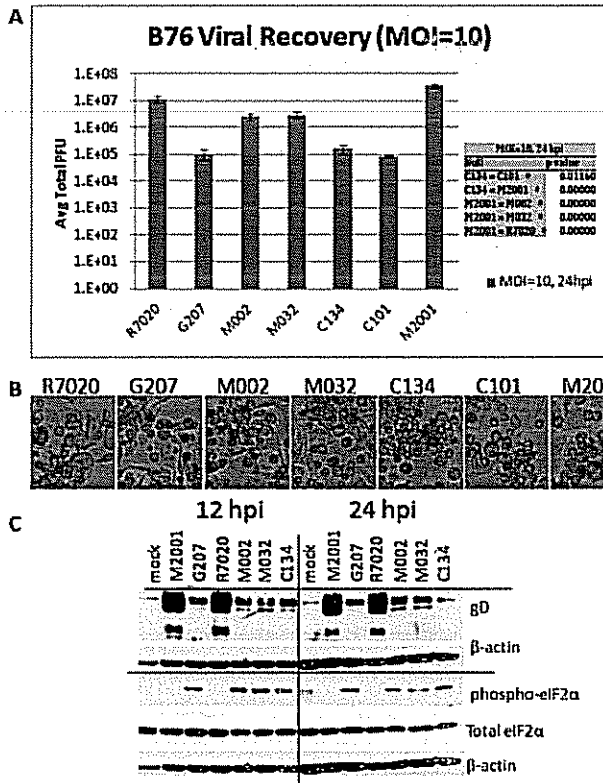


Figure 23: Composite of B76 murine MPNST cell line *in vitro* studies. A. Single-step replication study using a high MOI (10 PFU/cell), viral recovery data (24 hpi) shown with SD. **D.** Photomicrographs of cytopathic effect at high MOI for all α HSVs tested on B76 cells (density of 1.5×10^5 cells/well; 100X magnification). **C.** Immunostaining studies demonstrating synthesis of late gene product (glycoprotein D), phosphorylated and total eIF-2 α along with β -actin protein loading controls at 12 hpi (left panel) and 24 hpi (right panel).

The B76 MPNST cell line supports HSV replication and shows differential replication of $\Delta\gamma_{134.5}$ viruses (Figure 23A). Of the $\Delta\gamma_{134.5}$ viruses tested, M002 and M032 replicate best. C134 only generates 10^5 pfu and behaves similar to its parent virus C101 and G207 in the B76 cell line. The replication of M002 and M032 does not appear to be an eIF2 α dependent phenotype. Immunostaining (Figure 23C) shows the greatest gD accumulation in the M2001 and R7020 infected samples. The M002, M032 and C134 infected samples show evidence of eIF2 α phosphorylation at 12 hpi and less gD accumulation than the M2001 and R7020 infected samples, yet viral replication differs by 10x between these $\Delta\gamma_{134.5}$ viruses.

Summary and Analysis (231-Trig)

The 231-Trig cell line is an HSV sensitive murine MPNST that supports clinical grade virus replication. M032 replicates similar to M2001 in multistep and single step replication assays generating 10^7 PFU in both assays. The 231-Trig line supports efficient viral replication, including C101. It is most restrictive to G207 growth (Figure 24A,C).

In terms of early cytopathic effects (Figure 24B,D) minimal cytopathic effects were seen when low MOI was used, and all viruses produced cytopathic effects at high MOI.

Conclusion: The 231-Trig MPNST cells are a sensitive cell line. We intend to include this as one of the 2 oHSV sensitive MPNST cell lines in future studies as described in Subaim 1d.

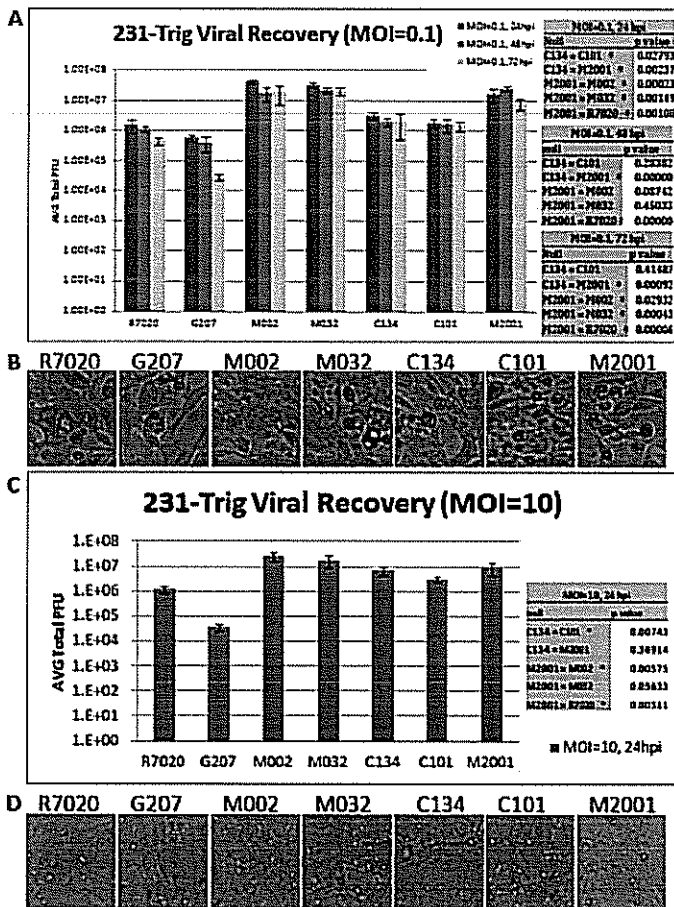


Figure 24: Composite of 231-Trigeminal murine MPNST cell line *in vitro* studies. A. Multistep Replication Study using a low multiplicity of infection (MOI: 0.1 plaque forming unit/cell) (PFU/cell). Viral recovery data shown at 24/ 48/ 72hpi with standard deviation (SD). B. Photomicrographs demonstrate cytopathic effect (CPE) in multistep replication effect (24hpi) for all oHSVs tested on 231-Trig cells (100X mag). C. Single-step replication study using a high MOI (10 PFU/cell), viral recovery data (24hpi) shown with SD. D. Photomicrographs of cytopathic effect at high MOI for all oHSVs tested on 231-Trig cells (density of 1.5×10^5 cells/well; 100X magnification).

Summary and Analysis (231-Trig cont'd.)

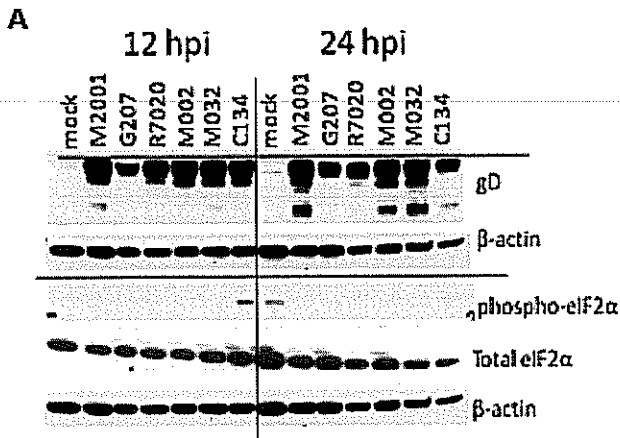


Figure 25: Composite of 231-Trigeminal murine MPNST cell line *in vitro* studies. A. Immunostaining studies demonstrating synthesis of late gene product (glycoprotein D), phosphorylated and total eIF-2α along with β-actin protein loading controls at 12hpi (left panel) and 24hpi (right panel).

All of the viruses tested produce abundant gD in the 231-Trig cell line. In terms of early cytopathic effects (Figure 25A) minimal cytopathic effects were seen when low MOI was used, and all viruses produced cytopathic effects at high MOI. M2001, M002, and M032 produce the greatest gD at 24hpi followed by C134. There is no evidence of p-eIF2α in the samples at 24hpi consistent with the permissive late protein phenotype of this cell line.

Conclusion: We intend to include this as one of the 2 oHSV sensitive MPNST cell lines in future studies as described in Subaim 1d.

*Summary and Analysis (A18)

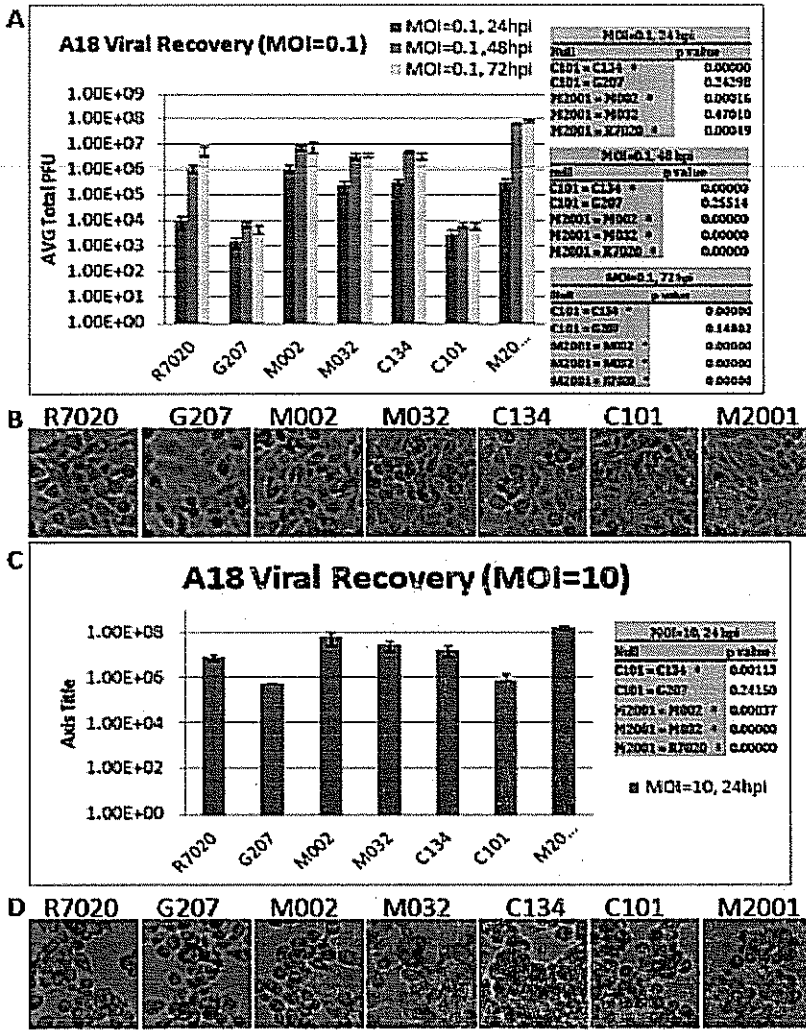


Figure 26: Composite of A18 murine MPNST cell lines *in vitro* studies. A. Multistep Replication Study using a low multiplicity of infection (MOI: 0.1 plaque forming unit/cell) (PFU/cell). Viral recovery data shown at 24/ 48/ 72hpi with standard deviation (SD). **B.** Photomicrographs demonstrate cytopathic effect (CPE) in multistep replication study (24hpi) for all oHSVs tested on A18 cells (100X mag). **C.** Single-step replication study using a high MOI (10 PFU/cell), viral recovery data (24hpi) shown with SD. **D.** Photomicrographs of cytopathic effect at high MOI for all oHSVs tested on A18 cells (density of 1.5e5 cells/well; 100X magnification).

The A18 cell murine MPNST cell line is also sensitive to HSV infection and replication. Unlike the 231-Trig line, however, there is greater replication variation between $\Delta\gamma_{134.5}$ viruses in this cell line. Of the $\Delta\gamma_{134.5}$ viruses tested, the M002, M032, and C134 viruses replicate the best (Figure 26A,C). The R7020 replicates well but initially produces less virus than the chimeric and IL12 containing viruses. The prototypical $\Delta\gamma_{134.5}$ viruses (G207 and C101) that induce protein shutoff in non-MPNST cell lines generate the least amount of virus in this cell line in multistep replication assays.

In terms of early cytopathic effects (Figure 26B,D) minimal cytopathic effects were seen when low MOI was used, and all viruses produced cytopathic effects at high MOI.

Conclusion The A18 cell line will be one of the 2 sensitive murine MPNST cell lines that we will use in future studies because it shows a greater differential effect on $\Delta\gamma_{134.5}$ replication.

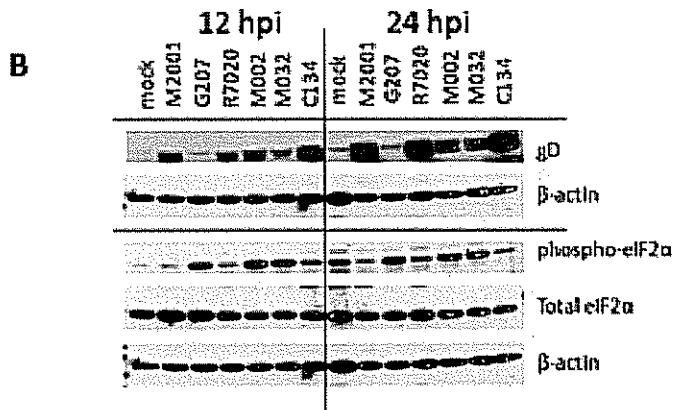
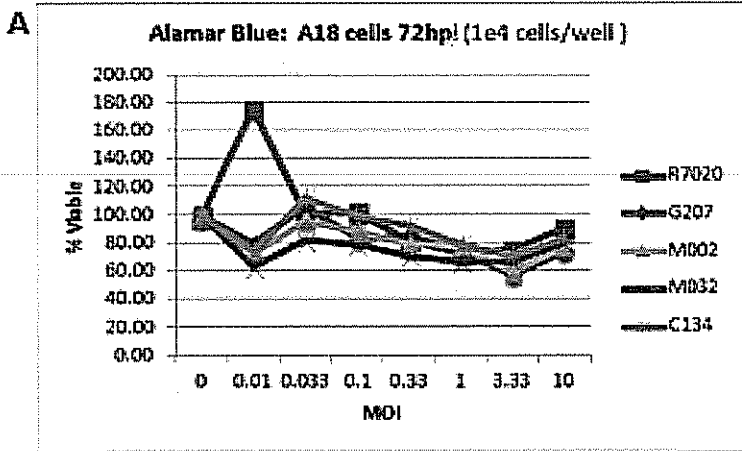


Figure 27: Composite of A18 murine MPNST cell line *in vitro* studies. **A.** Alamar Blue cell viability assay comparing clinical grade oHSVs (and the non-clinical grade oHSV M002) antitumor effect at 72hpi. **B.** Immunostaining studies demonstrating synthesis of late gene product (glycoprotein D), phosphorylated and total eIF-2 α along with β -actin protein loading controls at 12hpi (left panel) and 24hpi (right panel).

human tumor cell lines tested (Shah, 2007)

Summary and Analysis (A18 cont'd.)

In the Alamar Blue assay of cell viability, all viruses were somewhat effective against A18 (Figure 27 A).

Western blot analysis of the mutant viruses on A18 (Figure 27B) demonstrate decreased gD production in G207 and to some degree M002 and M032 infected cell samples. As expected, the greatest phosphorylation of eIF 2 α , was seen in G207, followed by M032 and M002, although these were not drastically different from R7020 and C134. By 24 hpi the greatest gD accumulation occurred in the M2001, R7020, and C134 infected cells. Consistent with the gD findings, less p-eIF2 α is detected in the M2001, R7020 and C134 infected samples.

Conclusion The A18 cell line will be one of the 2 sensitive murine MPNST cell lines that we will use in future studies because it shows a greater differential effect on $\Delta\gamma_{134.5}$ replication. The C134 recombinant differs from its parent virus (C101) in this cell line and is capable of maintaining late viral protein synthesis and precludes PKR mediated shutoff similar to that shown in other

Summary and Analysis (A599.)

The A599 MPNST cell line is sensitive to oHSV replication. M2001 produces 10^7 pfu in multistep replication assays (Figure 28A). M032 and M002 generate a similar amount of virus at 48 and 72h post infection as M2001. C134 initially replicates well in this cell line but over the next 48h of infection replication declines and the chimeric HSV replicates similar to its $\Delta\gamma_134.5$ parent virus C101. It is interesting that C134 infected cells appear pyknotic in CPE studies at low and high MOI and have a different appearance than the other $\Delta\gamma_134.5$ and the M2001 infected cells (Figure 28B and 28D). In single step replication assay, M032 and M002 performed similarly to M2001, while R7020 and G207 performed less well (Figure 28C).

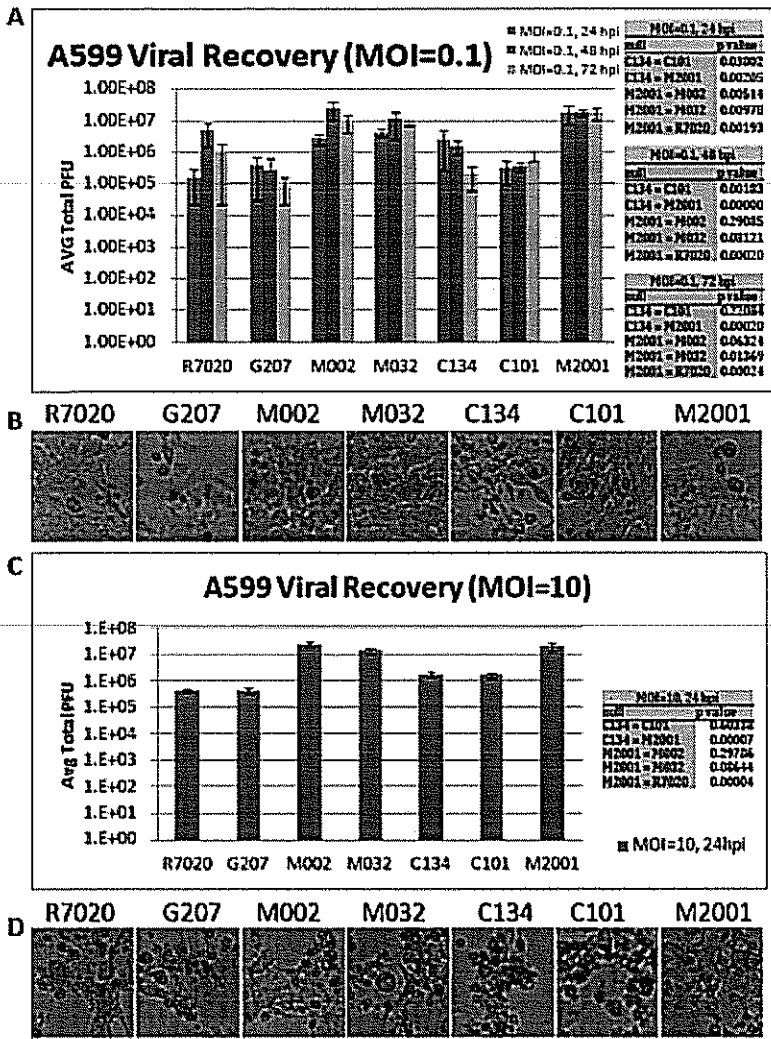


Figure 28: Composite of A599 murine MPNST cell line *in vitro* studies.
A. Multistep Replication Study using a low multiplicity of infection (MOI: 0.1 plaque forming unit/cell) (PFU/cell). Viral recovery data shown at 24/ 48/ 72hpi with standard deviation (SD). **B.** Photomicrographs demonstrate cytopathic effect (CPE) in multistep replication study (24hpi) for all oHSVs tested on A599 cells (100X mag). **C.** Single-step replication study using a high MOI (10 PFU/cell), viral recovery data (24hpi) shown with SD. **D.** Photomicrographs of cytopathic effect at high MOI for all oHSVs tested on A599 cells (density of 1.5e5 cells/well; 100X magnification).

Summary and Analysis (T265-luc)

The T265-luc human MPNST cell line is resistant to HSV infection. In multistep replication studies M2001 replicates the best followed by C134 and R7020. The replication pattern is interesting: in the R7020, C134, and to some extent M002 infected cells there is progressive increase in virus replication at 24, 48 and 72hpi. In contrast M032 and C101 show a decline in viral recovery over the 24, 48 and 72 h timepoints. While C134 and M032 generate similar peak viral levels they appear to do this with a different kinetic pattern (M032 early and C134 late) (Figures 29A,C)

Early cytopathic effect (Figure 29B,D) was particularly evident in the high MOI assay. As was seen in the Alamar blue assay below, this was likely due to non-replicative killing.

Conclusion: This is an interesting cell line that we intend to include in future studies as a representative resistant human cell line for future studies as described in Subaim 1d.

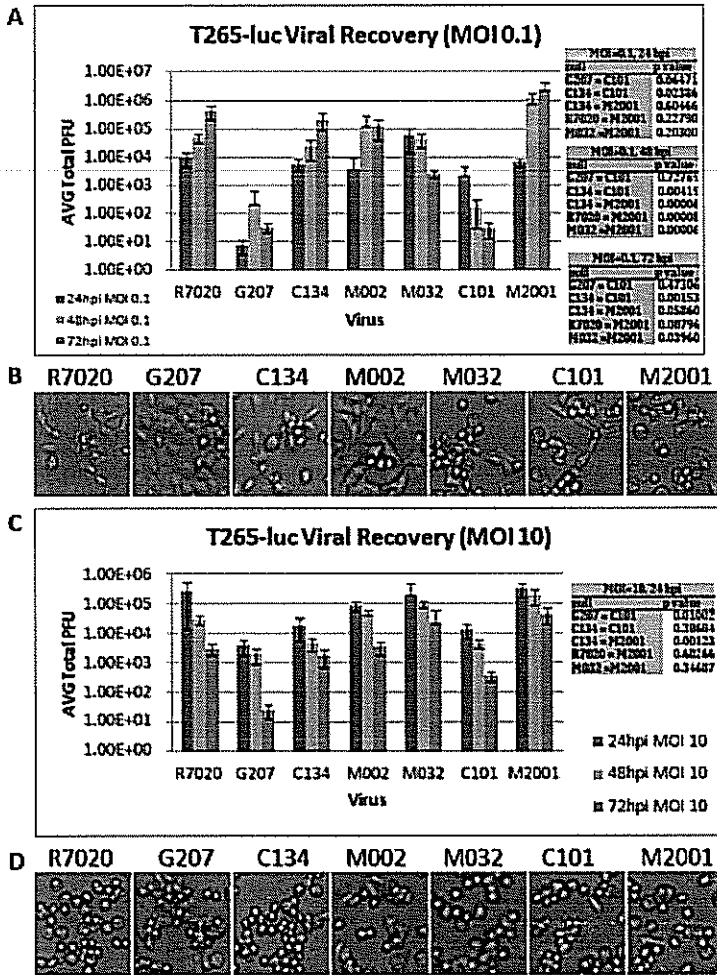


Figure 29: Composite of T265-luciferase human MPNST cell line *in vitro* studies. A. Multistep Replication Study using a low multiplicity of infection (MOI: 0.1 plaque forming unit/cell) (PFU/cell). Viral recovery data shown at 24/ 48/ 72hpi with standard deviation (SD). **B.** Photomicrographs demonstrate cytopathic effect (CPE) in multistep replication study (24hpi) for all oHSVs tested on T265-luc cells (100X mag). **C.** Single-step replication study using a high MOI (10 PFU/cell). viral recovery data (24hpi) shown with SD. **D.** Photomicrographs of cytopathic effect at high MOI for all oHSVs tested on T265-luc cells (density of 1.5e5 cells/well-100X magnification).

Summary and Analysis (T265-luc cont'd.)

In the Alamar Blue assay of cell viability, all viruses were particularly effective against T265-luc (Figure 30 A,B). At the highest MOI, the viruses were extremely effective producing about 80-100% CPE.

Western blot analysis of the mutant viruses on T265-luc (Figure 30C) demonstrated decreased production of gD, a late gene product, in M032 and to a lesser degree, G207. As expected, the greatest phosphorylation of eIF 2 α , was seen in G207, followed by M032 and M002. R7020 and M2001 showed similar p-eIF2 α staining as mock infected cells. C134 produced an intermediate level of eIF2 α staining somewhere between that of the $\gamma_{134.5}$ and M032 infected cell samples. This interesting pattern of eIF2 α phosphorylation combined with the replication findings shown in (Figure 29), warranted further study and thus this line was selected as one of the lines we will study in depth.

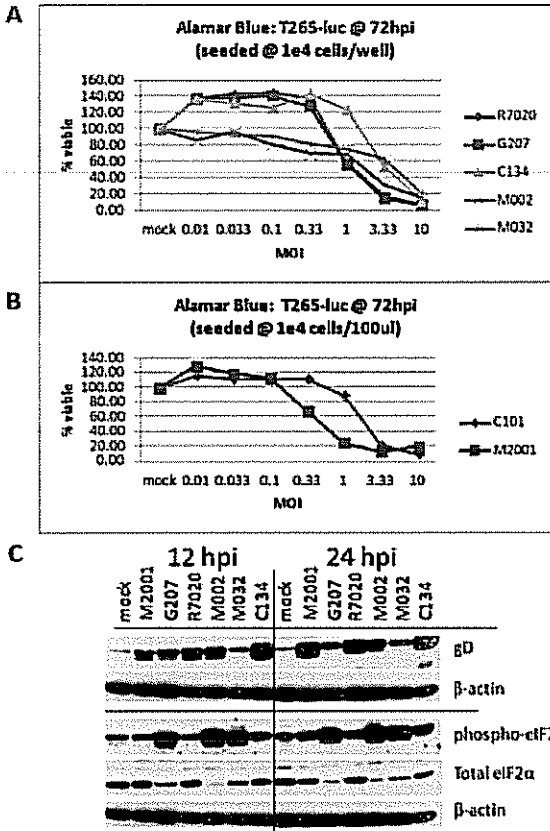


Figure 30: Composite of T265-luciferase human MPNST cell line *in vitro* studies. A. Alamar Blue cell viability assay comparing clinical grade oHSVs (and the non-clinical grade oHSV M002) antitumor effect at 72hpi. B. Alamar Blue cell viability assay comparing nonclinical grade oHSVs C101 ($\Delta\gamma_{134.5}$) vs. M2001 (wt) at 72hpi. C. Immunostaining studies demonstrating synthesis of late gene product (glycoprotein D), phosphorylated and total eIF-2 α along with β -actin protein loading controls at 12hpi (left panel) and 24hpi (right panel).

Summary and Analysis (S26T-luc)

The S26T-luc Human MPNST cell line is highly resistant to most of the $\Delta\gamma_134.5$ viruses tested. Wild-type HSV expressing GFP (M2001) was capable of sustained replication over a 72h period and generated between 10^4 and 10^5 PFU. R7020 by 72hpi generated virus in at 10^4 pfu. M032 replicates well initially (10^4 pfu 24hpi) but then declines over time (10^3 pfu 72hpi). C134 replicates poorly in this human MPNST cell lines behaving similar to the $\Delta\gamma_134.5$ parent virus C101 (figure 31 A).

Differences in replication kinetics between the viruses are less apparent in single step replication assays (Figure 31C)

Early cytopathic effect was particularly evident in the high MOI assay. (Figure 31B,D).

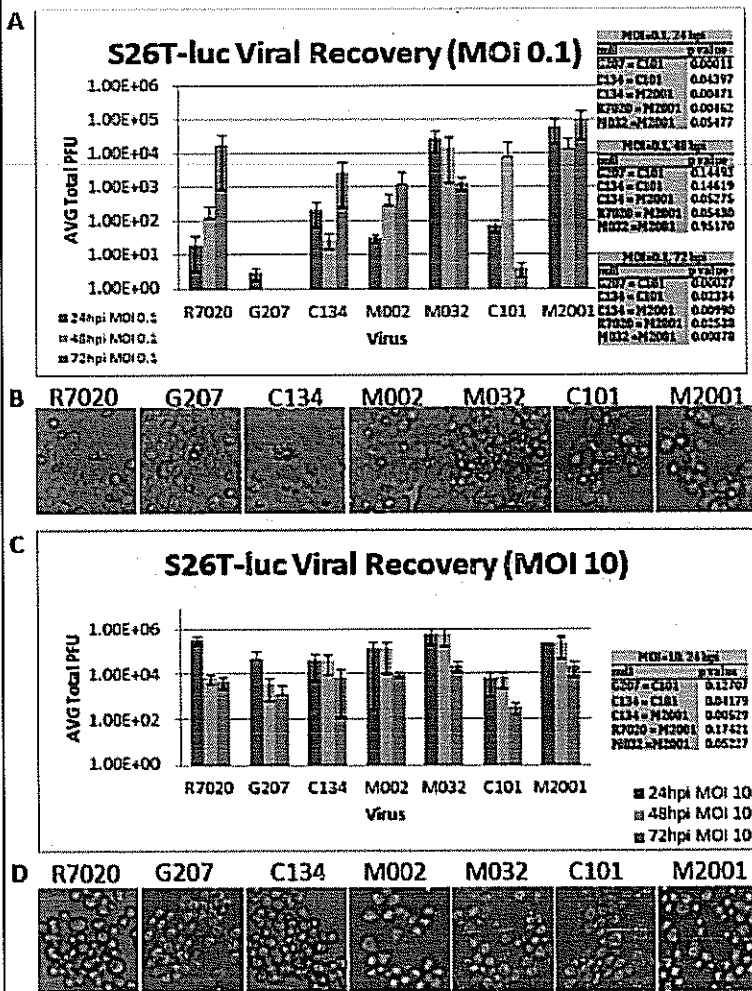


Figure 31: Composite of S26T-luciferase human MPNST cell line *in vitro* studies. A. Multistep Replication Study using a low multiplicity of infection (MOI: 0.1 plaque forming unit/cell) (PFU/cell). Viral recovery data shown at 24/ 48/ 72hpi with standard deviation (SD). **B.** Photomicrographs demonstrate cytopathic effect (CPE) in multistep replication study (24hpi) for all α HSVs tested on S26T-luc cells (100X mag). **C.** Single-step replication study using a high MOI (10 PFU/cell). viral recovery data (24hpi) shown with SD. **D.** Photomicrographs of cytopathic effect at high MOI for all α HSVs tested on S26T-luc cells (density of 1.5×10^5 cells/well; 100X magnification).

Summary and Analysis (S26T-luc cont'd.)

In the Alamar Blue assay of cell viability, all viruses were particularly effective against S26T-luc (Figure 32 A,B). At the highest MOI, the viruses were extremely effective producing about 65-80% CPE.

Western blot analysis of the mutant viruses on S26T-luc (Figure 39C) demonstrated significant production of gD, a late gene product, by R7020, M2001, and to a lesser extent, G207. M002, M032, and C134 had little to no expression of gD. There was an interesting pattern of phosphorylation of eIF 2 α , in all viruses, even M2001.

Conclusion: The 26T-luc is an interesting cell line that we intend to include in future studies as a representative resistant human cell line in Subaim 1d.

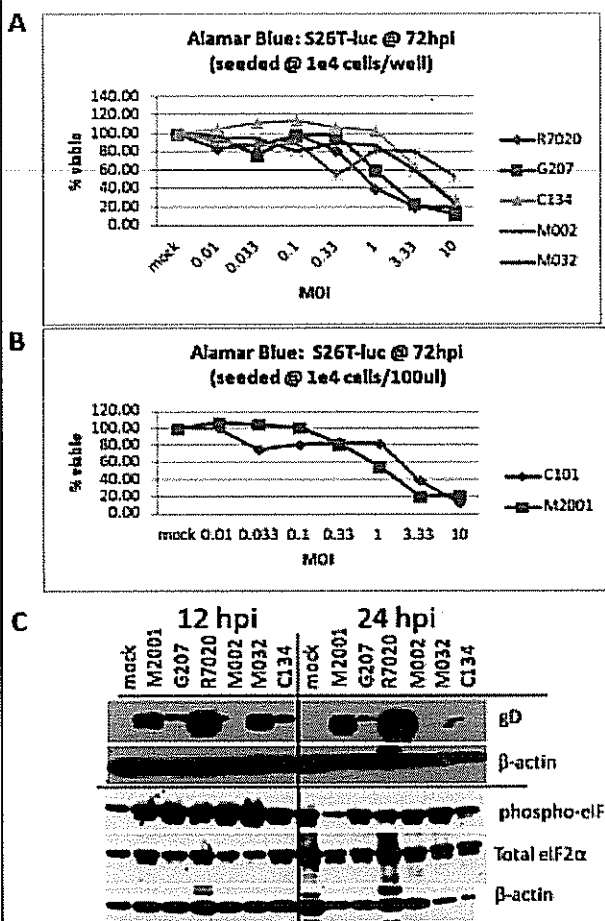


Figure 32: Composite of S26T-luciferase human MPNST cell line *in vitro* studies. A. Alamar Blue cell viability assay comparing clinical grade oHSVs (and the non-clinical grade oHSV M002) antitumor effect at 72hpi. B. Alamar Blue cell viability assay comparing nonclinical grade oHSVs C101 ($\Delta\gamma1$ 34.5) vs. M2001 (wt) at 72hpi. C. Immunostaining studies demonstrating synthesis of late gene product (glycoprotein D), phosphorylated and total eIF-2 α along with β -actin protein loading controls at 12hpi (left panel) and 24hpi (right panel).

Summary and Analysis (88-14-luc)

The 88-14-luc human MPNST cell line is resistant to HSV replication, similar to that seen in the S26T cell line shown in Figure 31. The viruses tested exhibit different replication patterns in multistep replication assays (Figure 33A). M2001, C134, and M002 increase viral replication over time whereas G207, C101, and M032 replication declines over the 72h culture period. At high MOI M032 produces as much virus as the wild-type HSV M2001.

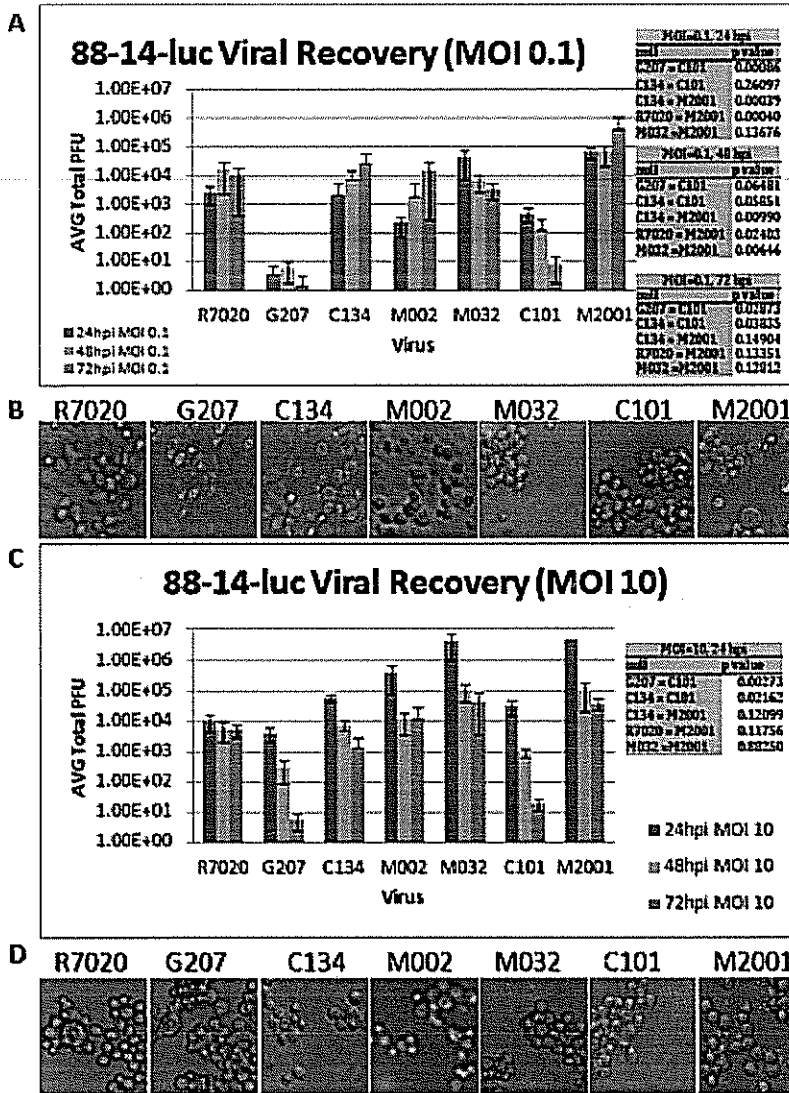


Figure 33: Composite of 88-14-luciferase human MPNST cell line *in vitro* studies. A. Multistep Replication Study using a low multiplicity of infection (MOI: 0.1 plaque forming unit/cell) (PFU/cell). Viral recovery data shown at 24/ 48/ 72hpi with standard deviation (SD). B. Photomicrographs demonstrate cytopathic effect (CPE) in multistep replication study (24hpi) for all oHSVs tested on 88-14-luc cells (100X mag). C. Single-step replication study using a high MOI (10 PFU/cell). viral recovery data (24hpi) shown with SD. D. Photomicrographs of cytopathic effect at high MOI for all oHSVs tested on 88-14-luc cells (density of 1.5e5 cells/well; 100X magnification).

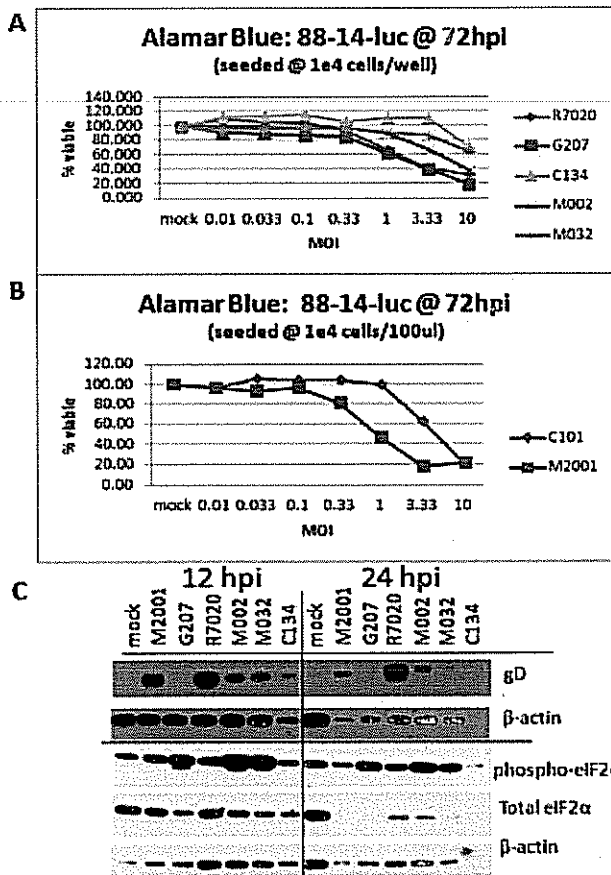


Figure 34: Composite of 88-14-luciferase human MPNST cell line *in vitro* studies. A. Alamar Blue cell viability assay comparing clinical grade oHSVs (and the non-clinical grade oHSV M002) antitumor effect at 72hpi. **B.** Alamar Blue cell viability assay comparing nonclinical grade oHSVs C101 ($\Delta\gamma$ 34.5) vs. M2001 (wt) at 72hpi. **C.** Immunostaining studies demonstrating synthesis of late gene product (glycoprotein D), phosphorylated and total eIF-2 α along with β -actin protein loading controls at 12hpi (left panel) and 24hpi (right panel).

In the Alamar Blue assay of cell viability, all viruses were particularly effective against S26T-luc (Figure 34 A,B). At the highest MOI, the viruses were extremely effective producing about 65-80% CPE.

Western blot analysis of the mutant viruses on 88-14 (Figure 34C) demonstrate significant production of gD, a late gene product, in M2001 and R7020. Lesser amounts were made in M002 and M032. As expected, the greatest phosphorylation of eIF 2 α , was seen in G207, followed by M032 and M002, although these were not drastically different from R7020 and C134. C134 samples are incapable of being interpreted in the western blot studies due to insufficient protein loading based upon the actin staining.

Summary and Analysis (90-8)

The 90-8 cell line exhibits intermediate sensitivity to HSV infection. M2001 replicates the best. The M002, M032, R7020, and C134 viruses replicate similarly. The G207 and C101 virus replicate poorly in this cell line (Figure 35 A,C). All of the viruses tested elicit early CPE, with some present even in the low MOI group (Figure 35 B, D)

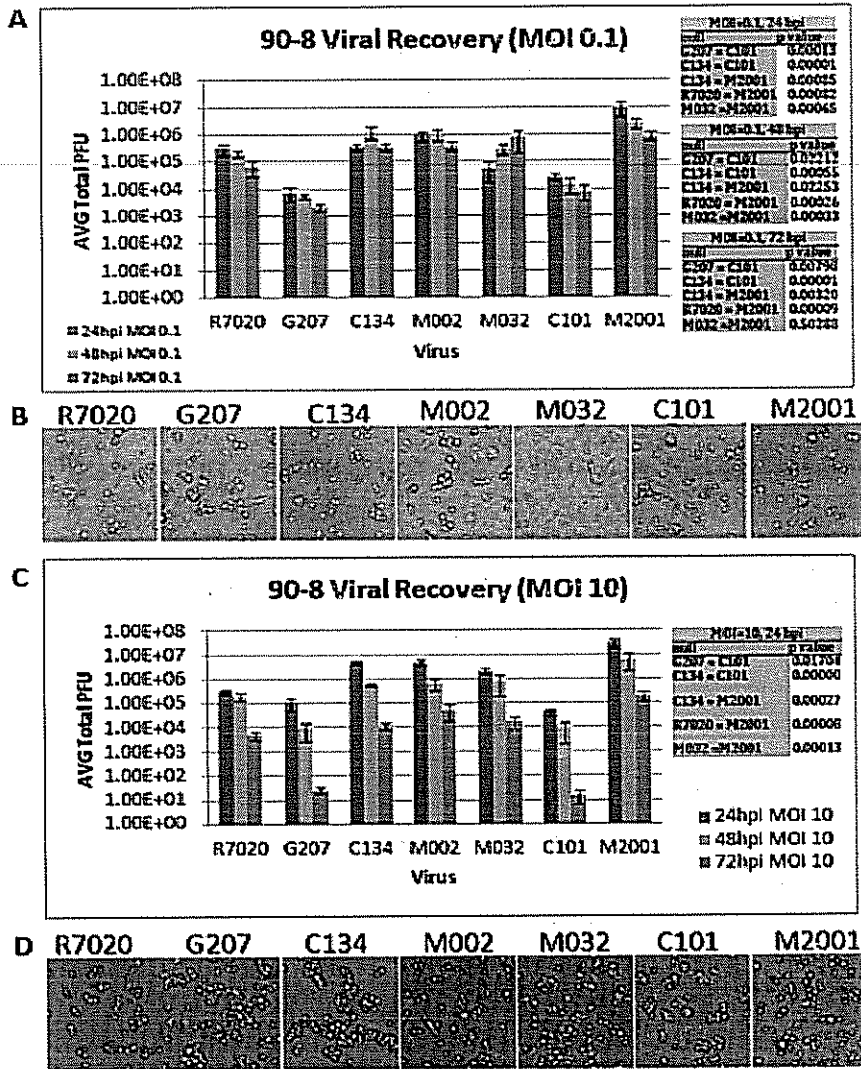


Figure 35: Composite of 90-8 human MPNST cell line *in vitro* studies. A. Multistep Replication Study using a low multiplicity of infection (MOI: 0.1 plaque forming unit/cell) (PFU/cell). Viral recovery data shown at 24/ 48/ 72hpi with standard deviation (SD). **B.** Photomicrographs demonstrate cytopathic effect (CPE) in multistep replication study (24hpi) for all oHSVs tested on 90-8 cells (100X mag). **C.** Single-step replication study using a high MOI (10 PFU/cell), viral recovery data (24hpi) shown with SD. **D.** Photomicrographs of cytopathic effect at high MOI for all oHSVs tested on 90-8 cells (density of 1.5e5 cells/well;100X magnification).

Summary and Analysis (90-8 cont'd.)

In the Alamar Blue assay of cell viability, all viruses were particularly ineffective against 90-8. These results are inconsistent with the CPE studies (shown in Figure 36 B and D) in which all of the viruses tested elicited morphologic evidence of cell damage and death.

Western blot analysis of the mutant viruses on 90-8 (Figure 36C) demonstrate significant production of gD, a late gene product, with the exception of G207, which had minimal expression of gD. M002 and M032 were intermediate. As expected, the greatest phosphorylation of eIF 2 α , was seen in G207, followed by M032 and M002.

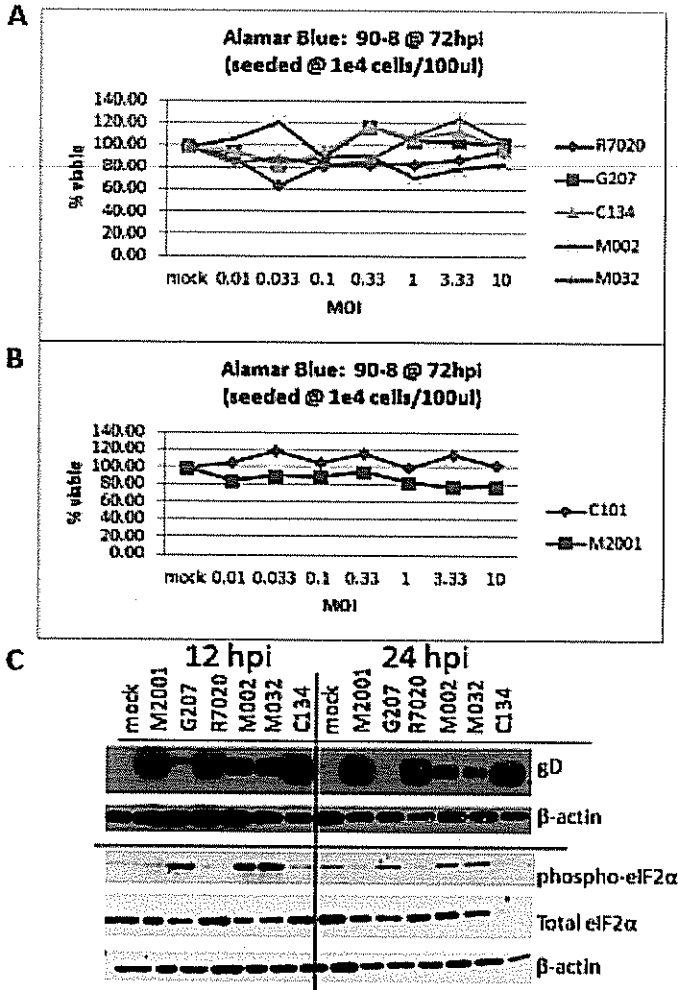


Figure 36: Composite of 90-8 human MPNST cell line *in vitro* studies. A. Alamar Blue cell viability assay comparing clinical grade oHSVs (and the non-clinical grade oHSV M002) antitumor effect at 72hpi. B. Alamar Blue cell viability assay comparing nondclinical grade oHSVs C101 ($\Delta\gamma 1$ 34.5) vs. M2001 (wt) at 72hpi. C. Immunostaining studies demonstrating synthesis of late gene product (glycoprotein D), phosphorylated and total eIF-2 α along with β -actin loading controls at 12hpi (left panel) and 24hpi (right panel).

Summary and Analysis (YST-1)

Human MPNST cell line YST-1 was sensitive to viral replication and cytopathic effects as shown in the accompanying figures. In the single step replication assay, all viruses were able to replicate, producing at least 1×10^5 pfu, with C134 resembling wild-type virus at 1×10^7 . This virus statistically replicated superiorly to C101 (Figure 37A).

In terms of cytopathic effects (37B) all viruses cytopathic effects at high MOI. This cell line this was categorized as *sensitive*.

Western blot analysis of the mutant viruses on YST-1 (Figure 37C) demonstrate significant production of gD, a late gene product, with the exception of G207, which had moderate expression of gD, along with M032. As expected, the greatest phosphorylation of eIF 2 α , was seen in G207, and M032 and M002, followed by R7020 and C134.

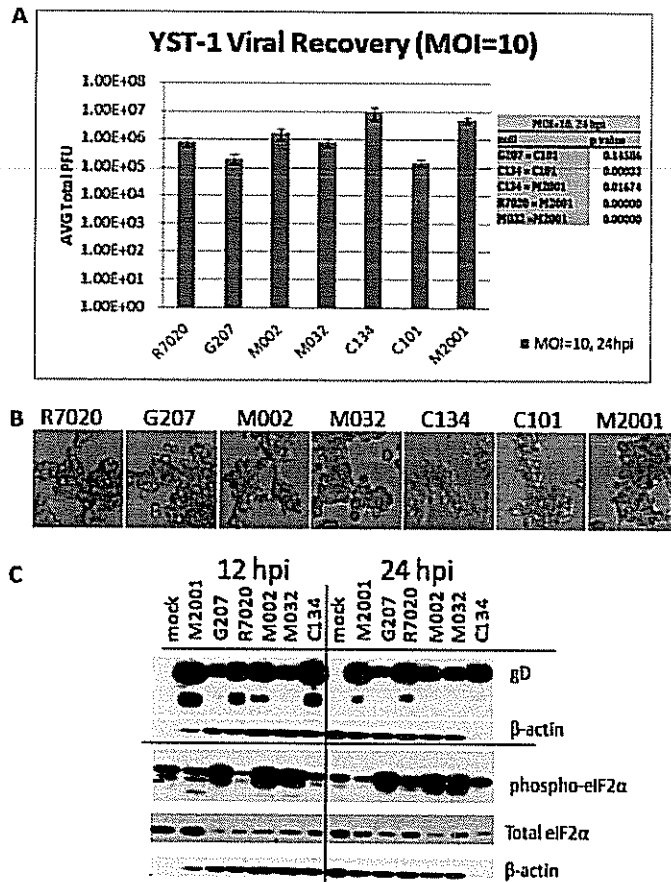
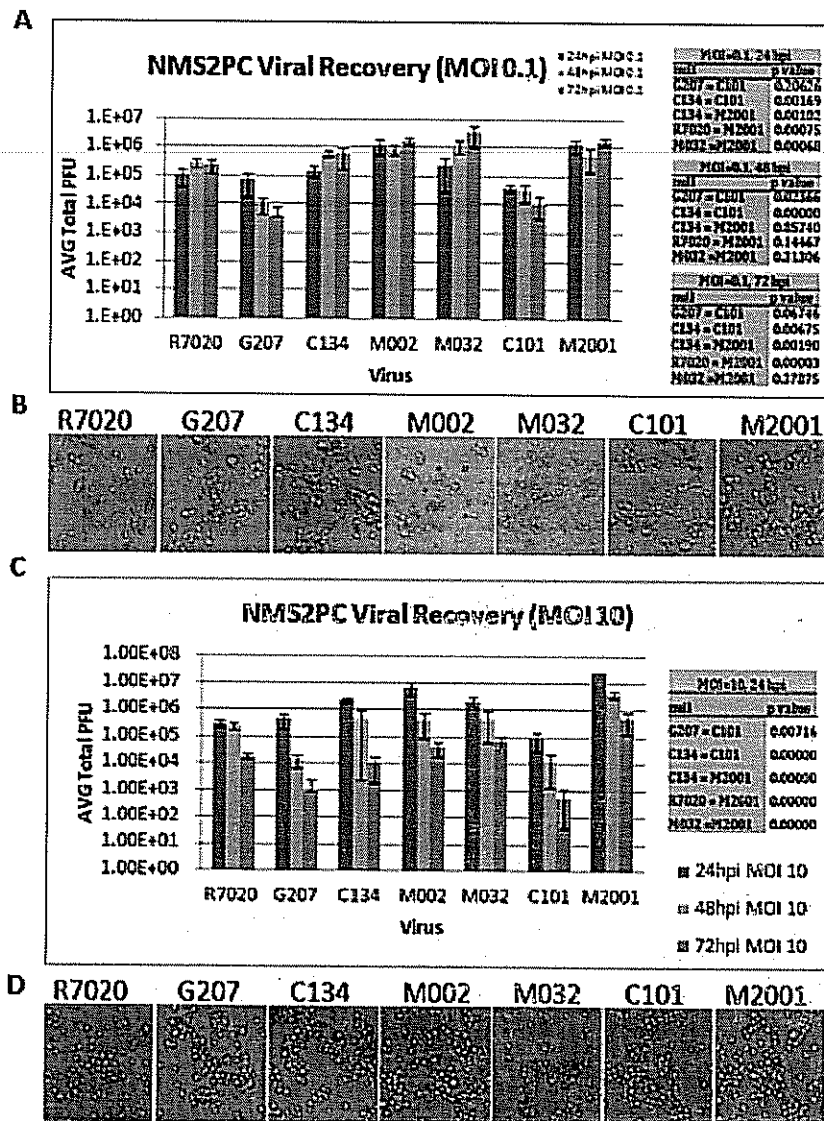


Figure 37: Composite of YST-1 human MPNST cell line *in vitro* studies.
A. Single-step replication study using a high MOI (10 PFU/cell), viral recovery data (24hpi) shown with SD. **B.** Photomicrographs of cytopathic effect at high MOI for all oHSVs tested on YST-1 cells (density of 1.5×10^5 cells/well; 100X magnification). **C.** Immunostaining studies demonstrating synthesis of late gene product (glycoprotein D), phosphorylated and total eIF-2 α along with β -actin protein loading controls at 12hpi (left panel) and 24hpi (right panel).

MPNST cell line allows the replication of all of our viral mutants under study and is sensitive to the virus as a cytotoxic agent.

Conclusion: YST-1 represents a human



Summary and Analysis (NMS2PC)

Human MPNST cell line NMS2PC was in general sensitive to viral replication and cytopathic effects as shown in the accompanying figures. In the multistep replication assay, no viruses reached to 1×10^7 pfu, with M002, M032, and C134 reaching or exceeding 1×10^6 pfu (Figure 38A). In the single step replication assay, all viruses were likewise intact for replication, replicating to at least 5×10^6 pfu, with M002 and M032 resembling wild-type virus at 1×10^8 pfu. These same 3 viruses statistically replicated superiorly to G207, C101, and R7020 (Figure 38C).

In terms of cytopathic effects (Figure 38B,D) all viruses produced some early cytopathic effect at both low and high MOI, although not to the degree of the line S462.

Conclusion: NMS2PC represents a human MPNST cell line that both allows the replication of all of our viral mutants under study and is more sensitive to the virus as a cytotoxic agent than most other human lines.

Figure 38: Composite of NMS2PC human MPNST cell line *in vitro* studies. A. Multistep Replication Study using a low multiplicity of infection (MOI: 0.1 plaque forming unit/cell) (PFU/cell). Viral recovery data shown at 24/ 48/ 72hpi with standard deviation (SD). B. Photomicrographs demonstrate cytopathic effect (CPE) in multistep replication study (24hpi) for all oHSVs tested on NMS2PC cells (100X mag). C. Single-step replication study using a high MOI (10 PFU/cell): viral recovery data (24hpi) shown with SD. D. Photomicrographs of cytopathic effect at high MOI for all oHSVs tested on NMS2PC cells (density of 1.5×10^5 cells/well; 100X magnification).

Summary and Analysis (NMS2PC cont'd.)

In the Alamar Blue assay of cell viability, all viruses were particularly ineffective against NMS2PC, even M2001 (Figure 39 A,B). At the highest MOI, the viruses were minimally effective producing about 20% CPE, except for C134.

Western blot analysis of the mutant viruses on NMS2PC (Figure 39C) demonstrate significant production of gD, a late gene product, with the exception of G207, which had minimal expression of gD. As expected, the greatest phosphorylation of eIF 2 α , was seen in G207, followed by M032 and M002, although these were not drastically different from R7020 and C134.

This interesting pattern of phosphorylation of eIF 2 α , combined with the replication findings above, warranted further study and thus this line was selected as one of the lines we will study in depth.

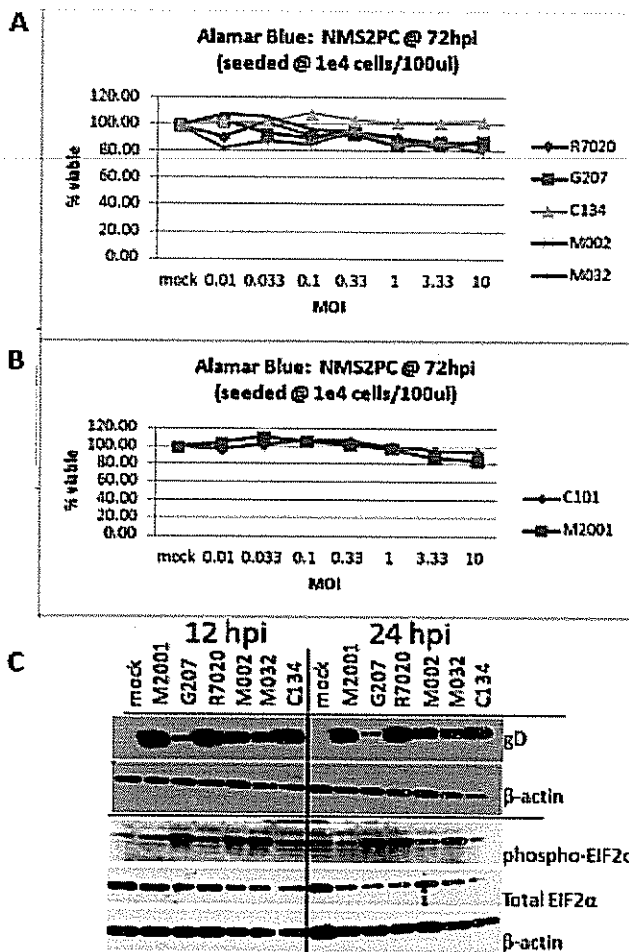


Figure 39: Composite of NMS2PC human MPNST cell line *in vitro* studies. A. Alamar Blue cell viability assay comparing clinical grade oHSVs (and the non-clinical grade oHSV M002) antitumor effect at 72hpi. B. Alamar Blue cell viability assay comparing nonclinical grade oHSVs C101 ($\Delta\gamma$ 1 34.5) vs. M2001 (wt) at 72hpi. C. Immunostaining studies demonstrating synthesis of late gene product (glycoprotein D), phosphorylated and total eIF-2 α along with β -actin protein loading controls at 12hpi (left panel) and 24hpi (right panel).

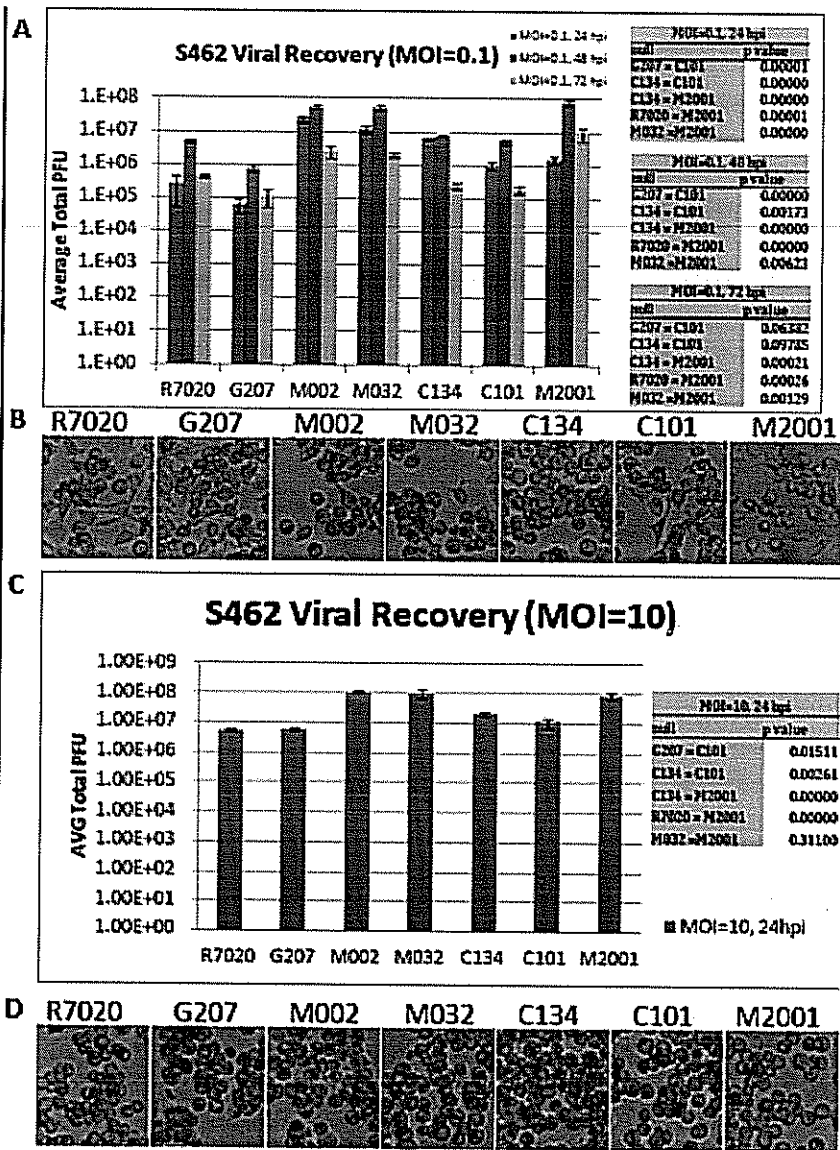


Figure 40: Composite of S462 human MPNST cell line *in vitro* studies.
A. Multistep Replication Study using a low multiplicity of infection (MOI: 0.1 plaque forming unit/cell) (PFU/cell). Viral recovery data shown at 24/ 48/ 72hpi with standard deviation (SD). **B.** Photomicrographs demonstrate cytopathic effect (CPE) in multistep replication study (24hpi) for all oHSVs tested on S462 cells (100X mag). **C.** Single-step replication study using a high MOI (10 PFU/cell). viral recovery data (24hpi) shown with SD. **D.** Photomicrographs of cytopathic effect at high MOI for all oHSVs tested on S462 cells (density of 1.5e5 cells/well:100X magnification).

particularly well in this line.

Summary and Analysis (S462)

Human MPNST cell line S462 was in general favorable for viral replication and cytopathic effects as shown in the accompanying figures. In the multistep replication assay, all viruses reached to at least 1×10^6 pfu, with M002, M032, and C134 reaching or exceeding 1×10^7 pfu (Figure 40A). In the single step replication assay, all viruses replicated to at least 5×10^6 pfu, with M002 and M032 resembling wild-typ virus at 1×10^8 . These same 3 viruses statistically replicated superiorly to G207, C101, and R7020 (Figure 40C).

In terms of cytopathic effects (40B,D) all viruses except R7020 and G207 produced significant cytopathic effects when low MOI was used, and all viruses produced cytopathic effects at high MOI. This cell line this was categorized as *sensitive*

Conclusion: S462 represents a human MPNST cell line that both highly supports the replication of all of our viral mutants under study and is uniformly sensitive to the virus as a cytotoxic agent. Viral mutants M002 and M032, and to a lesser degree, C134, replicated

Summary and Analysis (S462 cont'd.)

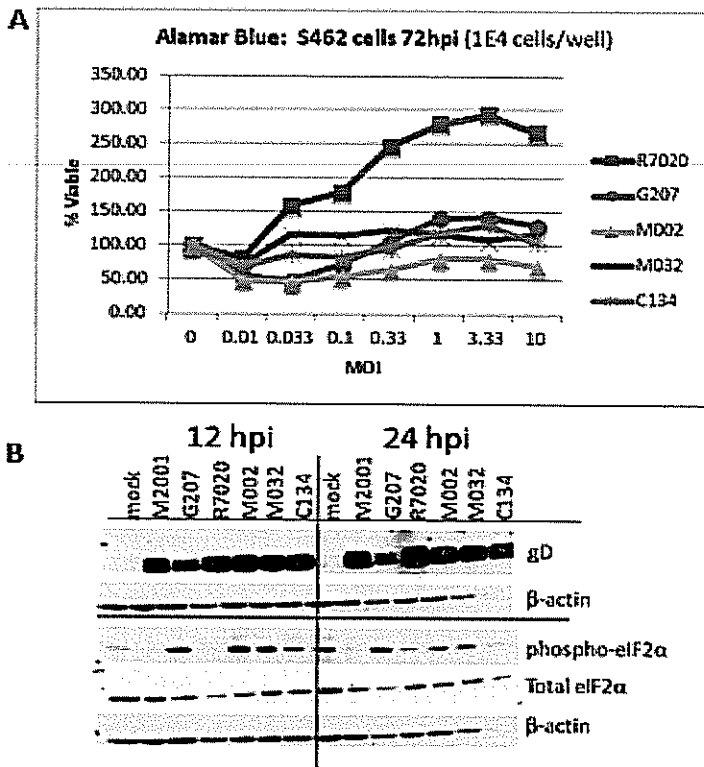


Figure 41: Composite of S462 human MPNST cell line *in vitro* studies. A. Alamar Blue cell viability assay comparing clinical grade oHSVs (and the non-clinical grade oHSV M002) antitumor effect at 72hpi. B. Immunostaining studies demonstrating synthesis of late gene product (glycoprotein D), phosphorylated and total eIF-2α along with β-actin protein loading controls at 12hpi (left panel) and 24hpi (right panel).

In the Alamar Blue assay of cell viability (Figure 41A), R7020 was particularly ineffective against S462 when compared to M2001. M002 performed relatively well, with the other viruses performing at an intermediate level. Of note, some viruses appeared to perform better at lower MOI; this is an artifact of performing the analysis at 72 hours, since higher MOIs produce an initial round of cell killing but allow regrowth of cells in a relatively low virus environment.

Western blot analysis of the mutant viruses on S462 (Figure 41B) demonstrate significant production of gD, a late gene product, with relative phosphorylation of eIF 2α, except in M2001, R7020; C134 as well shows these findings at 24 hpi. Interestingly, C134 shows modest activation at 12 hours, lessening at 24.

Conclusion This interesting pattern of phosphorylation of eIF 2α, combined with the replication findings above, warranted further study and thus this line was selected as one of the lines we will study in depth.

Summary and Analysis (HS-PSS)

Human MPNST cell line HS-PSS was in general favorable for viral replication and cytopathic effects as shown in the accompanying figures. All viruses in the single step replication assay replicated to at least 5×10^6 pfu, with M002, M032 and C134 all approaching wild-typ virus at $>5 \times 10^7$. These same 3 viruses statistically replicated superiorly to G207, C101, and R7020 (Figure 42A).

In terms of cytopathic effects (42B) all viruses produced significant cytopathic effects when high MOI was used. This cell line this was categorized as *uniformly sensitive*.

Conclusion: HS-PSS represents

a human MPNST cell line that both highly supports the replication of all of our viral mutants under study and is uniformly sensitive to the virus as a cytotoxic agent. Viral mutants M002, M032, and C134 replicated particularly well in this line.

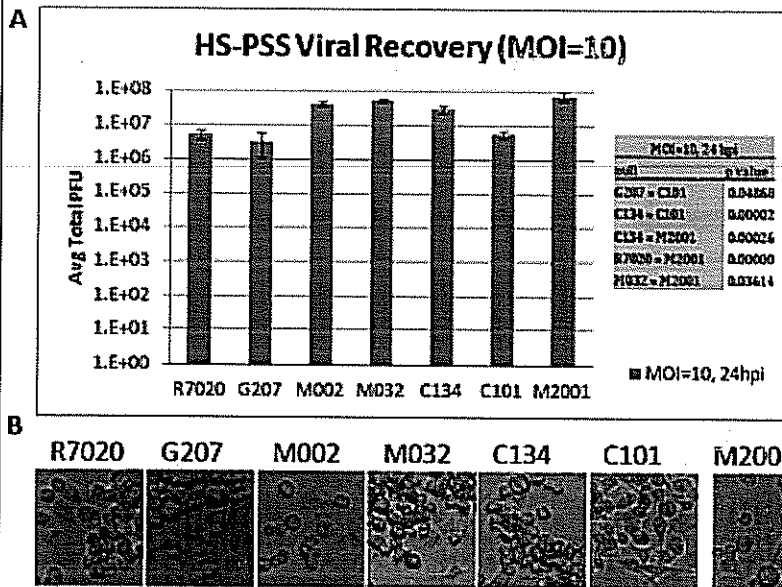


Figure 42: Composite of HS-PSS human MPNST cell line *in vitro* studies.
A. Single-step replication study using a high MOI (10 PFU/cell). viral recovery data (24hpi) shown with SD. **D.** Photomicrographs of cytopathic effect at high MOI for all oHSVs tested on HS-PSS cells (density of 1.5×10^5 cells/well; 100X magnification).

SubTask 1d. Correlate the data in the described experiments to identify oHSV-sensitive and oHSV-resistant MPNSTs and select 2 of each to study in the subsequent experiments.

Status: We have chosen representative HSV sensitive and resistant human and murine cell lines and are proceeding with studies involving these:

Human HSV Sensitive cell lines: (S462 and NMS2PC)

Human HSV-Resistant cell lines (T265-luc and S26T-luc)

Murine HSV Sensitive cell lines (A18 and 231 Trig)

Murine HSV Resistant cell lines (A382 and A202)

Based upon our preliminary analysis summarized for Figures 5-42, we have numerous MPNST cell lines (murine and human) available that will provide us with interesting scientific questions. In the event that we experience unanticipated pitfalls with the above cell lines, we have other candidate cell lines that we can use as a substitute for future studies.

SubTask 1e. Correlate the expression of alternative molecules on oHSV-resistant MPNSTs with the potential to engineer oHSVs that can utilize these receptors to enter cells that resist HSV entry.

Status: Our data show that even in HSV-resistant lines, the virus is capable of entry and replication. We are currently examining (as described in Subtask 1b) if the abundance of the HSV-entry molecule (nectin 1) alters viral entry and replication. These studies will identify if viral cell entry is the principal impediment to efficient viral replication or whether other viral functions (gene expression, protein synthesis, DNA replication, virus assembly, or egress) occurring after viral entry are suppressed by cellular antiviral responses leading to lower viral replication. Preliminary results suggest that the overexpression of nectin 1 can produce a small but reproducible improvement in viral recovery in one cell line but has no effect in the other cell line tested thus far (Figure 43).

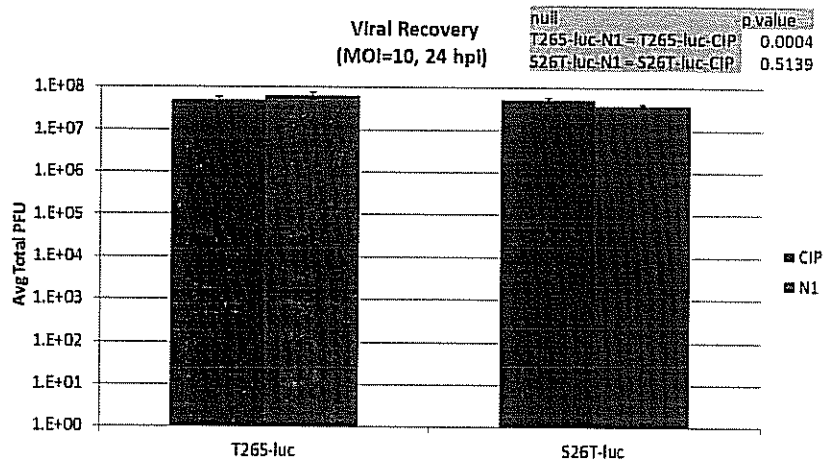


Figure 43 M2001 viral recovery following nectin-1 (N1) or mCherry (CIP) transduction in S26T-luc and T265-luc. There is a statistically significant difference in M2001 replication in the T265-luc nectin-1 overexpressing cell line. The virus recovery difference is small (state the number) and below the threshold (1/2 log) usually seen for biologically significant replication differences in in vitro replication assays. Nectin 1 overexpression did not result in a significant difference in viral recovery in the S26T cell line.

Task 2: Establish the most effective means of enhancing virus replication by modifying a HSV-resistant phenotype.

SubTask 2a. In Aim 2, we will test two different engineering solutions to enhance the expression of HSV "late genes" in both oHSV-sensitive and -resistant MPNST cell lines. We will use a combination of classical virology methods (plaque-titering at 24hr-intervals boost infection; single-step & multi-step replication assays) and FACS monitoring the extent and time course of oHSV infection based on expression of eGFP and other fluorescent markers by FACS assays

Status: These studies are commencing. We are focusing on the prototypical resistant and sensitive cell lines chosen for future studies. We are also investigating if the abundance of HSV entry receptor expression alters infection and spread in these cell lines (Figure 44).

SubTask 2b. Determine the ability of HSV-mediated expression of constitutively activated-MAP kinase kinase (MEK) will result in an increase in HSV late gene expression, higher HSV particle production and cytotoxicity.

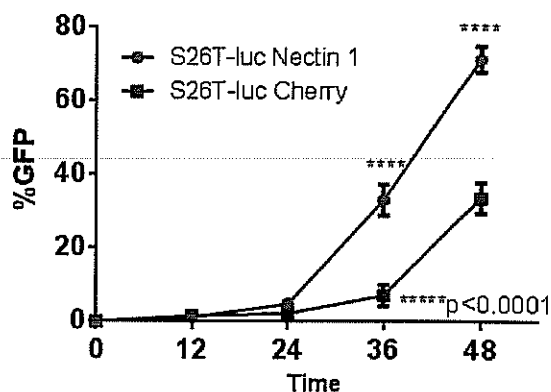


Figure 44: Summary of M2001 GFP Expression in S26T-Luc and in Nectin-1 overexpressing S26T-luc cells. These preliminary studies suggest that at low MOI the overexpression of nectin-1 may facilitate HSV spread.

Status: We have discovered two new and unexpected findings that will be pursued in follow up studies. The first novel discovery is that both of the IL-12 expressing $\Delta\gamma_134.5$ viruses, M002 and M032, are capable of late viral protein synthesis that surpasses that of other $\Delta\gamma_134.5$ viruses tested (C101 and G207) and can replicate as well as wild-type HSV in the MPNST tumor cells tested. However, unlike wild-type HSV or the two recombinants, R7020 and C134, the IL-12 expressing $\Delta\gamma_134.5$ viruses do not contain PKR-evasion genes. This is shown in Figure 45 Panel A, that M002 and M032 are unable to block PKR-mediated phosphorylation of eIF-2 α .

(Figure 45 Panel A p-eIF2 α immunostaining panel) This suggests that in the MPNST tumor cells the M002 and M032 oHSVs encode an alternative mechanism to allow late viral protein synthesis that differs from that of the C134 and R7020. There are two possible explanations: (i) either the expression of IL-12 enhances virus translation in the infected MPNST cell lines or (ii) that the M002 and M032 recombinants contain secondary mutations that enhance viral protein translation independent of eIF-2 regulation of translation initiation. Efforts are currently underway to identify genetic differences between the M002/M032 recombinants and the parent $\Delta\gamma_134.5$ recombinant used to construct the IL-12 expressing viruses.

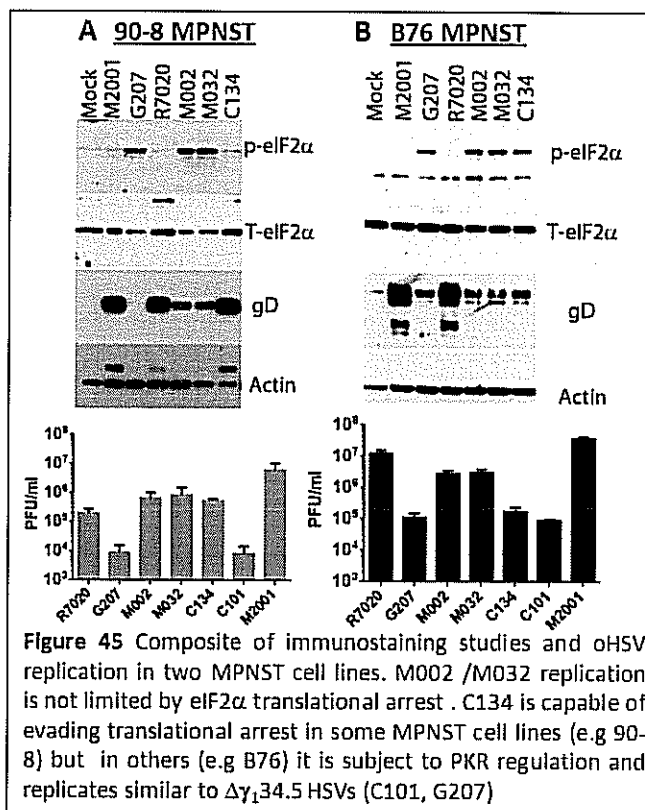


Figure 45 Composite of immunostaining studies and oHSV replication in two MPNST cell lines. M002 /M032 replication is not limited by eIF2 α translational arrest. C134 is capable of evading translational arrest in some MPNST cell lines (e.g 90-8) but in others (e.g B76) it is subject to PKR regulation and replicates similar to $\Delta\gamma_134.5$ HSVs (C101, G207)

The second novel finding is that certain MPNST cell lines restrict C134 late viral protein synthesis and replication. Preliminary studies show that in most of the MPNST cell lines, C134 is capable of PKR-evasion and replicates similar to the $\gamma_134.5$ containing viruses (R7020 and M2001). This is consistent with our prior studies in glioma tumors (Shah 2007). However, in select MPNST cell lines, C134 is unable to evade PKR-mediated translational arrest and its replication is restricted similarly to that seen with $\Delta\gamma_134.5$ virus (G207 and C101). This divergent late protein synthesis phenotype is summarized using 2 of the MPNST cell lines shown in Figure 45. In the Human MPNST 90-8 cell line, C134 is capable of evading translational arrest based upon decrease in eIF-2 α phosphorylation and increase in glycoprotein D expression in the C134 infected cells. In this cell line the $\Delta\gamma_134.5$ cell lines, G207, M002, and M032 induce phosphorylation of eIF-2 α and produce less glycoprotein D (a late HSV gene) than the recombinants

expressing PKR-evasion genes (M2001, R7020, and C134). This ability to synthesize late viral proteins also correlates with improved viral replication for the C134 recombinant. In contrast to the 90-8 cell line, the mouse B76 MPNST cell line activated eIF-2 α after infection by $\Delta\gamma_134.5$ oHSVs and chimeric C134, as indicated by its phosphorylation. Consonant with this, the synthesis of late gene product gD was downregulated in the $\Delta\gamma_134.5$ and C134 viruses and the recovery of infectious C134 virus assayed by plaque-forming ability was decreased to levels equivalent to that seen with the 3 $\Delta\gamma_134.5$ oHSVs. These cell lines will provide valuable tools for further characterization of the mechanism by which C134 and specifically the IRS1 gene targets PKR and the translational machinery. This work may in turn allow improved efficacy of C134 when ultimately tested in clinical trials.

SubTask 2c. Determine the ability of HSV-mediated expression of a human cytomegalovirus gene, IRS-1, that promotes late gene expression in CMV, to increase oHSV late gene expression, higher HSV particle production and MPNST cytotoxicity.

Status: These studies are near completion and as shown in Figures 5-42, We have tested if HCMV IRS1 expression improves $\Delta\gamma_134.5$ replication. The results show that in numerous MPNST cell lines (B86, 231-Trig, A18, T265-luc, 90-8, YST-1, and S462), C134 ($\Delta\gamma_134.5$, IRS1) replicates better than $\Delta\gamma_134.5$ virus or the cell line supports efficient late viral protein synthesis for all viruses. In many of these cell lines, the improved C134 replication correlates with improved late viral gene expression (e.g. gD expression) and PKR evasion (relative absence of p-eIF2 α) when compared to $\Delta\gamma_134.5$ virus. In contrast, in other cell lines (A387, A202, B91, B96, B97, B109, A292, A390, A391, B76, and S26T-luc) IRS1 expression does not benefit the virus leading to similar replication as a $\Delta\gamma_134.5$ virus.

SubTask 2d. Examine the impact of p38MAPK activation in MPNST tumors to have a positive or negative impact on the ability of these engineered oHSVs to display greater replication and oncolysis.

Status: See explanation in SubTask 2e. Based on our observations, these two tasks do not seem to be critical to the development of more effective oHSVs for treatment of MPNSTs and consequently will be deleted.

SubTask 2e. Correlate and compare the data sets obtained from the studies in oHSV-sensitive and -resistant MPNSTs using the caMEK viruses (R2660, R2636) and the IRS-1 viruses (C134, C154).

Status: One of the possible solutions to the issue of poor replication is the level of Mitogen-Activated Protein Kinase activation (phosphorylation), which is perceived as important for optimum late virus gene expression and optimum downregulation of PKR activation preventing eIF2 α activation which would shut-off protein synthesis. A strategy has been to consider exogenous expression of an upstream mediator, mitogen-activated protein kinase kinase (MEK 1/2). oHSVs expressing constitutively activated MEK (ca-MEK) or dominant negative MEK are available to study this. However, our studies show that most MPNSTs already have high levels of activated p38 MAPK and phosphorylated Erk1/Erk2, immediate downstream targets of MEK. Thus, a strategy of trying to coordinately upregulate MEK activation to achieve greater virus replication is likely not to be a worthwhile study. Based on our observations of elevated MEK with several MPNSTs, we are no longer considering that ca-MEK oHSV would be an effective strategy, unless we discover MPNSTs that would not already have phosphorylation of MEK.

SubTask 2f. Select the most appropriate (set of) oHSV virus(es) to advance to preclinical *in vivo* studies with human and mouse MPNSTs.

Status: Several studies remain to be completed before the candidate oHSVs can be appropriately selected. Preliminarily, we believe both M032 and C134 will prove to be the most attractive candidates. Once we have completed our evaluation of our panels of MPNSTs with regard to virus infectivity, virus replication and capacity of our experimental and clinical candidate HSVs to produce an oncolytic effect *in*

vitro, we will be able to select the most appropriate MPNST lines to use in our heterotopic and orthotopic models to evaluate the *in vivo* effects. In essence, the xenogeneic models with human tumors in immunocompromised mice will permit evaluation of the 3 clinical candidate viruses. In our syngeneic mouse models in immunocompetent mice, we will also be able to assess anti-tumor efficacy as it is affected by the host immune response. These studies are the basis of Milestone 4.

Task 3: Validate the ability of selected oHSV to produce an oncolytic anti-MPNST effect in established tumors in mouse models and quantify the capacity of a low dose of radiation to enhance this anti-tumor effect.

Status: None of the animal studies have been initiated since selection of the appropriate prototypic model tumors for these studies is still pending. We need a much more complete picture that was to be provided by the first 3 tasks to make an informed decision regarding the design of these animal studies. With a significant portion of the data in hand, we expect that we will be able to begin the studies associated with the Milestone during the second year of funding.

SubTask 3a. Tumor cells growing *in vivo* often display significant biologic differences from those growing *in vitro*. The first subtask will be to establish a baseline of the ability of oHSVs to infect and kill human or mouse MPNST cell lines transplanted into appropriate host mouse strains. The ability of generic $\Delta\gamma_134.5$ HSV (G207, NV1070) to produce an antitumor effect as observed in Task 1c *in vitro* will be determined by direct injection of bioluminescence-enabled human or mouse MPNSTs placed in an orthotopic location (sciatic nerve). Both oHSV-sensitive and oHSV-resistant MPNSTs will be compared.

Status: We have not initiated these experiments

SubTask 3b. Compare the abilities of selected oHSVs (e.g., M002, C134, R2660, etc) from previous studies to produce an enhanced anti-MPNST effect compared to that of the generic viruses. Oncolysis of orthotopically-placed oHSV-sensitive and oHSV-resistant MPNSTs will be compared.

Status: We have not initiated these experiments.

SubTask 3c. Determine whether or not a single low dose of radiation (2-5Gy) delivered to the tumor within 24 hrs of injection of selected oHSVs enhances the replication and spread of the virus yielding an enhanced anti-MPNST effect. Irradiation has a more pronounced and sometimes paradoxical effect *in vivo* than it does *in vitro* and thus, irradiation effects will not be explored *in vitro*.

Status: We have not initiated these experiments.

SubTask 3d. Compare and correlate the findings from these sub-tasks to select the most likely combination of oHSV and adjunctive therapy that will be most effective oncolytic, anti-MPNST modality for human or mouse MPNSTs transplanted orthotopically and test this combination in the P₀-GGF β 3 x Elux mouse against MPNST tumors that arise sporadically and spontaneously.

Status: We have not obtained sufficient data to be able to complete this subtask.

SubTask 3e. Review the entire data set to design studies that will be able to validate the selected oHSV with or without adjunctive therapy that can be advanced to a Phase I/II clinical trial to test the safety, identify unanticipated toxicities and establish preliminary evidence of efficacy in patients with MPNST.

Status: We have not obtained sufficient data to be able to complete this subtask.

Appendix i

High nectin-1 expression in malignant peripheral nerve sheath tumor cell lines benefits oncolytic herpes simplex viruses which compensate for $\gamma_134.5$ deficiency

ABSTRACT

Limited expression and distribution of nectin-1, the major herpes simplex virus-1 entry receptor, within tumors has been proposed as an impediment to oncolytic HSV (oHSV) therapy. To determine if resistance to oHSV in malignant peripheral nerve sheath tumors (MPNSTs) was explained by this hypothesis, nectin-1 expression and oHSV replication were assessed in a panel of MPNST tumor lines using an array of $\gamma_134.5$ -attenuated oHSVs and a wild-type (wt) $\gamma_134.5$ virus. Although a positive correlation between nectin-1 and viral replication was found for the wt virus ($R=0.75$, $P=0.03$), no correlation for the attenuated viruses was observed. The chimeric virus C134 which compensates for $\gamma_134.5$ attenuation by expression of CMV IRS1 was positively correlated ($R=0.62$, $P=ns$). To determine whether increased nectin-1 expression improved oHSV replication, the less-permissive cell lines were transduced with nectin-1. The results show that while this marginally improved wild-type virus replication, the attenuated virus derived ambiguous benefit. We then examined whether nectin-1 overexpression improved viral spread and found that it benefitted both attenuated and wild-type HSV. This improvement to cell-cell spread of fully attenuated oHSV in resistant cell lines did not approach that of the wild-type or C134 viruses. Additionally, spread of the attenuated virus in nectin-1 overexpressing resistant cells did not reflect the spread observed in permissive MPNST cell lines. Based on this evidence we propose that high nectin-1 expression in MPNSTs is a likely determinant in the success of oHSV therapy, but only with viruses that functionally compensate for the $\gamma_134.5$ deletion.

INTRODUCTION

Although great technical progress has been achieved by small-molecule cancer therapy, chemotherapeutic agents for several highly aggressive tumor types have remained marginally effective at best. A number of therapeutic alternatives have been proposed to treat these cancers. Recent research has revisited the mid-20th century strategy of employing viruses as oncolytic agents[1]. Advances allowing the manipulation of viral genetics have yielded a number of candidate viruses with tumor-selective cytotoxicity profiles[2]. Among these, oncolytic HSV-1 derivatives are particularly advantageous as the modifications conferring their tumor-selective properties do not severely attenuate their replication[3]. In addition, oHSV can tolerate large genetic inserts and anti-HSV medications are available in the event of adverse viral pathology. Current oHSV therapy is based on the attenuation of HSV-1 neurovirulence by deletion of the $\gamma_134.5$ genes. While the product of the $\gamma_134.5$ gene is necessary for classic HSV pathogenesis in healthy tissue[3], it is dispensable for replication in malignantly transformed cells, resulting in selective viral replication and cytotoxicity within cancer cells. These attenuated vectors have a clinically-verified safety profile in patients with malignant glioma and have produced measureable anti-tumor responses [4-7]. Although most oHSV efforts have focused on treatment of brain tumors, more recent work has explored the use of oHSV as an alternative therapy for other tumors of the central and peripheral nervous system, specifically malignant peripheral nerve sheath tumors (MPNSTs)[8-12]. MPNSTs are highly aggressive malignant neoplasms believed to originate within the Schwann cell lineage[13] and are most commonly associated with the genetic condition neurofibromatosis type-1 (NF1)[14]. As with malignant glioma, treatment options for MPNST tumors beyond surgery are scarce, resulting in a median survival of approximately 26 months[15, 16].

Despite significant progress in translating oHSV therapy from laboratory to clinic, clinical responses have been inconsistent. Thus, our current research efforts have focused on deciphering the mechanisms of oHSV resistance within the tumor environment. One proposed limitation is insufficient or heterogeneous expression of the HSV-1 entry receptors, resulting in limited establishment of the primary infection and subsequent spread of the progeny

virions [17-20]. The mechanisms and requirements governing HSV-1 entry have been widely reviewed [21-24]. Studies of viral surface protein knockouts and HSV-1 resistant cell lines have established that a minimum of four viral glycoproteins (gD, gB, and gH/gL) and a cellular glycoprotein D (gD)-interacting receptor are necessary and sufficient to trigger cellular entry [25-29]. To date, three functionally and structurally distinct cellular gD-interacting receptors have been discovered. Nectin-1, a cellular adhesion protein located at epithelial adherens and tight junctions [30] and the pre-synaptic junctions of neurons [30, 31], has been established as the major HSV-1 entry receptor for neurons [32, 33] and mucosal epithelium [34-36]. Nectin-1 is widely expressed in a variety of tissues [37, 38], including those of neural origin [39] as well as neoplasms of nervous tissue [40]. Herpes virus entry mediator (HVEM), a member of the tumour necrosis factor receptor family, has also been proven functional as an entry receptor [41] as well as the recently discovered, but more poorly understood, entry receptor 3-O-sulfated heparan sulfate (3-OS-HS) [42]. Other HSV-1 entry mediators include $\alpha v\beta 3$ integrins [43] which interact with glycoprotein H (gH) or heparan sulfate proteoglycan (HSPG) [44], paired immunoglobulin-like type 2 receptor- α (PILR α) [45], non-muscle myosin heavy chain IIA (NMMHCIIA) [46], and myelin-associated glycoprotein (MAG) [47] which have all been shown to interact with glycoprotein B (gB). Finally, other cell surface molecules have been shown to enhance HSV-1 entry including syndecans-1 and 2 [48], as well as macrophage receptor with collagenous structure (MARCO) [49], though the broad necessity of these in permitting HSV-1 infection and spread remains to be determined. These entry components have not yet been implicated in limiting the oncolytic capacity of oHSV, but no research has excluded that possibility.

Here, we have tested the hypothesis that expression of the HSV-1 entry receptor nectin-1 limits oHSV replication and spread in MPNST cells. The effects of increased nectin-1 expression in oHSV-resistant MPNST cell lines were evaluated using both wild-type and $\Delta\gamma_1 34.5$ attenuated viruses.

RESULTS

Viral recovery highlights MPNST cell lines permissive and resistant to oHSV replication

To determine whether MPNST cells are permissive to oHSV replication, the MPNST cell lines, or their derivatives, STS-26T, T265-2c, NMS2-PC, S462, YST-1, 90-8, ST88-14, and 2XSB were infected with a panel of genetically modified HSV-1. A number of these MPNST cell lines are commonly used throughout the MPNST literature and several have been further transduced in our studies with luciferase ("-luc") for future *in vivo* studies. MPNST cells were infected at a multiplicity of infection (MOI) of 10 (single-step replication assay) and MOI of 0.1 (multi-step replication assay) using C101 ($\gamma_1 34.5^{-/-}$, EGFP), G207 ($\gamma_1 34.5^{-/-}$, UL39-), R7020 (single copy $\gamma_1 34.5$), and M2001 ($\gamma_1 34.5^{+/+}$, EGFP) viruses. M2001 is representative of wild-type HSV-1 virus, while C101 has both regions of the neurovirulence gene $\gamma_1 34.5$ deleted. Both M2001 and C101 express EGFP. G207 is mutated in both regions of $\gamma_1 34.5$ and contains a lacZ insert in UL39, disabling expression of ICP6 the large subunit of ribonucleotide reductase. R7020, originally developed as an HSV vaccine, contains part of the U_S region of HSV-2 inserted into HSV-1(F) resulting in a loss of one copy of $\gamma_1 34.5$. [50] Both G207 and R7020 have been produced as cGMP product for oncolytic therapy.

Viral titers following infection of all MPNST cell lines at an MOI of 10 ranged as follows (Figures 1a-d): M2001 (5.1×10^6 to 1.8×10^8 PFU), R7020 (9.7×10^4 to 2.7×10^6), C101 (8.8×10^3 to 2.4×10^6 PFU), and G207 (3.5×10^4 to 2.9×10^6 PFU). Multi-step (MOI=0.1) data collected at 24, 48, and 72 hpi revealed a variety of responses across cell lines (see supplementary data).

On the basis of the single and multi-step replication data, the STS26T-luc and T265-luc cell lines were determined to be resistant to oHSV replication, while the S462-luc and NMS2-PC cell lines were identified as permissive.

MPNST cell lines express variable nectin-1 and HVEM entry receptor levels.

To examine the hypothesis that entry receptor availability is predictive of oHSV sensitivity, the expression intensity and distribution of nectin-1 and HVEM, for which there are validated antibodies, was measured in a panel of MPNST cell lines by flow cytometry. The mean fluorescence intensity was then converted to a known antibody binding capacity (ABC) by quantification beads, allowing receptor comparison across cell lines. Each MPNST cell line was >95% nectin-1 positive, compared to the isotype control, except for 90-8-luc and T265-luc which were both ~55% positive (Figure 2a). The mean ABC for nectin-1 ranged from 2,805 (90-8-luc cells) to 35,815 (2XSB cells). HVEM expression was generally low with <10% positive in most cell lines, except 2XSB (94.1%), YST-1 (59.0%), and S462-luc (19.6%) (Figure 2b). The mean ABC for HVEM across the entire population was also low; below 3,000 ABC, except 2XSB (11,353). With the exception of 2XSB and YST-1, the distribution of HVEM was low with no greater than 23% of any population expressing HVEM (Figure 2b). High levels of HVEM, ranging from 31,852 to 123,863 ABC were present in small sub-populations (0.54% to 2.98%) in each cell line (data not shown). As a negative control, the CHOK1 cell line, previously established as HSV entry receptor deficient[44], displayed no expression of nectin-1 or HVEM relative to isotype controls (data not shown). In summary, nectin-1 expression was more prominent in MPNST cell lines compared to HVEM. Because HVEM expression was negligible in the majority of MPNST cell lines, nectin-1 was assumed to be the primary HSV-1 entry receptor for MPNSTs.

Endogenous nectin-1 expression does not correlate significantly with oHSV replication

Guided by the single-step viral recovery and nectin-1 quantification described above, a correlative analysis was performed to test the hypothesis that increased nectin-1 in MPNSTs is predictive of greater sensitivity to oHSV, as has previously been reported in other tumor types. Pearson's correlation coefficients were calculated between viral recovery data and nectin-1 expression levels. Although a statistically significant positive association was found for the wild-type M2001 ($R=0.75$; $P=0.03$) (Figure 3a), replication of the attenuated oHSVs was not associated with entry receptor expression (Figures 3a-d).

Overexpression of nectin-1 in resistant cell lines

To evaluate the impact of increased nectin-1 expression on oHSV sensitivity in more controlled studies, the oHSV resistant cell lines STS26T-luc and T265-luc were transduced with a human nectin-1 expressing lentivirus, or an mCherry expressing control. Expression of nectin-1 and mCherry was confirmed by flow cytometry. As expected, nectin-1 expression was significantly increased compared to the corresponding parent (untransduced) cell lines. The results show that transduction increased nectin-1 expression in T265-N1 by 167 fold, compared to the parent line (T265-luc)(Figure 4a). Two daughter cell lines were isolated from the nectin-1 transduction of STS26T-luc cells: STS26T-N1HI which expressed 100 fold greater nectin-1 compared to the parent (Figure 4b) and STS26T-N1MED which contained an approximately 2:1 mix of two distinct populations respectively expressing 4 and 81 fold greater nectin-1 (Figure 4c). To determine if the lentivirus encoded nectin-1 was functional as an HSV-1 entry receptor, receptor deficient cell line CHOK1 was transduced (Figure 4d) and viral replication examined in these cells. Following infection with M2001, viral recovery yielded 6.9×10^6 PFU for the nectin-1 transduced cell line CHO-N1 as compared to 3.3 PFU for the parent CHOK1 (Figure 4e), proving that the nectin-1 overexpressed by our lentivirus was functional for HSV-1 entry.

Impact of nectin-1 overexpression on viral replication in resistant cell lines

If low nectin-1 expression diminishes the odds for oHSV to establish a primary infection, we would predict that increased nectin-1 expression would increase the number of initial entry events, resulting in subsequent replication and an increase in the production of virus. To determine the impact of increased nectin-1 expression on viral

replication both single-step and multi-step viral recovery assays were performed following nectin-1 transduction of the resistant T265-luc and STS26T-luc cell lines. Of note, no notable differences in viral recovery were observed between the parent and mCherry-transduced control cell lines (data not shown). At an MOI of 10 replication of M2001 was significantly improved (0.62 log increase) with lentivirus-based expression of nectin-1 in T265-luc cells, compared to the mCherry-transduced control (6.47×10^6 to 2.67×10^7 PFU; $P < 0.001$), while a significant 0.27 log decrease was observed for C101 (1.60×10^4 to 8.00×10^3 PFU; $P < 0.01$) (Figure 5a). For the multi-step replication assays (MOI=0.1) of C101 and M2001 in T265-N1, significantly different replication levels were detected at each timepoint, except C101 at 48 hpi (Figures 5b-c). Despite significant differences in replication titers for M2001, no differences greater than 0.5 log were noted for any timepoint except at 24 hpi (0.61 log increase).

Viral recoveries from the high nectin-1 (STS26T-N1HI) and medium-nectin 1 (STS26T-N1MED) expressing sub-lines were compared to the control line STS26T-Cherry. In the single-step assay, M2001 showed a significant increase ($P < 0.01$) in STS26T-N1MED and a significant decrease ($P < 0.01$) in STS26T-N1HI (Figure 5d), whereas viral recovery of C101 in single-step assays showed no significant changes within either cell line (Figure 5d). For the differences in M2001 viral recovery, no change was observed to be greater than 0.5 log.

For multi-step assays with M2001 in STS26T-N1MED, significantly greater (>0.5 log) recovery was observed at each timepoint, except 72 hpi (Figure 5e). Increased replication of M2001 in STS26T-N1HI was detected at 24 hpi ($P < 0.01$; 0.59 log) but significantly decreased in titer at later timepoints (0.39 and 1.20 log at 48 and 72 hpi, respectively). C101 replication in both of the nectin-1 transduced STS26T-luc lines showed consistently and significantly higher titers, compared to STS26T-Cherry at every timepoint (Figure 5f), with notable 3.8 and 1.5 log increases at 72 hpi for STS26T-N1MED and STS26T-N1HI, respectively. Interestingly, no statistically different viral recovery was noted between M2001 and C101 in the STS26T-N1MED cell line at the 72 hpi timepoint.

In summary, nectin-1 overexpression had little to no benefit to single-step HSV recovery rates in resistant MPNST cell lines, indicating the endogenous levels of nectin-1 are likely sufficient to establish an initial infection when a saturating amount of virus is used. The multi-step assay in T265-luc-N1 demonstrated no major trends in improvement to replication for either wild-type or attenuated virus, while increased nectin-1 in STS26T-luc showed significant benefits to both viruses.

Impact of nectin-1 overexpression on cell-cell spread in resistant cell lines

To determine if increased nectin-1 expression improved the rate of oHSV spread through a monolayer of resistant cells, the percentage of cells expressing virus-derived GFP (C101 or M2001) was assessed over time following infection at MOI=0.1. Compared to parental lines, M2001 spread more rapidly in all nectin-1 transduced cells (Figures 6a and c). At 36 hpi, the two nectin-1 transduced lines of STS26T-luc were greater than 85% positive for M2001, compared to 45% positive in the parent line. Similarly, T265-N1 was 95% positive at 36 hpi, compared to 22% of the parent line at the same timepoint. Despite the slower rate of spread in the parent lines, M2001 eventually spread to over 95% in both parent lines (STS26T-luc and T265-luc) by 72 hpi, demonstrating that all cells are normally susceptible to infection by the wild-type virus within the observed timeframe.

C101 was incapable of sustained infection in either of the resistant MPNST parent lines (T265-luc and STS26T-luc) as apparent by a decline in the percentage of GFP positive cells over time (Figures 6b and d). Increased nectin-1 expression improved C101 spread over time in both of the cell lines with 23% (T265-luc) and 27% (STS26T-luc) of the cells GFP positive at 72 hpi. STS26T-N1MED showed no significant change between 12 and 72 hpi in the percent positive, but was significantly higher compared to the parent line at all timepoints (Figure 6d).

For the purposes of comparison, S462-luc and NMS2-PC, two lines determined to be permissive to oHSV replication, were also analyzed for cell-cell spread by monitoring viral GFP expression. As expected, M2001 rapidly infected greater than 65% of both cell lines by 36 hpi (Figure 6e). In contrast to the resistant cell lines, C101 achieved 83% and 96% positive in NMS2-PC and S462-luc respectively by 60 hpi (Figure 6f).

In summary, increased nectin-1 expression in resistant MPNST cell lines positively influences cell-cell spread although more modestly for C101 as compared to M2001.

DISCUSSION

Attenuation of HSV-1 by mutation of the $\gamma_134.5$ gene renders the virus sensitive to the intrinsic host antiviral response and the Type I IFN pathway. In many instances, through the process of malignant transformation, numerous pathways involved in recognition and response to viral infection may be downregulated or inactivated in a tumor cell population. In theory, this diminishes the need for a virus competent in immune evasion and allows selective replication of $\gamma_134.5$ null viruses in cancerous cells as opposed to healthy tissue. Nonetheless, the handicap of the $\gamma_134.5$ deletion may still amplify the sensitivity of the virus to other environmental determinants such as entry receptor expression, especially when tumor cells exhibit any capacity for antiviral response.

All of the MPNST cell lines we studied demonstrated susceptibility to infection and replication by the four viruses we tested. At an MOI of 10, C101 and G207 yielded comparable viral titers (10^4 - 10^6 PFU). R7020 generally produced 10 fold higher titers than the $\gamma_134.5^{-/-}$ viruses. M2001 (wild-type $\gamma_134.5$, EGFP) produced the highest amount of virus and was ~ 100 fold higher than $\Delta\gamma_134.5$ viruses. Overall, the rank of each cell line by viral titer was similar to what has previously been reported between several of these MPNST cell lines infected with $\gamma_134.5$ wild-type (hrR3) and null (G207) viruses[9].

Although HSV-1 entry receptors have not been previously identified in MPNSTs, it has been established that nectin-1 is widely expressed in neurons and neural tissues[39, 40]. It is also accepted that nectin-1 is the major entry receptor for HSV-1 in neurons [32, 33]. Upon examination of nectin-1 and HVEM expression in our panel of MPNST cell lines, we found detectable levels of nectin-1 in all of the lines as measured by flow cytometry. HVEM was expressed in some MPNST cell populations (<23% positive) except the cell lines YST-1 and 2XSB which expressed the receptor across a majority of the population. In previous studies where detectable HVEM expression was observed in other cancer lines, nectin-1 was still attributed as the primary entry receptor [17, 18] similar to our conclusions for MPNST cells. Other purported entry receptors (e.g 3-OS-HS and nectin-2) were not examined. Although a commercially available antibody recognizing the 3-OS-HS entry receptor was not available, *in situ* hybridization studies in neuronal tissue have demonstrated that Schwann cells were consistently negative for the 3-O-sulfonyltransferases which modify heparan sulfate to 3-OS-HS[51], suggesting that this receptor may be similarly unexpressed in MPNST cells. Nectin-2 has only been shown useful as an HSV-1 entry receptor for laboratory derived gD mutants [52-54] and was not assessed here.

While two prior studies involving thyroid cancer[17] and head and neck squamous cell carcinoma (HNSCC)[18] cell lines demonstrated significant correlations between replication of NV1023, a derivative of R7020, and nectin-1 expression, we found no correlative associations between G207, C101, or R7020 and the MPNST cell lines studied. There was a strong and significant correlation for the representative wild-type virus M2001. Several cell lines acted as outliers and contributed to the poor correlation for the attenuated viruses. Although the tumor line 90-8-luc expressed the least amount of nectin-1 of all MPNST cell lines tested, it produced among the highest titers of oHSV compared to other cell lines. S462-luc is notable in that it consistently produced markedly higher titers of attenuated virus across all lines. Conversely, the 2XSB cell line which expressed the greatest nectin-1 of the cell lines tested ($\sim 2x$ that of S462-luc or $\sim 15x$ that of 90-8-luc) did not support good oHSV replication. While the $\gamma_134.5$ containing virus

M2001 replicated well in this line (1.82×10^8 PFU), the attenuated $\Delta\gamma_134.5$ viruses produced greater than 1000 fold less virus compared to M2001.

Nectin-1 overexpression in resistant MPNST cell lines demonstrated somewhat divergent assessments of viral replication. T265-N1 showed statistically and biologically significant improvement to M2001 replication, but none to C101. Nectin-1 overexpression in S26T-luc revealed statistically and biologically relevant improvement in multi-step replication of the attenuated C101 virus, but had no impact in the single-step assay. In our lab, interpretations of changes in viral titer are generally put in context of “biological significance” in addition to statistical significance. Our benchmark for determining biologically relevant changes as relayed through viral replication is assumed to be an absolute change in titer greater than 0.5 log.

In addition to the production of high viral titers, a major assumption of efficacy in oncolytic therapy is the ability of the virus to spread beyond its initial point of infection. Although entry receptors are necessary to mediate spread, the extent to which an increased level of nectin-1 impacts viral transfer has not yet been explored in oHSV research. To assess this, we utilized flow cytometry to monitor the percentage of cells expressing viral GFP from either C101 or M2001. The results demonstrate that a representative wild-type virus M2001 is capable of spreading to nearly all cells in every cell line tested, and that increased nectin-1 expression increases the velocity of this spread. This observation was noted for both M2001 and C101, and was achieved in all of the nectin-1 transduced lines, except for C101 in STS26T-N1MED. One characteristic of all the nectin-1 transduced cell lines (T265-N1HI, S26T-N1HI, S26T-N1MED, CHO-N1, and others unreported), as well as the highest endogenous nectin-1 expressing cell line 2XSB, was the increased formation of syncytia upon virus infection (see Supplementary Figure). This occurred with C101 and to a greater extent with M2001. The occurrence of increased HSV-1 induced syncytia with high nectin-1 expression has not been previously reported. We suggest that in some cases the cell-cell fusion resulting in the formation of syncytia in the high nectin-1 expressing lines diminishes the ability of the virus to exhaust the replication capacity of a single cell resulting in lower overall titers. For example, more rapid spread of M2001 was observed in S26T-N1HI compared to S26T-N1MED, however titers of M2001 were generally higher in S26T-N1MED. C101 also showed improved spread in the nectin-1 overexpressing cell lines with greater than 25% positive in T265-N1HI and S26TN1HI compared to <3% for the parents by 72 hpi. Despite the increased viral spread in the nectin-1 transduced resistant cell lines, the maximum spread was less than that observed in permissive MPNST cell lines with endogenous nectin-1 expression. For example in the permissive cell line S462-luc, C101 was capable of infecting and spreading through 96% of the cells within 60 hpi. These data show that while nectin-1 overexpression does benefit viral spread, high nectin-1 expression is not sufficient to generate oHSV permissivity in resistant cells and may only account for a minor component of the resistance to oHSV therapy. The facts that this disparity in spread occurred in transduced cell lines expressing greater than ~30 fold more nectin-1 than the highest endogenous levels in an MPNST cell line, and that C101 spread did not occur in S26T-N1MED, leads to the conclusion that cellular events that limit $\gamma_134.5$ null oHSV replication following entry are more important in limiting $\Delta\gamma_134.5$ infection and spread to neighboring cells. In contrast, M2001 replication correlates more closely with nectin-1 levels suggesting nectin-1 to be an upper limit to replication.

A potential limitation in the interpretation of these data is the assumption that increased nectin-1 expression by itself is directly responsible for HSV-1 entry and spread. It is possible that increased coexpression of intracellular nectin-1 interacting proteins such as afadin are also required to observe these effects. The cytoplasmic region of nectin-1- α , the full-length isoform used in this research, which binds to afadin via its PDZ domain, has been shown dispensable for two modes of HSV-1 spread, extracellular viral fusion and cell-cell fusion[55, 56]. There is, however, some controversy over the requirement of the nectin-1 cytoplasmic region and afadin interaction to mediate a third mode of spread, cell-cell transmission. Negative effects on HSV-1 spread have been observed in both nectin-1 PDZ mutants and following afadin knockdown[57, 58]. Other studies countering these conclusions have demonstrated the ability

of nectin-1 chimeras, lacking the native cytoplasmic and transmembrane domains, to permit cell-cell transmission in the same manner as wild-type nectin-1[55, 59]. The extent to which limited afadin interactions exist in cells with ectopically expressed nectin-1, and the subsequent impact on HSV-1 spread, remains to be determined.

The normal role of nectin-1 as a participant in cell adhesion and junction organization provokes questions regarding the cellular phenotype of the expressing cells. Nectin-1 cooperates in the formation of both neuronal (N) cadherin[60] and epithelial (E) cadherin-organized cell junctions[61], with each serving discreet functional roles in tissue while being commonly dysregulated during the progression of cancer [62]. While defining a positive relationship between nectin-1 and oHSV, Yu et al. additionally suggested an inverse correlation between nectin-1 expression and E-cadherin [18]. It is widely known that loss of E-cadherin results in a more migratory and metastatic phenotype in many cancers[63, 64]. As normal Schwann cells express both N-cadherin and E-cadherin[65, 66] and Schwann cell precursors express N-cadherin [67], the unique origin of MPNSTs may confound comparisons of oHSV/nectin-1 correlation with the previously mentioned studies involving epithelium-derived carcinomas [17, 18]. Nonetheless, the relation of oncolytic HSV to how MPNSTs and carcinomas differ in the organization and dysregulation of each junction type, and the consequent cellular phenotype, may influence the biological behavior of oHSV. Nectin-1 expression rather than acting only as an entry receptor may be indicative of a more global cellular phenotype that is permissive to oHSV that simple overexpression of nectin-1 does not recapitulate.

Finally, the inability of high nectin-1 expression to recapitulate a permissive phenotype for C101 in resistant cell lines implies first that the threshold for entry receptor expression to facilitate replication may be low as previously suggested [68]. Second, other post-entry events are likely the determinant of cellular resistance to the attenuated virus. In C101, loss of the $\gamma_134.5$ gene prevents the virus from reversing translational shutoff mediated by PKR activation[69]. In contrast, for the permissive cell lines such as NMS2-PC and S462-luc, $\gamma_134.5$ is relatively dispensable for successful replication and spread. In malignant cells, there are several known ways in which malignant cells can nominally suppress PKR activation and the lack of this suppression may explain the discrepancy between permissive and resistant MPNST cells. Hyperactive Ras/MEK signaling[70, 71] is one such pathway, however other research suggests that Ras signaling does not determine permissiveness to oHSV in MPNSTs[9]. Mutation or dysregulation of key components in the Type I interferon response pathway[72] may also explain a lack of anti-viral response and PKR activation. Further work is needed to determine if any of these pathways signal properly to permit PKR activation in oHSV resistant cell lines. Despite the mode of resistance to the attenuated virus, our work and others[19] conclude that high nectin-1 expression together with a virus capable of countering the innate anti-viral response by expression of the $\gamma_134.5$ gene, and presumably other immune evasion strategies, are likely indicators of successful HSV therapy.

In summary, the work presented here provides insight into one of the proposed determinants of oHSV efficacy. The fact that nectin-1 expression is proposed to have varied relevance to the $\gamma_134.5$ status of the oncolytic virus may have implications for the interpretation of results between studies using different viruses. While the first viruses used in clinical trials, G207 and HSV1716, were fully attenuated with no compensating loss for $\gamma_134.5$, subsequent second generation viruses have incorporated a number of strategies to counter this handicap. OHSVs derived from R7020 including NV1020 and NV1023 contain one functional copy of $\gamma_134.5$. M002 and Oncovex express cytokines to aid in immune recruitment. The chimeric C134 expresses the CMV IRS1 which effectively counters PKR activation. Other novel methods that aim to re-establish a selective wild-type HSV phenotype include rQnestin34.5 which re-expresses $\gamma_134.5$ with a tumor dependent promoter. The research here suggests that patients with tumors expressing high levels of nectin-1 would be candidates for oHSV therapy with second generation viruses containing enhancements that compensate for the loss of $\gamma_134.5$.

MATERIALS AND METHODS

Cell lines

MPNST cell lines STS26T-luc, T265-luc, ST88-14-luc, S462-luc, 90-8-luc, NMS2-PC, YST-1 and 2XSB and were provided by Dr. Steve Carroll (University of Alabama at Birmingham). STS26T-luc, T265-luc, and ST88-14-luc express firefly luciferase and have been previously described. S462-luc and 90-8-luc were transduced to express Renilla luciferase. HSV-1 entry receptor deficient cell line CHOK1 was generously provided by Dr. Yancey Gillespie (University of Alabama Birmingham). All MPNST cell lines were maintained in DMEM, 10% FBS, and 1% P/S. CHO-K1 cells were maintained in Ham's F12, 10% FBS, and 1% P/S. Vero cells were maintained in MEM and 5% BGS. All cell lines were confirmed to be free of Mycoplasma by DAPI staining and PCR.

Viruses

Viral replication assays

Viral replication was determined by limiting dilution plaque forming assays. MPNST cells were seeded 1.5×10^5 per well in a 24-well plate and allowed to adhere overnight. Cells were then washed with PBS and incubated for 2 hr with virus diluted in 100 μ l infection media (DMEM + 1% FBS). After 2 hr, infection media was removed and replaced with MPNST growth media. At the indicated time following infection, an equivalent volume of sterile milk was applied and the plate subjected to 3 cycles of freeze-thaw at -80°C . Lysate was collected, sonicated, serially diluted in Vero infection media (MEM + 1% BGS), and incubated on Vero monolayers for 2 hr. Following incubation, infection media was replaced with Vero growth media and 0.01% human AB serum (Corning Cellgro, Corning, NY). After 48 hr, plaques were counted following May-grunwald/methanol staining. All experiments were performed in triplicate and the average total plaque forming units (PFU) reported with standard deviation.

Viral entry receptor quantification

Expression of entry receptors was quantified by flow cytometry. In 6 well plates, 3×10^5 cells were seeded and allowed to adhere overnight. Cells were washed twice with PBS and non-enzymatically dissociated using CellStripper (Corning Cellgro, Corning, NY). Cells were twice washed in PBS, then incubated for 45 mins in either phycoerythrin (PE) conjugated mouse monoclonal antibodies to nectin-1 (R1.302)(Biolegend, San Diego, CA), HVEM (Biolegend, San Diego, CA), or PE-conjugated isotype control (BD Biosciences, San Jose, CA) according to the manufacturer's instructions. Antibody concentrations used were confirmed to be saturating. Cells were washed three times in FACS buffer (PBS + 2% FBS + 0.01% NaN_3) and immediately subjected to analysis using a FACSCaliber flow cytometer (Becton Dickinson, Franklin Lakes, NJ). Concurrently, Quantum Simply Cellular beads (Bangs Laboratories, Fisher, IN) were used according to manufacturer's instructions to determine the antibody binding capacity (ABC) of each cell line. Mean fluorescence analysis was performed using FlowJo (v 7.6.1; Tree Star, Ashland, OR) and the data converted to ABC using a script provided with the Quantum Simply Cellular kit. All measurements were averaged from three independently seeded wells, and the final ABC reported as the difference above the isotype control.

Correlation of nectin-1 and viral recovery

Pearson's correlation coefficients between nectin-1 expression and viral recovery were determined by analysis of the data in Prism 5 (GraphPad Software, La Jolla, CA). Cutoff for statistical significance was set at $P=0.05$.

Nectin-1 overexpression

A self-inactivating lentiviral vector was used to overexpress nectin-1 or control mCherry in oHSV resistant cell lines. Human nectin-1 clone (Clone ID: 8322523) was obtained from Open Biosystems (Thermo Scientific, ***). Nectin-1

cDNA was PCR amplified with 5 PRIME HotMasterMix (5 Prime, Gaithersburg, MD) using primers 5'-CGGATCCCGGGTTCGACCCGATGGCTCGGATGGGGCTT-3' and 5'-CCGGTTCGAGCGGCCGCTACACGTACCACTCCTTCTTGAA-3' (IDT, Coralville, IA) in a T100 Thermal Cycler (BioRad, Hercules, CA). A 1.5 kb PCR product was confirmed and column purified (Enzymax, Lexington, KY). (***** briefly describe recipient vector). To prepare the recipient vector, pLVmd.mUTA2-IPp was digested with Sall and NotI and subjected to electrophoresis to isolate the large fragment. Nectin-1 cDNA was then inserted into the linearized recipient vector using an InFusion HD Cloning Kit (Clontech, Mountain View, CA) according to the manufacturer's instructions. The InFusion product pCK2114 was sequenced at the insertion sites to confirm recombination and orientation of the nectin-1 gene. Lentivirus was assembled by co-transfection of pCK2114, pMD.G (VSVG pseudotype), and pDR8.91 (HIV packaging) in 293T cells under OptiMEM media (Gibco, ***). Control lentivirus was constructed using pLVmd.CIP, mCherry followed by IRES and puromycin N-acetyl-transferase. After 12 hr, transfection media was replaced with DMEM/F12 with 10% FBS. Lentiviral soup was collected 48 hr post-transfection, filtered through a 0.2 micron filter, and mixed with polybrene (8 µg/ml). Approximately 2×10^6 STS26T-luc or T265-luc cells were exposed to 1 ml of collected nectin-1 or mCherry lentivirus in 9 ml of MPNST growth media. Puromycin (5 µg/ml) was applied after 48 hr to select for transduced cells. Nectin-1 and mCherry transduced cells were additionally enriched by fluorescence activated cell sorting (FACS) to obtain pure populations (UAB Comprehensive Flow Cytometry Core, Birmingham, AL). HSV entry receptor deficient cell line CHOK1 was transduced with nectin-1 and infected with M2001 for viral recovery (as previously described for MPNST cell lines) to validate the entry receptor function of the nectin-1 construct.

HSV replication in nectin-1 overexpressing cell lines

The impact of increased nectin-1 expression on viral replication in resistant cell lines was determined as described above with the exception of replacing infection media with MPNST growth media and 0.01% human AB serum to minimize extracellular spread of the virus. Statistical significance was determined by two-tailed student's T-test assuming equal variance. Star notation indicating significant differences is as follows: (*) for $P < 0.05$, (**) for $P < 0.01$, and (***) for $P < 0.001$.

HSV spread as measured by GFP expression

The impact of nectin-1 overexpression on the cell-cell spread of virus was determined by multi-step infection and evaluation of viral GFP expression in the population by flow cytometry. Parent or nectin-1 transduced cells were seeded 1.5×10^5 cells per well in a 24 well plate and allowed to adhere overnight. Cells were incubated with C101, M2001, or mock for 2 hr at MOI=0.1 in infection media. Infection media was replaced with growth media and 0.01% human AB serum following incubation. At 12 hr intervals, cells were washed with PBS, trypsinized, and resuspended in FACS buffer. All washes were collected and added to dissociated cells. Cells were immediately analyzed by flow cytometry for viral GFP expression. Analysis in FlowJo used forward and side-scatter to gate on the main population of mock treated samples. The percent GFP positive of this population was assessed by defining the GFP (FL1) gate at 1% positive of the mock treated cells. The percentage of the infected cell population expressing GFP was then recorded. All data points were performed in triplicate, averaged, and the standard deviation reported.

FIGURES

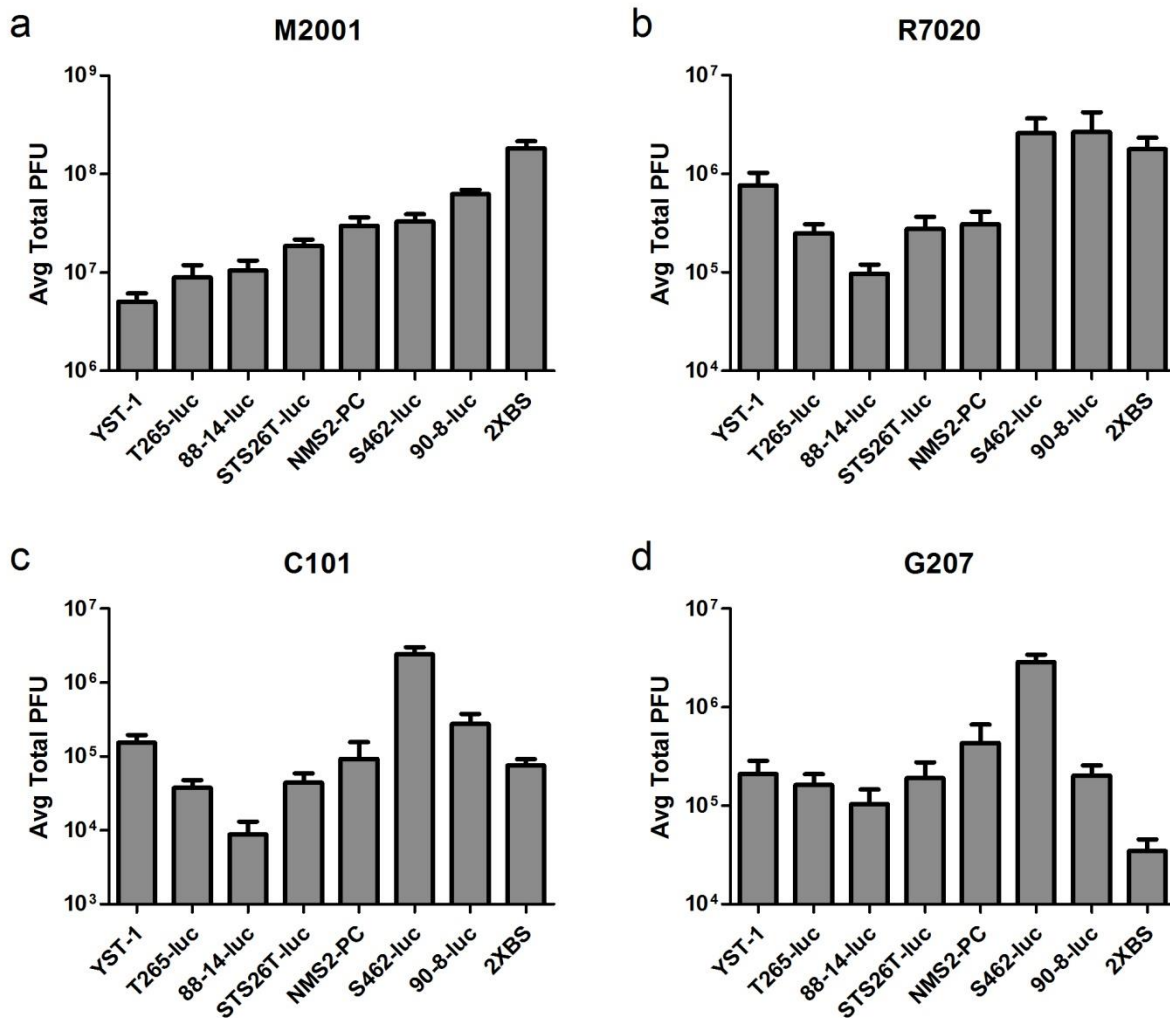
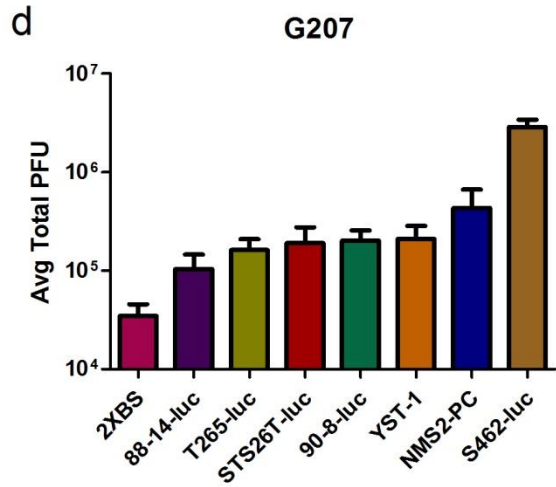
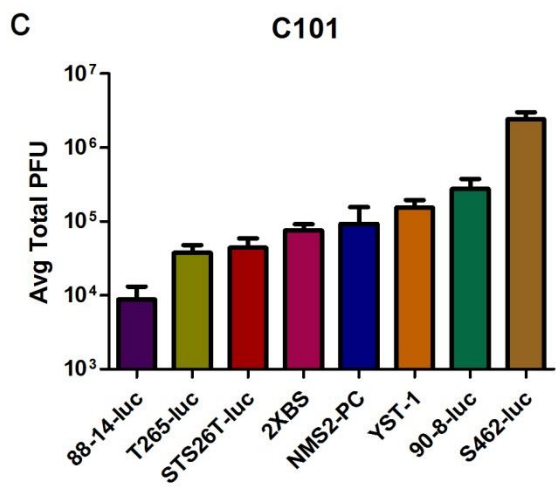
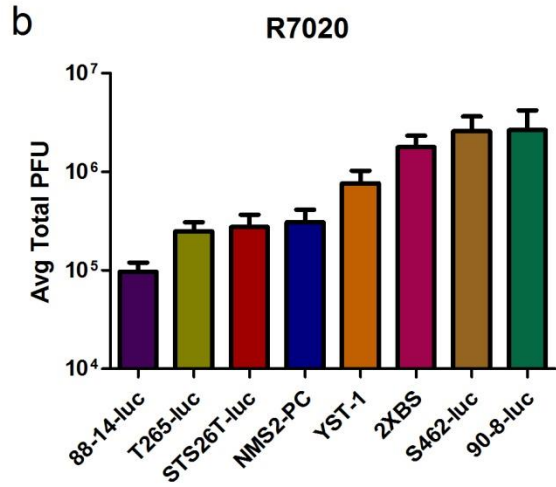
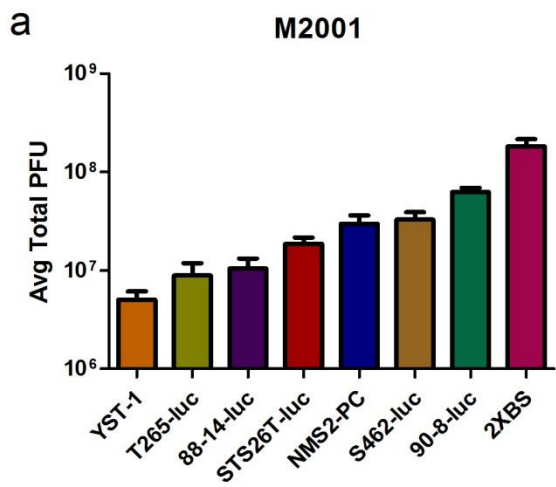
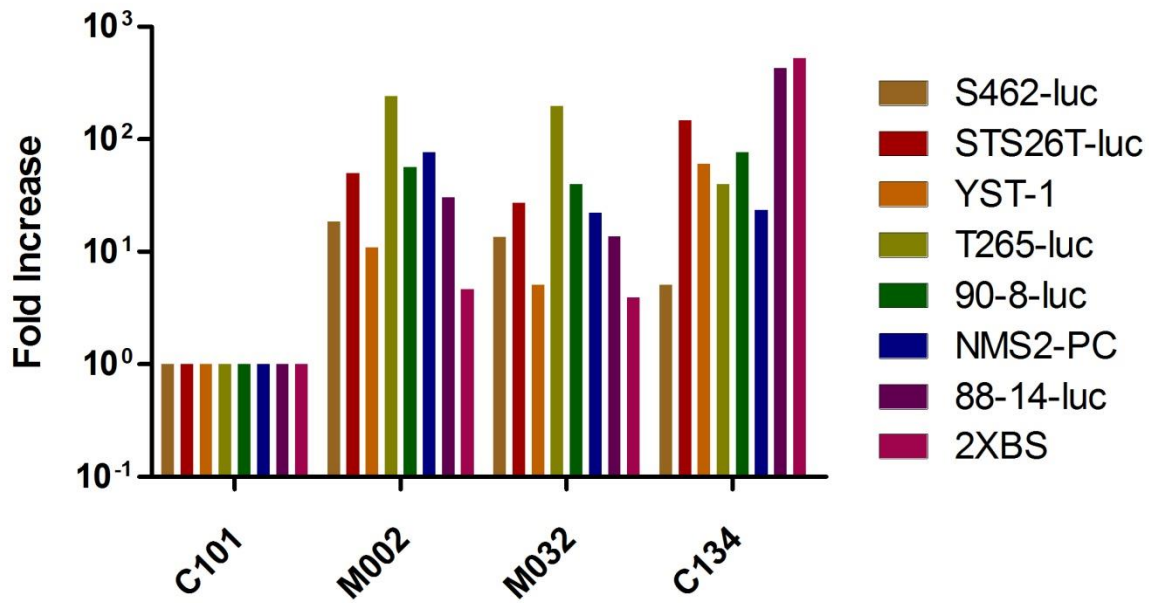
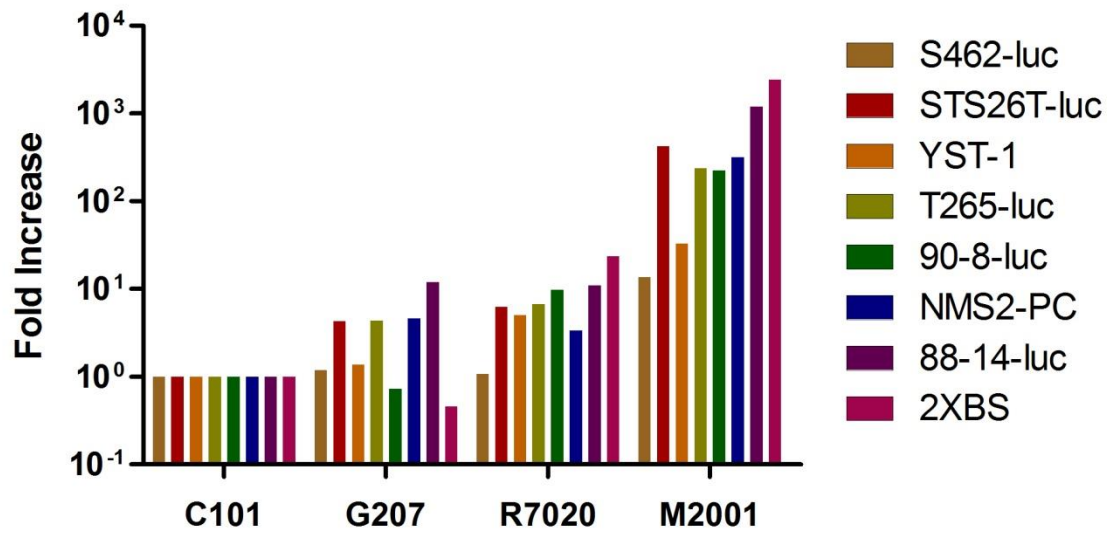


Figure 1: Single-step viral recovery in MPNST cell lines. MPNST cell lines were subjected to single-step (MOI=10, 24 hr) infection by viruses M2001 (a), R7020 (b), C101 (c), and G207 (d) and the viral titers reported as the average total plaque forming units (PFU) as determined through limiting dilution plaque formation. Error bars represent standard deviation. For each virus, a range of replication was observed between all cell lines with the largest differences observed in the double $\gamma_{134.5}$ deleted viruses C101 and G207. Resistant cell lines STS26T-luc and T265-luc as well as permissive lines S462-luc and NMS2-PC were identified and selected for further study.



Alternative Figure 1 (Ascending titer with same cell line color)



Alternative Figure 1 (all cell lines normalized to C101... represented as fold increase over C101)

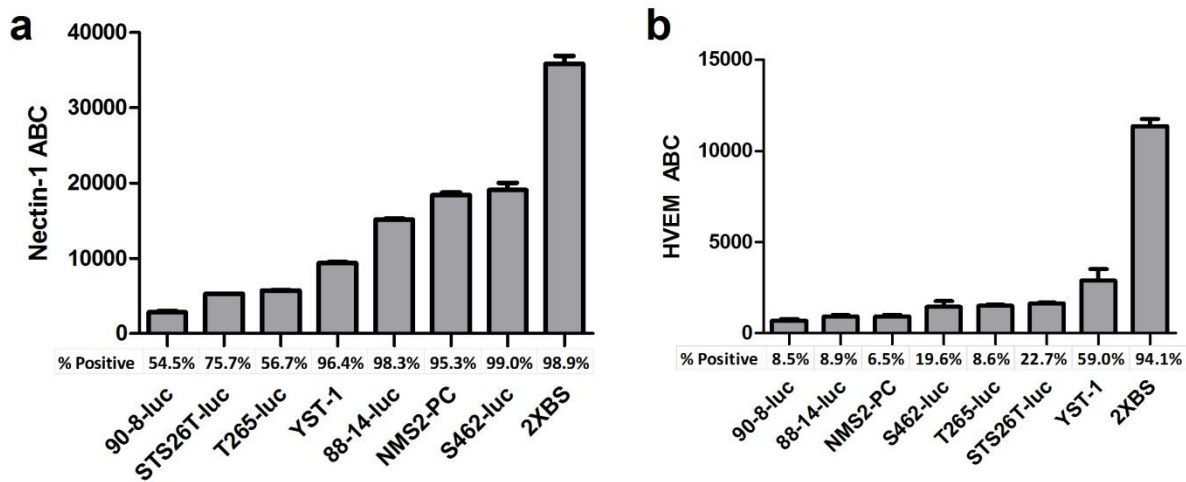


Figure 2: HSV-1 entry receptor expression in MPNST cell lines. Nectin-1 (a) and HVEM (b) entry receptor expression was assessed in all MPNST cell lines by flow cytometry using PE-conjugated antibodies. Mean fluorescence intensity was related to antibody binding capacity (ABC) using beads designed to bind set quantities of antibody. For each cell line, the percent of the population staining positively above the isotype control is also reported. A range of nectin-1 expression (a) is observed across all cell lines with the ABC of 2XSB nearly twice that of the next highest cell line. Some HVEM expression (b) was observed in several cell lines, but in much lower quantities than nectin-1.

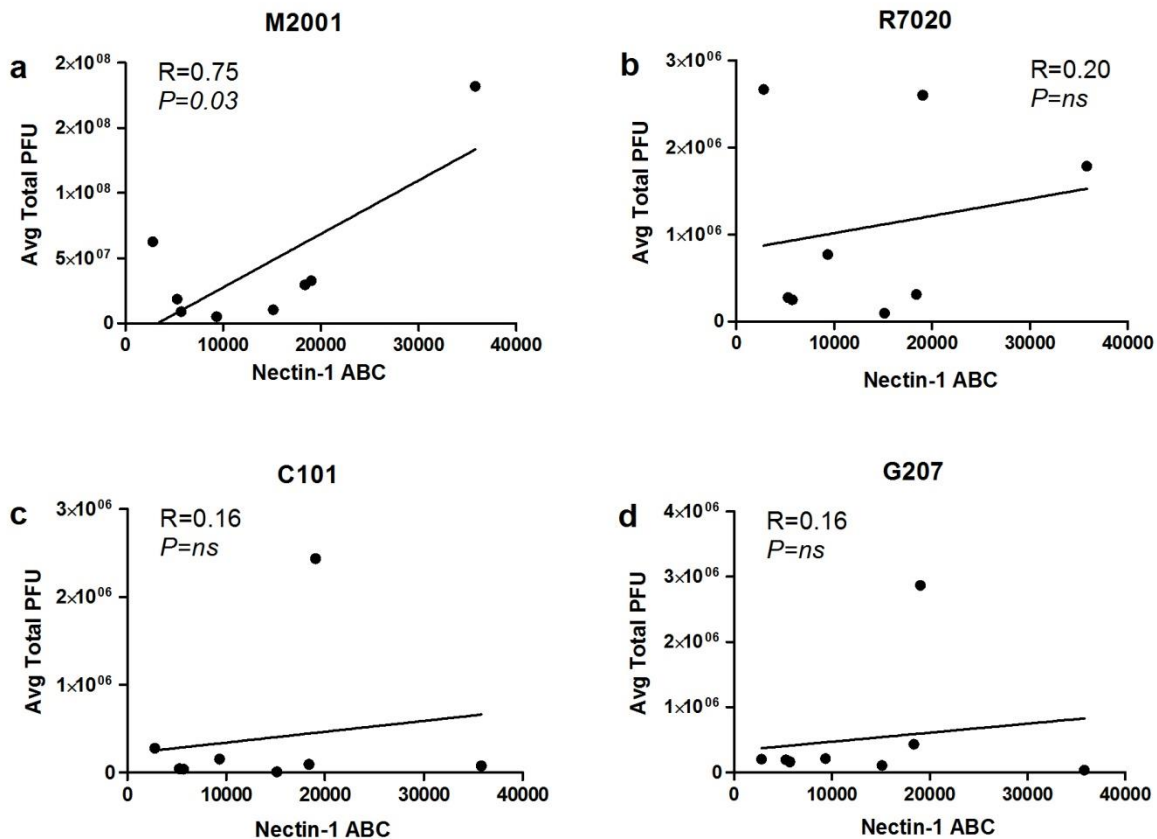


Figure 3: Correlation of nectin-1 expression with viral replication. Pearson's correlation coefficients were calculated between nectin-1 expression and each set of viral recovery data from M2001 (a), R7020 (b), C101 (c), and

G207 (d). A strong correlation ($R=0.75$) was noted for M2001 however the correlation was not statistically significant. Significance was set at $P<0.05$.

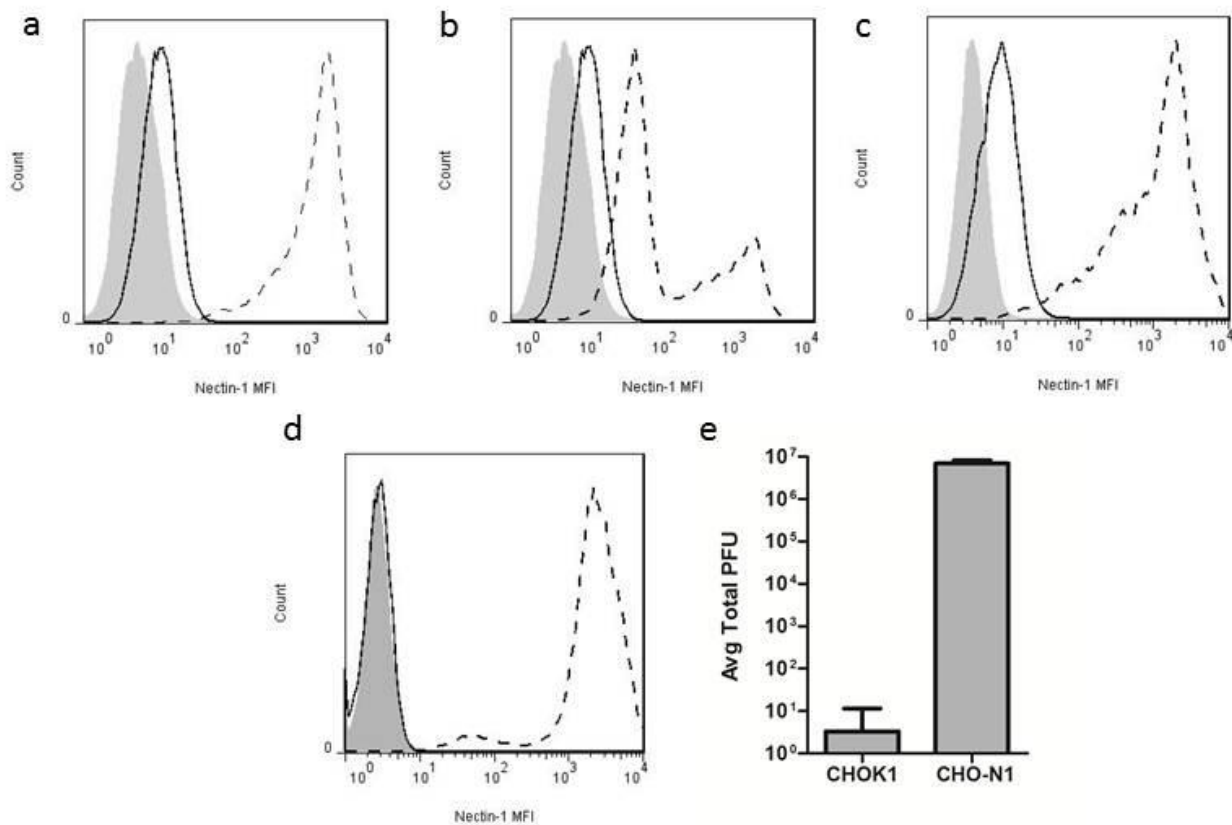


Figure 4: Functional overexpression of nectin-1 in resistant cell lines T265-luc and STS26T-luc. Nectin-1 was transduced via lentivirus into oHSV resistant cell lines STS26T-luc and T265-luc. Two lines derived from STS26T-luc were obtained by FACS: STS26T-N1HI (a) with a single high expressing population and STS26T-N1MED (b) with dual populations of increased nectin-1. Transduction followed by FACS in T265-luc yielded T265-N1 (c), a mainly high expressing population. Isotype control (shaded), parent (solid line), and transduced (dashed line) cell lines are shown. Nectin-1 deficient cell line CHOK1 was transduced to produce CHO-N1 (d) and infected with M2001 (MOI=10, 24 hr) to demonstrate functionality of the nectin-1 and subsequent viral replication (e).

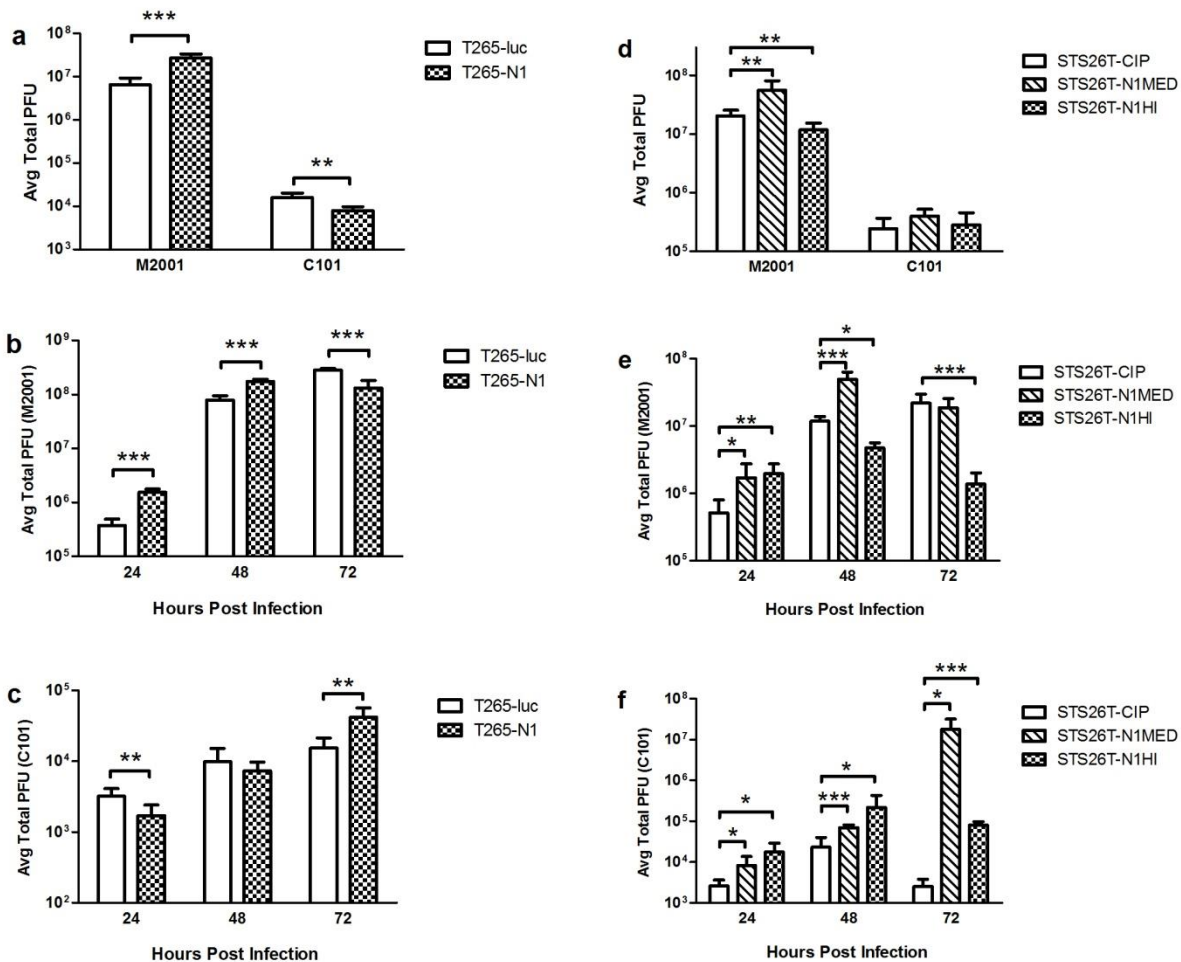


Figure 5: Impact of increased nectin-1 expression on viral replication. Single and multi-step replication assays using M2001 and C101 were performed in STS26T-luc and T265-luc transduced with nectin-1 or mCherry (Cherry). In the single-step assays for both STS26T-luc (a) and T265-luc (d), M2001 was increased significantly in T265-N1 and STS26T-N1MED, however was decreased for STS26T-N1HI. No significant increases using C101 were measured in any cell line. For T265-N1 in the multi-step assay, there were some significant increases in viral recovery following infection with M2001 (b) and C101 (c), though a greater than 0.5 log increase was not seen. In STS26T-N1MED and STS26T-N1HI, infection with M2001 showed divergent trends in viral titer over time (e) resulting in significantly higher titers in STS26T-N1MED at 48 hpi and in STS26T-N1HI significantly lower titers at 48 and 72 hpi compared to the control. Significant increases in titer were observed at all timepoints when these STS26T-luc nectin-1 overexpressers were infected with C101 (f). Notably at 72 hpi, both nectin-1 overexpressing lines were multiple orders of magnitude larger than STS26T-Cherry.

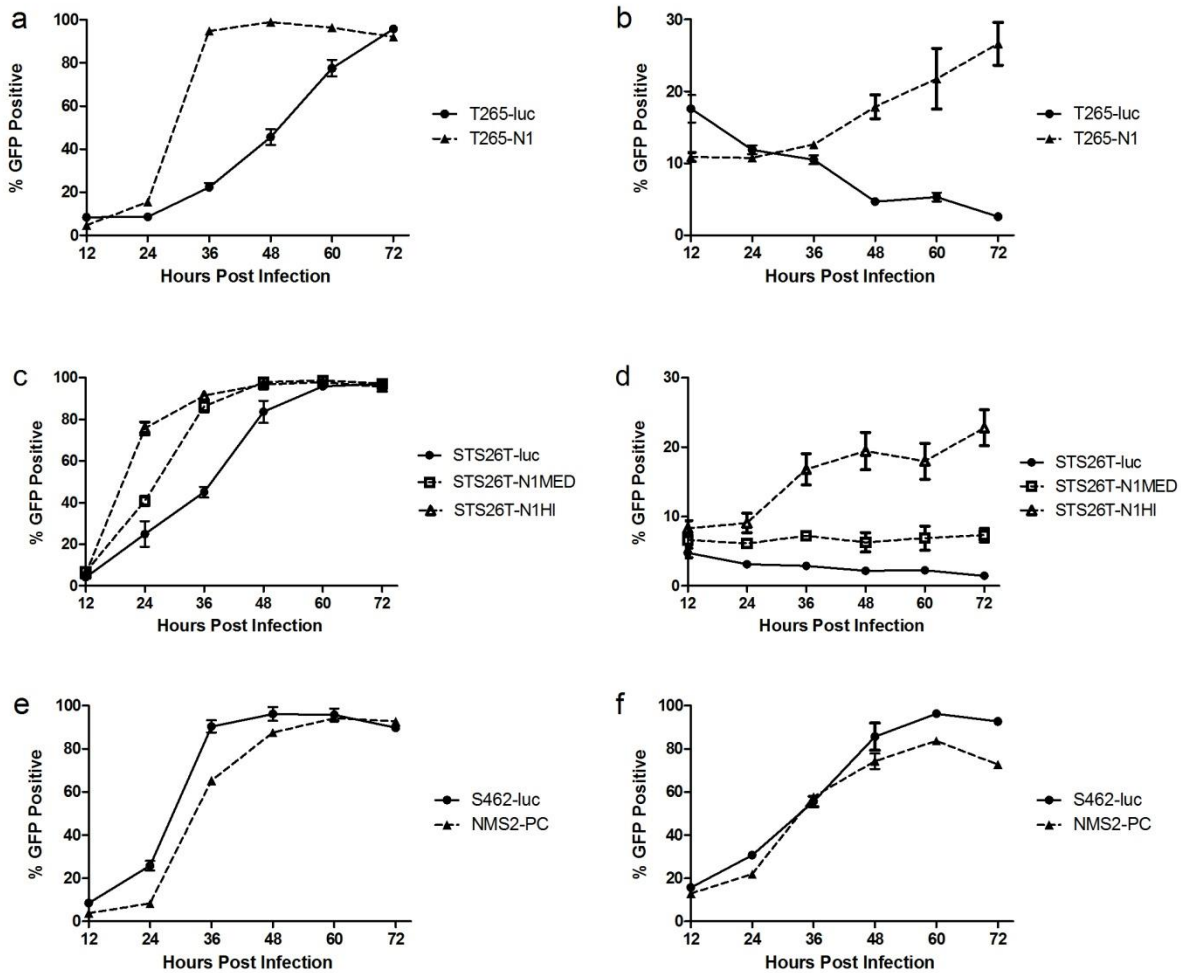


Figure 6: Impact of increased nectin-1 expression on viral spread. Whole populations of nectin-1 transduced cells or parent were monitored for viral spread following infection with M2001 or C101 at MOI=0.1. Spread was assessed by determining the percent of the population expressing viral GFP at 12 hr intervals for 72 hrs. As compared to the respective parent, infection with M2001 in T265-N1 (a), STS26T-N1MED (c), and STS26T-N1HI (c) showed substantially increased speed in the spread of the virus, similar to that seen in permissive cell lines S462-luc and NMS2-PC (e). Increased nectin-1 expression appears to enhance spread of wild-type virus. C101 showed improved spread in the highest nectin-1 expressing lines T265-N1 (b) and STS26T-N1HI (d) compared to their respective parent lines, however the percent positive at 72 hpi for these lines was achieved near 24 hpi by permissive cell lines (f). Increased nectin-1 implies a benefit to spread by attenuated virus C101 but does not mimic a permissive phenotype.

1. Kelly, E. and S.J. Russell, *History of oncolytic viruses: genesis to genetic engineering*. Molecular therapy, 2007. **15**(4): p. 651-659.
2. Russell, S.J., K.-W. Peng, and J.C. Bell, *Oncolytic virotherapy*. Nature biotechnology, 2012. **30**(7): p. 658-670.
3. Chou, J., et al., *Mapping of herpes simplex virus-1 neurovirulence to gamma 134.5, a gene nonessential for growth in culture*. Science, 1990. **250**(4985): p. 1262-1266.
4. Harrow, S., et al., *HSV1716 injection into the brain adjacent to tumour following surgical resection of high-grade glioma: safety data and long-term survival*. Gene therapy, 2004. **11**(22): p. 1648-1658.
5. Markert, J., et al., *Conditionally replicating herpes simplex virus mutant, G207 for the treatment of malignant glioma: results of a phase I trial*. Gene therapy, 2000. **7**(10): p. 867-874.
6. Rampling, R., et al., *Toxicity evaluation of replication-competent herpes simplex virus (ICP 34.5 null mutant 1716) in patients with recurrent malignant glioma*. Gene therapy, 2000. **7**(10): p. 859.
7. Markert, J.M., et al., *Phase Ib trial of mutant herpes simplex virus G207 inoculated pre-and post-tumor resection for recurrent GBM*. Molecular Therapy, 2008. **17**(1): p. 199-207.
8. Mahller, Y.Y., et al., *658. Oncolytic Herpes Virus Mutants Are Efficacious Against Malignant Peripheral Nerve Sheath Tumor Xenografts*. Molecular Therapy, 2006. **13**: p. S253-S254.
9. Mahller, Y.Y., et al., *Malignant peripheral nerve sheath tumors with high and low Ras-GTP are permissive for oncolytic herpes simplex virus mutants*. Pediatric blood & cancer, 2006. **46**(7): p. 745-754.
10. Mahller, Y.Y., et al., *Oncolytic HSV and erlotinib inhibit tumor growth and angiogenesis in a novel malignant peripheral nerve sheath tumor xenograft model*. Molecular Therapy, 2007. **15**(2): p. 279-286.
11. Mahller, Y., et al., *Molecular analysis of human cancer cells infected by an oncolytic HSV-1 reveals multiple upregulated cellular genes and a role for SOCS1 in virus replication*. Cancer gene therapy, 2008. **15**(11): p. 733-741.
12. Maldonado, A.R., et al., *Molecular engineering and validation of an oncolytic herpes simplex virus type 1 transcriptionally targeted to midkine-positive tumors*. The journal of gene medicine, 2010. **12**(7): p. 613-623.
13. Carroll, S.L. and N. Ratner, *How does the Schwann cell lineage form tumors in NF1?* Glia, 2008. **56**(14): p. 1590-1605.
14. Korf, B.R., *Malignancy in neurofibromatosis type 1*. The oncologist, 2000. **5**(6): p. 477-485.
15. Ingham, S., et al., *Malignant peripheral nerve sheath tumours in NF1: improved survival in women and in recent years*. European Journal of Cancer, 2011. **47**(18): p. 2723-2728.
16. Kolberg, M., et al., *Survival meta-analyses for > 1800 malignant peripheral nerve sheath tumor patients with and without neurofibromatosis type 1*. Neuro-oncology, 2013. **15**(2): p. 135-147.
17. Huang, Y.-Y., et al., *Nectin-1 is a marker of thyroid cancer sensitivity to herpes oncolytic therapy*. Journal of Clinical Endocrinology & Metabolism, 2007. **92**(5): p. 1965-1970.
18. Yu, Z., et al., *Nectin-1 expression by squamous cell carcinoma is a predictor of herpes oncolytic sensitivity*. Molecular Therapy, 2007. **15**(1): p. 103-113.
19. Wang, P., et al., *Expression of HSV-1 receptors in EBV-associated lymphoproliferative disease determines susceptibility to oncolytic HSV*. Gene therapy, 2012.
20. Friedman, G.K., et al., *Engineered herpes simplex viruses efficiently infect and kill CD133+ human glioma xenograft cells that express CD111*. Journal of neuro-oncology, 2009. **95**(2): p. 199-209.
21. Campadelli-Fiume, G., et al., *The multipartite system that mediates entry of herpes simplex virus into the cell*. Reviews in medical virology, 2007. **17**(5): p. 313-326.
22. Connolly, S.A., et al., *Fusing structure and function: a structural view of the herpesvirus entry machinery*. Nature Reviews Microbiology, 2011. **9**(5): p. 369-381.
23. Karasneh, G.A. and D. Shukla, *Herpes simplex virus infects most cell types in vitro: clues to its success*. Virology journal, 2011. **8**(1): p. 481.
24. Campadelli-Fiume, G., et al., *The novel receptors that mediate the entry of herpes simplex viruses and animal alphaherpesviruses into cells*. Reviews in medical virology, 2000. **10**(5): p. 305-319.
25. Forrester, A., et al., *Construction and properties of a mutant of herpes simplex virus type 1 with glycoprotein H coding sequences deleted*. Journal of Virology, 1992. **66**(1): p. 341-348.
26. Ligas, M.W. and D.C. Johnson, *A herpes simplex virus mutant in which glycoprotein D sequences are replaced by beta-galactosidase sequences binds to but is unable to penetrate into cells*. Journal of Virology, 1988. **62**(5): p. 1486-1494.

27. Cai, W., B. Gu, and S. Person, *Role of glycoprotein B of herpes simplex virus type 1 in viral entry and cell fusion*. Journal of virology, 1988. **62**(8): p. 2596-2604.
28. Pertel, P.E., et al., *Cell fusion induced by herpes simplex virus glycoproteins gB, gD, and gH-gL requires a gD receptor but not necessarily heparan sulfate*. Virology, 2001. **279**(1): p. 313-324.
29. Roop, C., L. Hutchinson, and D.C. Johnson, *A mutant herpes simplex virus type 1 unable to express glycoprotein L cannot enter cells, and its particles lack glycoprotein H*. Journal of virology, 1993. **67**(4): p. 2285-2297.
30. Rikitake, Y., K. Mandai, and Y. Takai, *The role of nectins in different types of cell-cell adhesion*. J Cell Sci, 2012. **125**(Pt 16): p. 3713-22.
31. Mizoguchi, A., et al., *Nectin an adhesion molecule involved in formation of synapses*. The Journal of cell biology, 2002. **156**(3): p. 555-565.
32. Richart, S.M., et al., *Entry of herpes simplex virus type 1 into primary sensory neurons in vitro is mediated by nectin-1/HveC*. Journal of virology, 2003. **77**(5): p. 3307-3311.
33. Simpson, S.A., et al., *Nectin-1/HveC mediates herpes simplex virus type-1 entry into primary human sensory neurons and fibroblasts*. Journal of neurovirology, 2005. **11**(2): p. 208-218.
34. Shah, A., et al., *HSV-1 infection of human corneal epithelial cells: receptor-mediated entry and trends of re-infection*. Molecular vision, 2010. **16**: p. 2476.
35. Akhtar, J., et al., *HVEM and nectin-1 are the major mediators of herpes simplex virus 1 (HSV-1) entry into human conjunctival epithelium*. Investigative ophthalmology & visual science, 2008. **49**(9): p. 4026-4035.
36. Linehan, M.M., et al., *In vivo role of nectin-1 in entry of herpes simplex virus type 1 (HSV-1) and HSV-2 through the vaginal mucosa*. Journal of virology, 2004. **78**(5): p. 2530-2536.
37. Menotti, L., et al., *The murine homolog of human Nectin1delta serves as a species nonspecific mediator for entry of human and animal alpha herpesviruses in a pathway independent of a detectable binding to gD*. Proc Natl Acad Sci U S A, 2000. **97**(9): p. 4867-72.
38. Geraghty, R.J., et al., *Entry of alphaherpesviruses mediated by poliovirus receptor-related protein 1 and poliovirus receptor*. Science, 1998. **280**(5369): p. 1618-1620.
39. Haarr, L., et al., *Transcription from the gene encoding the herpesvirus entry receptor nectin-1 (HveC) in nervous tissue of adult mouse*. Virology, 2001. **287**(2): p. 301-309.
40. Guzman, G., et al., *Expression of entry receptor nectin-1 of herpes simplex virus 1 and/or herpes simplex virus 2 in normal and neoplastic human nervous system tissues*. Acta virologica, 2006. **50**(1): p. 59.
41. Montgomery, R.I., et al., *Herpes simplex virus-1 entry into cells mediated by a novel member of the TNF/NGF receptor family*. Cell, 1996. **87**(3): p. 427-436.
42. Shukla, D., et al., *A Novel Role for 3-O-Sulfated Heparan Sulfate in Herpes Simplex Virus 1 Entry*. Cell, 1999. **99**(1): p. 13-22.
43. Parry, C., et al., *Herpes simplex virus type 1 glycoprotein H binds to α v β 3 integrins*. Journal of general virology, 2005. **86**(1): p. 7-10.
44. Shieh, M.-T., et al., *Cell surface receptors for herpes simplex virus are heparan sulfate proteoglycans*. The Journal of cell biology, 1992. **116**(5): p. 1273-1281.
45. Arii, J., et al., *Entry of herpes simplex virus 1 and other alphaherpesviruses via the paired immunoglobulin-like type 2 receptor α* . Journal of virology, 2009. **83**(9): p. 4520-4527.
46. Arii, J., et al., *Non-muscle myosin IIA is a functional entry receptor for herpes simplex virus-1*. Nature, 2010. **467**(7317): p. 859-862.
47. Suenaga, T., et al., *Myelin-associated glycoprotein mediates membrane fusion and entry of neurotropic herpesviruses*. Proceedings of the National Academy of Sciences, 2010. **107**(2): p. 866-871.
48. Bacsa, S., et al., *Syndecan-1 and syndecan-2 play key roles in herpes simplex virus type-1 infection*. Journal of General Virology, 2011. **92**(4): p. 733-743.
49. MacLeod, D.T., et al., *HSV-1 exploits the innate immune scavenger receptor MARCO to enhance epithelial adsorption and infection*. Nature communications, 2013. **4**.
50. Meignier, B., R. Longnecker, and B. Roizman, *In vivo behavior of genetically engineered herpes simplex viruses R7017 and R7020: construction and evaluation in rodents*. Journal of Infectious Diseases, 1988. **158**(3): p. 602-614.
51. Lawrence, R., et al., *The principal neuronal gD-type 3-O-sulfotransferases and their products in central and peripheral nervous system tissues*. Matrix biology, 2007. **26**(6): p. 442-455.

52. Warner, M.S., et al., *A cell surface protein with herpesvirus entry activity (HveB) confers susceptibility to infection by mutants of herpes simplex virus type 1, herpes simplex virus type 2, and pseudorabies virus.* Virology, 1998. **246**(1): p. 179-189.
53. Lopez, M., et al., *Nectin2 α (PRR2 α or HveB) and nectin2 δ are low-efficiency mediators for entry of herpes simplex virus mutants carrying the Leu25Pro substitution in glycoprotein D.* Journal of virology, 2000. **74**(3): p. 1267-1274.
54. Martinez, W.M. and P.G. Spear, *Structural features of nectin-2 (HveB) required for herpes simplex virus entry.* Journal of virology, 2001. **75**(22): p. 11185-11195.
55. Krummenacher, C., et al., *Cellular localization of nectin-1 and glycoprotein D during herpes simplex virus infection.* Journal of virology, 2003. **77**(16): p. 8985-8999.
56. Subramanian, R.P., J.E. Dunn, and R.J. Geraghty, *The nectin-1 α transmembrane domain, but not the cytoplasmic tail, influences cell fusion induced by HSV-1 glycoproteins.* Virology, 2005. **339**(2): p. 176-191.
57. Sakisaka, T., et al., *Requirement of interaction of nectin-1 α /HveC with afadin for efficient cell-cell spread of herpes simplex virus type 1.* Journal of virology, 2001. **75**(10): p. 4734-4743.
58. Keyser, J., et al., *Role of AF6 protein in cell-to-cell spread of Herpes simplex virus 1.* FEBS letters, 2007. **581**(28): p. 5349-5354.
59. Even, D.L., A.M. Henley, and R.J. Geraghty, *The requirements for herpes simplex virus type 1 cell-cell spread via nectin-1 parallel those for virus entry.* Virus research, 2006. **119**(2): p. 195-207.
60. Togashi, H., et al., *Interneurite affinity is regulated by heterophilic nectin interactions in concert with the cadherin machinery.* The Journal of cell biology, 2006. **174**(1): p. 141-151.
61. Takai, Y. and H. Nakanishi, *Nectin and afadin: novel organizers of intercellular junctions.* Journal of cell science, 2003. **116**(1): p. 17-27.
62. Jeanes, A., C. Gottardi, and A. Yap, *Cadherins and cancer: how does cadherin dysfunction promote tumor progression?* Oncogene, 2008. **27**(55): p. 6920-6929.
63. Takeichi, M., *Cadherins in cancer: implications for invasion and metastasis.* Current opinion in cell biology, 1993. **5**(5): p. 806-811.
64. Vleminckx, K., et al., *Genetic manipulation of E-cadherin expression by epithelial tumor cells reveals an invasion suppressor role.* cell, 1991. **66**(1): p. 107-119.
65. Friedrich Jr, V.L. and D.R. Colman, *Novel E-cadherin-mediated adhesion in peripheral nerve: Schwann cell architecture is stabilized by autotypic adherens junctions.* The Journal of cell biology, 1995. **129**(1): p. 189-202.
66. Wanner, I.B. and P.M. Wood, *N-cadherin mediates axon-aligned process growth and cell-cell interaction in rat Schwann cells.* The Journal of neuroscience, 2002. **22**(10): p. 4066-4079.
67. Wanner, I.B., et al., *Role of N-cadherin in Schwann cell precursors of growing nerves.* Glia, 2006. **54**(5): p. 439-459.
68. Krummenacher, C., et al., *Comparative usage of herpesvirus entry mediator A and nectin-1 by laboratory strains and clinical isolates of herpes simplex virus.* Virology, 2004. **322**(2): p. 286-299.
69. Shah, A., et al., *Enhanced antiglioma activity of chimeric HCMV/HSV-1 oncolytic viruses.* Gene therapy, 2007. **14**(13): p. 1045-1054.
70. Farassati, F., A.-D. Yang, and P.W. Lee, *Oncogenes in Ras signalling pathway dictate host-cell permissiveness to herpes simplex virus 1.* Nature cell biology, 2001. **3**(8): p. 745-750.
71. Smith, K.D., et al., *Activated MEK suppresses activation of PKR and enables efficient replication and in vivo oncolysis by $\Delta\gamma$ 134. 5 mutants of herpes simplex virus 1.* Journal of virology, 2006. **80**(3): p. 1110-1120.
72. Honda, K., A. Takaoka, and T. Taniguchi, *Type I interferon gene induction by the interferon regulatory factor family of transcription factors.* Immunity, 2006. **25**(3): p. 349-360.

Appendix ii

Poster session: Comprehensive Cancer Center Retreat, Oct. 29 2012, **“Effect of Oncolytic Herpes Simplex Virus Replication in MPNST Cell Lines Over-Expressing Nectin-1”** Joshua D. Jackson, Adrienne McMorris, Jennifer Coleman, Justin Roth, Steven Carroll, Kevin Cassady, James Markert

Abstract: We propose in this research to study the capacity of various oncolytic Herpes Simplex Viruses (oHSVs) to elicit regression of malignant peripheral nerve sheath tumors (MPNSTs) through virally induced cell lysis and immune recruitment. As rare and aggressive tumors of glial origin, MPNSTs frequently arise from patients with type-1 neurofibromatosis, but also form spontaneously. Five year survival ranges from 16-52%, and a lack of dependable treatment options suggests oHSV as a novel candidate to treat these malignancies. HSV is an attractive therapy because it is neurotropic and readily tolerates therapeutic transgene inserts up to 30 kb for high-level expression in infected cells. HSV has been proposed as an oncolytic therapy for tumors derived of neuronal lineage and has already been safely used in Phase I clinical trials for patients with glioblastoma multiforme. Despite promising results in select patients, others experienced less dramatic clinical response to the therapy. One potential explanation to the variability in oHSV efficacy is the absence or limiting concentration of the primary HSV entry receptor Nectin-1 on the surface of target cells. While this is a theoretical concern, it is expected that Nectin-1 concentrations in MPNST cell lines are sufficient to allow efficient viral entry. Preliminary results regarding the impact of human Nectin-1 over-expression (by lentiviral transduction in MPNST cell lines) on oHSV viral recovery are presented here. In the future, it is expected that the study of events following viral entry will explain the observed variations of *in vitro* data and clinical response to oHSV. Proposals involving innate viral defense responses and intracellular metabolic effects on host susceptibility, as well as correlative *in vivo* studies using xenogeneic and syngeneic murine models, are under development.

Appendix iii

Poster Presentation. November 2012 McMorris, JD Jackson, KA Cassady, JM Markert, and J Roth "Nectin-1 expression effects on oncolytic HSV replication in Malignant Peripheral Nerve Sheath Tumors (MPNSTs)." Annual Biomedical Research Conference for Minority Student (ABRCMS) Sand Francisco CA.

Malignant peripheral nerve sheath tumors (MPNSTs) are resistant to chemotherapy and radiation. Surgical resection is the mainstay of current therapy but results in significant morbidity. An alternate therapy is needed. Phase I b studies have shown that genetically engineered oncolytic Herpes Simplex Viruses (oHSV) are safe and selectively replicate and lyse tumor cells while leaving non-malignant neurons intact. To determine if oHSVs could provide an effective alternative treatment we investigated the ability of these oHSVs to replicate in a panel of MPNST cell lines. Preliminary results show variable oHSV replication in the different cell lines and low levels of nectin-1 expression: the principal HSV entry receptor. We hypothesized that low levels of Nectin-1 surface expression on MPNST tumors limits the efficacy of oHSV vectors. To test this hypothesis, we created a lentivirus expression construct to stably express nectin 1 in one of the more resistant MPNST cell lines. Viral entry and oHSV recovery results of the nectin-1 entry receptor protein transduction into MPNST cell lines will then be examined to determine if the nectin-1 expression level in resistant MPNSTs is a rate limiting step in oHSV therapy.

Supporting Data

Please Figures attached

NECTIN-1 EXPRESSION EFFECT ON ONCOLYTIC HERPES SIMPLEX VIRUS (oHSV)
REPLICATION IN MALIGNANT PERIPHERAL NERVE SHEATH TUMORS (MPNSTs)

Adrienne McMorris

Dr. Kevin Cassady, Dr. James Markert, Dr. Justin Roth

University of Alabama Birmingham

Malignant Peripheral Nerve Sheath Tumors

- Malignant peripheral nerve sheath tumors (MPNSTs) are rare cancers but only 30 - 50% of patients survive beyond 5 years after diagnosis.
- MPNSTs are neoplasms derived from schwann cells and can occur from sporadic or inherited mutations.
- Patients who inherit the trait for MPNSTs previously have a disease known as neurofibromatosis type 1 (NF1).
- Neurofibromatosis patients have a mutated neurofibromin gene that controls the suppression of tumors. As a result of the mutation patients develop benign and malignant tumors



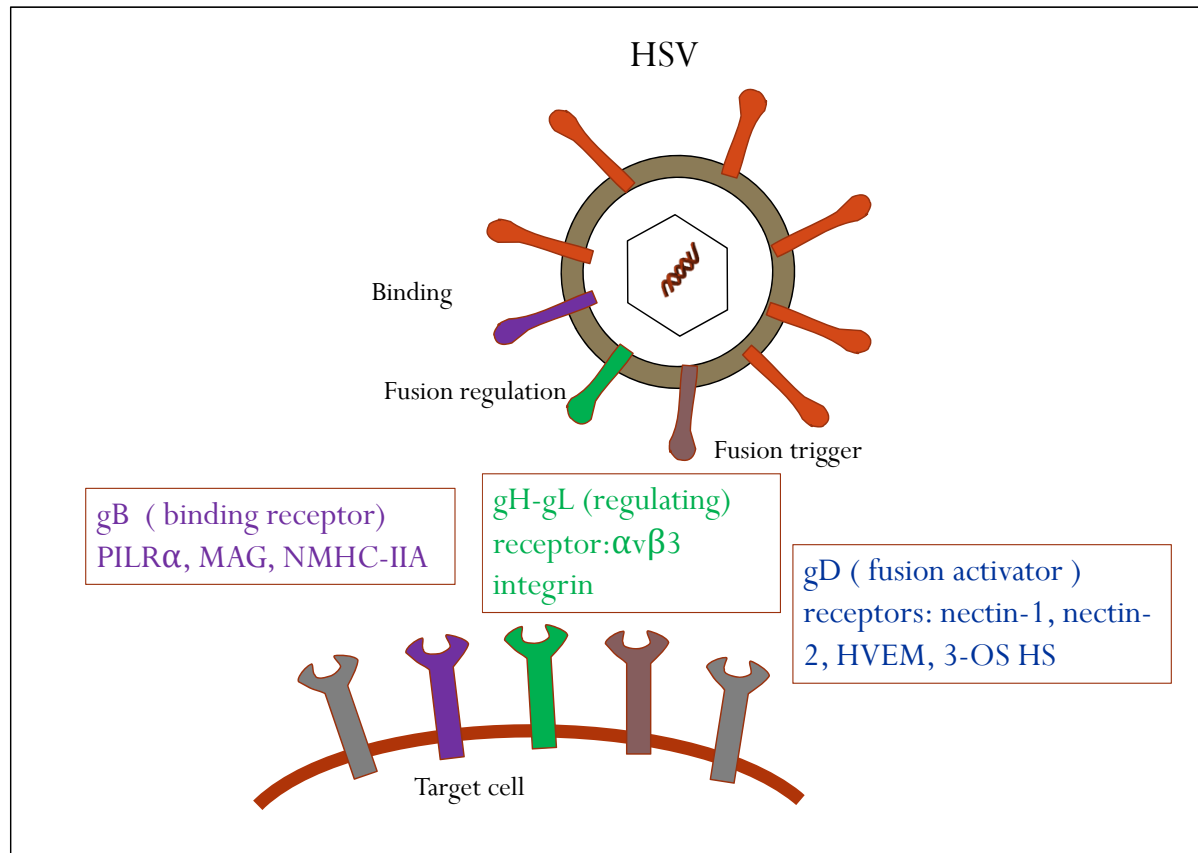
Herpes Simplex Virus



Insert schematic of ICP34.5 (-) HSV genome

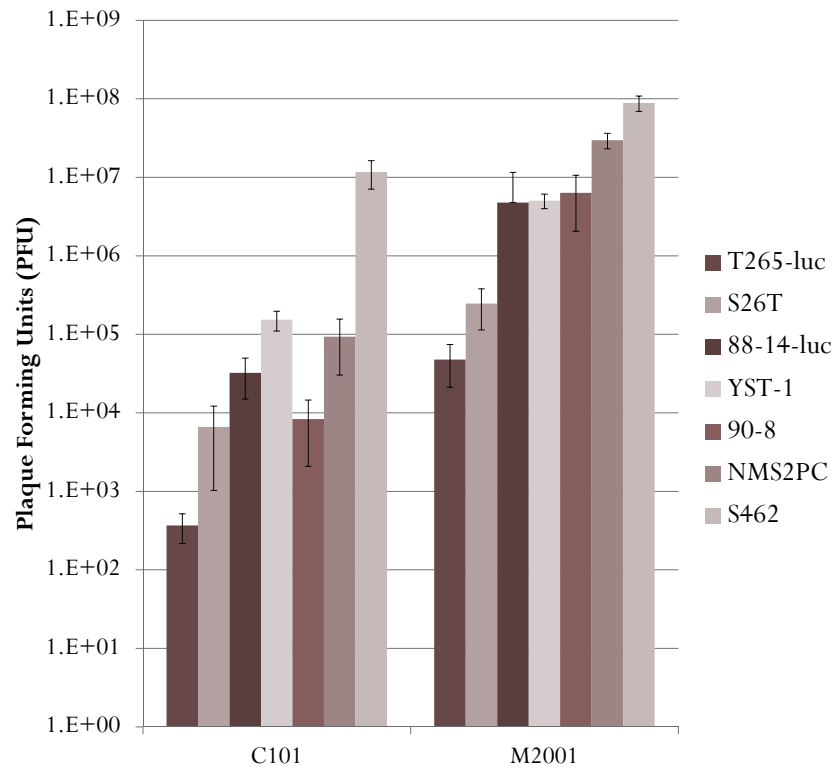
- Most commonly know as causing cold sores.
- Cold sore caused when virus replicates and kills cells.
- Modified to selectively replicate in tumor cells. (Do animation and show schematic when you reach this point and then discuss briefly how the g134.5 gene is a neurovirulence gene and how deletion of this renders the virus non-pathogenic except in tumor cells)

HSV Entry Into MPNSTs

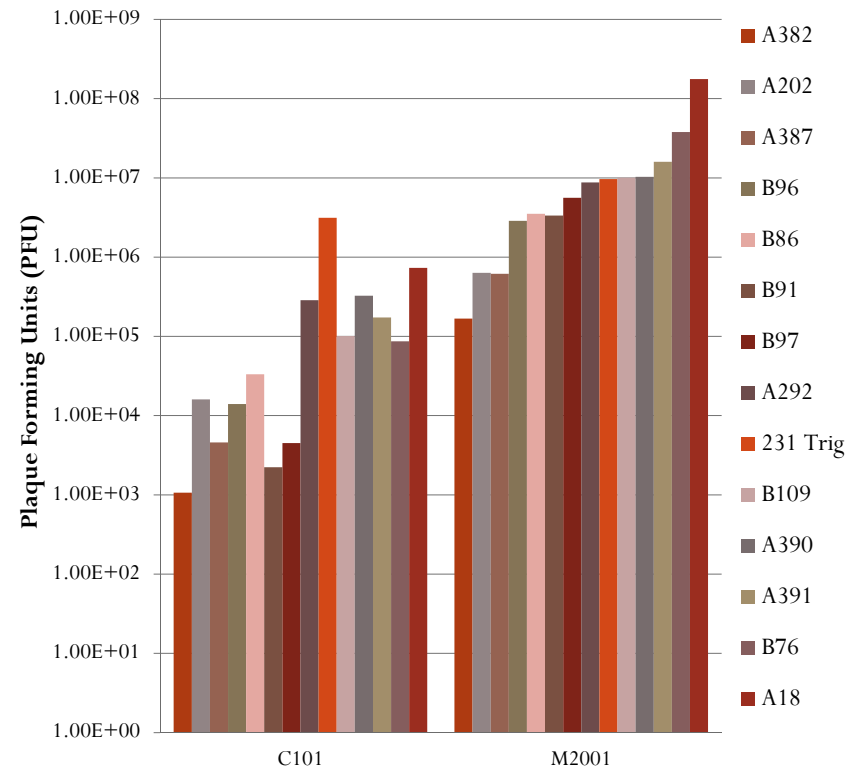


- HSV contains glycoproteins gD, gB, and gH-gL
- Interact with correlating cell receptors
- The principal HSV entry receptor on most cells is Nectin -1 (also called PVLR-1 or CD111)

Viral Replication Varies by Cell Line

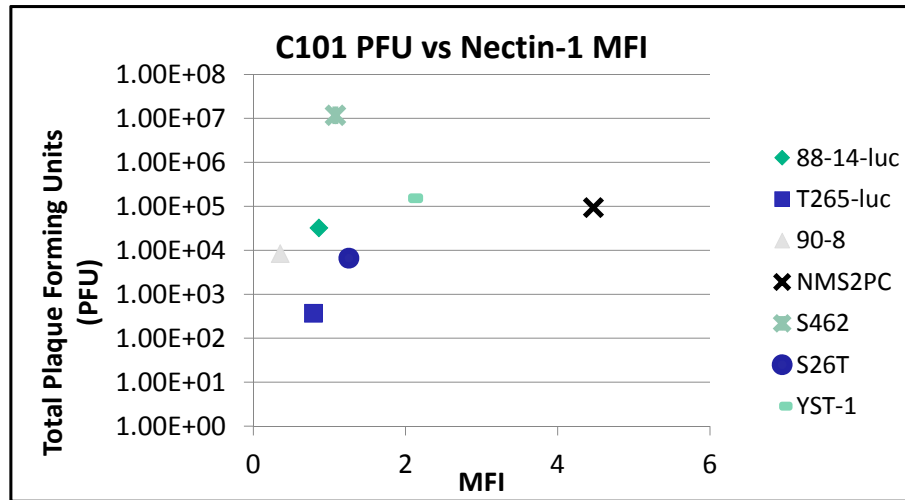


Human MPNST Viral Recovery

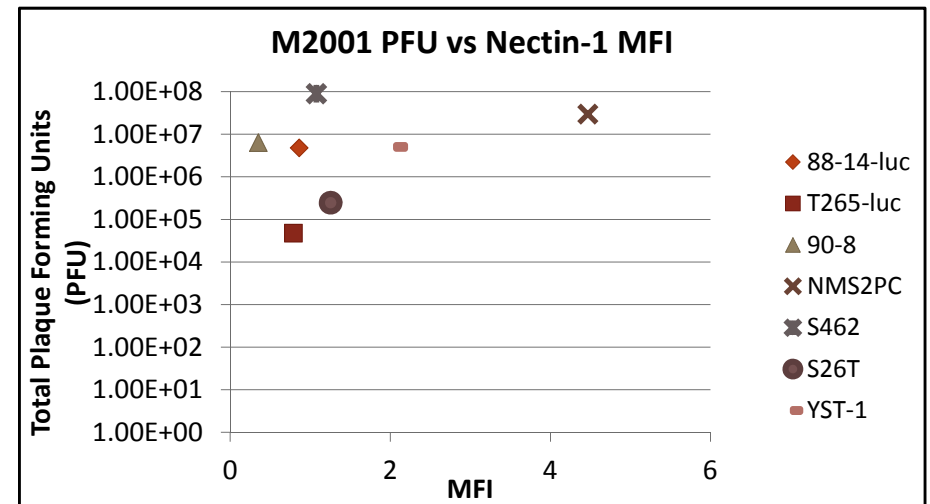


Murine MPNST Viral Recovery

Comparing Viral Recovery with Nectin-1 Expression



PFU of C101 HSV in cell lines 88-14-luc, T265-luc, 90-8, NMS2PC, S462, S26T, and YST-1 plotted against nectin-1 MFI after a 24 Hour Infection



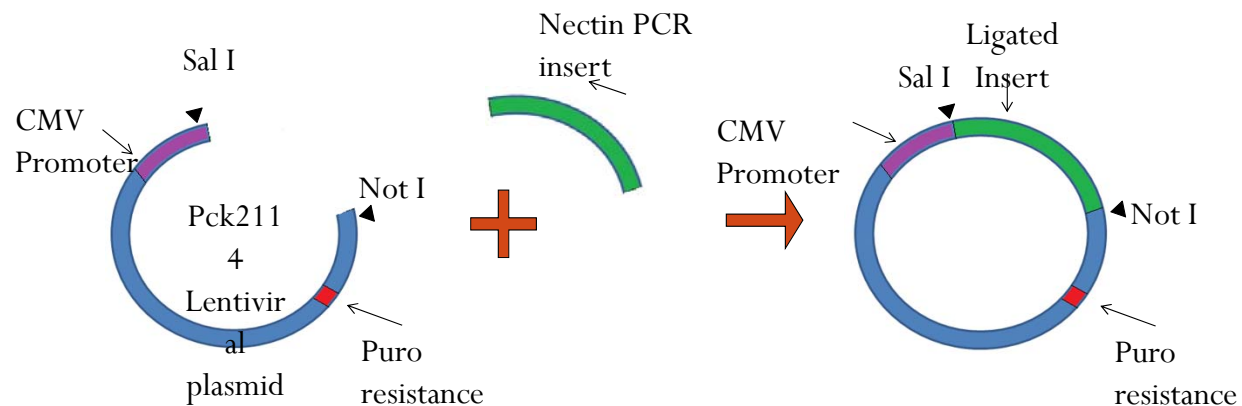
PFU of M2001 HSV in cell lines 88-14-luc, T265-luc, 90-8, NMS2PC, S462, S26T, and YST-1 plotted against nectin-1 MFI after a 24 Hour infection

Hypothesis

We hypothesize that the variability in oHSV-1 replication is due to differences Nectin-1 entry receptor (abundance or expression levels) between MPNST cell lines.

Include a CARTOON OF groups of CELLS WITH RELATIVELY LITTLE nectin (on left) and a group with large amounts of nectin (on the right) and show virus not entering the group on the left leading to low amounts of viral recovery. Show the virus on the right entering multiple cells (through the nectin receptor) and then replicating leading to higher viral recovery

Creating a nectin-1 expressing lentivirus



Slide 8

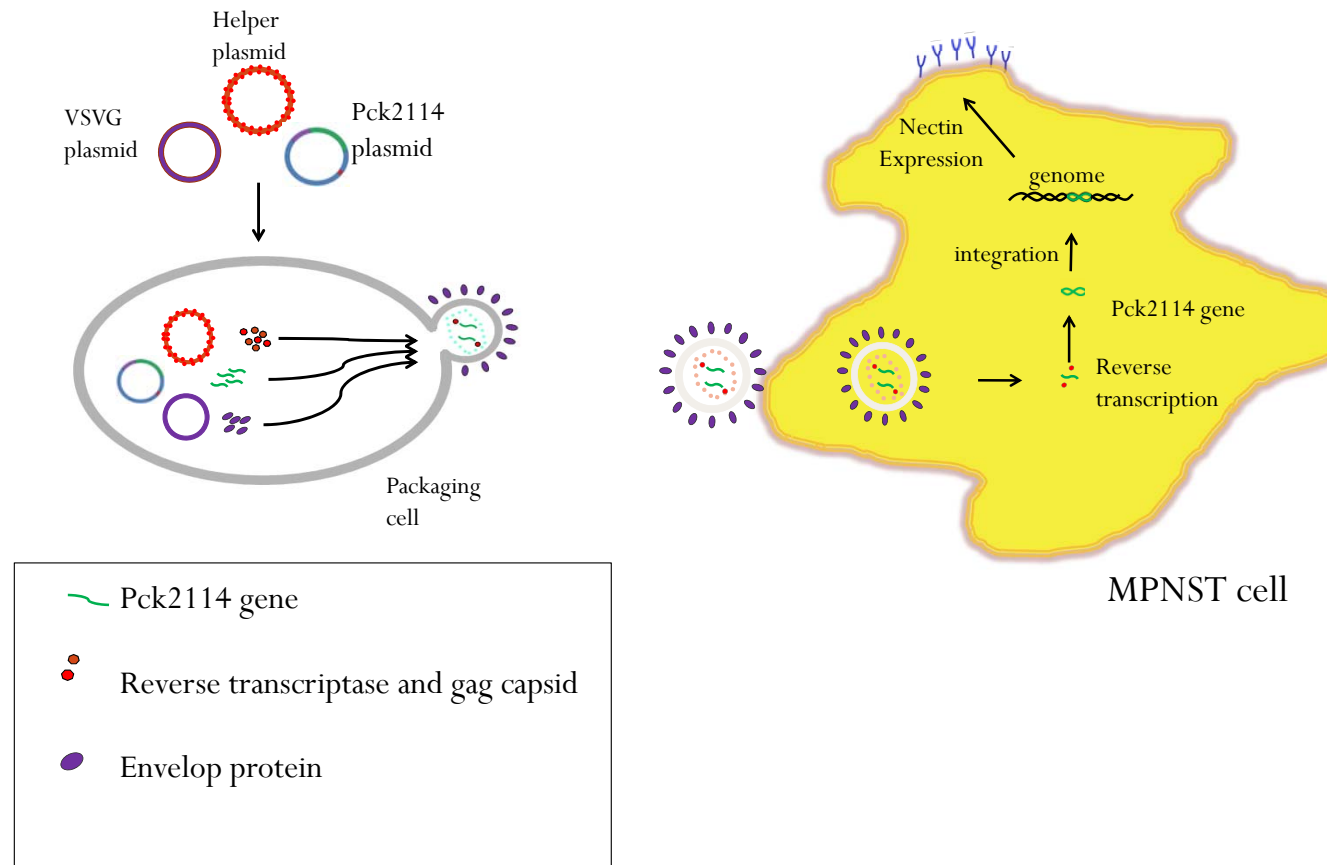
KAC1 Do you want to make this image more sexy consider using the Geneious program and include the annotated image and / or a picture of the structure of Nectin 1

Kevin A. Cassady, M.D., 2/8/2013

KAC2 Make your figures bigger the audience is unable to see all of this.

Kevin A. Cassady, M.D., 2/8/2013

Creating MPNST cell line overexpressing Nectin-1

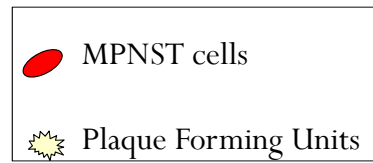


Production of Nectin-1-Expressing Lentivirus.

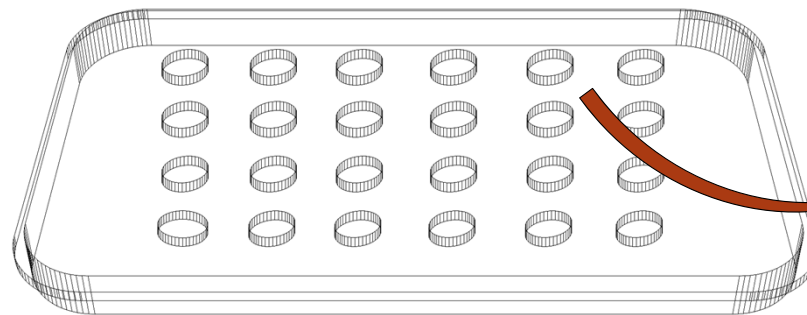
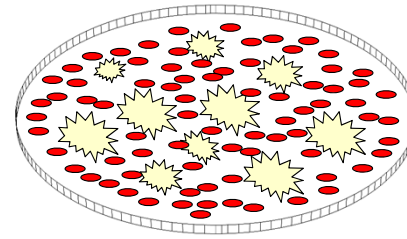
KAC3 ANIMATE THIS SO YOU Go through the steps

Kevin A. Cassady, M.D., 2/8/2013

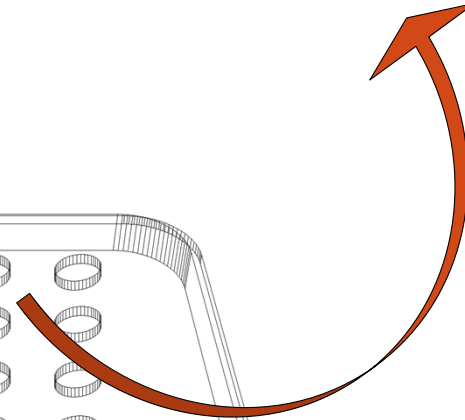
Viral Recovery Study



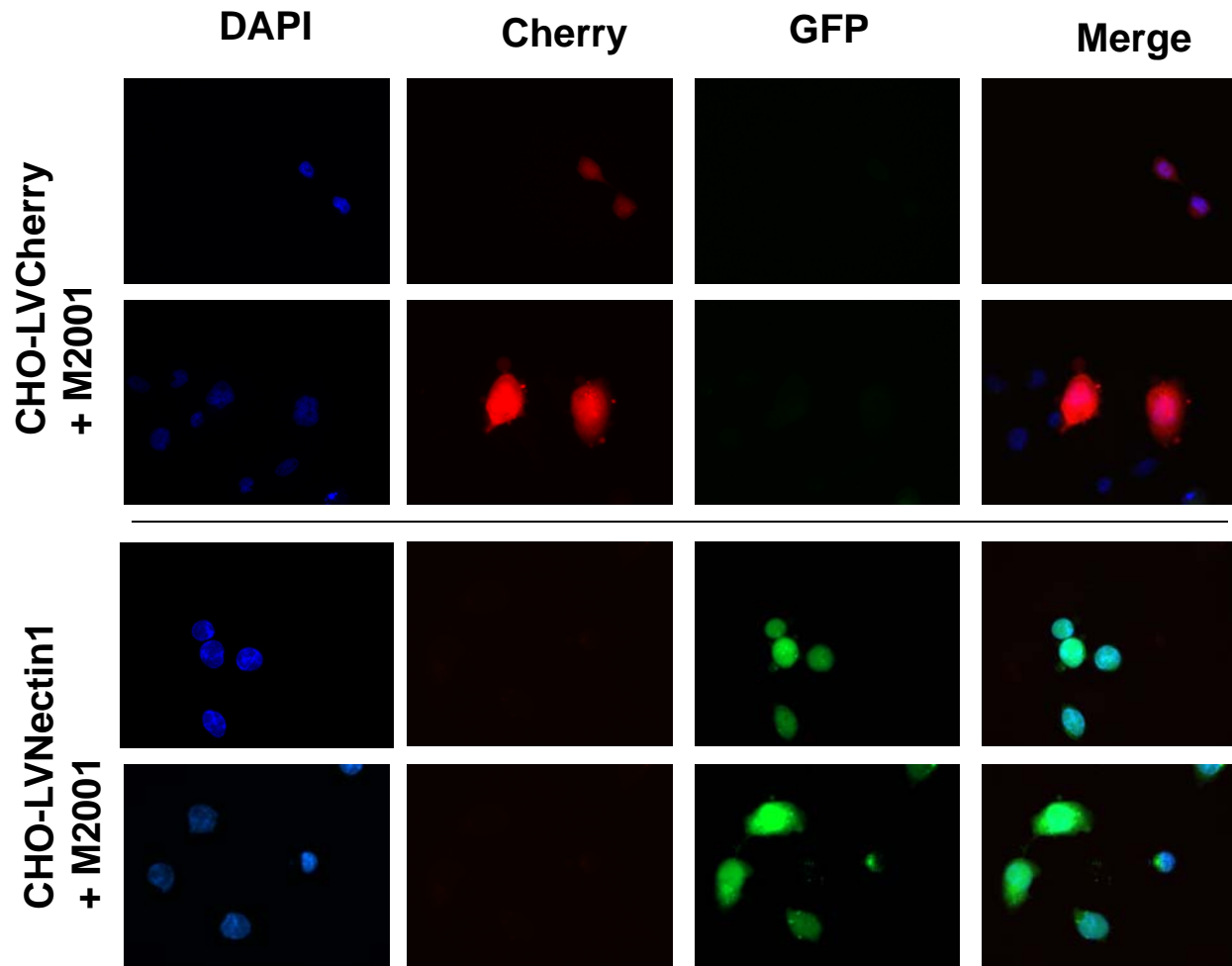
Well with HSV infected
MPNST cells



24 well titer plate

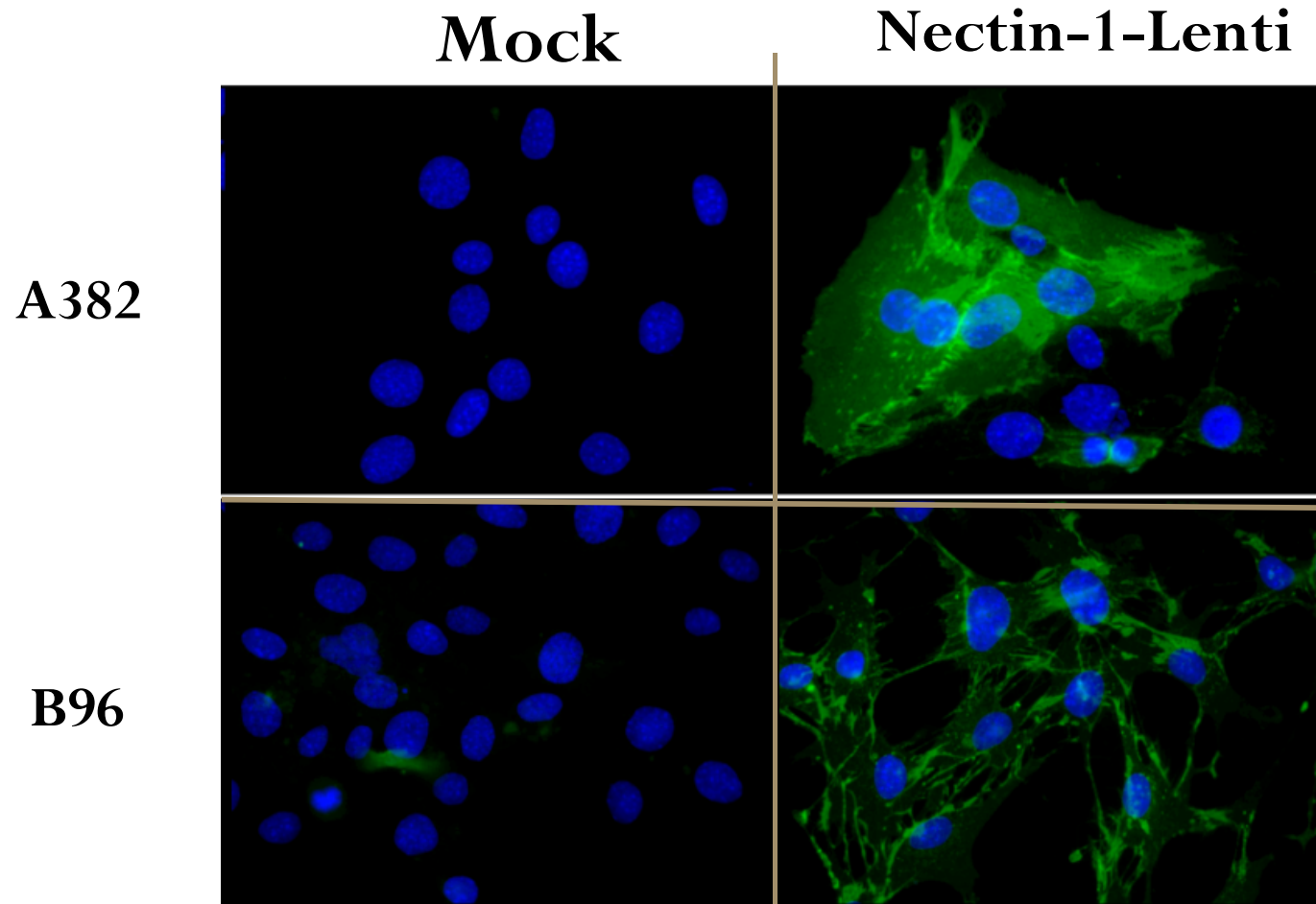


Testing the functionality of Lenti Virus



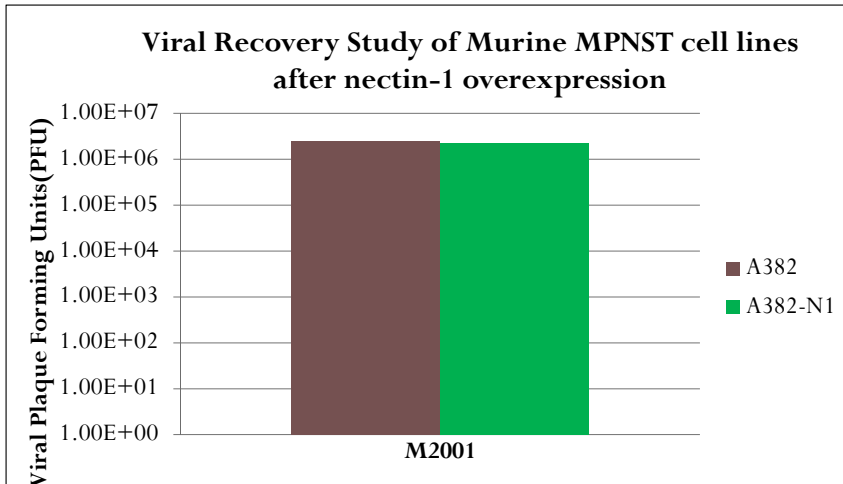
Demonstration of functional nectin-1 Lenti viral construct.

Nectin-1 Overexpression

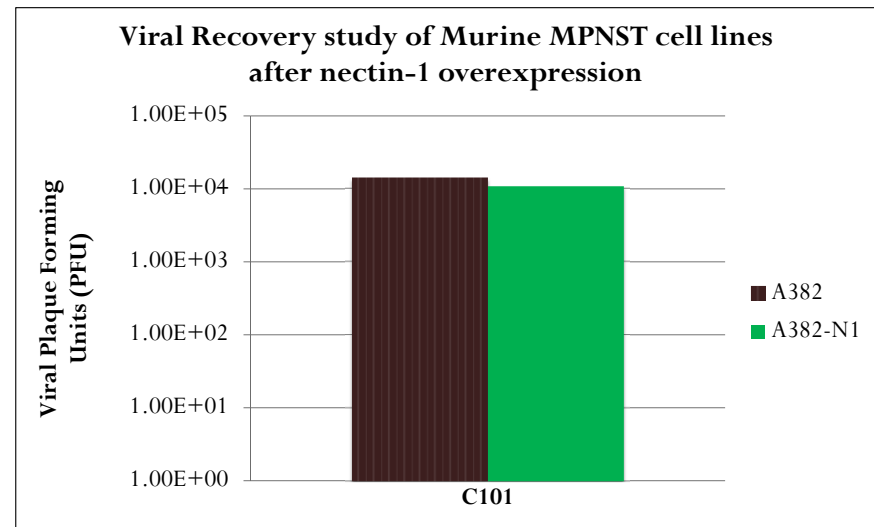


Mouse cell lines A382 and B96, mock and nectin overexpressed, stained with PE and DAPI

Viral Recovery After Nectin-1 overexpression



PFU of A382 (before overexpressing nectin) and A382-N1(after overexpressing nectin) in M2001 cell line after a 24 Hour incubation period.



PFU of A382 (before overexpressing nectin) and A382-N1(after overexpressing nectin) in C101 cell line after a 24 Hour incubation period

Summary & Discussion

- Results show no significant correlation between nectin 1 expression and susceptibility of MPNSTs for Dg134.5 vectors based upon viral replication. KAC5
- Suggest internal mechanisms controlling infectivity of cells KAC4

Slide 14

KAC4 I would hold off on this at this time!

Kevin A. Cassady, M.D., 2/8/2013

KAC5 Also Hold off on this as well

Kevin A. Cassady, M.D., 2/8/2013

Human MPNST	Mycoplasma contamination	Mycoplasma eliminated	Clearance method	Viral recovery? Single step	Viral recovery? Multi-step	Establishes in vivo flank tumors?
88-14-luc	no			yes	yes	yes (Carroll)
STS26T-luc	no			yes	yes	yes (Carroll/Markert)
T265-luc	no			yes	yes	no (Carroll/Markert)
YST-1	no			yes	yes	yes (Carroll)
S462	yes	yes	lenti w/ puro	yes	yes	no (Markert)
NMS2-PC	no			yes	yes	no (Markert)
90-8	yes	yes	lenti w/ puro	yes	yes	no (Markert)
2XSB	yes	yes	BM Cyclin (Roche)	yes	yes	Testing
HS-PSS	yes	no	BM Cyclin (Roche)	yes	yes	-

Murine MPNST						
231 trigeminal	no			yes	yes	
A18	yes	yes	BM Cylin (Roche)	yes	yes	
A202	no			yes	yes	
A292	no			yes	yes	yes (Carroll)
A382	no			yes	yes	
A387	no			yes	yes	
A390	yes	no		yes	yes	
A391	no			yes	yes	
B91	no			yes	yes	yes (Carroll)
B96	no			yes	yes	
B97	yes	no		yes	yes	yes (Carroll)
B109	no			yes	yes	
B76	yes	no		yes	yes	yes (Carroll)
A599	no			yes	yes	

Table 1: Summary of data for MPNST cell lines.

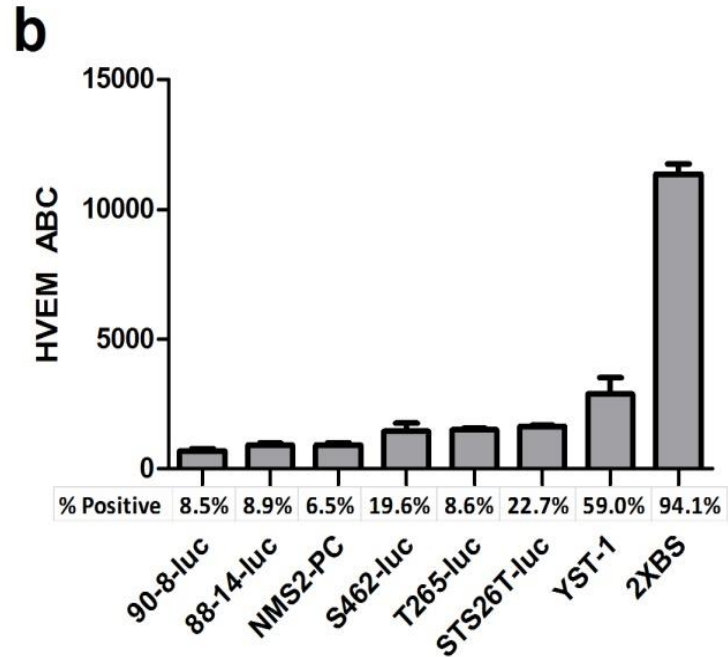
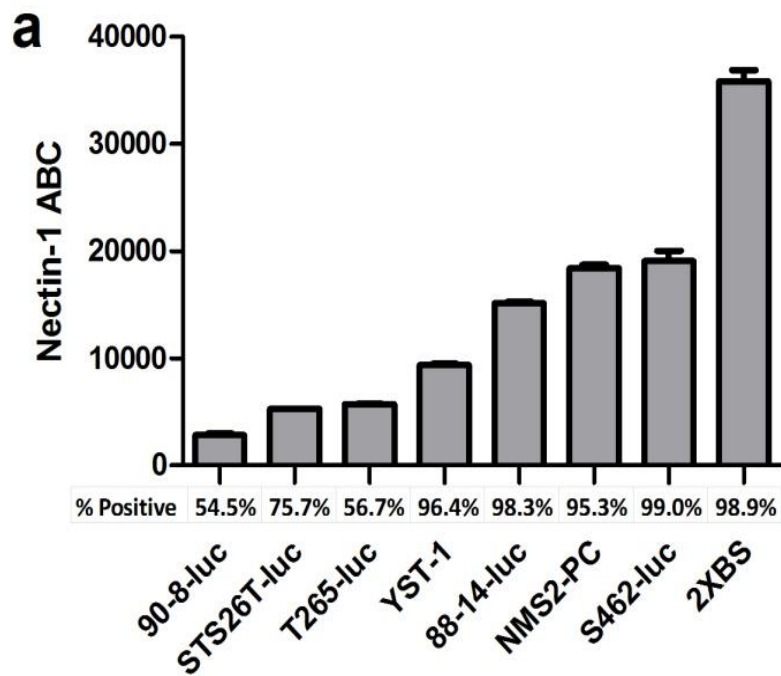


Figure 1 (Sub Task 1a): HSV-1 entry receptor expression in MPNST cell lines. Nectin-1 (a) and HVEM (b) entry receptor expression was assessed in all MPNST cell lines by flow cytometry using PE-conjugated antibodies. Mean fluorescence intensity was related to antibody binding capacity (ABC) using beads designed to bind set quantities of antibody. For each cell line, the percent of the population staining positively above the isotype control is also reported. A range of nectin-1 expression (a) is observed across all cell lines with the ABC of 2XSB nearly twice that of the next highest cell line. Some HVEM expression (b) was observed in several cell lines, but in much lower quantities than nectin-1.

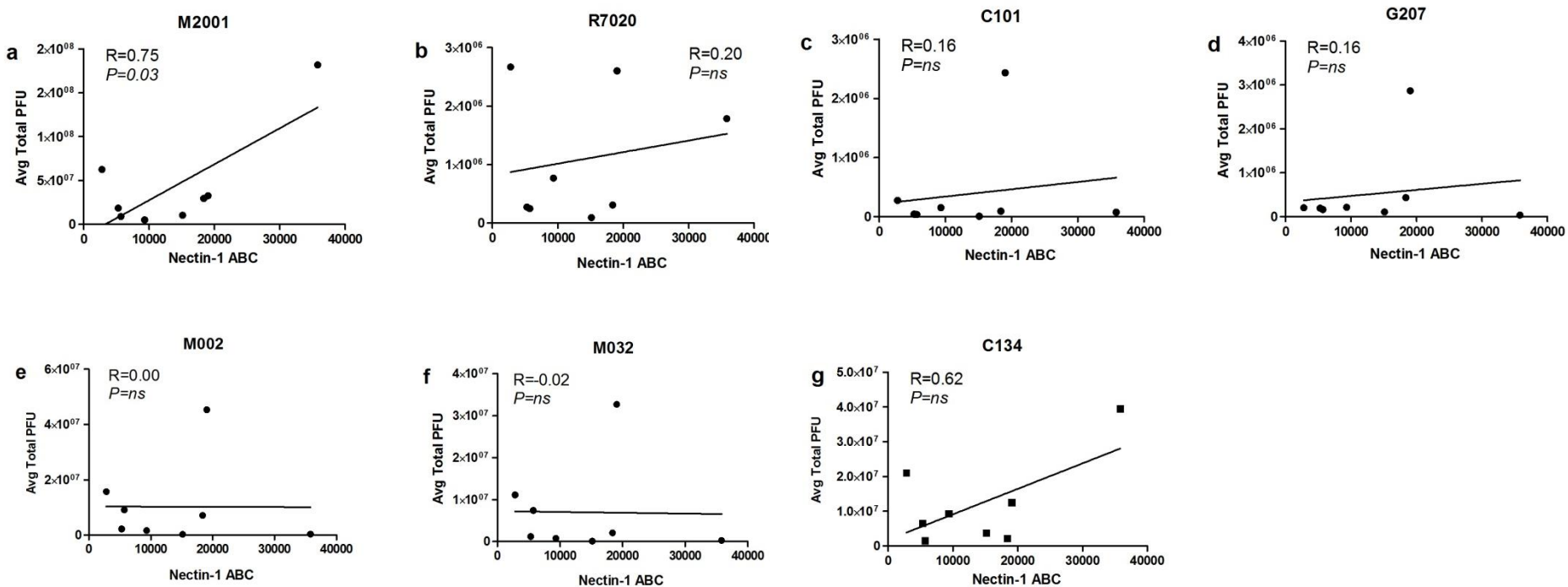


Figure 2 (Sub Task 1a & 1d): Correlation of nectin-1 expression with viral replication. Pearson's correlation coefficients were calculated between nectin-1 expression and each set of viral recovery data from M2001 (a), R7020 (b), C101 (c), G207 (d), M002 (e), M032 (f), and C134 (g). A statistically significant correlation ($R=0.75$) was noted for M2001. A strong correlation ($R=0.62$) was also noted for the chimeric virus C134 but the correlation was not statistically significant. Significance was set at $P<0.05$.

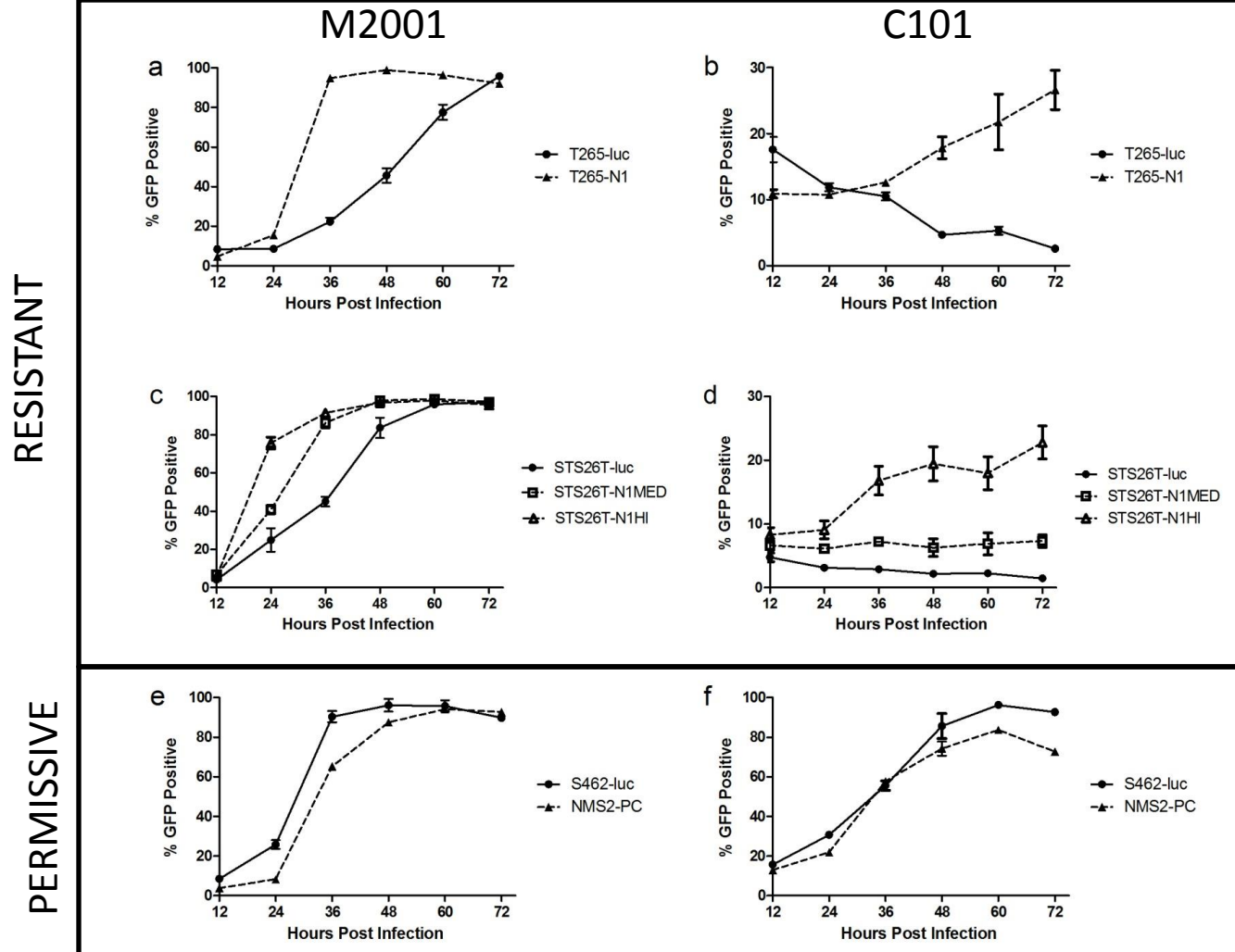
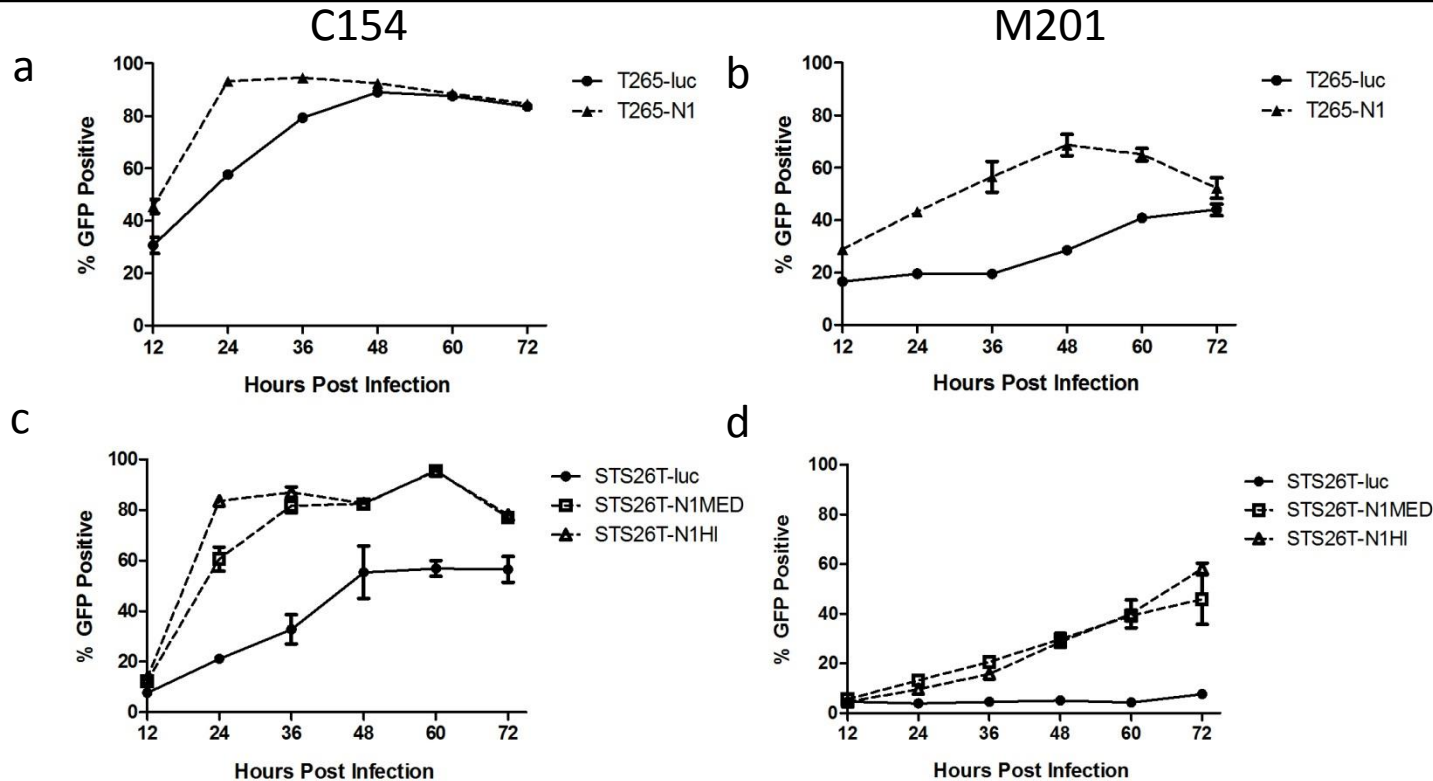


Figure 3 (Sub Task 1b): Spread of wild-type and attenuated oHSV in resistant and permissive cell lines. Whole populations of nectin-1 transduced cells or parent were monitored for viral spread following infection with M2001 or C101 at MOI=0.1. Spread was assessed by determining the percent of the population expressing viral GFP at 12 hr intervals for 72 hrs. As compared to the respective parent, infection with M2001 in T265-N1 (a), STS26T-N1MED (c), and STS26T-N1HI (c) showed substantially increased speed in the spread of the virus, similar to that seen in permissive cell lines S462-RLIP and NMS2-PC (e). Increased nectin-1 expression appears to enhance spread of wild-type virus. C101 showed improved spread in the highest nectin-1 expressing lines T265-N1 (b) and STS26T-N1HI (d) compared to their respective parent lines, however the percent positive at 72 hpi for these lines was achieved near 24 hpi by permissive cell lines (f). Increased nectin-1 implies a benefit to spread by attenuated virus C101 but does not mimic a permissive phenotype.

RESISTANT



PERMISSIVE

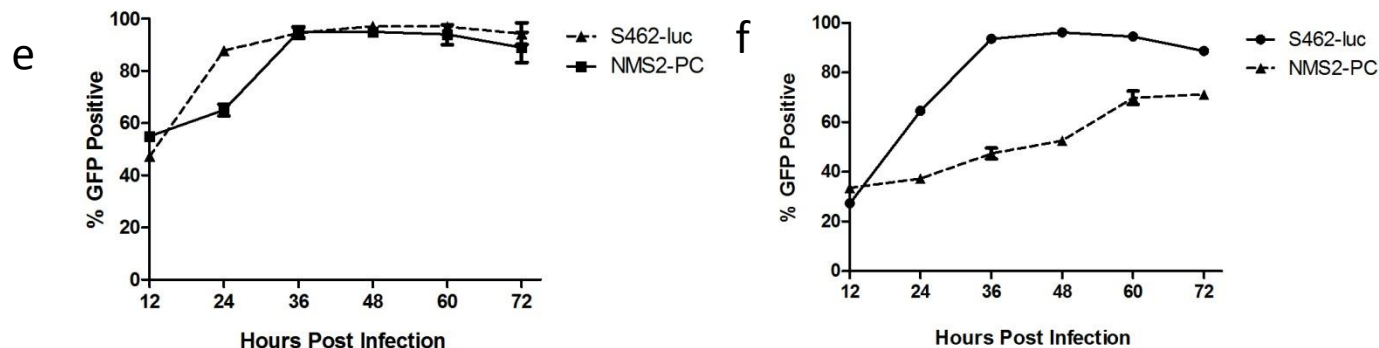


Figure 4 (Sub Task 1b): Spread of engineered oHSV in resistant and permissive cell lines. The spread of engineered oHSVs C154 (A,C,E) and M201 (B,D,F) was measured by monitoring expression of GFP in infected cells over time by flow cytometry. OHSVs C154 and M201 are GFP expressing variants of C134 and M002 respectively. Resistant cell lines T265-luc (A-B) and STS26T-luc (C-D) and the nectin-1 overexpressing variants were used. Permissive lines S462-luc and NMS2-PC are shown for comparison (E-F).

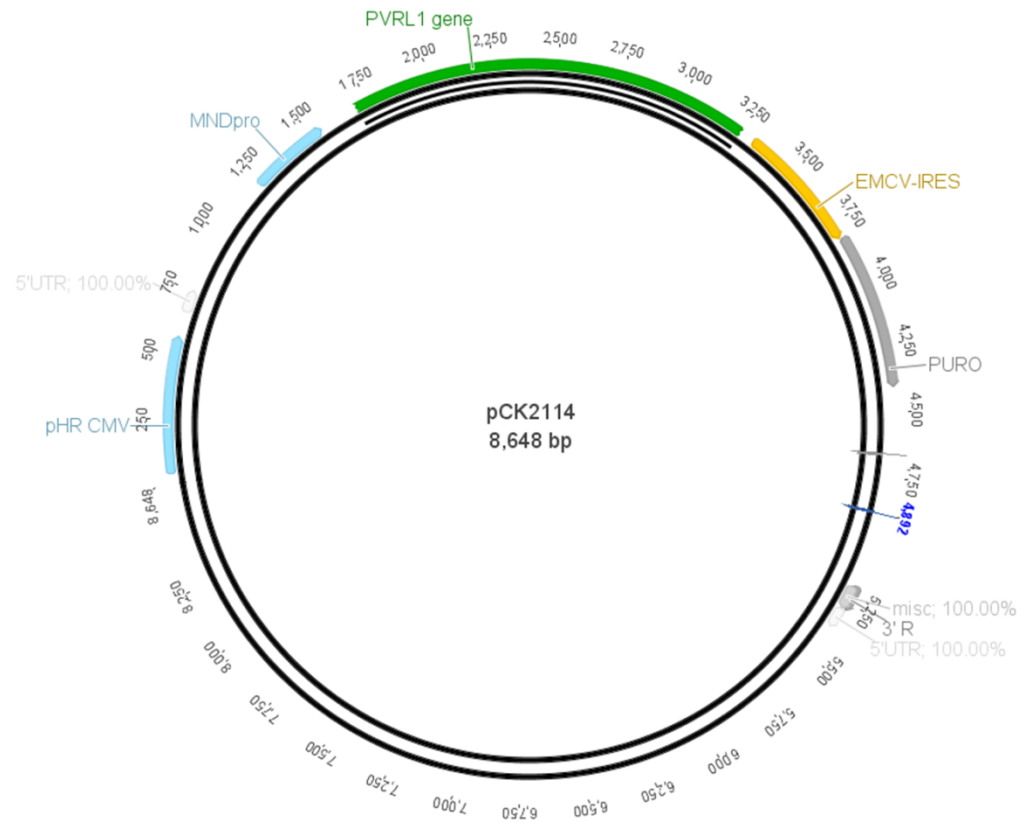


Figure 5 (Sub Task 1b): Plasmid map of pCK2114 encoding full length nectin-1 gene (PVRL1). A self-inactivating lentiviral vector was used to overexpress nectin-1 or control mCherry in oHSV resistant cell lines. Human nectin-1 clone (Clone ID: 8322523) was obtained from Open Biosystems (Thermo Scientific). Nectin-1 cDNA was PCR amplified with 5 PRIME HotMasterMix (5 Prime, Gaithersburg, MD) using primers 5'-CGGATCCCGGGTCGACCCGATGGCTCGGATGGGGCTT-3' and 5'-CCGGTTCGAGCGGCCGCGCTACACGTACCACTCCTTCTTGAA-3' (IDT, Coralville, IA) in a T100 Thermal Cycler (BioRad, Hercules, CA). A 1.5 kb PCR product was confirmed and column purified (Enzymax, Lexington, KY). To prepare the recipient vector, pLVmnd.mUTA2-IPp was digested with Sall and NotI and subjected to electrophoresis to isolate the large fragment. Nectin-1 cDNA was then inserted into the linearized recipient vector using an InFusion HD Cloning Kit (Clontech, Mountain View, CA) according to the manufacturer's instructions. The InFusion product pCK2114 was sequenced at the insertion sites to confirm recombination and orientation of the nectin-1 gene. Lentivirus was assembled by co-transfection of pCK2114, pMD.G (VSVG pseudotype), and pDR8.91 (HIV packaging) in 293T cells under OptiMEM media (Gibco). Control lentivirus was constructed using pLVmnd.CIP, mCherry followed by IRES and puromycin N-acetyl-transferase.

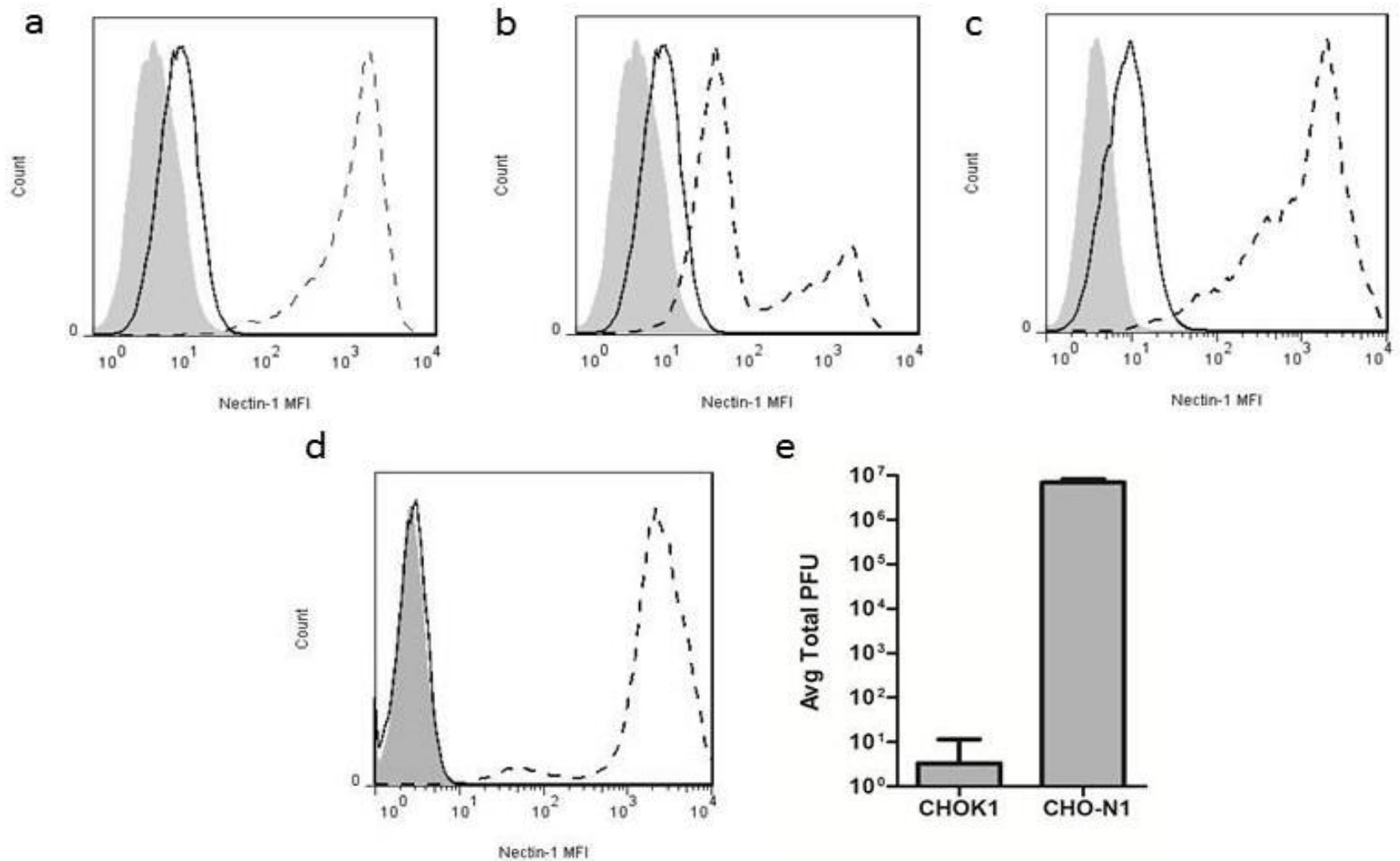
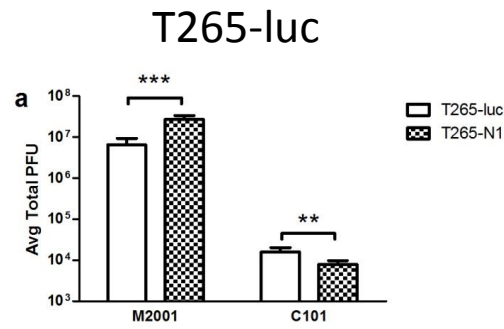
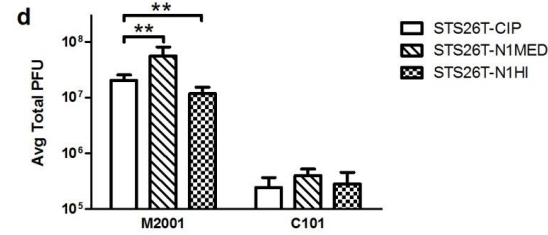


Figure 6 (Sub Task 1b): Functional overexpression of nectin-1 in resistant cell lines T265-luc and STS26T-luc. Nectin-1 was transduced via lentivirus into oHSV resistant cell lines STS26T-luc and T265-luc. Two lines derived from STS26T-luc were obtained by FACS: STS26T-N1HI (a) with a single high expressing population and STS26T-N1MED (b) with dual populations of increased nectin-1. Transduction followed by FACS in T265-luc yielded T265-N1 (c), a mainly high expressing population. Isotype control (shaded), parent (solid line), and transduced (dashed line) cell lines are shown. Nectin-1 deficient cell line CHOK1 was transduced to produce CHO-N1 (d) and infected with M2001 (MOI=10, 24 hr) to demonstrate functionality of the nectin-1 and subsequent viral replication (e).

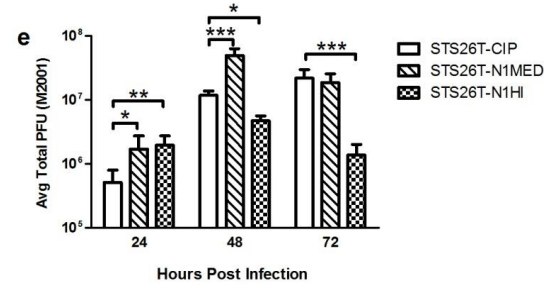
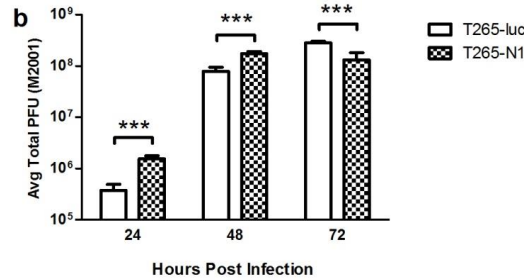
MOI=10



STS26T-luc



M2001
MOI=0.1



C101
MOI=0.1

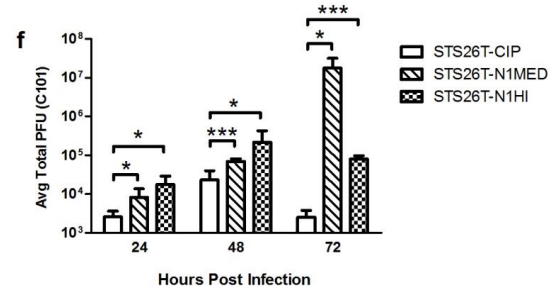
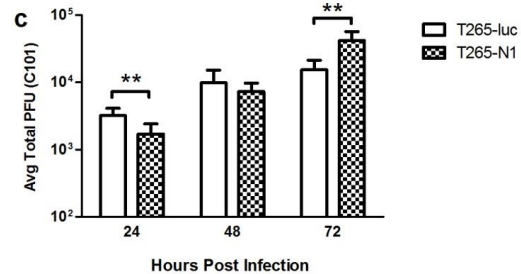


Figure 7 (Sub Task 1b): Impact of increased nectin-1 expression on viral replication. Single and multi-step replication assays using M2001 and C101 were performed in STS26T-luc and T265-luc transduced with nectin-1 or mCherry (CIP). In the single-step assays for both STS26T-luc (a) and T265-luc (d), M2001 was increased significantly in T265-N1 and STS26T-N1MED, however was decreased for STS26T-N1HI. No significant increases using C101 were measured in any cell line. For T265-N1 in the multi-step assay, there were some significant increases in viral recovery following infection with M2001 (b) and C101 (c), though a greater than 0.5 log increase was not seen. In STS26T-N1MED and STS26T-N1HI, infection with M2001 showed divergent trends in viral titer over time (e) resulting in significantly higher titers in STS26T-N1MED at 48 hpi and in STS26T-N1HI significantly lower titers at 48 and 72 hpi compared to the control. Significant increases in titer were observed at all timepoints when these STS26T-luc nectin-1 overexpressers were infected with C101 (f). Notably at 72 hpi, both nectin-1 overexpressing lines were multiple orders of magnitude larger than STS26T-CIP.

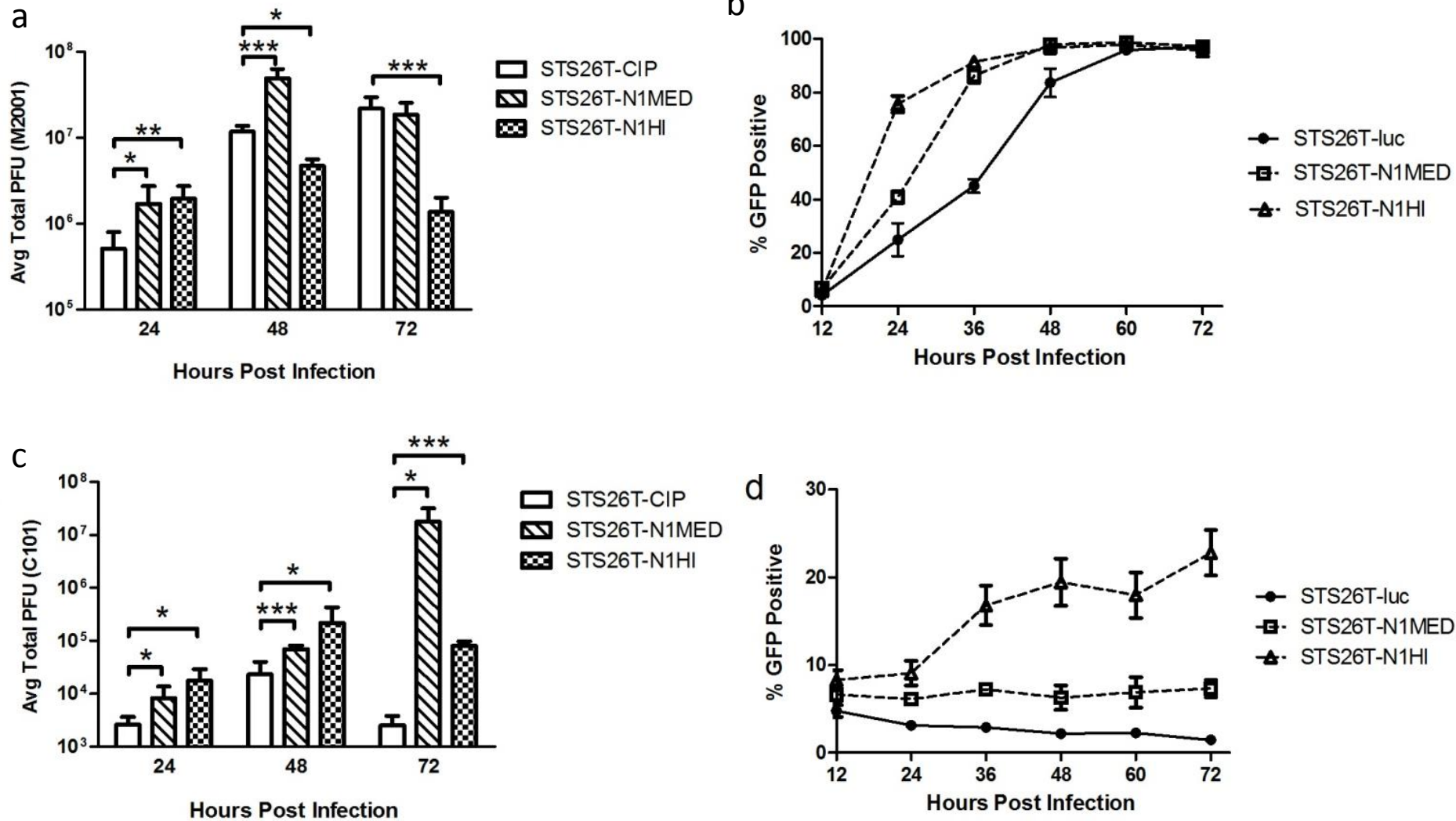


Figure 8 (Sub Task 1b): Comparison of viral recovery and viral spread in STS26T-luc and nectin-1 overexpressing STS26T-luc cells. Viral spread of both M2001 (b) and C101 (d) is increased in cell line STS26T-N1HI as compared to STS26T-N1MED. However viral recovery of M2001 in STS26T-N1MED is increased over STS26T-N1HI at 48 and 72 hpi (a) and with C101 at 72 hpi (c).

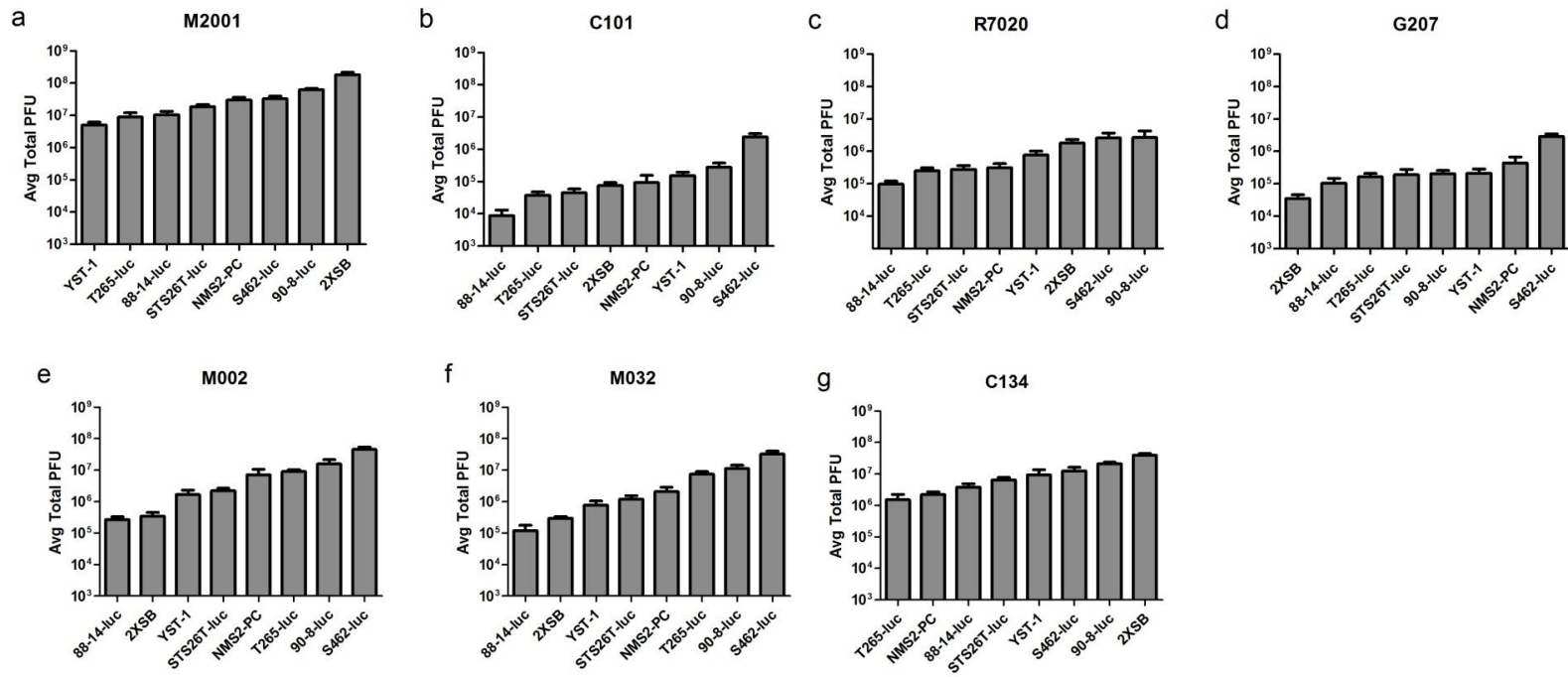


Figure 9 (Sub Task 1c): Single-step viral recovery in MPNST cell lines. MPNST cell lines were subjected to single-step (MOI=10, 24 hr) infection by viruses M2001 (a), R7020 (b), C101 (c), G207 (d), M002 (e), M032 (f), C134 (g) and the viral titers reported as the average total plaque forming units (PFU) as determined through limiting dilution plaque formation. Error bars represent standard deviation. For each virus, a range of replication was observed between all cell lines with the largest differences observed in the double $\gamma_134.5$ deleted viruses C101 and G207. Resistant cell lines STS26T-luc and T265-luc as well as permissive lines S462-luc and NMS2-PC were identified and selected for further study.

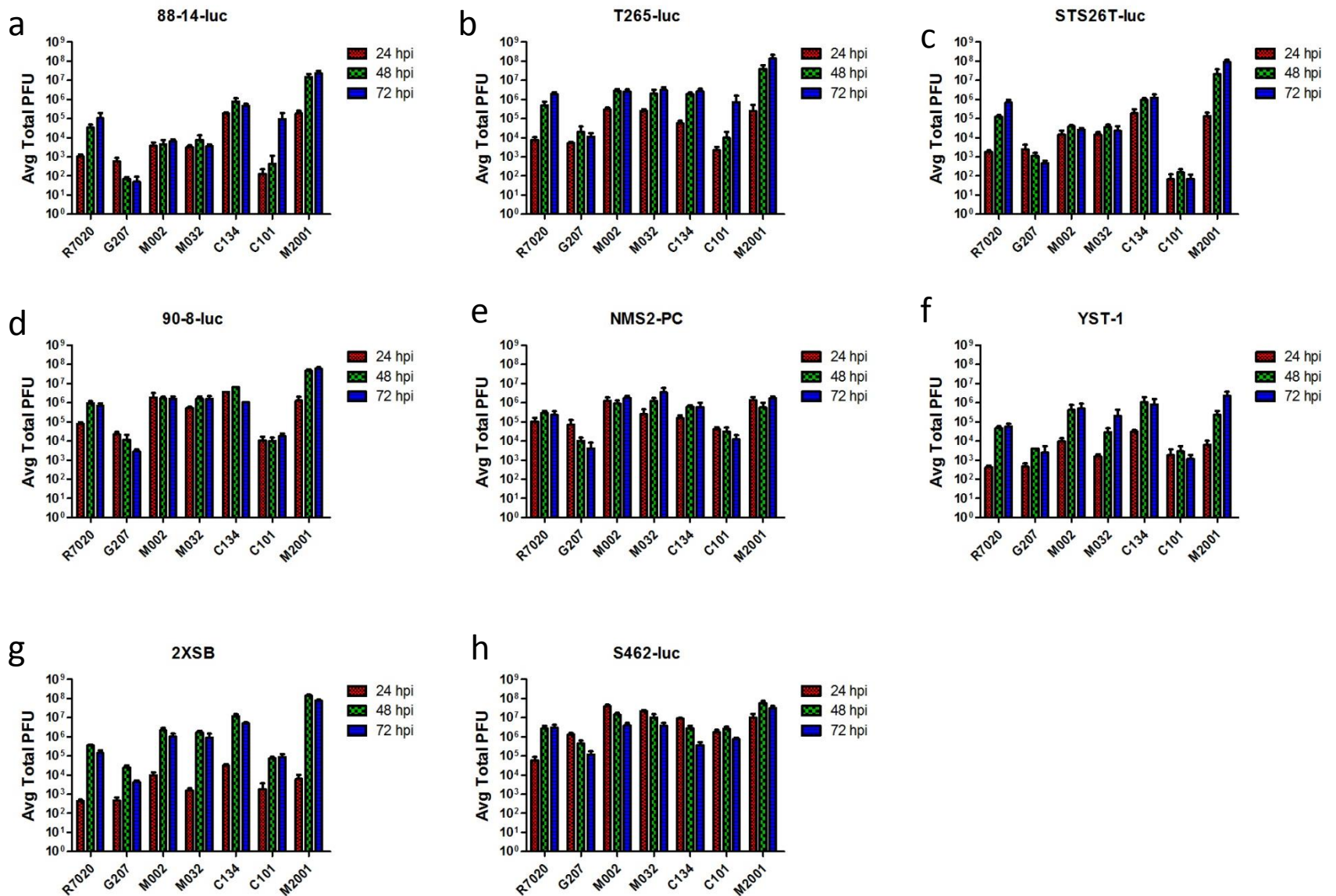


Figure 10 (Sub Task 1c): Multistep-step viral recovery in MPNST cell lines. MPNST cell lines were subjected to multi-step (MOI=0.1 at 24, 48, and 72 hpi) infection by viruses M2001 (a), R7020 (b), C101 (c), G207 (d), M002 (e), M032 (f), C134 (g) and the viral titers reported as the average total plaque forming units (PFU) as determined through limiting dilution plaque formation. Error bars represent standard deviation. In general, permissive cell lines permit replication of attenuated viruses (e.g. C101, G207) closer to that reported for wild type M2001. Resistant lines T265-luc (b) and STS26T-luc(c) generally have suppressed replication of G207 and C101 compared to M2001.

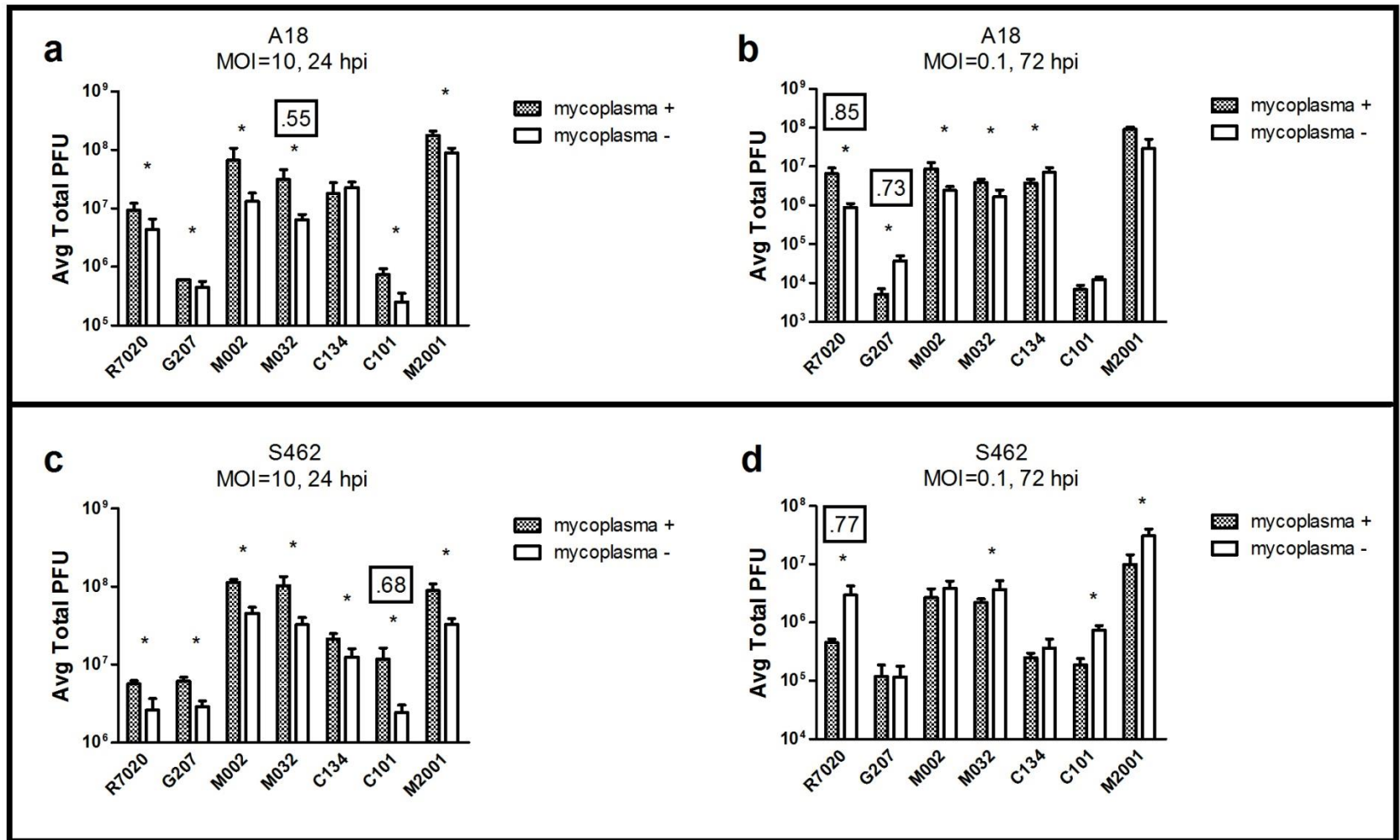


Figure 11 (Sub Task 1c): Comparison of viral recovery before and after mycoplasma contamination. Cell lines A18 (a-b) and S462 (c-d) (human) were discovered to be mycoplasma contaminated following original viral recovery. Following elimination of the contamination, viral recovery was performed again. Viral recovery at MOI of 10 (a and c) and a representative MOI of 0.1 timepoint (72 hpi) (b and d) are reported. While statistically significant differences were observed for a number of the viruses, only titer differences greater than 1.0 logs are considered biologically significant, since this is the known range of titer variation in HSV-1 (boxed numbers indicate fold change greater than 0.5 log). The overall trend in viral recovery remains the same and does not change assessment of these cell lines as permissive to viral replication.

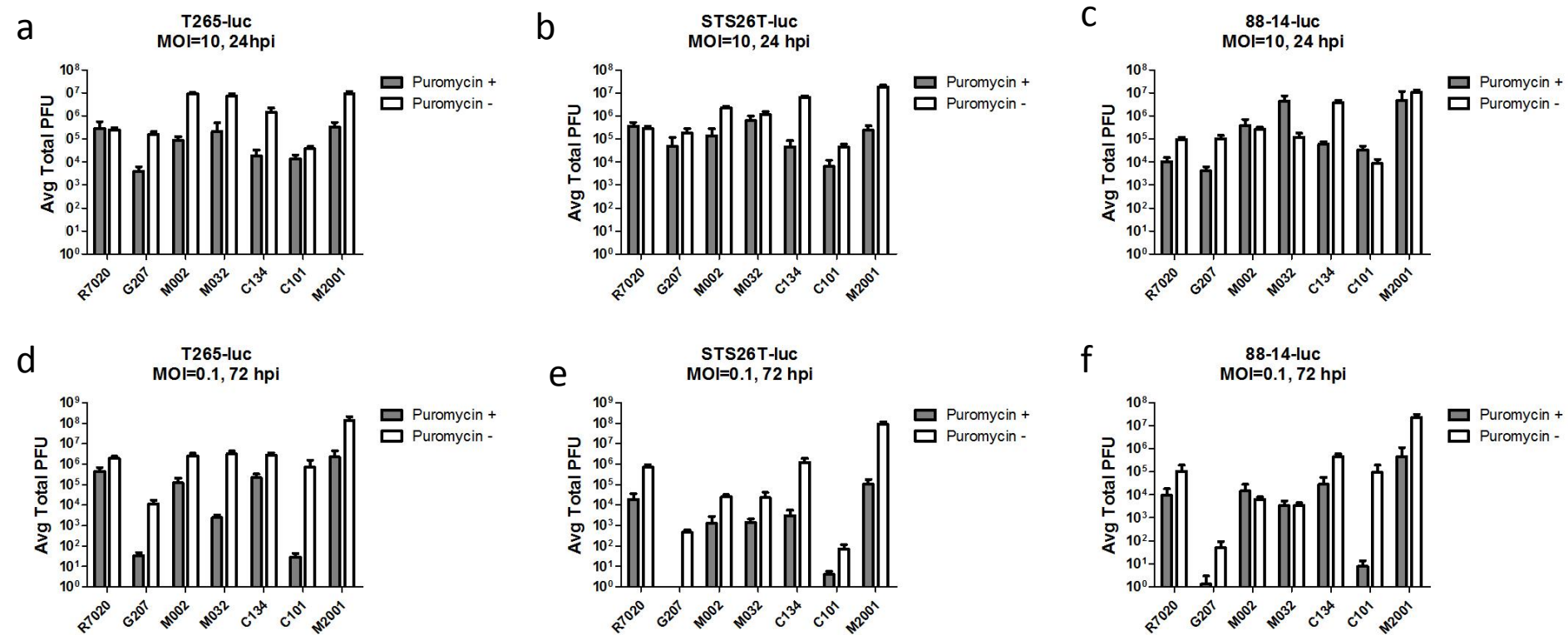


Figure 12 (Sub Task 1c): Comparison of viral recovery with and without puromycin. Viral recovery in cell lines T265-luc (a,d), STS26T-luc (b,e), and 88-14-luc (c,f) was suspected of being influenced by the use of puromycin in the maintenance media. Following removal of puromycin, the viral recovery assay was performed again. Viral recovery at MOI of 10 (a-c) and a representative MOI of 0.1 timepoint (72 hpi) (d-f) are reported. The majority of the timepoints and viruses tested are statistically different and, especially in the multistep assay, have increases in titer greater than 10 fold (one log). This confirms an overall trend that the presence of puromycin suppresses viral replication, especially at later timepoints in a multistep assay. All further data and conclusions are based on the data reported without puromycin.

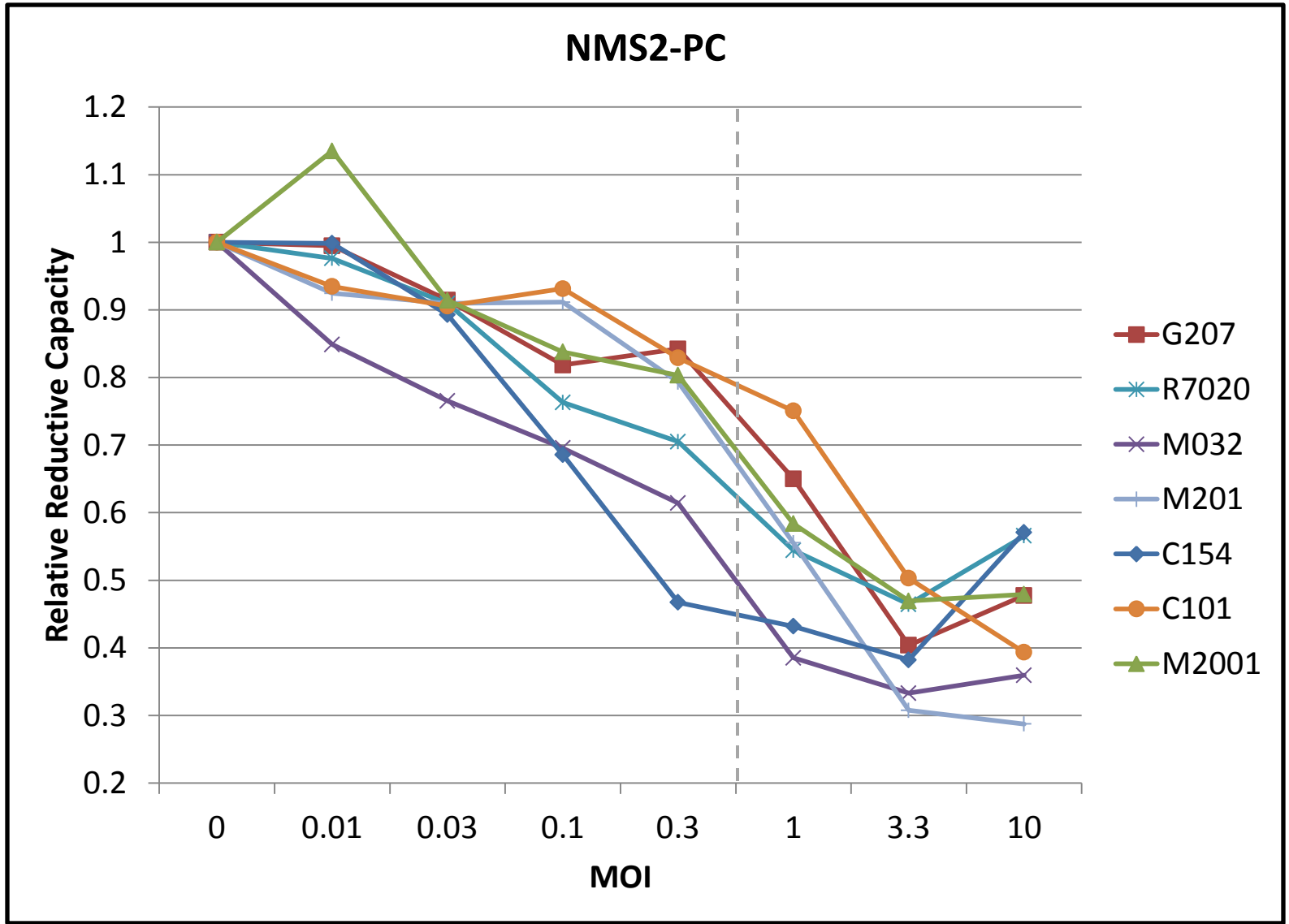


Figure 13 (Sub Task 1c): Alamar blue cytotoxicity assay in NMS2-PC: NMS2-PC cells were infected at various MOIs to establish the threshold for cytotoxicity and assayed for by Alamar blue at 72 hpi. As the cytotoxicity begins for most viruses below an MOI of 1 (dashed line), this cell line is confirmed to be permissive to replication and spread.

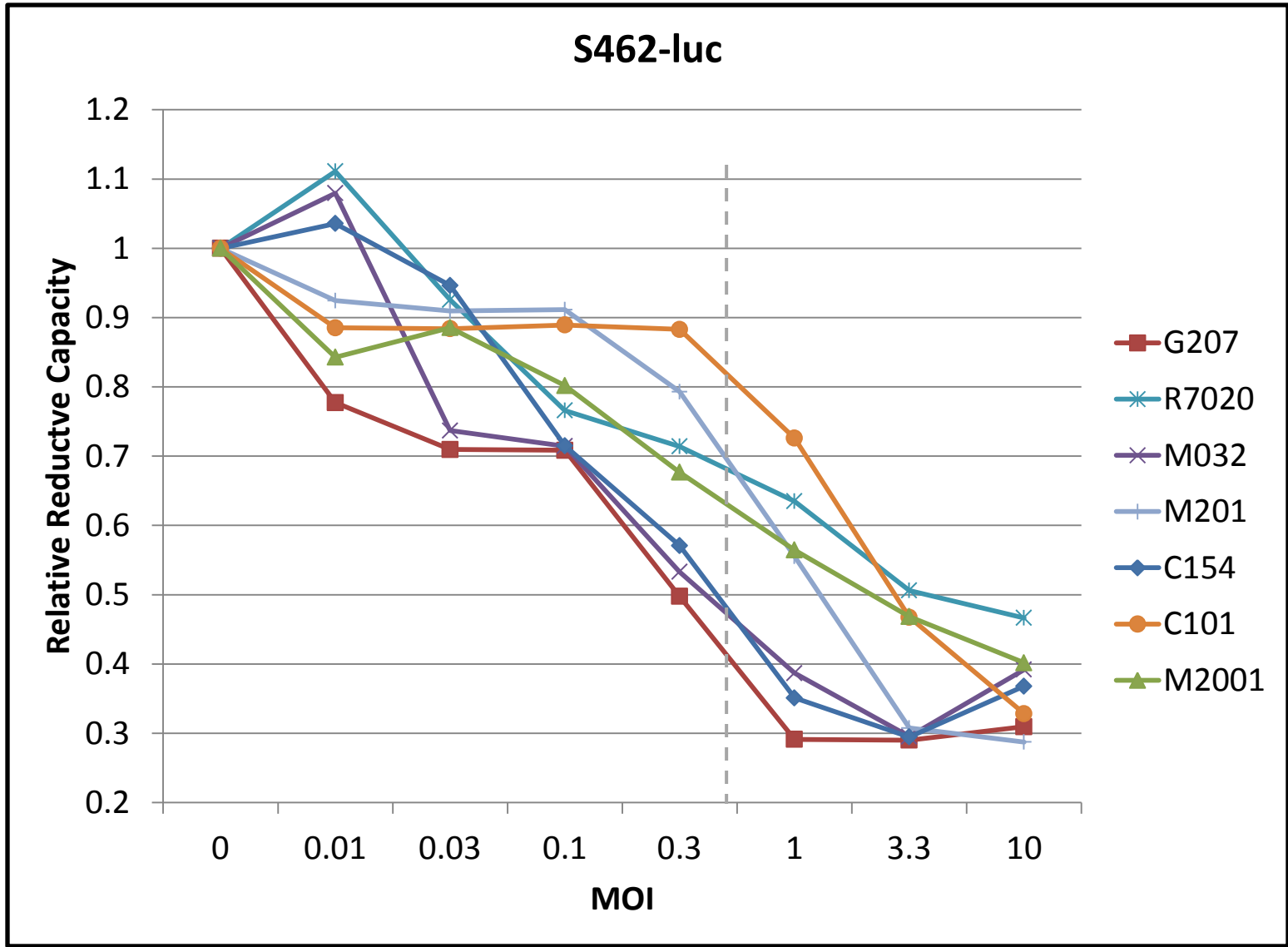


Figure 14 (Sub Task 1c): Alamar blue cytotoxicity assay in S462-luc: S462-luc cells were infected at various MOIs to establish the threshold for cytotoxicity and assayed for by Alamar blue at 72 hpi. As the cytotoxicity begins for most viruses below an MOI of 1 (dashed line), this cell line is confirmed to be permissive to replication and spread.

STS26T-luc

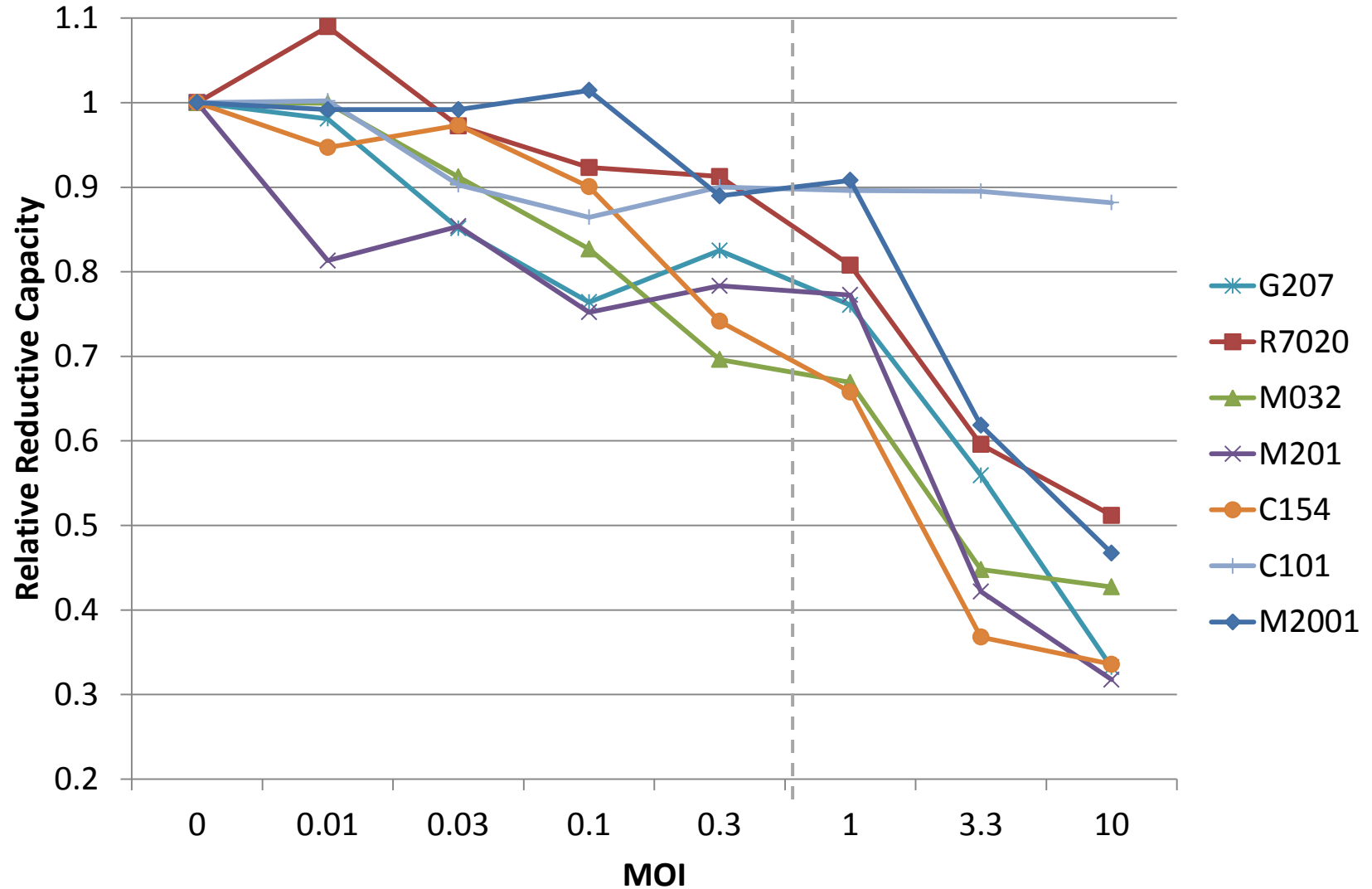


Figure 15 (Sub Task 1c): Alamar blue cytotoxicity assay in STS26T-luc: STS26T-luc cells were infected at various MOIs to establish the threshold for cytotoxicity and assayed for by Alamar blue at 72 hpi. As the cytotoxicity begins for most viruses above an MOI of 1 (dashed line), this cell line is confirmed to be resistant to replication and spread.

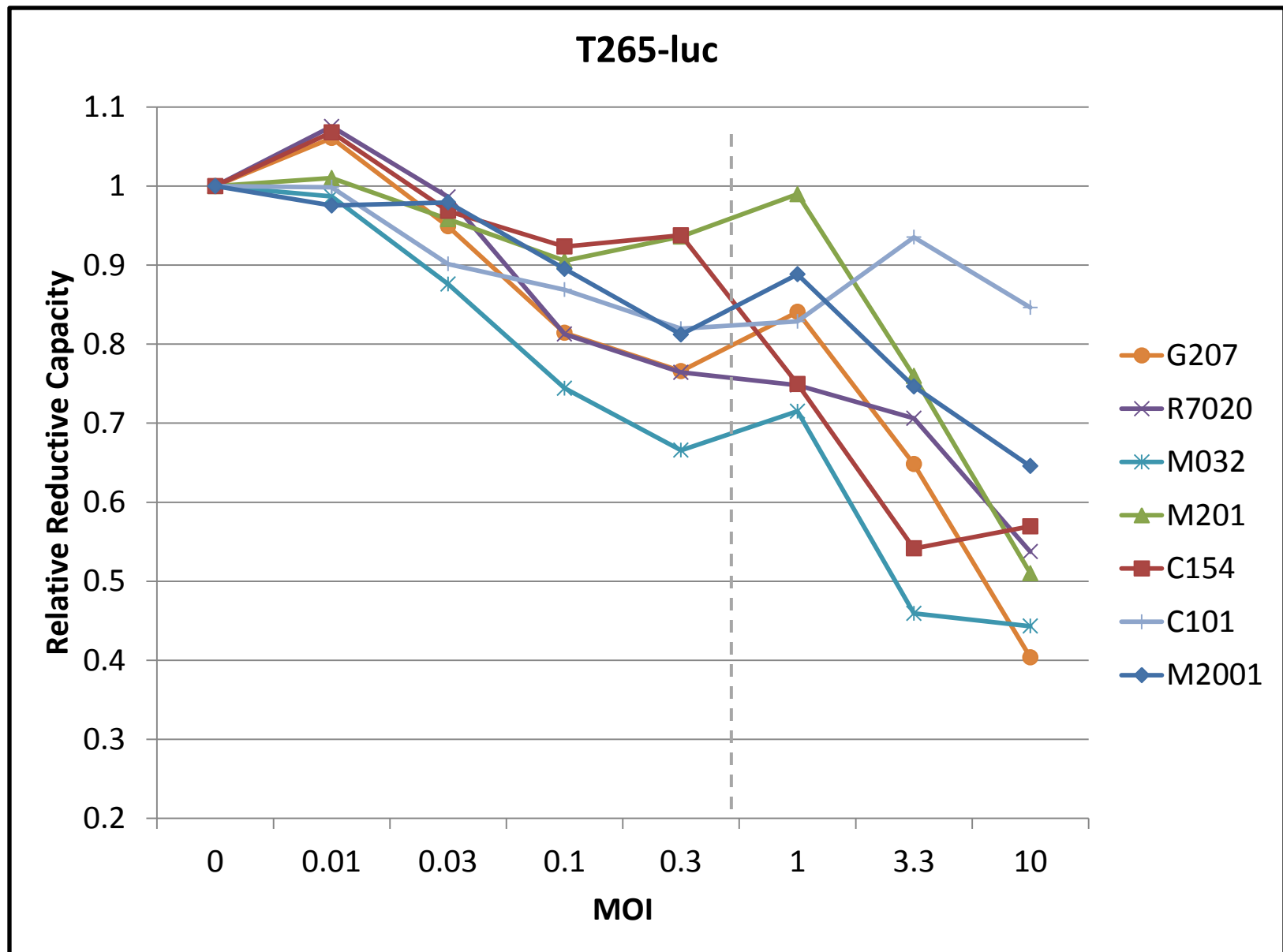


Figure 16 (Sub Task 1c): Alamar blue cytotoxicity assay in T265-luc: T265-luc cells were infected at various MOIs to establish the threshold for cytotoxicity and assayed for by Alamar blue at 72 hpi. As the cytotoxicity begins for most viruses above an MOI of 1 (dashed line), this cell line is confirmed to be resistant to replication and spread.

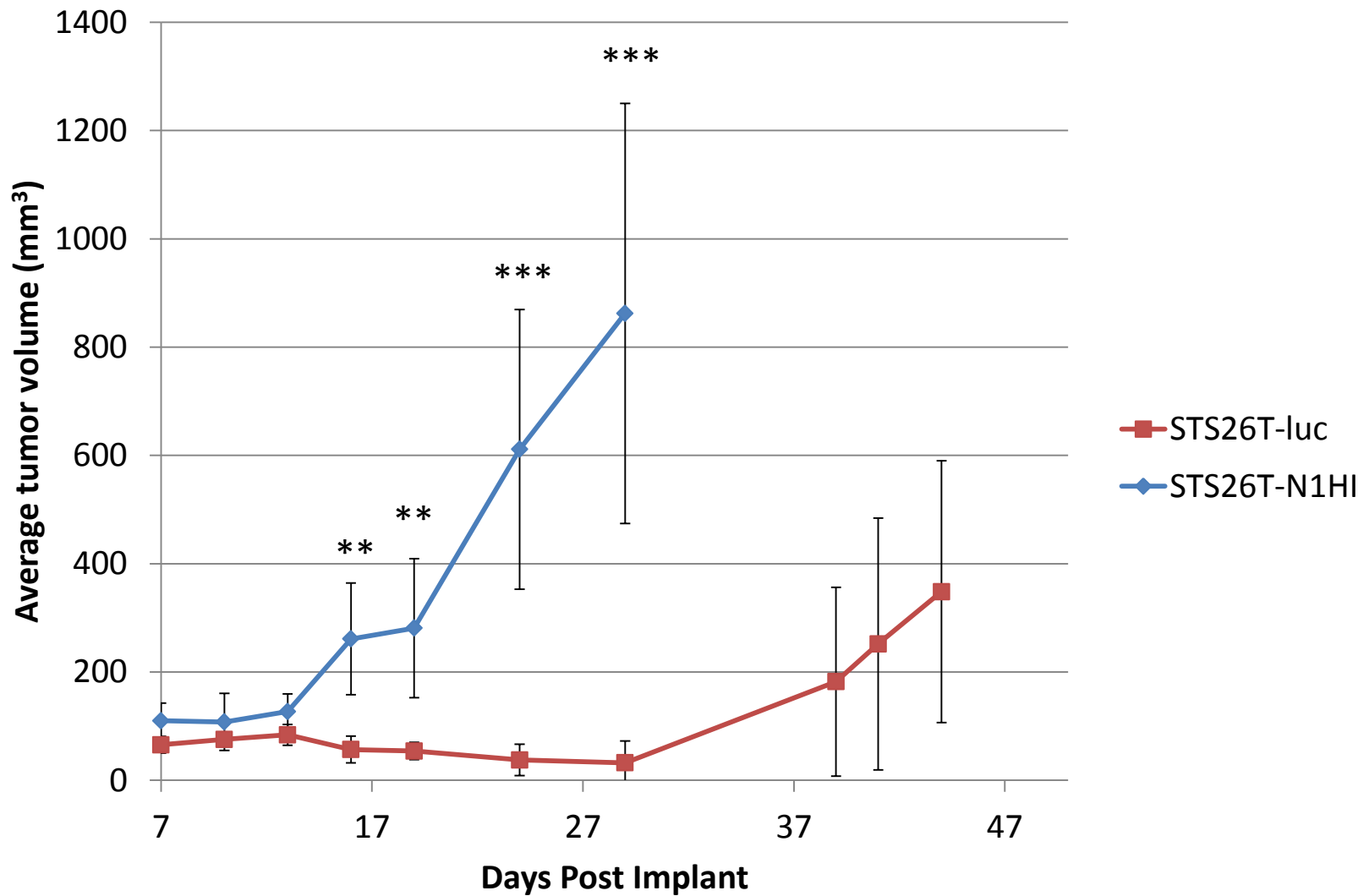


Figure 17 (Sub Task 1d): *In vivo* growth of MPNST tumors STS26T-luc and STS26T-N1HI (ongoing): 5e6 cells from STS26T-luc and the nectin-1 overexpressing STS26T-N1HI were aseptically implanted subcutaneously in the flanks of nude mice in 200 uL methylcellulose. Volume measurements are reported as the mean of 6 tumors with standard deviation. The cohort of mice bearing nectin-1 overexpressing tumors were sacrificed at day 29 post implant based on tumor volume. The parent cell line STS26T-luc took approximately 3 weeks longer to begin growth compared to the nectin-1 overexpressing daughter line. Growth of STS26T-luc tumors have not reached the sacrifice criteria and are ongoing. Star notation as follows: ** $P < 0.01$, *** $P < 0.001$.

S26T-luc Tumor Volume

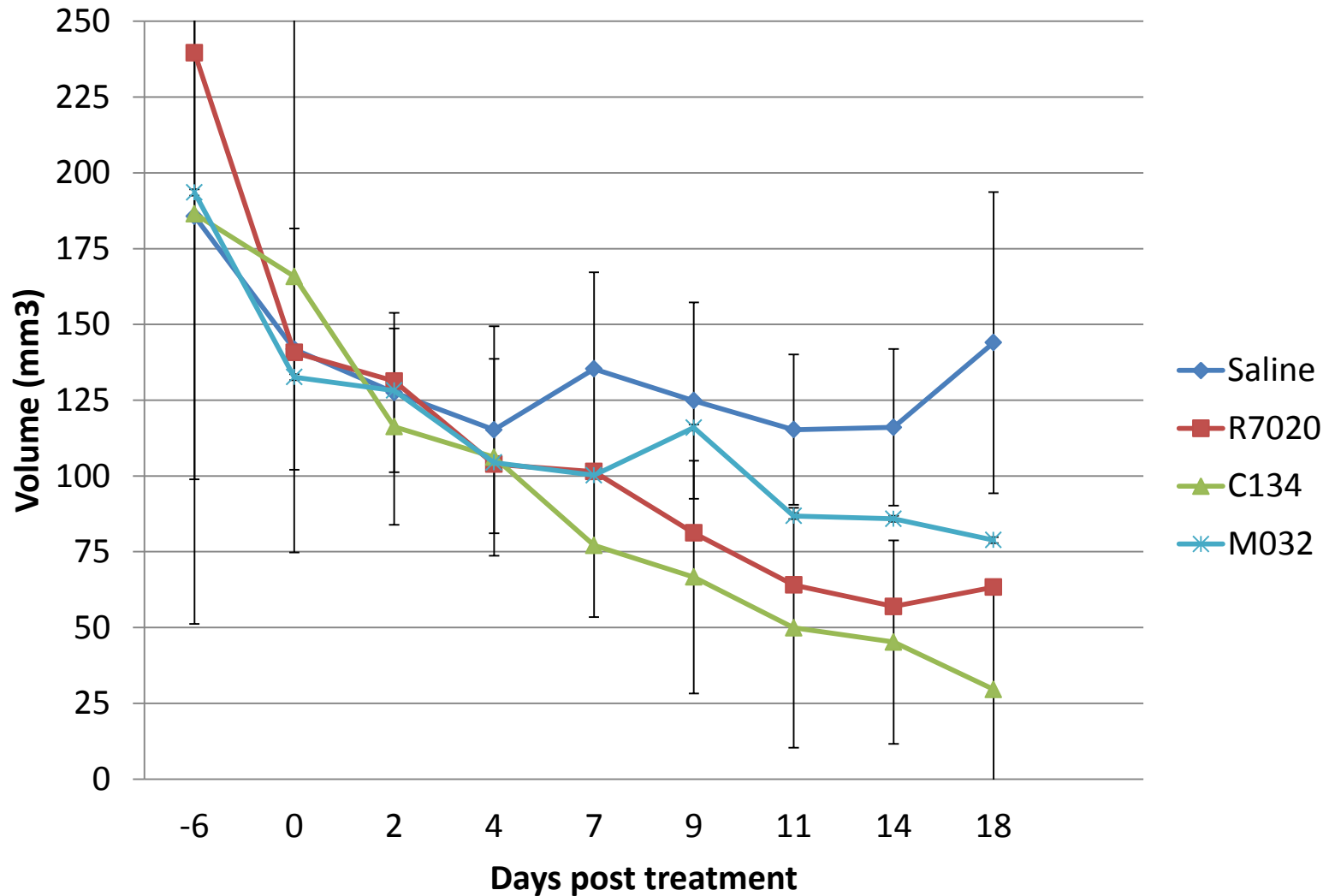


Figure 18 (Sub Task 2f): *In vivo* pilot experiment of oHSV effects on MPNST tumor STS26T-luc (ongoing): 5e6 cells from STS26T-luc were aseptically implanted subcutaneously in the flanks of nude mice in 200 uL DMEM. Volume measurements are reported as the mean of 8 tumors (standard deviation shown for saline and C134). At 14 days post implant, 1e7 PFU of viruses R7020, M002, C134, or 50 uL of saline were injected into the tumor and caliper measurements taken to track tumor volume. This study is ongoing however at day 18 post treatment, there is a statistically significant difference ($P < 0.001$) between the second generation virus C134 and saline treatment

Appendix i

Poster session: The same poster was presented at both of the listed presentations.

UAB GBS/JHS Student Retreat, May 9 2014, **“Effect of Oncolytic Herpes Simplex Virus Replication in MPNST Cell Lines Over-Expressing Nectin-1”** Joshua D. Jackson, Adrienne McMorris, Jennifer Coleman, Justin Roth, Steven Carroll, Kevin Cassady, James Markert

Comprehensive Cancer Center Retreat, Nov. 5 2013, **“Effect of Oncolytic Herpes Simplex Virus Replication in MPNST Cell Lines Over-Expressing Nectin-1”** Joshua D. Jackson, Adrienne McMorris, Jennifer Coleman, Justin Roth, Steven Carroll, Kevin Cassady, James Markert

ABSTRACT

We propose in this research to study the capacity of various oncolytic Herpes Simplex Viruses (oHSVs) to elicit regression of malignant peripheral nerve sheath tumors (MPNSTs) through virally induced cell lysis and immune recruitment. As rare and aggressive tumors of glial origin, MPNSTs frequently arise from patients with type-1 neurofibromatosis, but also form spontaneously. Five year survival ranges from 16-52%, and a lack of dependable treatment options suggests oHSV as a novel candidate to treat these malignancies. HSV is an attractive therapy because it is neurotropic and readily tolerates therapeutic transgene inserts up to 30 kb for high-level expression in infected cells. HSV has been proposed as an oncolytic therapy for tumors derived of neuronal lineage and has already been safely used in Phase I clinical trials for patients with glioblastoma multiforme. Despite promising results in select patients, others experienced less dramatic clinical response to the therapy. One potential explanation to the variability in oHSV efficacy is the absence or limiting concentration of the primary HSV entry receptor Nectin-1 on the surface of target cells. While this is a theoretical concern, it is expected that Nectin-1 concentrations in MPNST cell lines are sufficient to allow efficient viral entry. Preliminary results regarding the impact of human Nectin-1 over-expression (by lentiviral transduction in MPNST cell lines) on oHSV viral recovery are presented here. In the future, it is expected that the study of events following viral entry will explain the observed variations of in vitro data and clinical response to oHSV. Proposals involving innate viral defense responses and intracellular metabolic effects on host susceptibility, as well as correlative in vivo studies using xenogeneic and syngeneic murine models, are under development.

Appendix ii

Supporting Data

Supporting data figures can be found on the following pages.

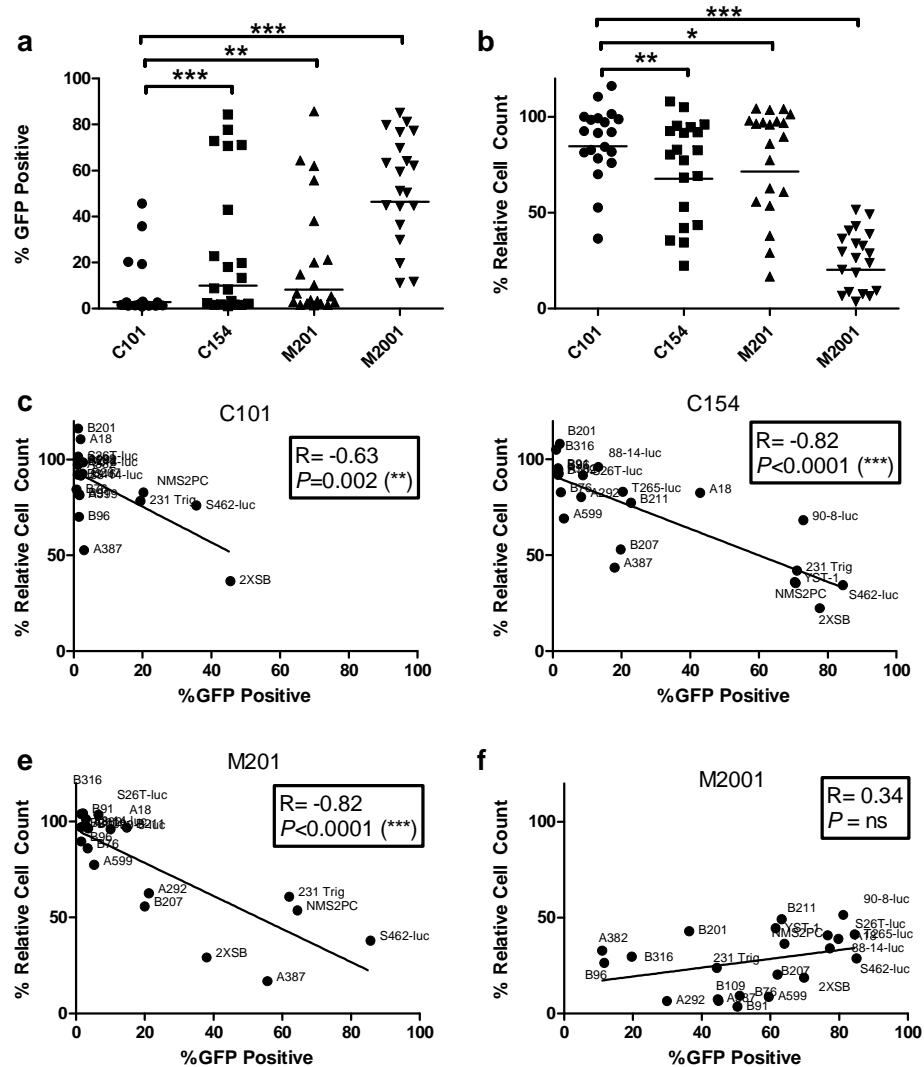


Figure 1 (SubTask 1b): Assessment of multi-step viral productivity by GFP and cell count measurements. All eight human and fourteen mouse MPNST cell lines were infected with the viruses C101 (R3616 + eGFP), C154 (C134 + eGFP), M201 (M002 + eGFP), or M2001 (HSV-1 F strain + eGFP) at a multiplicity of infection (MOI) of 0.1. Cells were collected at 48 hours post infection (hpi) and subjected to FACS analysis for viral GFP expression. Total cell counts for mock and infected cells were measured using standard fluorescent counting beads (Bangs Labs) according to the manufacturer's directions. Both second generation viruses C154 and M201 demonstrated significantly higher GFP positive cells (a) and reduction in relative cell counts (b) as compared to C101. As expected the wild-type virus also demonstrated these increases (a-b). Means for each group are plotted. Student's paired t test was used in the statistical analysis. Data for each cell line was gathered in triplicate and averaged. To test the validity of measuring these two variables, we correlated the % GFP positive measurement and the % relative cell count for each cell line. For the attenuated viruses there was a strong and significant association with the GFP and cell count measurements (c-e) but not for the wild-type virus (f) as calculated by Pearson's correlation. Star notation defined as follows: (*) $P < 0.05$, (**) $P < 0.01$, (***) $P < 0.001$.

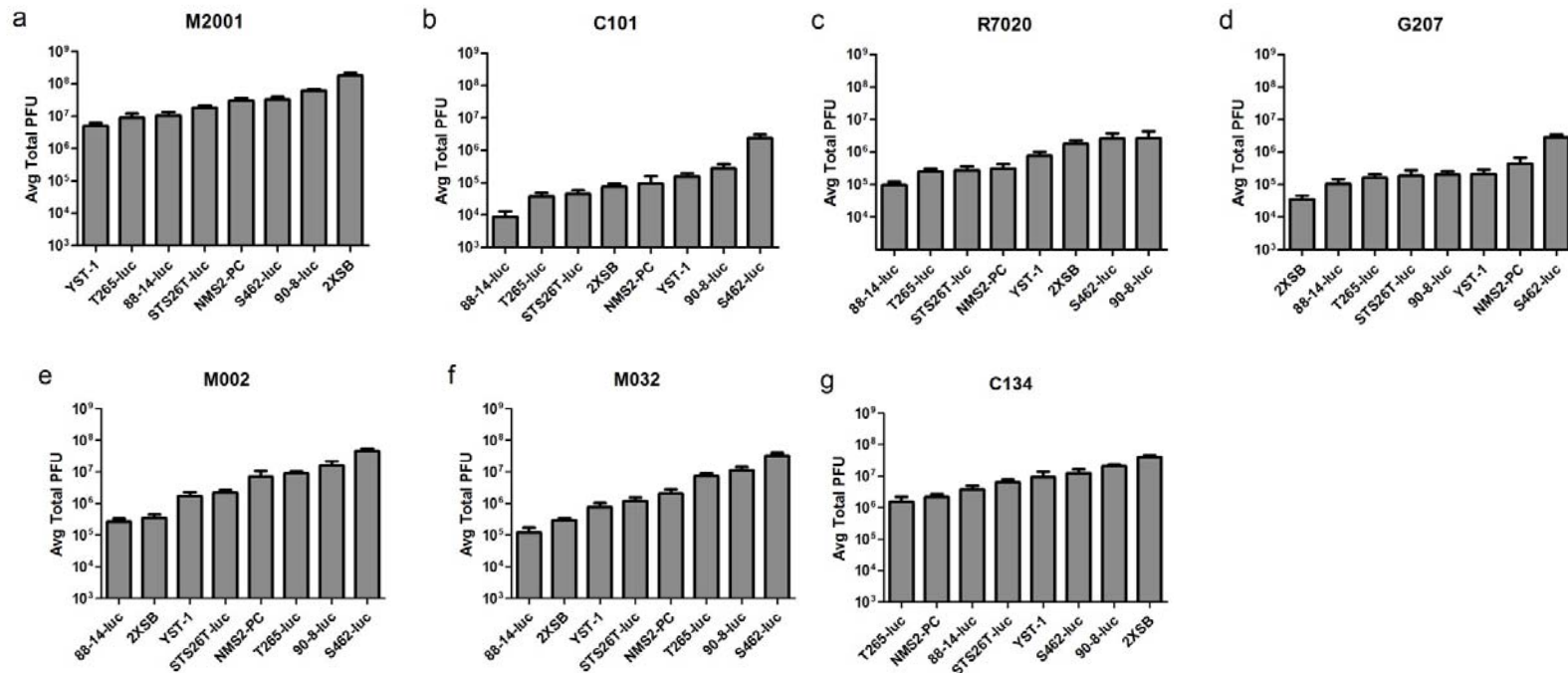


Figure 2 (SubTask 1c): Single-step viral recovery in MPNST cell lines. MPNST cell lines were subjected to single-step (MOI=10, 24 hr) infection by viruses M2001 (a), R7020 (b), C101 (c), G207 (d), M002 (e), M032 (f), C134 (g) and the viral titers reported as the average total plaque forming units (PFU) as determined through limiting dilution plaque formation. Error bars represent standard deviation. For each virus, a range of replication was observed between all cell lines with the largest differences observed in the double $\gamma_134.5$ deleted viruses C101 and G207. Resistant cell lines STS26T-luc and T265-luc as well as permissive lines S462-luc and NMS2-PC were identified and selected for further study.

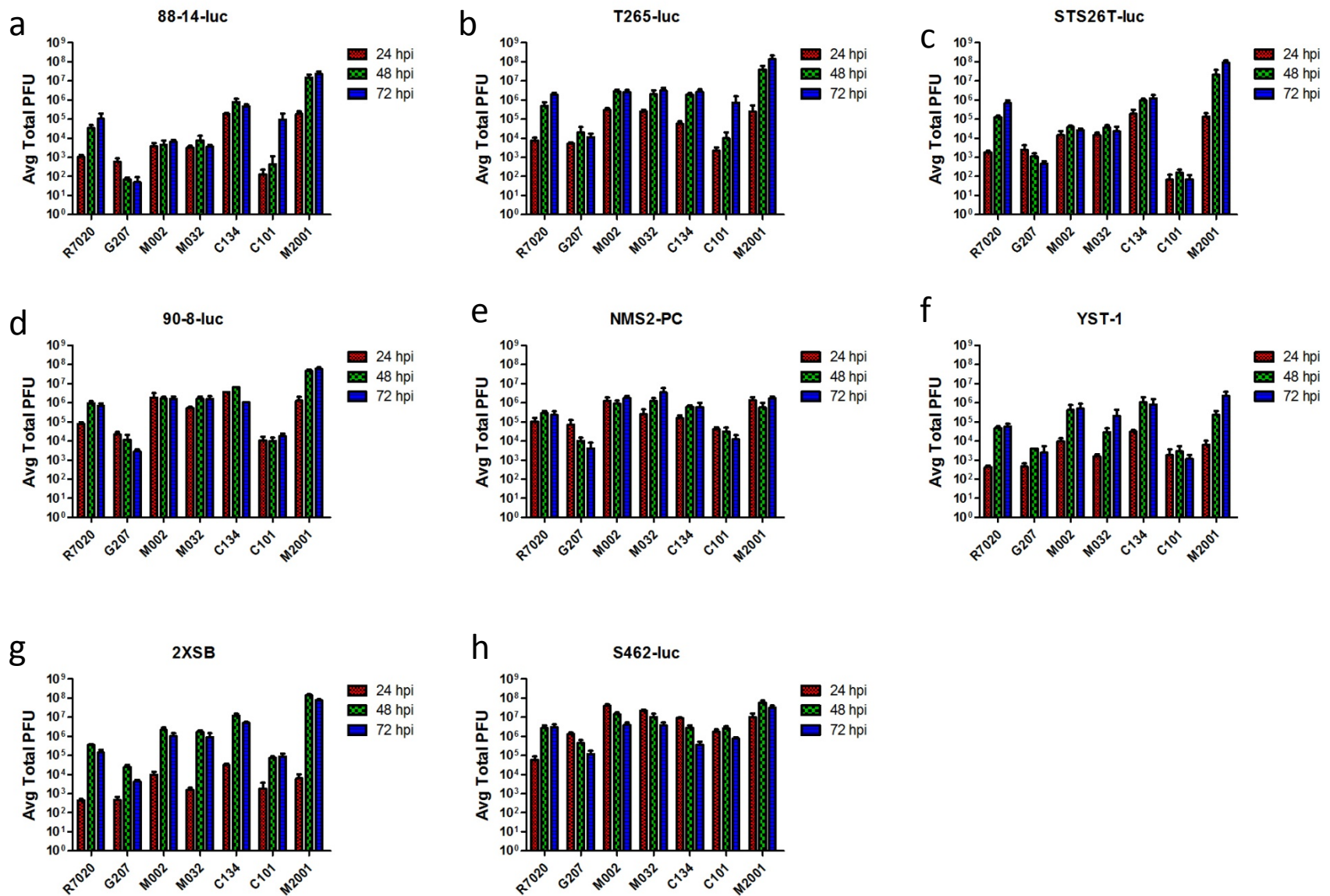


Figure 3 (SubTask 1c): Multistep-step viral recovery in MPNST cell lines. MPNST cell lines were subjected to multi-step (MOI=0.1 at 24, 48, and 72 hpi) infection by viruses M2001 (a), R7020 (b), C101 (c), G207 (d), M002 (e), M032 (f), C134 (g) and the viral titers reported as the average total plaque forming units (PFU) as determined through limiting dilution plaque formation. Error bars represent standard deviation. In general, permissive cell lines permit replication of attenuated viruses (e.g. C101, G207) closer to that reported for wild type M2001. Resistant lines T265-luc (b) and STS26T-luc(c) generally have suppressed replication of G207 and C101 compared to M2001.

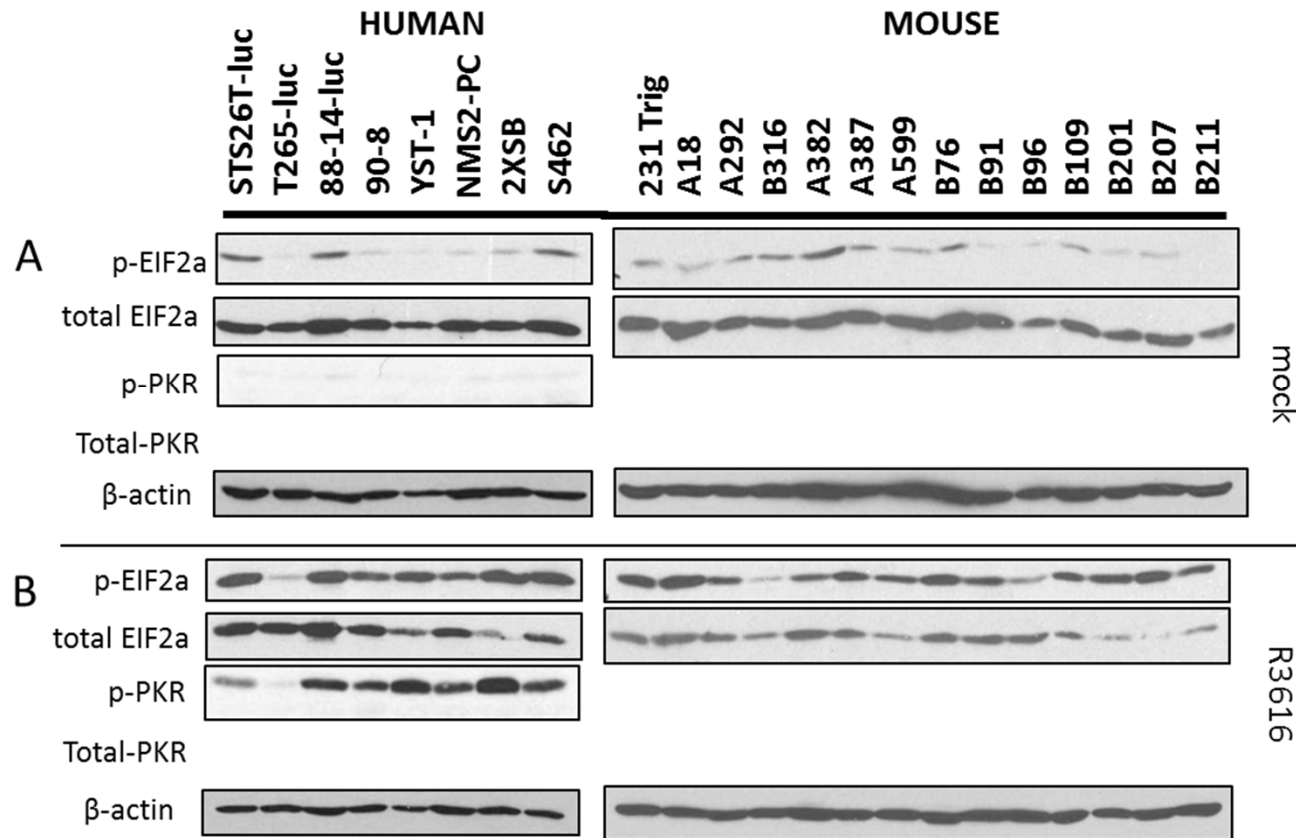


Figure 4 (SubTask 2a): MPNST cell lines mock or R3616 infected (MOI=1, 12 hpi). Mouse and human MPNST cell lines were mock infected (A) or infected with R3616 (MOI=1) (B) for 1 hr under normal serum (7%) conditions. Media was replaced at 1 hr. Lysates were collected in Laemelli buffer at 12 hpi, subjected to SDS-PAGE. The following antibodies were used pEIF2a (Cell Signaling #3398), total EIF2a (Cell Signaling #5324), pPKR (Cell Signaling #3076), total PKR (Santa Cruz #SC-707), and beta actin (Sigma-Aldrich #A3853). Nearly all MPNST cell lines respond to R3616 with eIF2a phosphorylation. Human cell lines additionally demonstrate PKR phosphorylation in nearly all cell lines including all oHSV permissive cell lines.

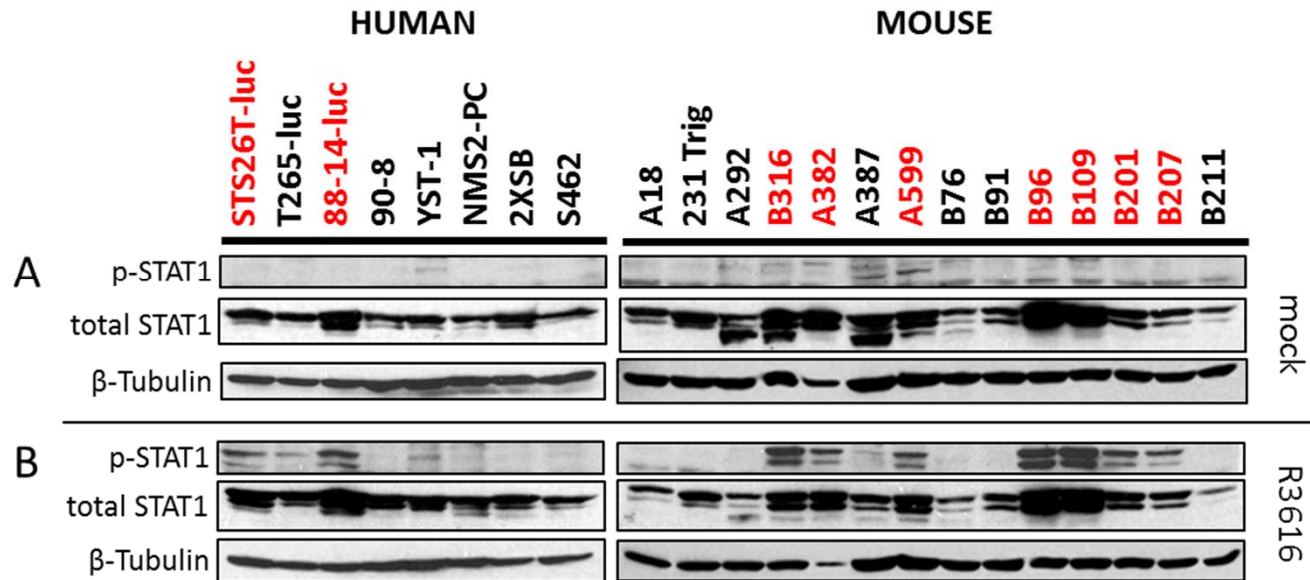


Figure 5 (SubTask 2a): MPNST cell lines mock or R3616 infected (MOI=1, 6 hpi). Mouse and human MPNST cell lines were mock infected (A) or infected with R3616 (MOI=1) (B) for 1 hr under normal serum (7%) conditions. Media was replaced at 1 hr. Lysates were collected in Laemmli buffer at 6 hpi, subjected to SDS-PAGE. The following antibodies were used pSTAT1 (Y701) (Cell Signaling #9167), STAT1 (Cell Signaling #9172), and beta tubulin (Cell Signaling #2128). Only certain MPNST cell lines (red lettering) respond to R3616 with STAT1 phosphorylation.

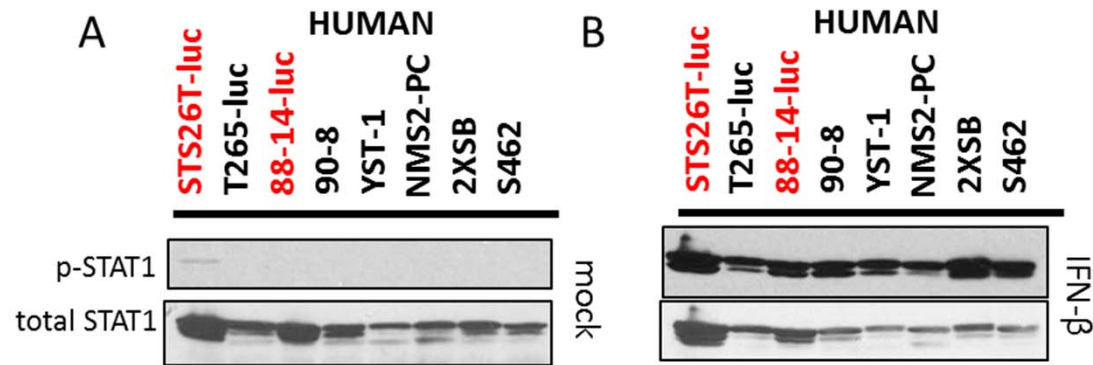


Figure 6 (SubTask 2a): MPNST cell lines treated with or without IFN-β. Human MPNST cell lines were treated with fresh growth media (A) or 200 IU/ml of recombinant human IFN-β for 30 minutes. Lysates were collected in Laemmli buffer at 30 minutes after treatment and subjected to SDS-PAGE. The following antibodies were used pSTAT1 (Y701) (Cell Signaling #9167), STAT1 (Cell Signaling #9172). All human MPNST cell lines respond to IFN-β by phosphorylating STAT1 including those cell lines which did not respond to R3616 with STAT1 phosphorylation (black lettering) (Figure 5).

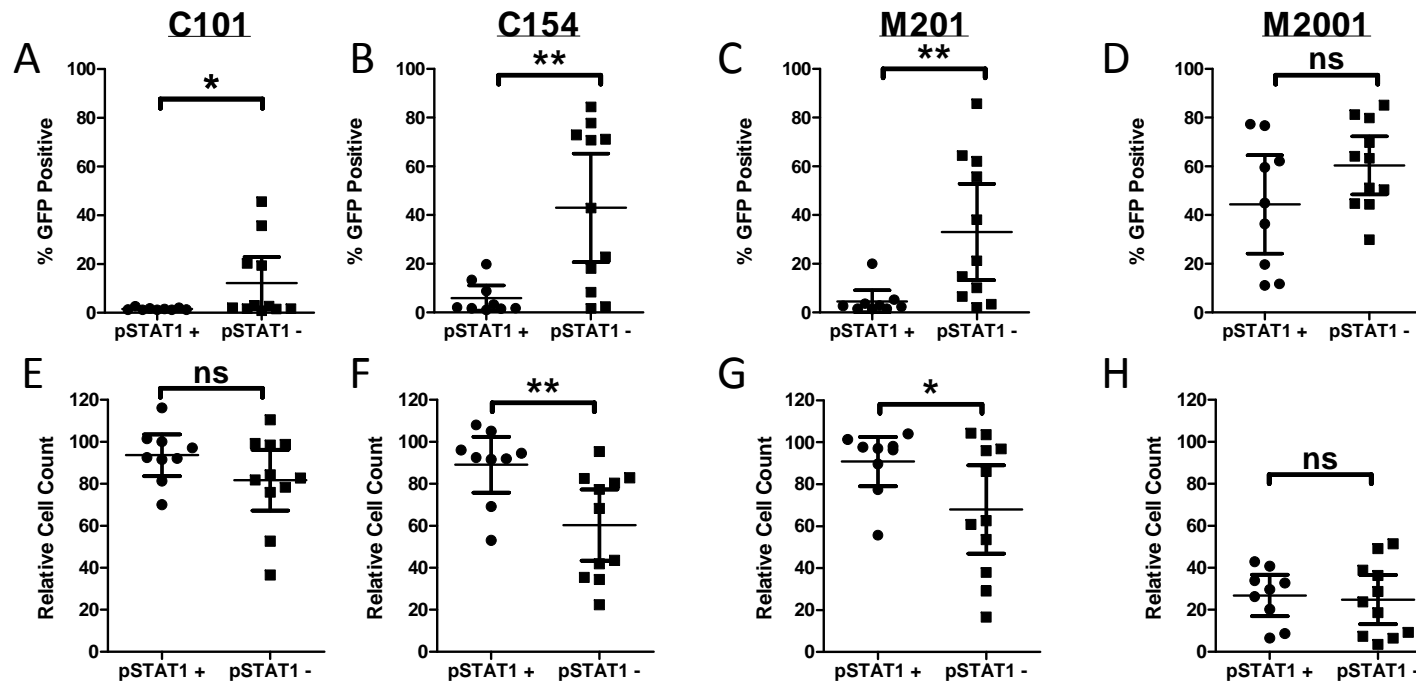


Figure 7 (SubTask 2a): Comparison of measures of viral productivity in STAT1 responsive and unresponsive MPNST cell lines. Data obtained from Figure 1 was grouped into STAT1 responsive and unresponsive groups based upon the observations made in Figure 5. Student's t test with Welch's correction were performed for each group. There was significant association with the STAT1 response for the oHSVs C101, C154, and M201 by both measurements of %GFP positive (A-C) and % relative cell count (E-G) except for the % relative cell count in C101 (E). No significance was observed for either measurement for the wild-type virus M2001 (D and H) indicating that the ability of the cell to activate STAT1 is irrelevant during infection with the wild-type HSV-1. Star notation defined as follows: (*) $P < 0.05$, (**) $P < 0.01$, (***) $P < 0.001$.

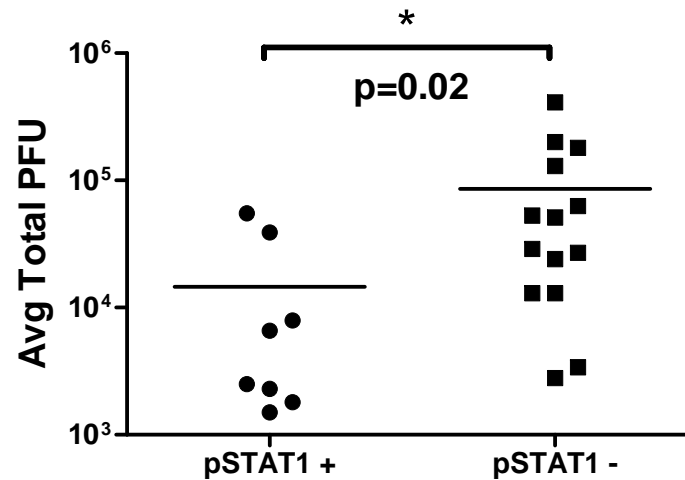


Figure 8 (SubTask 2a): Comparison of measures of R3616 replication capacity in STAT1 responsive and unresponsive MPNST cell lines. All human and mouse MPNST cell lines were infected with the $\Delta\gamma_134.5$ oHSV R3616 at an MOI of 1 for 24 hpi. Cells were titered in the standard fashion (Jackson *et al.*) and viral plaques counted in triplicate and reported as the average total plaque forming unit (PFU). Grouping of cell lines by STAT1 response as determined in Figure 5 revealed statistically significant lower titers of R3616 in cells which could respond to the virus by activation of the STAT1 pathway.

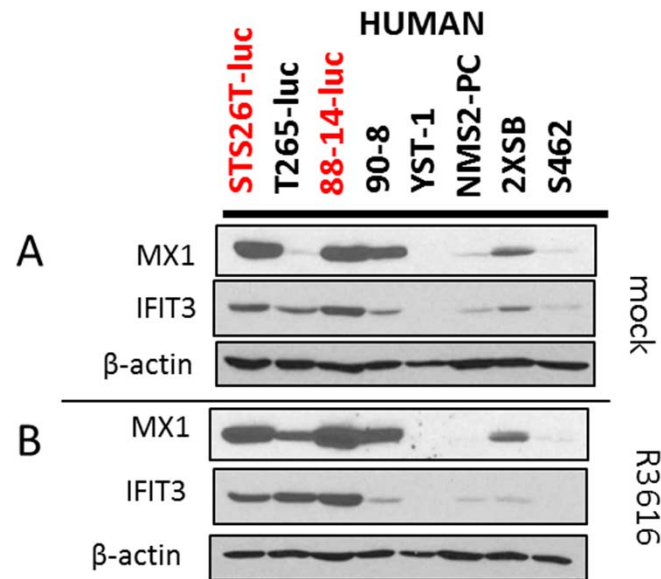


Figure 9 (SubTask 2a): ISG expression by human MPNST cell lines mock or R3616 infected (MOI=1, 12 hpi). Human MPNST cell lines were mock infected (A) or infected with R3616 (MOI=1) (B) for 1 hr under normal serum (7%) conditions. Media was replaced at 1 hr. Lysates were collected in Laemelli buffer at 12 hpi, subjected to SDS-PAGE. The following antibodies were used: MX1 (ProteinTech #13750-1-AP), IFIT3 (ProteinTech # 15201-1-AP), and beta actin (Sigma-Aldrich #A3853). Cell lines which were capable are STAT1 responsive (red lettering) show high basal levels of ISGs prior to infection whereas permissive lines S462, NMS2-PC, and YST-1 do not.

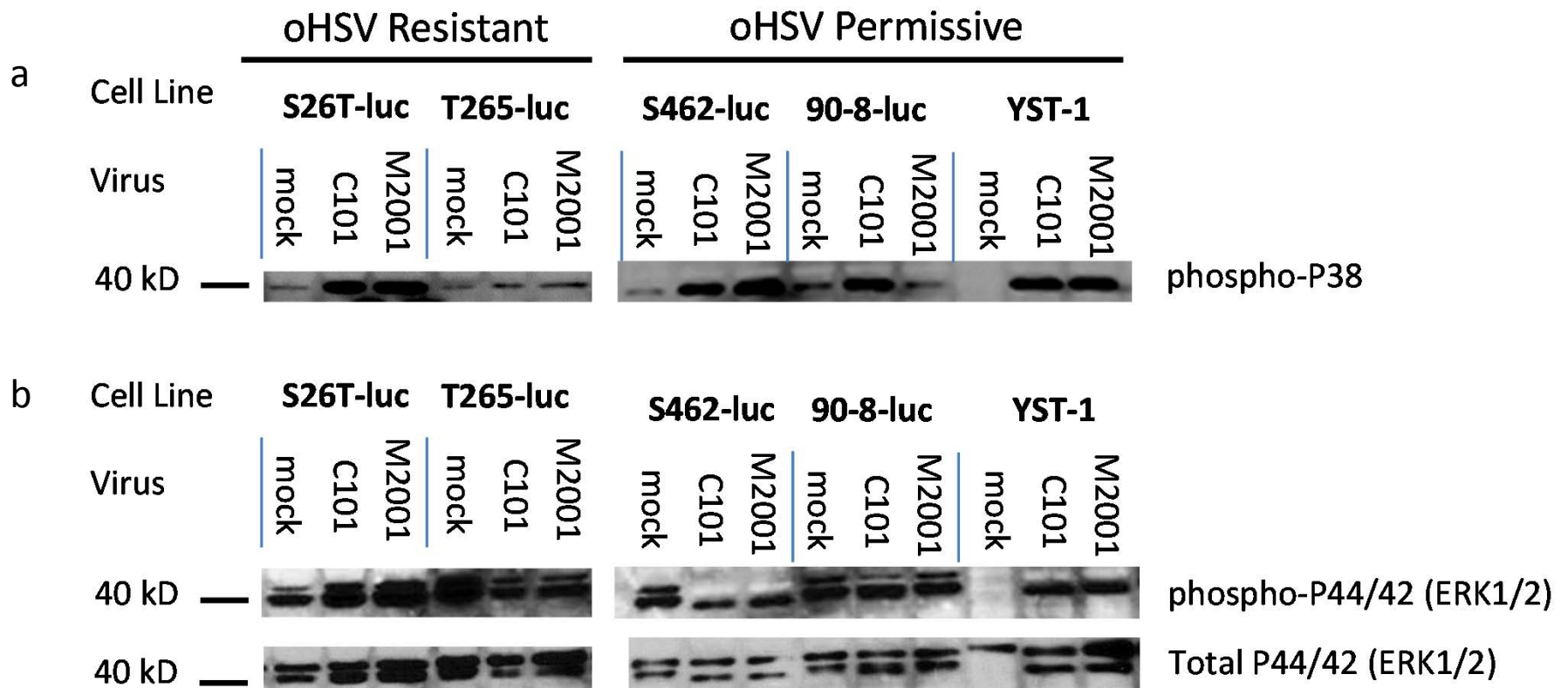


Figure 10 (Subtask 2b and d): P38 and ERK1/2 activation in resistant and permissive cell lines. MPNST cells were infected with mock, C101 or M2001 virus at an MOI of 10 and lysates collected 12 hpi. Immunoblots for phospho-P38 (a) indicate that P38 is activated in all permissive cell lines upon infection as well as the resistant line STS26T-luc. ERK 1/2 activation is apparent in all resistant and permissive MPNST cell lines (b). Basal levels of ERK 1/2 activation are apparent in all mock infected MPNST cell lysates except the permissive line YST-1 (b).

Appendix iii

Manuscript published in *Gene Therapy* can be found on the following pages.

SHORT COMMUNICATION

Assessment of oncolytic HSV efficacy following increased entry-receptor expression in malignant peripheral nerve sheath tumor cell lines

JD Jackson¹, AM Morris¹, JC Roth², JM Coleman¹, RJ Whitley², GY Gillespie^{1,3}, SL Carroll^{4,5}, JM Markert^{1,2,6} and KA Cassady^{2,6}

Limited expression and distribution of nectin-1, the major herpes simplex virus (HSV) type-1 entry-receptor, within tumors has been proposed as an impediment to oncolytic HSV (oHSV) therapy. To determine whether resistance to oHSVs in malignant peripheral nerve sheath tumors (MPNSTs) was explained by this hypothesis, nectin-1 expression and oHSV viral yields were assessed in a panel of MPNST cell lines using $\gamma_134.5$ -attenuated ($\Delta\gamma_134.5$) oHSVs and a $\gamma_134.5$ wild-type (wt) virus for comparison. Although there was a correlation between nectin-1 levels and viral yields with the wt virus ($R=0.75$, $P=0.03$), there was no correlation for $\Delta\gamma_134.5$ viruses (G207, R7020 or C101) and a modest trend for the second-generation oHSV C134 ($R=0.62$, $P=0.10$). Nectin-1 overexpression in resistant MPNST cell lines did not improve $\Delta\gamma_134.5$ oHSV output. While multistep replication assays showed that nectin-1 overexpression improved $\Delta\gamma_134.5$ oHSV cell-to-cell spread, it did not confer a sensitive phenotype to resistant cells. Finally, oHSV yields were not improved with increased nectin-1 *in vivo*. We conclude that nectin-1 expression is not the primary obstacle of productive infection for $\Delta\gamma_134.5$ oHSVs in MPNST cell lines. In contrast, viruses that are competent in their ability to counter the antiviral response may derive benefit with higher nectin-1 expression.

Gene Therapy advance online publication, 14 August 2014; doi:10.1038/gt.2014.72

INTRODUCTION

Malignant peripheral nerve sheath tumors (MPNSTs) are a highly aggressive cancer of the peripheral nervous tissue believed to originate within the Schwann cell lineage¹ and are most commonly associated with the genetic condition neurofibromatosis type-1. Treatment options for MPNSTs beyond surgery are inadequate, resulting in a median survival of only 26 months.² Oncolytic virotherapy by attenuated herpes simplex type-1 viruses (oHSVs) has been proposed as an alternative to chemotherapy and radiotherapy for the treatment of MPNSTs.^{3–7} HSVs with $\gamma_134.5$ neurovirulence gene deletions are safe in humans and have been shown to selectively replicate in tumor cells.⁸ These attenuated $\Delta\gamma_134.5$ oHSVs have a clinically verified safety profile in patients with malignant glioma and have been associated with measurable antitumor responses.^{9–13} However, these patient responses have varied widely, likely due to tumor susceptibility. Therefore, we have sought to further elucidate the mechanisms of oHSV resistance.

In our initial investigation into potential oHSV resistance mechanisms within MPNSTs, we have tested the hypothesis that oHSV resistance is attributable to the insufficient expression of HSV-1 entry receptors by tumor cells.^{14–18} Four viral glycoproteins (gD, gB and gH/gL) and a cellular glycoprotein D (gD)-interacting receptor have been demonstrated as necessary and sufficient to trigger cellular entry.^{19–23} Of the three cellular HSV-1 gD-interacting

receptors, nectin-1, a cellular adhesion protein expressed in epithelial cells,²⁴ fibroblasts and neurons,²⁵ has been proposed as the major HSV-1 entry receptor.²⁶ Herpes virus entry mediator (HVEM)²⁷ and 3-O-sulfated heparan sulfate (3-OS-HS)²⁸ have also been demonstrated to facilitate HSV-1 entry. Additional cell-surface molecules that interact with other viral glycoproteins have been identified, though the broad necessity of these in permitting HSV-1 infection and spread remains to be determined and the lack of these molecules has not yet been implicated in limiting the oncolytic capacity of oHSV.

Here, we have investigated the hypothesis that HSV entry-receptor expression is a determinant of oHSV efficacy in MPNST cells and have identified whether an increase in entry-receptor expression improves the viral yield and spread of oHSVs. The influence of entry-receptor expression was examined in the context of an array of viral genotypes, including a representative wild-type (wt) $\gamma_134.5$ HSV-1, a fully attenuated $\Delta\gamma_134.5$ oHSV, and an attenuated second-generation oHSV capable of host antiviral evasion. We report the following conclusions: (1) correlation of nectin-1 expression with viral production capacity appears more important in viruses which are genetically competent to counter the intrinsic antiviral response, (2) increased expression of entry-receptor molecules modestly improves cell-cell spread of $\Delta\gamma_134.5$ oHSVs, but yields little benefit to viral production and (3) increases in entry-receptor expression do not render resistant MPNST cell lines permissive to $\Delta\gamma_134.5$ oHSV infection.

¹Department of Neurosurgery, University of Alabama at Birmingham, Birmingham, AL 35233, USA; ²Department of Pediatrics, University of Alabama at Birmingham, Birmingham, AL 35233, USA; ³Department of Microbiology, University of Alabama at Birmingham, Birmingham, AL 35233, USA; ⁴Department of Pathology, University of Alabama at Birmingham, Birmingham, AL 35233, USA; ⁵Department of Pathology and Laboratory Medicine, Medical University of South Carolina, Charleston, SC, USA and ⁶Department of Cell, Developmental and Integrative Biology, University of Alabama at Birmingham, Birmingham, AL 35233, USA. Correspondence: Dr J Markert, 510 20th Street South, FOT 1060, Birmingham, AL 35294, USA.

E-mail: markert@uab.edu

Received 17 March 2014; revised 30 May 2014; accepted 25 June 2014

RESULTS AND DISCUSSION

MPNST cell lines have been previously identified as susceptible to oHSV infection and cytotoxicity.³ To examine the correlation between viral production capacity and entry-receptor expression, human MPNST cell lines STS-26T, T265-2c, NMS2-PC, S462, YST-1, 90-8, ST88-14 and 2XSB, or their luciferase-expressing derivatives ('-luc'), were first infected at a multiplicity of infection (MOI) of 10 (single-step replication assay) with a panel of genetically modified HSV-1 and cellular lysates collected 24 h post infection (h.p.i.) for viral recovery analysis (Supplementary Figure 1). The viral yields from this assay are presented in correlation with nectin-1 expression in Figures 1a–e.

HSV-1 entry receptors have not been previously identified in MPNSTs or cells of the Schwann cell lineage. Upon examination of nectin-1 and HVEM expression in our panel of MPNST cell lines, we found detectable levels of nectin-1 in all of the lines, with population-wide (>95%) expression of nectin-1 in five of eight cell lines (Figure 1f). Population-wide expression of HVEM in MPNST cell lines was observed in only one of eight lines (Supplementary Figure 2D); therefore, HVEM was excluded as a candidate for the major entry receptor in MPNSTs. The other established entry receptor 3-OS-HS was not examined in this study due to the lack of a commercially available antibody. However, HSV-1 infection of the resistant cell lines selected for further study (STS26T-luc and T265-luc) was found to be dependent on nectin-1 expression alone by nectin-1 neutralization assays (Supplementary Figure 2).

Pearson's correlation coefficients were calculated between viral recovery data and nectin-1 expression levels. Possible positive associations were found for the wt M2001 ($R = 0.75$; $P = 0.03$) and attenuated second-generation oHSV C134 ($R = 0.62$, $P = 0.10$) viruses (Figures 1a and b). While prior studies involving thyroid cancer¹⁴ and head and neck squamous cell carcinoma¹⁵ cell lines demonstrated correlation between viral yields of oHSV NV1023 (a derivative of R7020) and nectin-1 expression, no such associations were observed for G207, C101 or R7020 oHSVs suggesting that the specific viral genotype influences the outcome of infection.

The lack of a clear association of nectin-1 expression with attenuated $\Delta\gamma_{134.5}$ oHSV viral yields led us to further evaluate the functional impact of increased entry-receptor expression on oHSV sensitivity. To assess this, the oHSV-resistant cell lines, T265-luc and STS26T-luc were transduced with full-length human nectin-1 (nectin-1a) using lentivirus LV2114CK. An mCherry expressing lentivirus was used as a control and confirmed that transduction alone did not alter viral production (data not shown).

If low entry-receptor expression diminishes the ability of oHSV to establish an initial infection, we would predict that increased nectin-1 expression would increase the initial opportunity for entry, resulting in replication within a greater number of cells and an increase in the total production of virus. To determine the impact of increased nectin-1 expression on viral yields in MPNSTs, single-step (MOI=10, 24 h.p.i.) and multistep (MOI=0.1, 24, 48, 72 h.p.i.; Supplementary Figure 3) viral recovery assays were performed using the parent and nectin-1 transduced cell lines. Because the

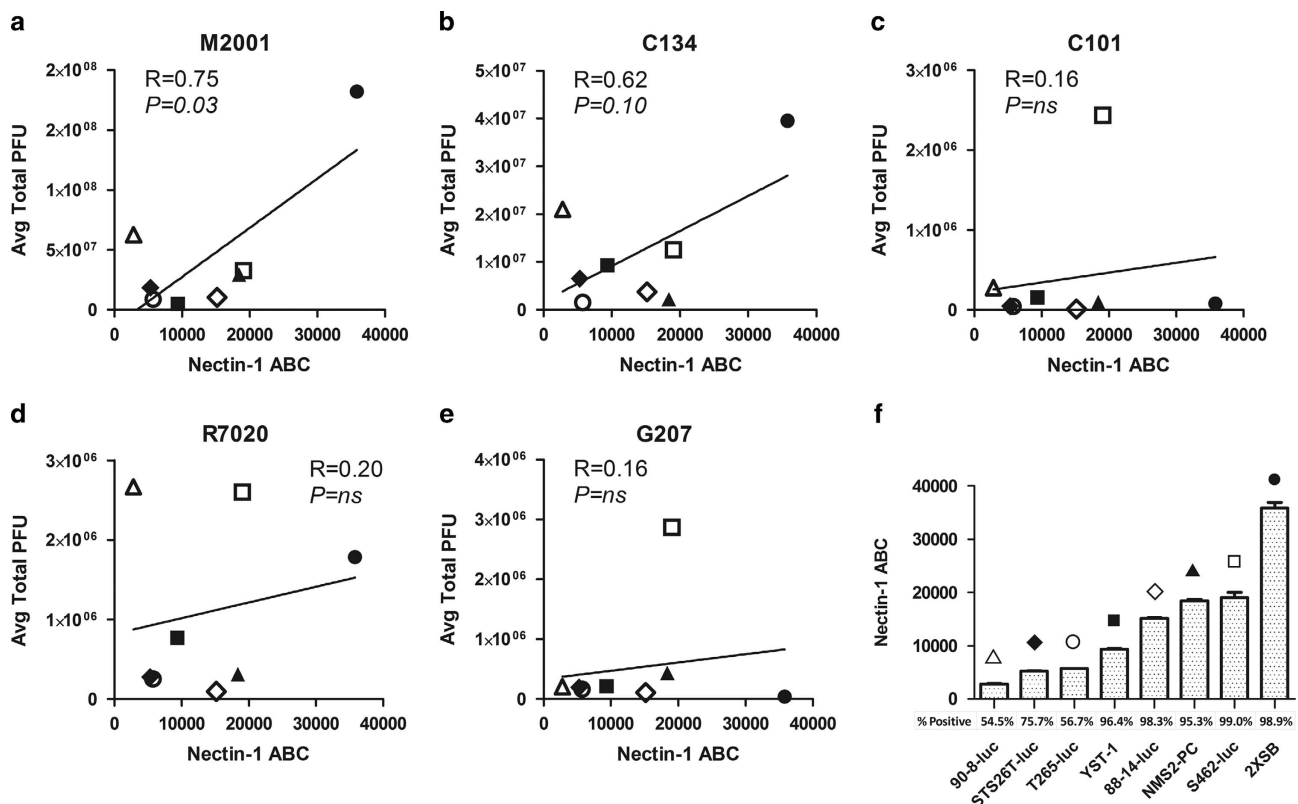


Figure 1. Correlation of nectin-1 expression with viral titers. Pearson's correlation coefficients (a–e) were calculated between the viral titering data from M2001, C134, C101, R7020, G207 (Supplementary Figure 1) and the nectin-1 expression levels (f) from cell lines 90-8-luc (open triangle), STS26T-luc (closed diamond), T265-luc (open circle), YST-1 (closed square), 88-14-luc (open diamond), NMS2-PC (closed triangle), S462-luc (open square), and 2XSB (closed circle). A strong and significant correlation was noted for M2001. Cells were infected in triplicate by a single-step replication assay (MOI=10) and the lysates collected and titered at 24 h.p.i. Nectin-1 expression was quantified by flow cytometry after incubation with phycoerythrin (PE)-conjugated mouse monoclonal antibody with subsequent quantification using antibody quantification beads. The percentage of the cell population staining above the isotype control is also reported. Receptor quantification was performed in triplicate with the standard deviation reported.

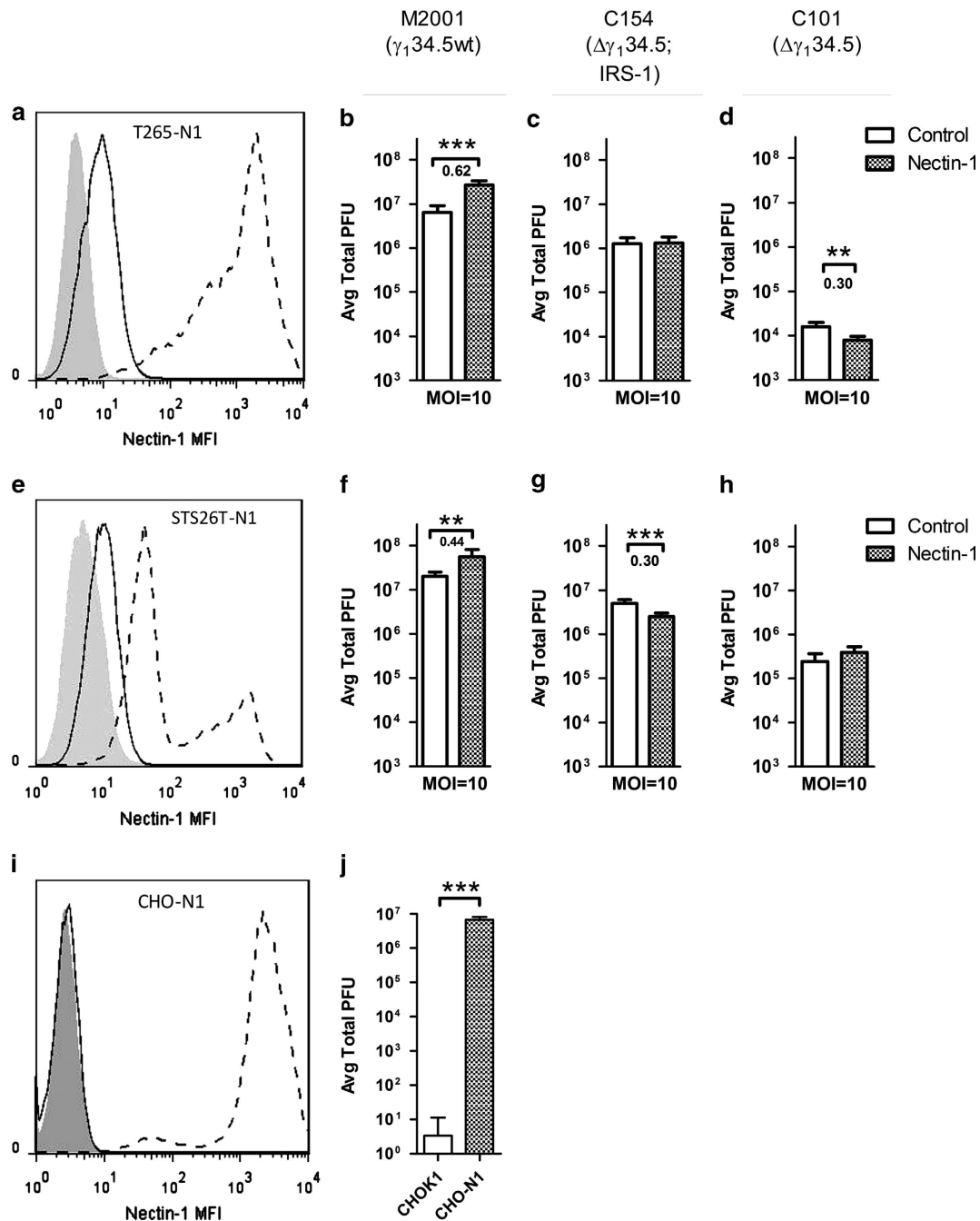


Figure 2. Overexpression of nectin-1 in resistant cells and impact on single-step replication assays. Nectin-1 was transduced via lentivirus into oHSV-resistant cell lines T265-luc (a) and STS26T-luc (e) as well as control cell line CHO-K1. Isotype control (shaded), parent (solid line) and transduced (dashed line) cell lines are shown. Transduction of the nectin-1-deficient cell line (i) demonstrated function as an entry receptor as apparent by M2001 replication (j). The impact of nectin-1 overexpression in resistant cell lines was tested by single-step (MOI= 10) replication by viruses M2001 (b, f), C154 (c, g) and C101 (d, h) and compared with control cell lines. Significance was determined by two-tailed Student's *t*-test with unequal variance. Significance was set at $P < 0.05$. For cells with significant changes in titer, the logarithm of the absolute value of the increase was reported below the significance marking. Changes in titer greater than 0.5 log are considered to be biologically relevant. ** $P > 0.01$ and *** $P > 0.001$.

reliable titering repeatability of HSV is within approximately 0.5 log, only changes in titer greater than 0.5 log are considered to be biologically relevant. The nectin-1 transduction of T265-luc and STS26T-luc resulted in abundant nectin-1 expression in T265-N1 and STS26T-N1 cell lines, respectively (Figures 2a and e). While increased entry-receptor expression improved the yields of a representative wt virus (Figures 2b and f), the increased expression did not improve the titers of a next-generation oHSV C154, an EGFP

expressing variant of C134 (Figures 2c and g) or first-generation $\Delta\gamma_1 34.5$ oHSV C101 (Figures 2d and h). To demonstrate that increased nectin-1 expression would be expected to improve viral production, the HSV receptor-deficient cell line CHO-K1 was transduced with nectin-1. A significant and greater than 5 log increase in wt HSV-1 titers was observed (Figures 2i and j).

Interaction with HSV entry receptors is essential for initial HSV entry as well as the subsequent cell-to-cell spread of HSV.²⁹

To assess the effect of increased nectin-1 expression on viral spread, we measured viral GFP expression in MPNST cells over the time in multistep assays following infection with GFP expressing C101 and C154 (Figure 3) or M2001 (Supplementary Figure 4). The results show that nectin-1 overexpression improved the ability of C101 to undergo cell-to-cell spread and increased the proportion of cells infected from 3 to 27% and from 1 to 7% of the cell population in T265-N1 and STS26T-N1 in multistep replication assays (MOI=0.1, 24, 48 and 72 h.p.i.) respectively (Figures 3a and b). Despite this improved spread in resistant lines, the maximum spread was much less than that observed in the naturally permissive S462-luc and NMS-2PC MPNST cell lines, where C101 was capable of infecting >80% of the cells (Figure 3c). This suggests that endogenous levels of entry receptors are sufficient to permit infection and sustain $\Delta\gamma_1,34.5$ oHSV spread in these lines and that increased entry-receptor expression is not sufficient to render resistant cell lines with a permissive phenotype. Of note, the overexpressed nectin-1 levels far exceeded the highest

endogenous levels in the permissive lines (Supplementary Figure 5), suggesting that restricted entry is not an explanation for MPNST resistance to oHSVs. This conclusion is further supported by the fact that infection of the same cell lines with a second-generation oHSV (that is, C134 or C154) capable of evading the antiviral response³⁰ resulted in approximately 10-100 fold increase in viral titers and notably greater cell-to-cell spread as compared with C101 (Figures 3d and e).

To determine the extent to which *in vivo* studies recapitulated these results, athymic nude mice were engrafted with either parent or nectin-1 expressing cell lines. Of the resistant cell lines, only STS26T-luc and the nectin-1 overexpressing variant established flank tumors. Tumors were injected with 1×10^7 plaque forming units of C101 or C154, and viral recovery was measured on days 3 and 5 post injection. Similar to the *in vitro* results (Figure 3g and h), the next-generation virus had a >10-fold viral production advantage over the $\Delta\gamma_1,34.5$ oHSV C101, however neither virus demonstrated an increased viral titer between days 3

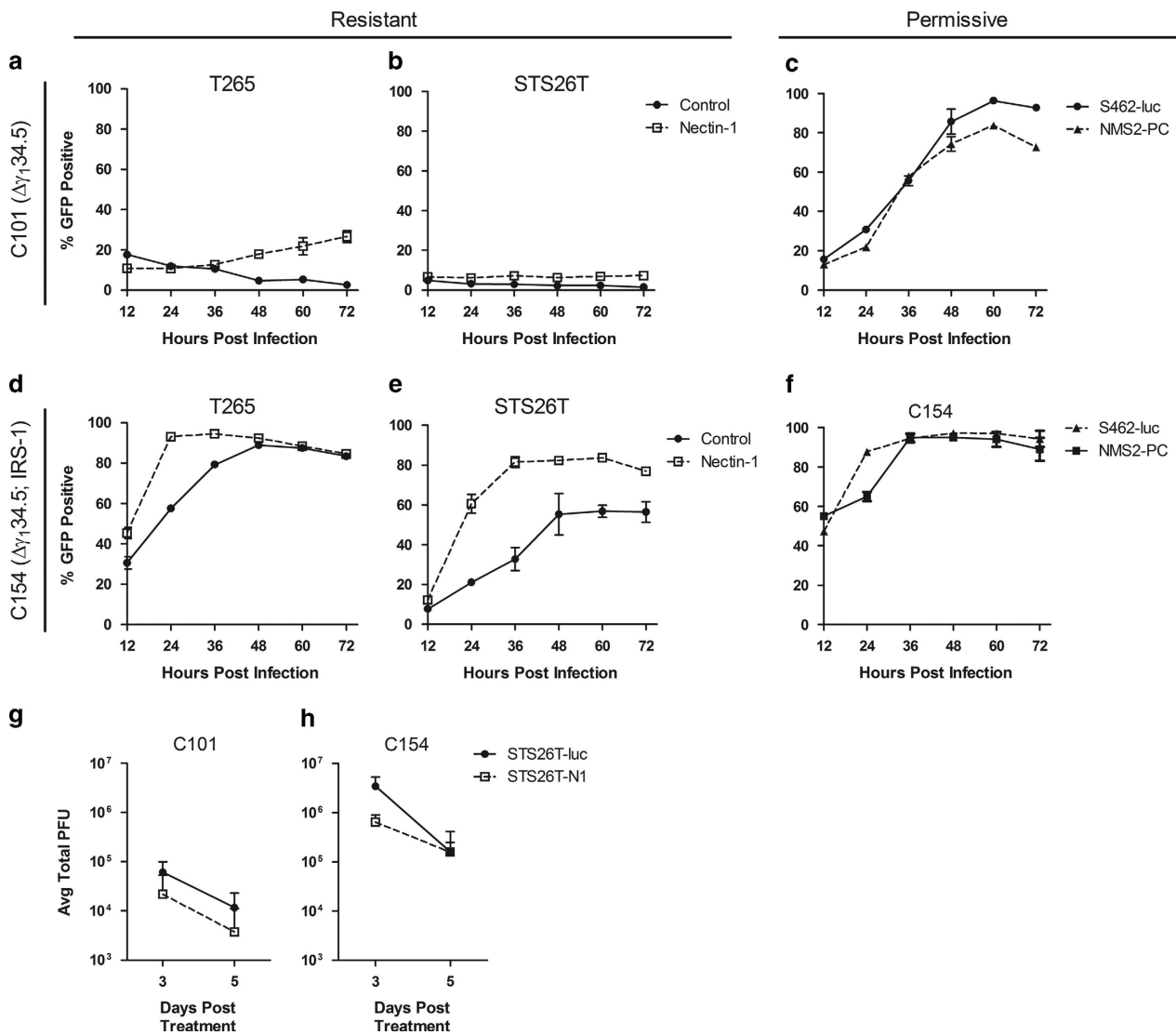


Figure 3. Impact of increased nectin-1 expression on oHSV spread *in vitro* and viral recovery *in vivo*. Resistant cell lines STS26T-luc and T265-luc and their nectin-1 transduced variants, as well as permissive cell lines S462-luc and NMS2-PC, were infected in a multistep assay (MOI=0.1) with fully attenuated oHSV C101 (a–c) or second-generation C154 expressing HCMV IRS1 (d–f) and monitored by flow cytometry over time for viral infection as evident by expression of viral GFP. STS26T-luc and STS26T-N1 cells were engrafted in the flanks of nude mice and following tumor formation were injected with 1×10^7 plaque forming units (PFU) of C101 or C154. Tumors were harvested and viral titers determined at days 3 and 5 following infection (g and h). Data are representative of four tumors with standard deviation reported.

and 5 even with increased nectin-1 expression. Tumors were also collected for immunohistochemistry and staining for HSV-1 confirmed that increased nectin-1 expression did not benefit oHSV spread between days 3 and 5 (data not shown). The *in vivo* results therefore confirmed that neither the first- nor the second-generation oHSVs derived a benefit to viral output from increased entry-receptor expression.

In summary, the work presented here provides insight into one of the proposed determinants of oHSV therapeutic efficacy. We conclude that the primary mode of MPNST resistance to $\Delta\gamma_134.5$ oHSVs is not due to limited expression of nectin-1. Despite the primary conclusions of previously published work that entry-receptor expression is predictive of a productive infection by oHSV, we suggest that the use of viruses in these previous studies which contained at least one functional copy of the $\gamma_134.5$ gene (NV1023)^{14,15,18} or $\gamma_134.5$ under a nestin promoter (rQnestin34.5)¹⁶ is in line with our conclusions that viruses which are genetically competent to counter the intrinsic antiviral response benefit the most from increased entry-receptor expression. Similarly in our work, the wt HSV-1 and C134 viruses derived greater benefit from higher entry-receptor expression than did the first-generation $\Delta\gamma_134.5$ oHSVs. Furthermore, the work of Wang *et al*¹⁶ showed that only the $\gamma_134.5$ containing virus was able to substantially benefit from increased nectin-1 expression while the $\Delta\gamma_134.5$ control virus did not. Future work should therefore include the characterization of the capacity for an intrinsic antiviral response as the major mechanism for oHSV resistance in MPNSTs.

MATERIALS AND METHODS

Cell lines

MPNST cell lines STS26T-luc, T265-luc, ST88-14-luc, S462-luc, 90-8-luc, NMS2-PC, YST-1 and 2XSB were provided by Dr Steve Carroll (University of Alabama at Birmingham). Cell lines STS26T-luc, T265-luc, and ST88-14-luc express firefly luciferase and have been previously described.³¹ S462-luc and 90-8-luc were transduced *via* lentivirus to express Renilla luciferase. HSV-1 entry receptor-deficient cell line CHO-K1 was generously provided by Dr Yancey Gillespie (University of Alabama, Birmingham). All MPNST cell lines were maintained in DMEM, 10% FBS, and 1% P/S. CHO-K1 cells were maintained in Ham's F12, 10% FBS and 1% P/S. Vero cells were obtained from American Type Culture Collection (Manassas, VA, USA) and maintained in MEM and 5% BGS. All cell lines were confirmed to be free of Mycoplasma by DAPI staining and PCR detection.

Viruses

All viruses have been previously described. Briefly, M2001 was constructed by insertion of the gene encoding EGFP under the control of the CMV immediate early promoter into the U_L3-U_L4 intergenic region of the prototypical wt HSV-1 (F) strain.³² C101 and C134 were derived from the $\Delta\gamma_134.5$ mutant HSV-1 R3616 by insertion respectively of the *EGFP* or *HCMV IRS1* genes under the control of the CMV immediate early promoter in the U_L3-U_L4 intergenic region.³³ C154 is derived from C134 by insertion of EGFP into the deletion loci of $\gamma_134.5$. G207 (Medigene, Inc., San Diego, CA, USA) is a clinical grade oHSV derived from R3616 with the additional insertion of *lacZ* in the U_L39 region.³⁴ R7020 (kindly provided by Bernard Roizman; University of Chicago, Chicago, IL, USA), is a clinical grade oHSV derived from HSV-1 (F) strain by insertion of a region of the HSV-2 genome encoding glycoproteins G, D, I and a portion of E into one of the internal repeat regions of HSV-1 (F) disrupting one copy of the neurovirulence gene $\gamma_134.5$.³⁵

Viral titering assays

Viral titers were determined by limiting dilution plaque formation assays as previously described.³³ MPNST cells were incubated for 2 h with virus diluted in 100 μ l infection media (DMEM + 1% FBS) and replaced with growth media after infection. An equivalent volume of sterile milk was added and the plate subjected to three cycles of freeze-thaw at -80°C . Lysate was collected, sonicated, serially diluted in Vero infection media (MEM + 1% BGS), and incubated on Vero monolayers. Infection media was replaced with growth media containing 0.01% human AB serum (Corning Cellgro, Corning, NY, USA). After 48 h, plaques were counted following May-Grunwald/methanol staining as previously described. All experiments were performed in triplicate and the average total plaque forming units reported with standard deviation.

Viral entry-receptor quantification

Expression of entry receptors was quantified by flow cytometry using either phycoerythrin-conjugated mouse monoclonal antibodies to nectin-1 (R1.302) (Biolegend, San Diego, CA, USA), HVEM (Biolegend), or isotype control (BD Biosciences, San Jose, CA, USA). Antibody concentrations used were confirmed to be saturating. Cells analyzed using a FACSCaliber flow cytometer (Becton Dickinson, Franklin Lakes, NJ, USA). Concurrently, Quantum Simply Cellular beads (Bangs Laboratories, Fisher, IN, USA) were used to determine the antibody binding capacity of each cell line. Mean fluorescence analysis was performed using FlowJo (v 7.6.1; Tree Star, Ashland, OR, USA) and the receptor-mean fluorescence intensity data converted to antibody binding capacity using a script provided with the Quantum Simply Cellular kit. All measurements were averaged from three independently seeded wells, and the final antibody binding capacity reported as the difference above the isotype control.

Correlation of nectin-1 and viral recovery

Pearson's correlation coefficients between nectin-1 expression and viral recovery were determined by analysis of the data in Prism 5 (GraphPad Software, La Jolla, CA, USA). Cutoff for statistical significance was set at $P < 0.05$.

Nectin-1 overexpression

A self-inactivating lentiviral vector was used to overexpress nectin-1 or control mCherry in oHSV-resistant cell lines. Human nectin-1 clone (Clone ID: 8322523) was obtained from Open Biosystems (Thermo Scientific, Waltham, MA, USA). Nectin-1 cDNA was PCR amplified using primers 5'-CGGATCCCGGGTTCGACCCGATGGCTC GGATGGGGCTT-3' and 5'-CCGGTCCGAGCGCGCCGCTACACGTAC CACTCCTTCTGGAA-3' (IDT, Coralville, IA, USA) in a T100 Thermal Cycler (Bio-Rad, Hercules, CA, USA). The recipient vector has been previously described.³⁶ An intermediate lenti-vector was first constructed by insertion of an IRES-puromycin *N*-acetyl-transferase cassette into the *NotI*- and *EcoRI*-digested pLVmnd lentivirus. The intermediate construct was then digested with *Sall* and *NotI* for subsequent insertion of the PCR-amplified Nectin-1 cDNA. The sequence of the coding region of the resulting lentiviral vector pCK2114 was verified. The control lentivirus (pLVmnd.CIP) was similarly constructed by insertion of mCherry upstream of the IRES-puromycin *N*-acetyl-transferase cassette in the intermediate virus. Lentiviruses were produced by co-transfection of pCK2114 or pLVmnd.CIP with pMD.G (VSFG pseudotype), and pCMV. deltaR8.91 (HIV packaging) in 293T cells using Lipofectamine 2000 and OptiMEM media (Gibco, Carlsbad, CA, USA). After 12 h, transfection media was replaced with DMEM/F12 with 10% FBS. Lentiviral-enriched supernatant was collected 48 h post transfection, filtered through a 0.22-micron filter, and mixed with polybrene (8 $\mu\text{g ml}^{-1}$). STS26T-luc and T265-luc cells were

subsequently transduced with the resulting lentiviruses enriched by puromycin selection ($5 \mu\text{g ml}^{-1}$), followed by fluorescence activated cell sorting to obtain pure populations (UAB Comprehensive Flow Cytometry Core, Birmingham, AL, USA).

HSV titers in nectin-1 overexpressing cell lines

The impact of increased nectin-1 expression on viral titers in resistant cell lines was determined as described above with the exception of replacing infection media with MPNST growth media and 0.01% human AB serum to minimize extracellular spread of the virus. Statistical significance was determined by two-tailed Student's *T*-test assuming equal variance. Star notation indicating significant differences is as follows: (*) for $P < 0.05$, (**) for $P < 0.01$ and (***) for $P < 0.001$.

HSV spread as measured by GFP expression

Cells were incubated with virus or mock infected for 2 h at MOI=0.1 in infection media. Infection media was replaced with growth media and 0.01% human AB serum following incubation. Cells were harvested at 12 h intervals and analyzed by flow cytometry. The percent GFP-positive measurement was assessed by defining the GFP (FL1) gate at 1% positive of the mock-treated cells. The percentage of the infected cell population expressing GFP was then recorded. All data points were performed in triplicate, averaged, and the standard deviation reported.

In vivo viral recovery

Six-week-old athymic nude (nu/nu) mice (NCI-Frederick, Frederick, VA, USA) were obtained and allowed to adjust for a period of 2 weeks. Bilateral, subcutaneous tumors were engrafted in the flank by injection of 5×10^6 cells suspended in 50:50 BD Matrigel (Becton Dickinson) and serum-free DMEM. Four tumors were used for each virus and timepoint. When tumors reached an average size of 300 mm^3 , 1×10^7 plaque forming units of oHSV suspended in saline-buffered solution was injected intratumorally. At days 3 and 5 following infection, mice were euthanized and tumors recovered in DMEM and kept on ice. After tumors were mechanically dissociated, an equivalent volume of sterile milk was added to the homogenate and viral titering was performed as described above. Titers are plotted with standard deviation.

CONFLICT OF INTEREST

JMM, GYG, and RJW are co-founders, stockholders and consultants for Cathexer, Inc., which holds intellectual property related to oncolytic HSV.

ACKNOWLEDGEMENTS

Funding for this research was provided through DOD-W81XWH-10-NFRP-IIRA-NF1001157, P20 CA151129-03, P01 CA71933-15 and P50 CA97247-05. Special thanks to Enid Keyser in the UAB Comprehensive Flow Cytometry Core for assistance in cell sorting and Dr Bernard Roizman for providing R7020.

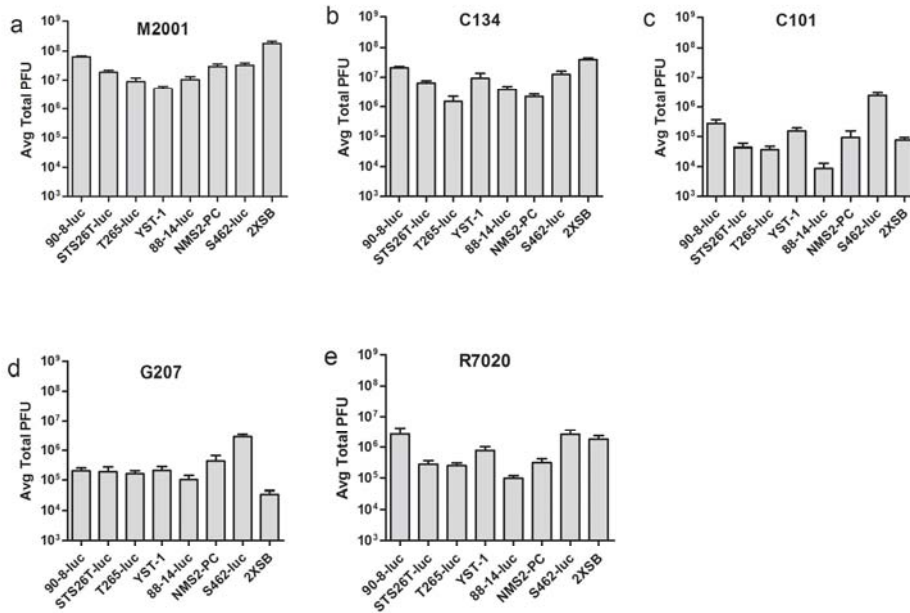
REFERENCES

- Carroll SL, Ratner N. How does the Schwann cell lineage form tumors in NF1? *Glia* 2008; **56**: 1590–1605.
- Kolberg M, Høland M, Ågesen TH, Brekke HR, Liestøl K, Hall KS *et al*. Survival meta-analyses for > 1800 malignant peripheral nerve sheath tumor patients with and without neurofibromatosis type 1. *Neuro-oncology* 2013; **15**: 135–147.
- Mahller YY, Rangwala F, Ratner N, Cripe TP. Malignant peripheral nerve sheath tumors with high and low Ras-GTP are permissive for oncolytic herpes simplex virus mutants. *Pediatric Blood Cancer* 2006; **46**: 745–754.
- Mahller YY, Vaikunth SS, Currier MA, Miller SJ, Ripberger MC, Hsu Y-H *et al*. Oncolytic HSV and erlotinib inhibit tumor growth and angiogenesis in a novel malignant peripheral nerve sheath tumor xenograft model. *Mol Ther* 2007; **15**: 279–286.

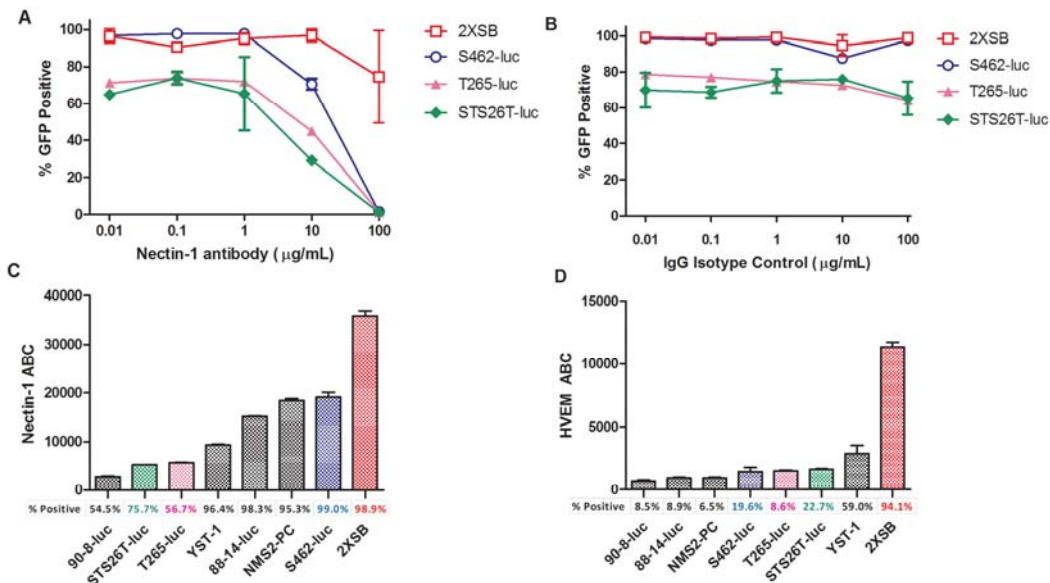
- Farassati F, Pan W, Yamoutpour F, Henke S, Piedra M, Frahm S *et al*. Ras signaling influences permissiveness of malignant peripheral nerve sheath tumor cells to oncolytic herpes. *Am J Pathol* 2008; **173**: 1861–1872.
- Maldonado AR, Klanke C, Jegga AG, Aronow BJ, Mahller YY, Cripe TP *et al*. Molecular engineering and validation of an oncolytic herpes simplex virus type 1 transcriptionally targeted to midkine-positive tumors. *J Gene Med* 2010; **12**: 613–623.
- Mahller Y, Sakthivel B, Baird W, Aronow B, Hsu Y, Cripe T *et al*. Molecular analysis of human cancer cells infected by an oncolytic HSV-1 reveals multiple upregulated cellular genes and a role for SOCS1 in virus replication. *Cancer Gene Ther* 2008; **15**: 733–741.
- Chou J, Kern ER, Whitley RJ, Roizman B. Mapping of herpes simplex virus-1 neurovirulence to gamma 134.5, a gene nonessential for growth in culture. *Science* 1990; **250**: 1262–1266.
- Harrow S, Papanastassiou V, Harland J, Mabbs R, Petty R, Fraser M *et al*. HSV1716 injection into the brain adjacent to tumour following surgical resection of high-grade glioma: safety data and long-term survival. *Gene Therapy* 2004; **11**: 1648–1658.
- Markert J, Medlock M, Rabkin S, Gillespie G, Todo T, Hunter W *et al*. Conditionally replicating herpes simplex virus mutant, G207 for the treatment of malignant glioma: results of a phase I trial. *Gene Therapy* 2000; **7**: 867–874.
- Ramplung R, Cruickshank G, Papanastassiou V, Nicoll J, Hadley D, Brennan D *et al*. Toxicity evaluation of replication-competent herpes simplex virus (ICP 34.5 null mutant 1716) in patients with recurrent malignant glioma. *Gene Therapy* 2000; **7**: 859.
- Markert JM, Liechty PG, Wang W, Gaston S, Braz E, Karrasch M *et al*. Phase Ib trial of mutant herpes simplex virus G207 inoculated pre- and post-tumor resection for recurrent GBM. *Mol Ther* 2008; **17**: 199–207.
- Markert JM, Razdan SN, Kuo H-C, Cantor A, Knoll A, Karrasch M *et al*. A phase I trial of oncolytic HSV-1, G207, given in combination with radiation for recurrent GBM demonstrates safety and radiographic responses. *Mol Ther* 2014; **22**: 1048–1055.
- Huang Y-Y, Yu Z, Lin S-F, Li S, Fong Y, Wong RJ. Nectin-1 is a marker of thyroid cancer sensitivity to herpes oncolytic therapy. *J Clin Endocrinol Metab* 2007; **92**: 1965–1970.
- Yu Z, Adusumilli PS, Eisenberg DP, Darr E, Ghossein RA, Li S *et al*. Nectin-1 expression by squamous cell carcinoma is a predictor of herpes oncolytic sensitivity. *Mol Ther* 2007; **15**: 103–113.
- Wang P, Currier M, Hansford L, Kaplan D, Chioocca E, Uchida H *et al*. Expression of HSV-1 receptors in EBV-associated lymphoproliferative disease determines susceptibility to oncolytic HSV. *Gene Therapy* 2012; **20**: 761–769.
- Friedman GK, Langford CP, Coleman JM, Cassidy KA, Parker JN, Markert JM *et al*. Engineered herpes simplex viruses efficiently infect and kill CD133+ human glioma xenograft cells that express CD111. *J Neuro-oncology* 2009; **95**: 199–209.
- Chen C-h, Chen W-Y, Lin S-F, Wong RJ. Epithelial mesenchymal transition enhances response to oncolytic herpes viral therapy through nectin-1. *Human Gene Ther* 2014; **25**: 539–551.
- Forrester A, Farrell H, Wilkinson G, Kaye J, Davis-Poynter N, Minson T. Construction and properties of a mutant of herpes simplex virus type 1 with glycoprotein H coding sequences deleted. *J Virol* 1992; **66**: 341–348.
- Ligas MW, Johnson DC. A herpes simplex virus mutant in which glycoprotein D sequences are replaced by beta-galactosidase sequences binds to but is unable to penetrate into cells. *J Virol* 1988; **62**: 1486–1494.
- Cai W, Gu B, Person S. Role of glycoprotein B of herpes simplex virus type 1 in viral entry and cell fusion. *J Virol* 1988; **62**: 2596–2604.
- Pertel PE, Fridberg A, Parish ML, Spear PG. Cell fusion induced by herpes simplex virus glycoproteins gB, gD, and gH-gL requires a gD receptor but not necessarily heparan sulfate. *Virology* 2001; **279**: 313–324.
- Roop C, Hutchinson L, Johnson DC. A mutant herpes simplex virus type 1 unable to express glycoprotein L cannot enter cells, and its particles lack glycoprotein H. *J Virol* 1993; **67**: 2285–2297.
- Rikitake Y, Mandai K, Takai Y. The role of nectins in different types of cell-cell adhesion. *J Cell Sci* 2012; **125**: 3713–3722.
- Mizoguchi A, Nakanishi H, Kimura K, Matsubara K, Ozaki-Kuroda K, Katata T *et al*. Nectin an adhesion molecule involved in formation of synapses. *J Cell Biol* 2002; **156**: 555–565.
- Richart SM, Simpson SA, Krummenacher C, Whitbeck JC, Pizer LI, Cohen GH *et al*. Entry of herpes simplex virus type 1 into primary sensory neurons in vitro is mediated by nectin-1/HveC. *J Virol* 2003; **77**: 3307–3311.
- Montgomery RI, Warner MS, Lum BJ, Spear PG. Herpes simplex virus-1 entry into cells mediated by a novel member of the TNF/NGF receptor family. *Cell* 1996; **87**: 427–436.
- Shukla D, Liu J, Blaiklock P, Shworak NW, Bai X, Esko JD *et al*. A novel role for 3-O-sulfated heparan sulfate in herpes simplex virus 1 entry. *Cell* 1999; **99**: 13–22.

- 29 Even DL, Henley AM, Geraghty RJ. The requirements for herpes simplex virus type 1 cell–cell spread via nectin-1 parallel those for virus entry. *Virus Res* 2006; **119**: 195–207.
- 30 Shah A, Parker J, Gillespie G, Lakeman F, Meleth S, Markert J *et al*. Enhanced antiglioma activity of chimeric HCMV/HSV-1 oncolytic viruses. *Gene Therapy* 2007; **14**: 1045–1054.
- 31 Byer SJ, Eckert JM, Brossier NM, Clodfelder-Miller BJ, Turk AN, Carroll AJ *et al*. Tamoxifen inhibits malignant peripheral nerve sheath tumor growth in an estrogen receptor–independent manner. *Neuro-oncology* 2011; **13**: 28–41.
- 32 Friedman GK, Haas MC, Kelly VM, Markert JM, Gillespie GY, Cassady KA. Hypoxia moderates γ 134. 5-deleted herpes simplex virus oncolytic activity in human glioma xenoline primary cultures. *Transl Oncol* 2012; **5**: 200.
- 33 Cassady KA. Human cytomegalovirus TRS1 and IRS1 gene products block the double-stranded-RNA-activated host protein shutoff response induced by herpes simplex virus type 1 infection. *J Virol* 2005; **79**: 8707–8715.
- 34 Mineta T, Rabkin SD, Yazaki T, Hunter WD, Martuza RL. Attenuated multi-mutated herpes simplex virus-1 for the treatment of malignant gliomas. *Nat Med* 1995; **1**: 938–943.
- 35 Meignier B, Longnecker R, Roizman B. *In vivo* behavior of genetically engineered herpes simplex viruses R7017 and R7020: construction and evaluation in rodents. *J Infect Dis* 1988; **158**: 602–614.
- 36 Gerson SL. Cotransduction with MGMT and ubiquitous or erythroid-specific GFP lentiviruses allows enrichment of dual-positive hematopoietic progenitor cells *in vivo*. *ISRN Hematol* 2012; **2012**.

Supplementary Information accompanies this paper on Gene Therapy website (<http://www.nature.com/gt>)

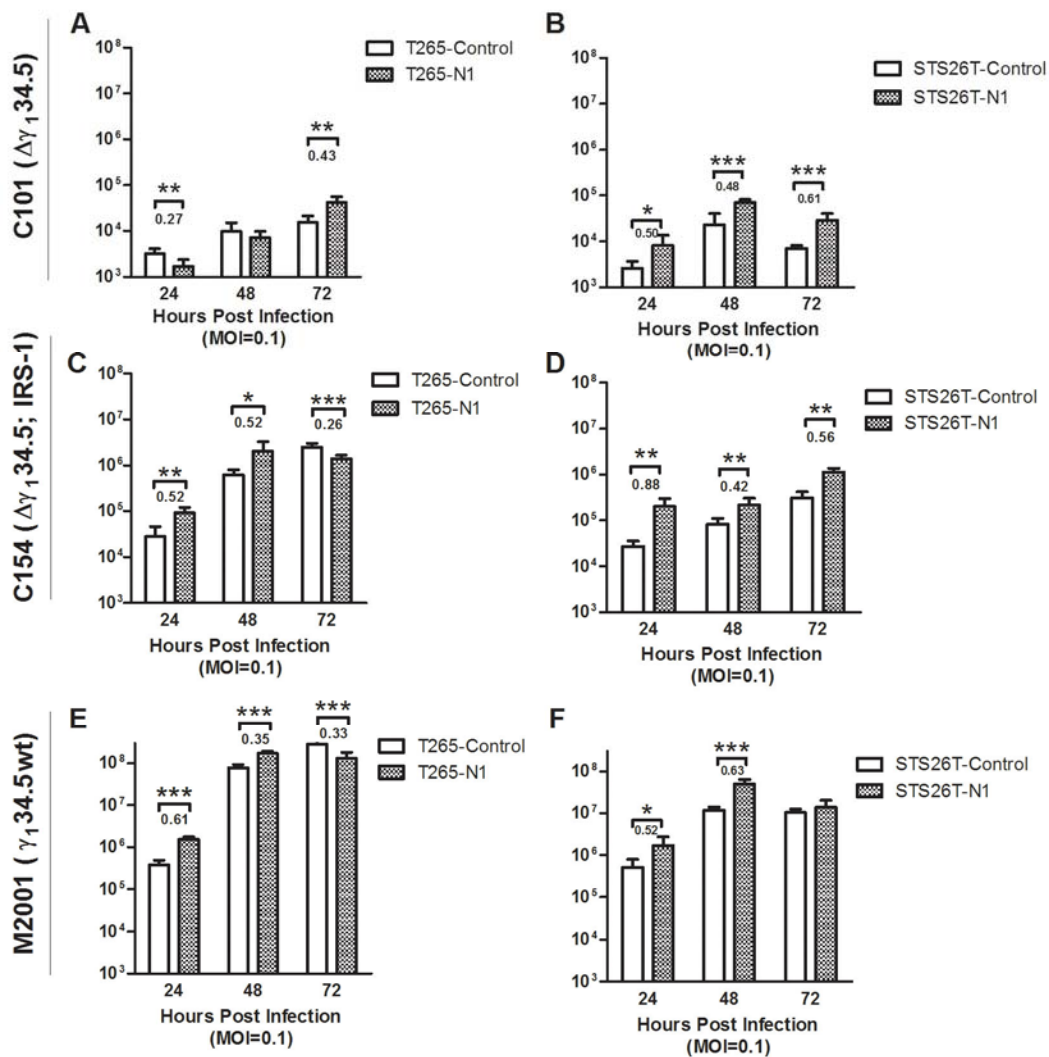


Supplemental Figure 1: Single-step viral recovery in MPNST cell lines. MPNST cell lines were subjected to single-step (MOI=10, 24 hr) infection by viruses M2001 (a), C134 (b), C101 (c), G207 (d), and R7020 (e) and the viral titers reported as the average total plaque forming units (PFU) as determined through limiting dilution plaque formation assay. Data were collected in triplicate and the standard deviation reported.



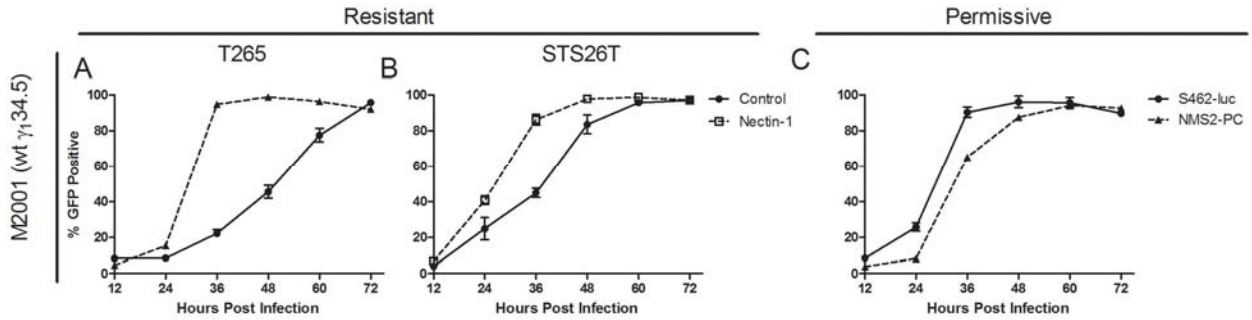
Supplemental Figure 2: Nectin-1 dependence of productive HSV-1 infection in resistant MPNST cell lines. MPNST cells were seeded 3×10^4 cells per well in 96 well plates and allowed to adhere overnight. Nectin-1 antibody (clone R1.302, Biologend) (A) or mouse IgG1 isotype control (Cell Signaling) (B) was diluted in growth media and incubated with cells at 4°C for 30

minutes. Cells were then infected with GFP expressing wt HSV-1 M2001 at an MOI of 5 and incubated at 37 °C for 20 hrs (S26T-luc, T265-luc, and S462-luc) or 12 hrs (2XSB). The earlier timepoint of analysis for 2XSB was necessary due to the rapid infection and deterioration of these cells at longer timepoints. Cells were trypsinized and resuspended in FACS buffer and analyzed by flow cytometry for GFP expression. The % GFP positive is calculated as the percentage of viable cells which have a GFP intensity greater than an uninfected control. Measurements were taken in duplicate and the standard deviation reported. Nectin-1 (C) and HVEM (D) expression was quantified by flow cytometry after incubation with PE-conjugated mouse monoclonal antibody (Biolegend) with subsequent quantification using antibody quantification beads (Bangs Labs). The percentage of cells staining above the isotype control is also reported. Receptor quantification was performed in triplicate with the standard deviation reported.

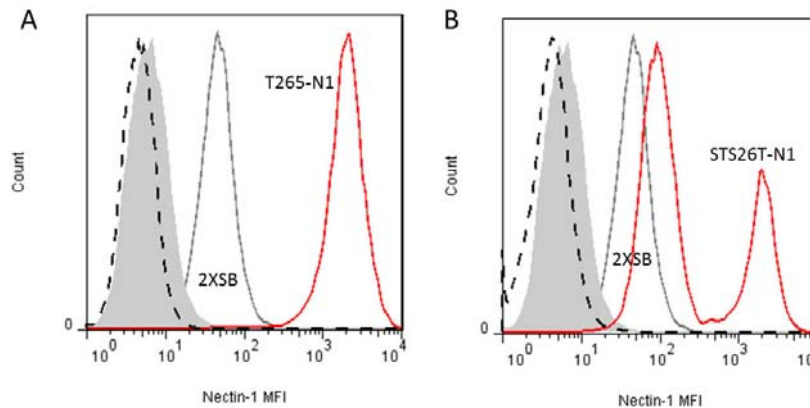


Supplemental Figure 3: Impact of increased nectin-1 expression on multi-step viral replication. Multi-step (MOI=0.1) replication assays using C101 (A,B), C154 (C,D), and M2001 (E,F)

viruses were performed in S26T-luc and T265-luc transduced with nectin-1 or control lentivirus. Samples were collected at the indicated timepoints following infection and titered using standard limiting dilution plaque formation assays. Data were collected in triplicate and the standard deviation reported. Comparison was made between nectin-1 overexpressing cells and control by 2-tailed Student's t-test. Significance was set at $P < 0.05$. For cells with significant changes in titer, the logarithm of the increase is reported below the significance marking.



Supplemental Figure 4: Impact of increased nectin-1 expression on wild-type HSV-1 spread in vitro. Resistant cell lines T265-luc (A) and STS26T-luc (B) and their nectin-1 transduced variants as well as permissive cell lines S462-luc and NMS2-PC (C) were infected in a multi-step assay (MOI=0.1) with GFP expressing wild-type HSV-1 M2001 and monitored over time for viral infection as evident by expression of viral GFP monitored by flow cytometry.



Supplemental Figure 5: Comparison of nectin-1 expression in 2XSB to nectin-1 overexpressing cell lines T265-N1 (A) and STS26T-N1 (B). Cell lines were analyzed by flow cytometry as described in the submitted manuscript. Dashed black or solid red lines respectively represent unlabeled or nectin-1 labeled resistant cell lines T265-N1 or STS26T-N1. Resistant cell lines in each graph are shown to express nectin-1 at an intensity greater than the highest natural nectin-1 expressing cell line 2XSB (gray line). Unlabeled 2XSB is also shown (shaded gray).

Appendix i

1 **TITLE:** STAT1 and NFκB inhibitors diminish basal interferon stimulated gene expression and improve the
2 productive infection of oncolytic HSV in malignant peripheral nerve sheath tumor cells

3 **RUNNING TITLE:** Basal ISG Expression Diminishes oHSV Productivity

4 **AUTHORS:** Joshua D. Jackson¹, James M. Markert^{1,2,3}, Li, Li¹, Steven L. Carroll⁴, and Kevin A. Cassady^{2,5}

5 **AFFILIATIONS:**

6 1 Department of Neurosurgery, 2 Department of Pediatric, 3 Department of Cell, Developmental and
7 Integrative Biology, University of Alabama at Birmingham, Birmingham, AL 35233, USA; 4 Department of
8 Pathology and Laboratory Medicine, Medical University of South Carolina, Charleston, SC, 29425,USA; 5
9 Nationwide Children's Hospital and The Ohio State University, OH 43205, USA

10 **CORRESPONDING AUTHOR:**

11 Kevin A. Cassady, M.D.

12 Center for Childhood Cancer and Blood Diseases

13 The Research Institute at Nationwide Children's Hospital

14 The Ohio State University College of Medicine

15 700 Children's Drive

16 Columbus, Ohio 43205

17 614-722-2798

18 Kevin.Cassady@Nationwidechildrens.org

19 **FUNDING:** Funding for this research was provided through DOD-W81XWH-10-NFRP-IIRA-NF1001157,
20 P20 CA151129-03, P01 CA71933-15 and P50 CA97247-05.

21 **CONFLICT OF INTEREST:** JMM is a co-founder, stockholder and consultant for Catherex, Inc., which
22 holds intellectual property related to oncolytic HSV.

23 **WORD COUNT: 5,948**

24 **FIGURES: 6**

25 **KEY WORDS:** STAT1, ISG, NFκB, oHSV,

26

27 **ABSTRACT**

28 Interferon stimulated genes (ISGs) encode diverse proteins that mediate intrinsic antiviral resistance in
29 infected cells. We hypothesized that malignant peripheral nerve sheath tumor (MPNST) cells resist the
30 productive infection of oncolytic herpes simplex virus (oHSV) through activation of the JAK/STAT1
31 pathway and resultant upregulation of ISGs. Twenty-one human and mouse MPNST cell lines were used
32 to explore the relationship between STAT1 activation and the productive infection of $\Delta\gamma_134.5$ oHSVs.
33 STAT1 activation in response to oHSV infection was found to associate with diminished $\Delta\gamma_134.5$ oHSVs
34 replication and spread. Multi-day pre-treatment, but not co-treatment, with a JAK inhibitor significantly
35 improved viral titer and spread. ISG expression was found to be elevated prior to infection and could
36 be downregulated when treated with the JAK inhibitor. This suggested that the JAK/STAT1 pathway is
37 active prior to infection. Overexpression of the transcription factors that promote ISG expression
38 increased basal ISG levels and significantly decreased oHSV titers in normally permissive cells. A possible
39 link between activation of the NF κ B pathway and ISG expression was established through the expression
40 of inhibitor of κ B (I κ B) which decreased basal STAT1 transcription and ISG expression. These results
41 demonstrate that basal ISG expression prior to infection contributes to the resistance of $\Delta\gamma_134.5$ oHSVs
42 in MPNST cell lines.

43 Implication: While cancer-associated ISG expression has been previously reported to impart resistance
44 to chemotherapy and radiotherapy, we show that basal ISG expression also contributes to oncolytic HSV
45 resistance.

46

47

48 **Introduction:**

49 Malignant peripheral nerve sheath tumors (MPNSTs) are a highly aggressive cancer of the
50 peripheral nervous system derived from cells of the Schwann cell lineage. Patients have a median
51 survival of 26 months following diagnosis (1). Beyond advances in surgical resection, further treatment
52 with chemotherapy and radiation has not demonstrated an overall benefit to survival (2, 3). A
53 promising alternative approach is the use of conditional replicating oncolytic herpes simplex viruses
54 type-1 (oHSVs) to treat MPNSTs. These oHSVs have been safely used in clinical trials in a number of
55 cancer types, however, the tumor response has varied and we anticipate this would be true for patients
56 with MPNSTs. We have previously demonstrated that MPNST cell lines exhibit variable oHSV
57 susceptibility (4), and we have sought to understand the potential mechanisms of resistance that are
58 detrimental to oHSV therapy.

59 The predominant paradigm for tumor resistance to oHSV has been the extent to which
60 oncogenic signaling cascades, namely Ras and the mitogen-activated protein kinases (5), suppress the
61 activation of protein kinase R (PKR) (6). PKR is one of the better studied antiviral kinases, and its activity
62 upon late-gene expression and replication in $\gamma_134.5$ -deleted HSVs has been well described. In brief, HSV
63 produces double-stranded RNA (dsRNA) during viral gene transcription which induces PKR dimerization,
64 auto-phosphorylation, and activation. Activated PKR phosphorylates its substrate eukaryotic initiation
65 factor 2 alpha (eIF2 α), a rate limiting factor in protein translation initiation, leading to translational
66 arrest in the infected cell. Wild-type HSV counters translational arrest through the expression of the
67 neurovirulence gene $\gamma_134.5$ which encodes a multifunctional viral protein, infected cell protein 34.5
68 (ICP34.5). ICP34.5 recruits a host phosphatase, protein phosphatase 1 alpha (PP1 α), to dephosphorylate
69 eIF2 α thus restoring protein translation in the infected cell. Though wild-type HSV causes lethal
70 encephalitis in the central nervous system, deletion of one or both copies of the diploid $\gamma_134.5$ gene
71 attenuates the virus allowing the safe administration of oHSV as an anti-tumor therapy. Attenuated

72 oHSV is believed to have a selective replication advantage in malignant cells that complement the loss of
73 $\gamma_134.5$ through oncogenic processes such as Ras-induced suppression of PKR.

74 In addition to PKR, cells express a diverse set of pattern recognition receptors (PRRs) that detect
75 pathogen associated molecular patterns (PAMPs) such as viral nucleic acids. Stimulation of certain PRRs
76 including retinoic acid-inducible gene I (RIG-I), melanoma differentiation antigen 5 (MDA5), stimulator of
77 interferon genes (STING), and members of the toll-like receptor (TLR) family ultimately lead to the
78 activation of transcription factors which promote expression of the Type-I interferons IFN α and IFN β
79 which are potent antiviral cytokines. As extracellular cytokines, Type-I IFNs interact with
80 transmembrane IFN-alpha receptors (IFNARs) in an autocrine and paracrine manner leading to the
81 activation of the intracellular Janus kinases JAK1 and TYK2. The specific activation of JAK1 and TYK2
82 results in the phosphorylation of signal transducer and activator of transcription 1 (STAT1) and STAT2,
83 which together with interferon regulatory factor 9 (IRF9) form the heterotrimeric transcription factor
84 interferon stimulated gene factor 3 (ISGF3). The ISGF3 complex localizes to the nucleus where it
85 promotes transcription from interferon stimulated response elements (ISRE) in the promoter regions of
86 several hundred interferon stimulated genes (ISGs). ISGs have diverse functions which modulate viral
87 and cellular functions to promote intrinsic antiviral resistance. The functions of ISGs include direct
88 inhibition of specific viral mechanisms (e.g. myxovirus resistance 1, MX1), inhibition of global cellular
89 processes involving transcription and translation (e.g. PKR; and 2'-5'-oligoadenylate synthetase 1, OAS1),
90 or increased expression of PRRs and IFN/STAT1 signaling modulators to promote amplification of the
91 antiviral response (e.g. RIG-I; MDA5; interferon-induced protein with tetratricopeptide repeats 3, IFIT3).

92 The research presented here tests the hypothesis that the upregulation of ISGs in MPNST cell
93 lines is associated with resistance to oHSV. Our results show that: (1) PKR activation is evident in the
94 majority of MPNST cell lines and therefore PKR activation is not specifically associated with oHSV
95 resistant phenotypes; (2) STAT1 activation is observed in 10 of 21 MPNST cell lines and is statistically

96 associated with diminished productivity of both a first generation $\Delta\gamma_134.5$ oHSV and a second generation
97 $\Delta\gamma_134.5$ oHSV, C134, capable of evading PKR-mediated translational arrest; (3) resistant MPNST cell
98 lines exhibit greater ISG expression than oHSV sensitive lines prior to oHSV infection suggesting they are
99 primed toward an antiviral state; (4) pre-treatment of resistant MPNST tumor lines with a small-
100 molecule JAK inhibitor reduces basal ISG expression and improves viral replication and spread; (5)
101 conversely, ISGF3 overexpression in MPNST cell lines increased ISG expression and decreased oHSV
102 replication; and finally (6) we have provided evidence that basal expression of ISGs may be dependent
103 on the NF κ B signaling network.

104

105 **Materials and Methods:**

106

107 **Cell lines and viruses.** Human MPNST cell lines or their firefly luciferase expressing derivatives (“-luc”) (4) as
108 well as MPNSTs lines derived from a genetically engineered mouse model(7) have been previously described. All
109 MPNST cell lines were maintained in growth media containing DMEM with 10% fetal bovine serum and 10 mM
110 L-glutamine (Sigma). The African green monkey kidney cell line Vero was obtained from the ATCC and
111 maintained in MEM with 5% bovine growth serum. All viruses except M201 have been previously described (4,
112 8). M201 is an oHSV with CMVp-GFP inserted in between UL3 and UL4, and murine IL-12 inserted in $\gamma_134.5$
113 locus. M201 was constructed as follows: M002 (mIL-12 virus) (8) DNA and pCK1029 (contains UL3 and UL4
114 flanking sequence) plasmid DNA linearized by restriction digest with SacI were co-transfected with
115 Lipofectamine in RSC cells. When the cytopathic effect (CPE) reached >90%, cells were collected in 50% sterile
116 skim milk solution, subjected to 3 freeze/thaw cycles of -80°C / 37°C, and stored at -80°C. Next, we performed
117 three rounds of plaque purification and selection on Vero cells for green fluorescence positive plaques.
118 Candidate viral DNAs were verified by Southern blot. Isolated viral DNAs were digested with PstI, separated on
119 1% agarose gel, transferred to Zeta-Probe membrane, and then hybridized to alkaline phosphatase labeled

120 pCK1037 (UL3 and UL4 flanking fragments inserted in pUC18 backbone plasmid). Expected band sizes of 2.0 and
121 1.2kb were observed. The final candidates were expanded for experimental stocks.

122

123 **Reagents.** The small molecule inhibitors ruxolitinib (Selleckchem) and TPCA-1 (Selleckchem) were
124 stored as 10mM aliquots in DMSO (Sigma). Primary antibodies were obtained as follows: p-T446-PKR
125 (3076), p-S51-eIF2 α (3398), eIF2 α (2103), p-Y701-STAT1 (9167), STAT1 (9172), MDA5 (5321), RIG-I
126 (3743), p-S536-NF κ B/P65 (3033), NF κ B/P65 (3987) I κ B (4814), p-MEK1/2 (2338), MEK1/2 (4694), p-
127 ERK1/2 (4376), and ERK1/2 (9102) from Cell Signaling; MX1 (13750), OAS1 (14955), IFIT3 (15201), STAT2
128 (16674), and IRF9 (14167) from Proteintech; HSV ICP4 (H1A021; Virusys), PKR (sc707; Santa Cruz) and β -
129 actin (A2228; Sigma). Horseradish peroxidase (HRP) conjugated goat anti-mouse (Immunopore) and
130 goat anti-rabbit antibodies were used as secondary antibodies.

131

132 **Viral productivity assays.** Viral recovery (replication) assays have been previously described (4) with the
133 following modifications: final virus inoculum was composed of virus and 150 μ l regular growth media
134 (10% FBS); incubation time was 1 hr followed by addition of growth media up to 1 mL per well in 24 well
135 plates. Viral spread assays have been previously described (4). In brief, cells were seeded 1.5×10^5 per
136 well in 24 well plates and infected at an MOI of 0.1 with GFP expressing viruses or mock infected (media
137 alone). After 48 hrs, cells were subjected to flow cytometry to assess the percentage of the population
138 positive for viral GFP. When described, Flow Cytometry Absolute Count Standard fluorescent beads
139 (Bangs Laboratories) were added to the final suspension of cells to calculate the ratio of cells surviving
140 infection compared to mock infected samples. All samples were collected in triplicate and the means
141 reported.

142

143 **Lentivirus construction and transduction.** Cloning methods and construction of lentivector plasmids are
144 provided as supplemental information. Our method of lentivirus production has been previously
145 described (4). Stable cell lines were produced via lentiviral transduction of the target cell lines. When
146 appropriate, hygromycin (Sigma) selection was applied no earlier than 48 hrs after transduction at a final
147 concentration of 300 µg/ml for 3-5 days.

148

149 **Western blotting.** Cellular lysates were collected on ice in RIPA buffer (10 mM Tris-Cl pH 8.0, 1 mM
150 EDTA, 1% Triton X100, 0.1% sodium deoxycholate, 0.1% SDS, 140 mM NaCl) with protease inhibitor
151 cocktail (Roche) and diluted in 4x sample buffer (240 mM Tris-Cl pH 6.8, 40% glycerol, 4% SDS, 20% β-
152 mercaptoethanol, 0.04% bromophenol blue). Samples were denatured at 98°C for five minutes, chilled
153 on ice, and separated by polyacrylamide gel electrophoresis. Proteins were transferred to a
154 nitrocellulose membrane (Thermo Scientific) and blocked for 1 hour at room temperature with 5% dry
155 milk (S.T. Jerrell Co.) or bovine serum albumin (Fisher). Membranes were incubated overnight at 4°C
156 with primary antibody diluted in Tris-buffered saline with 0.1% Tween-20 (TBST). Membranes were
157 repeatedly washed with TBST, incubated for 1 hr with secondary antibody diluted in TBST (1:20,000) at
158 room temperature, and subsequently washed with TBST. Membranes were wetted with SuperSignal
159 West Pico Chemiluminescent Substrate (Thermo Scientific) for 3 minutes and exposed to blue x-ray film
160 (Research Products International).

161

162 **Luciferase assays.** The STS26T-luc and ST8814-luc cell lines used in reporter assays have been previously
163 transduced with firefly luciferase under a constitutive CMV promoter. These cell lines were further
164 transduced via lentivirus with a nanoluciferase reporter (with a C-terminal PEST sequence) (Promega)
165 under the control of either ISRE or NFκB promoters. Luminescence assays were performed in opaque

166 96-well plates with the Nano-Glo Dual Luciferase Reporter Assay (Promega) according to the
167 manufacturer's instructions. Luminescence was measured using a FLUOStar Optima (BMG Labtech)
168 plate reader. Nanoluciferase activity was normalized to that of firefly luciferase and reported as
169 arbitrary units. Data were collected in triplicate or quadruplicate.

170

171 **Statistical analysis.** Statistical analysis was performed using Prism 5 (GraphPad Software). For analysis
172 involving multiple cell lines, a one-tailed Mann-Whitney U test was used. Student's t test was used for
173 inhibitor and transduction experiments within individual cell lines. For all analyses, the cutoff for
174 statistical significance was set at $P < 0.05$. The following notation was used: (ns) $P > 0.05$, (*) $P \leq 0.05$,
175 (**) $P \leq 0.01$, (***) $P \leq 0.001$.

176

177

178 **Results:**

179

180 ***Activation of PKR in response to oHSV infection***

181 To assess the contribution of antiviral signaling pathways to oHSV resistance in MPNSTs, we
182 assessed PKR activation and eIF2 α phosphorylation in response to R3616, a $\Delta\gamma_134.5$ oHSV (kindly
183 provided by Dr. Bernard Roizman, University of Chicago, Chicago, IL). The relevant characteristics of
184 R3616 and other viruses used in the following experiments are provided in Supplemental Table 1. We
185 first determined the susceptibility of 8 human and 13 mouse MPNST cell lines by viral recovery assay 24
186 hr after cells were infected at a multiplicity of infection (MOI) of 1. Titers of recovered virus ranged
187 from 7.9×10^3 to 4.1×10^5 plaque forming units (PFU) for human cell lines and 1.5×10^3 to 2.0×10^5 PFU for
188 mouse lines (Fig. 1 A-B). While mouse lines yielded 3-fold lower average titers of virus than human-

189 derived lines (3.2×10^4 and 9.5×10^5 PFU respectively), the distributions of human and mouse lines were
190 statistically indistinguishable (Supplemental Figure 1). Immunoblots against phosphorylated PKR (p-PKR)
191 and p-eIF2 α in human cell lines, or p-eIF2 α in mouse cell lines, revealed PKR activation and eIF2 α
192 phosphorylation following R3616 infection (Fig 1 C-D) at 12 hpi in nearly all cell lines tested. There was
193 no apparent difference in p-PKR/p-eIF2 α between cell lines with high or low viral recovery. We
194 conclude that activation of PKR is not sufficient to exclusively define the resistant phenotypes observed
195 in MPNST cell lines.

196 ***Activation of STAT1 in response to oHSV infection and association with viral productivity***

197 Because deletion of the HSV $\gamma_134.5$ gene increases HSV-1 sensitivity to Type-I IFNs (9) which
198 activate STAT1, we hypothesized that oHSV-induced activation of STAT1 was associated with decreased
199 viral productivity in MPNST cells. We determined that 6 hpi was the optimal time to observe STAT1
200 Y701 phosphorylation (Supplementary Fig. 2). R3616 infection induced STAT1 activation in 3 of 8 (38%)
201 human (Fig. 2A) and in 7 of 13 (54%) mouse cell lines (Fig. 2B). When exposed to exogenous IFN β (200
202 IU/ml) STAT1 Y701 phosphorylation was evident in all human MPNST cell lines indicating that
203 mechanisms for signal transduction were functional (Supplemental Fig. 3). When R3616 titers from all
204 MPNST cell lines were sorted into STAT1 unresponsive (pSTAT1-) and STAT1 responsive (pSTAT1+)
205 groups, cell lines which were STAT1 responsive were associated with significantly lower viral recovery
206 (Fig. 2C). To further test the association of the STAT1 response of each cell line with viral productivity,
207 we assessed viral spread within an *in vitro* monolayer. In this assay, the percentage of cells infected with
208 an eGFP expressing $\Delta\gamma_134.5$ virus (C101) in a multi-step infection (MOI=0.1, 48 hpi) was measured by
209 flow cytometry. Similar to the viral recovery studies, cells lines which responded to $\Delta\gamma_134.5$ infection by
210 activating STAT1 demonstrated significantly lower viral spread (Fig. 2D). To determine if differences in
211 STAT1 activation was cyto-protective following oHSV infection, we measured the number of gated cells
212 by flow cytometry at 48 hpi following multi-step infection with C101 and compared the counts to mock

213 infected cells. The results showed a trend toward higher cell counts (lower cytotoxicity) after C101
214 infection in STAT1 responsive cell lines, however, this was not statistically significant (Fig. 2E).

215 To identify if the STAT1 response was associated with diminished oHSV productivity in the
216 setting of a $\Delta\gamma_134.5$ oHSV capable of PKR evasion, we repeated the spread and cytotoxicity studies using
217 C134, a chimeric $\Delta\gamma_134.5$ oHSV expressing the human cytomegalovirus (HCMV) IRS1 gene product which
218 inhibits PKR-mediated translational arrest. Immunoblots against PKR and eIF2 α verified that C134
219 inhibited PKR-induced eIF2 α phosphorylation in MPNST tumor cells (Fig 3A) similar to what has been
220 observed in other cell lines (10). In a viral spread assay with C154 (an eGFP expressing variant of C134),
221 we found that similar to the results with C101, the spread and cytotoxic effect of C154 was significantly
222 diminished in STAT1 responsive cell lines (Fig 3B and 3C). Next, to identify if the productivity of wild-type
223 HSV-1 was associated with STAT1 response, we repeated the spread and cytotoxicity assays with a wild-
224 type HSV-1(F) that expresses eGFP (M2001). The results show that unlike $\Delta\gamma_134.5$ oHSVs, the STAT1
225 response was not significantly associated with wild-type HSV-1 spread or cytotoxicity in the MPNST cell
226 lines (Fig. 3 D-E). Both viral spread and cytotoxicity induced by M2001 was generally high in all cell lines
227 compared to the $\Delta\gamma_134.5$ attenuated viruses.

228 These results demonstrate that the restricted productivity of $\Delta\gamma_134.5$ oHSVs is significantly
229 associated with the capacity of a cell to activate the STAT1 signaling cascade in response to $\Delta\gamma_134.5$
230 oHSV infection. This association exists irrespective of PKR mediated translational arrest inasmuch as
231 the spread and cytotoxicity of C134, a $\Delta\gamma_134.5$ HSV capable of PKR evasion, is also restricted in these
232 STAT1 responsive cell lines. In contrast, the productivity of wild-type HSV-1 was not associated with the
233 capacity for a STAT1 response in similar assays.

234

235 ***Modulation of STAT1 activation by the JAK inhibitor ruxolitinib***

236

237 Next, to determine whether the observed STAT1 activation was directly responsible for
238 diminished $\Delta\gamma_134.5$ viral productivity in resistant MPNST cell lines, we inhibited STAT1 Y701
239 phosphorylation using the JAK1/2 inhibitor ruxolitinib. We hypothesized that by inhibiting this response,
240 $\Delta\gamma_134.5$ oHSV productivity could be improved. To test this hypothesis, we treated the oHSV resistant
241 MPNST cell lines STS26T-luc and ST8814-luc with 250 nM ruxolitinib (Rux) or vehicle (DMSO) following
242 $\Delta\gamma_134.5$ oHSV infection. Co-treatment with ruxolitinib did not improve $\Delta\gamma_134.5$ oHSV infection and
243 spread compared to DMSO in multi-step (low MOI) assay with C101 (Fig. 4A) despite the fact that
244 ruxolitinib co-treatment prevented STAT1 Y701 phosphorylation (Fig. 4G). In viral recovery assays,
245 ruxolitinib co-treatment did not improve R3616 replication in a single-step (MOI=1) assays (Fig. 4B), but
246 did slightly improve R3616 replication in multi-step (MOI=0.1) replication assays in both cell lines (Fig.
247 4C).

248 Multi-step replication assays, using a low virus/cell ratio and longer timepoints (24 vs. 48 hpi),
249 challenge the virus to undergo multiple rounds of replication and spread beyond the initially infected
250 cells. The modest increases in viral titer observed in the multi-step assay (Fig 4C), but not the single-step
251 assay, led us to hypothesize that uninfected cells in the multi-step assay benefitted to some degree from
252 “pre-treatment” with ruxolitinib prior to becoming infected. To further test the effects of pre-
253 treatment, the above experiments were repeated by exposing cells to ruxolitinib for 48 hrs followed by
254 removal of the inhibitor prior to infection and addition of DMSO following infection. The results show
255 that pre-treatment alone with ruxolitinib (Rux + DMSO) significantly improved the spread of C101 (Fig.
256 4D) as well as titers of R3616 in both single-step and multi-step assays in both cell lines (Fig. 4E-F)
257 compared to DMSO pre-treatment (DMSO + DMSO). Interestingly, pre-treatment alone, whereby cells
258 were washed of ruxolitinib prior to infection, did not inhibit subsequent oHSV-induced STAT1
259 phosphorylation (Fig. 4G). Sequential pre-and co-treatment with ruxolitinib (Rux +Rux) further

260 improved viral spread beyond pre-treatment alone (Fig. 4 D), however, it did not significantly improve
261 viral replication in either the single-step or multi-step viral recovery assays (Fig. 4 E-F). Similar
262 improvements were obtained with a M002 series oHSV (8) (Supplemental Fig. 4). To explain the unique
263 effects of pre-treatment, we hypothesized that ruxolitinib inhibited low-level stimulation and activation
264 of the JAK/STAT pathway in the STS26T-luc and ST8814-luc cell lines. To test this hypothesis, we stably
265 transduced these cell lines with a nano-luciferase reporter under the control of a series of ISRE promoter
266 elements and showed that ruxolitinib diminished the basal (uninfected) ISRE reporter activity in a
267 concentration-dependent manner relative to DMSO (Fig 4H). An assessment of protein expression by
268 western blot revealed that the expression of five representative ISGs (MDA5, RIG-I, MX1, IFIT3, and
269 OAS1) decreased following 48 hr treatment with ruxolitinib as compared to DMSO (Fig. 4I). We
270 conclude that basal STAT1/ISRE promoter activity leads to ISG expression which negatively impacts the
271 productive infection of oHSVs.

272

273 ***Effect of ISG upregulation on oHSVs***

274

275 To determine the extent to which basal ISGs expression occurs among other MPNST cell lines,
276 we evaluated the relative levels of five ISGs (MDA5, RIG-I, MX1, IFIT3, and OAS1) by immunoblot in all
277 human MPNST cell lines. The results show that for the 5 probed ISGs, greater protein expression was
278 detected in the cell lines ST8814-luc, T265-luc, 2XSB, STS26T-luc, and 90-8-luc whereas YST-1, NMS2-PC,
279 and S462-luc had low or undetectable ISG expression (Fig 5A). The low ISG expression in S462-luc is
280 notable since this cell line was the most permissive to oHSV infection producing the highest viral titers of
281 MPNST cell lines tested. We hypothesized that higher basal ISG expression would increase oHSV
282 resistance in S462-luc. Previously published studies have shown that co-expression of the ISGF3

283 component transcription factors (STAT1, STAT2, and IRF9) results in elevated basal ISG expression (11).
284 Overexpression of ISGF3 in S462-luc similarly resulted in elevated ISG expression (Fig 5B). ISGF3
285 overexpression in S462-luc led to greater than 10 fold reduction of R3616 titers in both single-step and
286 multi-step replication assays (Fig. 5C-D). In the resistant cell lines STS26T-luc and 88-14-luc, ISGF3
287 overexpression further elevated expression of ISGs (Fig. 5B) resulting in even lower titers of R3616 (Fig.
288 5C-D) further confirming that increasing ISGF3 activity and subsequent ISG expression in MPNST cell
289 lines diminishes oHSV productivity.

290

291 ***NFκB signaling and basal ISG expression***

292 Recent reports have implicated the transcription factor NFκB, specifically the p65/RelA subunit,
293 in promoting low level expression of IFNβ (12) resulting in higher basal ISG expression. We hypothesized
294 that MPNST cell lines with constitutively active NFκB increased ISG expression in oHSV resistant cell
295 lines. To assess this, immunoblots were performed and showed relatively high p65 phosphorylation in
296 the resistant cell lines STS26T-luc and ST8814-luc (Fig. 6A) suggesting elevated NFκB activity. To identify
297 if basal ISRE transcriptional activity and ISG expression was related to NFκB transcriptional activity, we
298 stably expressed the inhibitor of κB (IκB), a native inhibitor of NFκB, with S32A/S36A mutations that
299 prevent proteasomal degradation and act as an NFκB “super repressor.” The results show that IκB-
300 super repressor (IκB-SR) expression decreases both NFκB and ISRE reporter activity (Fig. 6B). In contrast,
301 control transduction had no effect upon NFκB or ISRE activity. IκB-SR expression also led to decreased
302 expression of ISGs (Fig 6C). Together these results suggest that constitutive stimulation of the NFκB
303 pathway can be related to the basal stimulation of ISRE elements and ISG expression.

304 Previous reports have shown that the small-molecule inhibitor TPCA-1, a dual inhibitor of IκB
305 kinase (IKK) (a positive regulator of NFκB) and JAK1, can benefit the productivity of the oncolytic viruses

306 vesicular stomatitis virus (VSV) and encephalomyocarditis virus (EMCV) (13, 14). We hypothesized that
307 TPCA-1 could also benefit oHSV by downregulating expression of ISGs. Indeed, TPCA-1 inhibited the
308 activity of both NF κ B (Fig. 6D) and ISRE (Fig 6E) nano-luciferase reporters in a concentration dependent
309 manner and reduced ISG expression in the treated cells (Fig. 6F). To test the effect of TPCA-1 on oHSV
310 productivity, we used combinations of pre-treatment and co-treatment with TPCA-1 or DMSO, similar to
311 the ruxolitinib studies described above. As with ruxolitinib, co-treatment (DMSO + TPCA1) with TPCA-1
312 did not significantly improve $\Delta\gamma_134.5$ infection and spread, however, pre-treatment (TPCA1 + DMSO)
313 was sufficient to significantly improve the spread of both of the $\Delta\gamma_134.5$ recombinants C101 and M201 in
314 the ST8814-luc and STS26T-luc cell lines (Fig. 6 G-H). Interestingly, in contrast to the C101 and M201,
315 the $\Delta\gamma_134.5$ PKR evasion virus C154 benefited from either TPCA-1 co-treatment or from pre-treatment
316 alone (Fig. 6I). Pre-treatment followed by co-treatment (TPCA1 + TPCA1) further improved spread in the
317 majority of conditions tested.

318

319 **DISCUSSION:**

320 The oHSVs engineered within our lab are derived from HSV-1 mutants with dual deletions of the
321 $\gamma_134.5$ neurovirulence gene rendering them safe to administer in the CNS (15). While healthy,
322 untransformed cells restrict $\Delta\gamma_134.5$ oHSV replication, a partial explanation for the oncolytic selectivity
323 of $\Delta\gamma_134.5$ HSVs for cancerous tissue is that the malignantly transformed nature of these cells results in a
324 defective antiviral response which effectively complements the loss of the $\gamma_134.5$ gene product ICP34.5.
325 However, despite the wide array of cancer types that are susceptible to oHSVs, resistance is also
326 commonly observed. In an *in vivo* setting, resistance can be attributed to inefficient delivery methods,
327 low interstitial penetration, tumor heterogeneity, and activation of the innate and adaptive immune
328 response. However, resistance is common *in vitro* and therefore, to the extent that tumor cell lines

329 maintain the phenotype of the tumors from which they are derived, implies that the cancer cells
330 themselves can independently restrict or resist oHSV infection and replication through intrinsic
331 mechanisms.

332 Our previous work has suggested that $\Delta\gamma_134.5$ oHSVs are restricted by mechanisms related to
333 the antiviral response in MPNSTs (4). It has been established that hyperactive Ras signaling through
334 MEK/ERK imparts an oHSV permissive phenotype to cells by suppressing activation of PKR (6), yet there
335 exist conflicting reports about the role of Ras signaling and oHSV in the context of MPNSTs (16, 17). Our
336 observations of MEK/ERK phosphorylation (Supplemental Fig. 5) support the finding that elevated Ras
337 signaling exists in both permissive and resistant MPNST cell lines (16), suggesting that it is not predictive
338 of a permissive phenotype. Furthermore, our current findings show that PKR activation is not
339 exclusively predictive of oHSV resistance. Additionally, the productivity of C134, an oHSV capable of
340 evading the PKR response, is apparently diminished in STAT1 responsive cells despite the inhibition of
341 PKR. In contrast, wild-type HSV-1 did not appear to be affected by the STAT1 response. This would be
342 predicted by the observation that R3616/C101 (9, 18) and C134 (18) replication is substantially inhibited
343 by IFN β exposure, while wild-type HSV-1 replication is not (9, 18). This suggests that PKR-mediated
344 translational arrest, while a critical obstacle, is not the sole impediment to $\Delta\gamma_134.5$ oHSV replication in
345 MPNST cells.

346 While viral productivity in MPNST tumor lines was found to be associated with an oHSV-induced
347 STAT1 response, co-treatment with ruxolitinib to inhibit STAT1 phosphorylation did not substantially
348 benefit oHSV productivity in the MPNST lines. Instead, ruxolitinib pre-treatment alone was sufficient to
349 improve oHSV replication and spread, despite the fact that STAT1 could still be phosphorylated upon
350 removal of the inhibitor. We propose that the capacity of a cell to phosphorylate STAT1 in response to
351 oHSV infection is likely reflective of the basal upregulation of the PRRs which are also ISGs that initiate
352 the IFN/JAK/STAT1 signaling cascade (e.g. RIG-I and MDA5). This association may also indicate basal

353 upregulation of other ISGs that are directly antagonistic to oHSV replication. The downregulation of
354 basal ISRE activity and ISG expression following pre-treatment with ruxolitinib demonstrates that a
355 reduction of the levels of antiviral effectors is sufficient to improve oHSV infection and spread. The
356 presence of faint p-Y701 STAT1 staining in some of the uninfected oHSV resistant MPNST cell lines at
357 baseline (e.g. STS26T-luc and A382 in Fig 2A) further supports the presence of basal STAT1 activity.

358 While basal expression of ISGs has been previously documented in a number of tumor-derived
359 cell lines (19-23), this has not been previously shown for MPNSTs. However in the context of oHSV
360 infection, Mahller *et al.* showed through gene expression analysis that the “JAK/STAT pathway” and
361 “Tyrosine Phosphorylation of STAT protein” were significantly upregulated in response to G207 (a lacZ
362 expressing variant of R3616) in a panel of MPNST cell lines (24). Knockdown of suppressor of cytokine
363 signaling 1 (SOCS1), a negative regulator of STAT1, decreased the viral titers of the G207 by more than
364 10 fold in the highly permissive cell line S462.

365 Activation of the JAK/STAT pathway and ISG expression limits the efficacy of other oncolytic
366 viruses including vesicular stomatitis virus (19, 22, 23, 25), measles virus (20), Newcastle Disease virus
367 (21), respiratory syncytial virus (26), Semliki Forest virus (27), and adenovirus (28, 29). In several of
368 these studies inhibitors of JAK/STAT1 signaling enhanced viral productivity (19, 22, 23, 25, 27). With
369 respect to HSV, a head and neck squamous cell carcinoma, which became radio-resistant through the
370 upregulation of STAT1 and other ISGs, suppressed the replication of oHSV R3616 by 40 fold compared to
371 the original tumor (30). Haseley *et al.* found that overexpression of the extracellular matrix protein
372 cysteine rich 61 (CYR61) induced upregulation of type-1 IFNs and ISGs which suppressed oHSV
373 productivity in glioma cells (31). Although $\Delta\gamma_134.5$ HSVs are known to be sensitive to exogenous IFN (9,
374 18), presumably through the upregulation of ISGs by STAT1, these appear to be the only reports in the
375 literature between a cancer-associated STAT1/ISG signature and resistance to oHSV.

376 The STAT1/ISG expression signature has been detected in a number of patient tumor specimens
377 including glioblastoma (32, 33), squamous cell carcinoma (34), melanoma (35), leukemia (36), breast
378 (36-38), ovarian (36), and pancreatic (28) cancers suggesting that cancer-associated STAT1/ISG
379 expression is not an *in vitro* artifact. In these reports it is not possible to determine whether the STAT1
380 signature is a phenotype driven by the intrinsic nature of the tumor cells (autocrine activation) or
381 whether expression of this signature occurs in response to inflammatory stimuli from the surrounding
382 microenvironment (paracrine activation). Regardless of the mechanism, the expression of STAT1 or the
383 STAT1/ISG signature has been implicated in the resistance of cancer to radiation (30, 39, 40) and
384 chemotherapy (39, 41, 42). ISG expression in MPNSTs may offer a possible explanation for the lack of
385 efficacy by these treatment modalities in patients with MPNSTs (2, 3).

386 It has been shown that innate immune effectors including microglia, macrophages, and natural
387 killer cells actively restrict replication of oncolytic HSV *in vivo* (43, 44). Although the debate is ongoing,
388 oHSV treatment may be beneficial as an immunotherapy by activating cytotoxic T lymphocytes (CTLs)
389 which are associated with tumor clearance (45, 46). Paradoxical responses to oHSV have been reported
390 whereby tumor cells which were characterized as oHSV resistant *in vitro* were more susceptible to the
391 anti-tumor effect of oHSV *in vivo* (46). While we have demonstrated STAT1 activation to be detrimental
392 to oHSV productivity *in vitro*, it will be necessary to identify how tumor cells that are STAT1 responsive
393 interact with the peripheral immune elements in this context since the efficacy of certain
394 immunotherapies and the recruitment of CTLs is dependent upon the Type-I IFN response (47).

395 Finally, the driver for basal ISG expression in tumor cells remains incompletely understood.
396 Virally induced NFκB activation is known to promote IFNβ transcription (48), but the extent to which the
397 constitutive NFκB activation, which is commonly overserved in certain cancers, affects IFNβ expression is
398 unclear. There is some evidence that upstream signaling components of the NFκB pathway,
399 independent of NFκB-driven gene expression, may be involved in STAT1 cross-talk (49, 50). Further

400 work is needed to determine the prevalence of NFκB-related ISG expression and the complete
401 mechanism in MPNSTs.

402 In conclusion, our current research has identified a previously unexplored determinant of oHSV
403 productivity in MPNSTs. We believe the novel finding of basal ISG expression in MPNST cells may have
404 further implications for MPNST biology and their treatment with conventional anti-tumor therapies.

405

406 **ACKNOWLEDGEMENTS:** Special thanks to the UAB Comprehensive Flow Cytometry Core, UAB Heflin
407 Genetics Center for Genomic Science, and Dr. Bernard Roizman (University of Chicago, Chicago, IL) for
408 providing R3616.

- 410 1. Kolberg M, Høland M, Ågesen TH, Brekke HR, Liestøl K, Hall KS, et al. Survival meta-analyses for >
411 1800 malignant peripheral nerve sheath tumor patients with and without neurofibromatosis type 1.
412 *Neuro-oncology*. 2013;15:135-47.
- 413 2. Wong WW, Hirose T, Scheithauer BW, Schild SE, Gunderson LL. Malignant peripheral nerve
414 sheath tumor: analysis of treatment outcome. *Int J Radiat Oncol Biol Phys*. 1998;42:351-60.
- 415 3. Zehou O, Fabre E, Zelek L, Sbidian E, Ortonne N, Banu E, et al. Chemotherapy for the treatment
416 of malignant peripheral nerve sheath tumors in neurofibromatosis 1: a 10-year institutional review.
417 *Orphanet J Rare Dis*. 2013;8:127.
- 418 4. Jackson JD, McMorris AM, Roth JC, Coleman JM, Whitley RJ, Gillespie GY, et al. Assessment of
419 oncolytic HSV efficacy following increased entry-receptor expression in malignant peripheral nerve
420 sheath tumor cell lines. *Gene Ther*. 2014;21:984-90.
- 421 5. Farassati F, Yang A-D, Lee PW. Oncogenes in Ras signalling pathway dictate host-cell
422 permissiveness to herpes simplex virus 1. *Nat Cell Biol*. 2001;3:745-50.
- 423 6. Smith KD, Mezhir JJ, Bickenbach K, Veerapong J, Charron J, Posner MC, et al. Activated MEK
424 suppresses activation of PKR and enables efficient replication and in vivo oncolysis by $\Delta\gamma 134$. 5 mutants
425 of herpes simplex virus 1. *J Virol*. 2006;80:1110-20.
- 426 7. Kazmi SJ, Byer SJ, Eckert JM, Turk AN, Huijbregts RP, Brossier NM, et al. Transgenic mice
427 overexpressing neuregulin-1 model neurofibroma-malignant peripheral nerve sheath tumor progression
428 and implicate specific chromosomal copy number variations in tumorigenesis. *Am J Pathol*.
429 2013;182:646-67.
- 430 8. Parker JN, Gillespie GY, Love CE, Randall S, Whitley RJ, Markert JM. Engineered herpes simplex
431 virus expressing IL-12 in the treatment of experimental murine brain tumors. *Proc Natl Acad Sci USA*.
432 2000;97:2208-13.
- 433 9. Cheng G, Brett M-E, He B. Val 193 and Phe 195 of the $\gamma 134.5$ protein of herpes simplex virus 1
434 are required for viral resistance to interferon- α/β . *Virology*. 2001;290:115-20.
- 435 10. Shah A, Parker J, Gillespie G, Lakeman F, Meleth S, Markert J, et al. Enhanced antiglioma activity
436 of chimeric HCMV/HSV-1 oncolytic viruses. *Gene Ther*. 2007;14:1045-54.
- 437 11. Cheon H, Holvey-Bates EG, Schoggins JW, Forster S, Hertzog P, Imanaka N, et al. IFNbeta-
438 dependent increases in STAT1, STAT2, and IRF9 mediate resistance to viruses and DNA damage. *EMBO J*.
439 2013;32:2751-63.
- 440 12. Basagoudanavar SH, Thapa RJ, Nogusa S, Wang J, Beg AA, Balachandran S. Distinct roles for the
441 NF-kappa B RelA subunit during antiviral innate immune responses. *J Virol*. 2011;85:2599-610.
- 442 13. Cataldi M, Shah NR, Felt SA, Grdzlishvili VZ. Breaking resistance of pancreatic cancer cells to an
443 attenuated vesicular stomatitis virus through a novel activity of IKK inhibitor TPCA-1. *Virology*.
444 2015;485:340-54.
- 445 14. Du Z, Whitt MA, Baumann J, Garner JM, Morton CL, Davidoff AM, et al. Inhibition of type I
446 interferon-mediated antiviral action in human glioma cells by the IKK inhibitors BMS-345541 and TPCA-
447 1. *J Interferon Cytokine Res*. 2012;32:368-77.
- 448 15. Chou J, Kern ER, Whitley RJ, Roizman B. Mapping of herpes simplex virus-1 neurovirulence to
449 gamma 134.5, a gene nonessential for growth in culture. *Science*. 1990;250:1262-6.
- 450 16. Mahller YY, Rangwala F, Ratner N, Cripe TP. Malignant peripheral nerve sheath tumors with high
451 and low Ras-GTP are permissive for oncolytic herpes simplex virus mutants. *Pediatr Blood Cancer*.
452 2006;46:745-54.

- 453 17. Farassati F, Pan W, Yamoutpour F, Henke S, Piedra M, Frahm S, et al. Ras signaling influences
454 permissiveness of malignant peripheral nerve sheath tumor cells to oncolytic herpes. *Am J Pathol.*
455 2008;173:1861-72.
- 456 18. Cassady KA, Saunders U, Shimamura M. $\Delta\gamma 134$. 5 Herpes Simplex Viruses Encoding Human
457 Cytomegalovirus IRS1 or TRS1 Induce Interferon Regulatory Factor 3 Phosphorylation and an Interferon-
458 Stimulated Gene Response. *J Virol.* 2012;86:610-4.
- 459 19. Paglino JC, van den Pol AN. Vesicular stomatitis virus has extensive oncolytic activity against
460 human sarcomas: rare resistance is overcome by blocking interferon pathways. *J Virol.* 2011;85:9346-58.
- 461 20. Berchtold S, Lampe J, Weiland T, Smirnow I, Schleicher S, Handgretinger R, et al. Innate immune
462 defense defines susceptibility of sarcoma cells to measles vaccine virus-based oncolysis. *J Virol.*
463 2013;87:3484-501.
- 464 21. Wilden H, Fournier P, Zawatzky R, Schirmmacher V. Expression of RIG-I, IRF3, IFN- β and IRF7
465 determines resistance or susceptibility of cells to infection by Newcastle Disease Virus. *Int J Oncol.*
466 2009;34:971-82.
- 467 22. Escobar-Zarate D, Liu Y, Suksanpaisan L, Russell S, Peng K. Overcoming cancer cell resistance to
468 VSV oncolysis with JAK1/2 inhibitors. *Cancer Gene Ther.* 2013;20:582-9.
- 469 23. Moerdyk-Schauwecker M, Shah NR, Murphy AM, Hastie E, Mukherjee P, Grdzlishvili VZ.
470 Resistance of pancreatic cancer cells to oncolytic vesicular stomatitis virus: role of type I interferon
471 signaling. *Virology.* 2013;436:221-34.
- 472 24. Mahller Y, Sakthivel B, Baird W, Aronow B, Hsu Y, Cripe T, et al. Molecular analysis of human
473 cancer cells infected by an oncolytic HSV-1 reveals multiple upregulated cellular genes and a role for
474 SOCS1 in virus replication. *Cancer Gene Ther.* 2008;15:733-41.
- 475 25. Liu Y-P, Suksanpaisan L, Steele MB, Russell SJ, Peng K-W. Induction of antiviral genes by the
476 tumor microenvironment confers resistance to virotherapy. *Sci Rep.* 2013;3.
- 477 26. Echchgadda I, Chang T-H, Sabbah A, Bakri I, Ikeno Y, Hubbard GB, et al. Oncolytic targeting of
478 androgen-sensitive prostate tumor by the respiratory syncytial virus (RSV): consequences of deficient
479 interferon-dependent antiviral defense. *BMC cancer.* 2011;11:43.
- 480 27. Ruotsalainen J, Kaikkonen M, Niittykoski M, Martikainen M, Lemay C, Cox J, et al. Clonal
481 variation in interferon response determines the outcome of oncolytic virotherapy in mouse CT26 colon
482 carcinoma model. *Gene Ther.* 2014.
- 483 28. Monsurrò V, Beghelli S, Wang R, Barbi S, Coin S, Di Pasquale G, et al. Antiviral state segregates
484 two molecular phenotypes of pancreatic adenocarcinoma: potential relevance for adenoviral gene
485 therapy. *J Transl Med.* 2010;8:10.
- 486 29. Liikanen I, Monsurrò V, Ahtiainen L, Raki M, Hakkarainen T, Diaconu I, et al. Induction of
487 interferon pathways mediates in vivo resistance to oncolytic adenovirus. *Mol Ther.* 2011;19:1858-66.
- 488 30. Khodarev NN, Beckett M, Labay E, Darga T, Roizman B, Weichselbaum RR. STAT1 is
489 overexpressed in tumors selected for radioresistance and confers protection from radiation in
490 transduced sensitive cells. *Proc Natl Acad Sci U S A.* 2004;101:1714-9.
- 491 31. Haseley A, Boone S, Wojton J, Yu L, Yoo JY, Yu J, et al. Extracellular Matrix Protein CCN1 Limits
492 Oncolytic Efficacy in Glioma. *Cancer Res.* 2012;72:1353-62.
- 493 32. Duarte CW, Willey CD, Zhi D, Cui X, Harris JJ, Vaughan LK, et al. Expression signature of
494 IFN/STAT1 signaling genes predicts poor survival outcome in glioblastoma multiforme in a subtype-
495 specific manner. *PLoS One.* 2012;7:e29653.
- 496 33. Cosset É, Petty TJ, Dutoit V, Cordey S, Padioleau I, Otten-Hernandez P, et al. Comprehensive
497 metagenomic analysis of glioblastoma reveals absence of known virus despite antiviral-like type I
498 interferon gene response. *Int J Cancer.* 2014;135:1381-9.
- 499 34. Laimer K, Spizzo G, Obrist P, Gastl G, Brunhuber T, Schäfer G, et al. STAT1 activation in squamous
500 cell cancer of the oral cavity. *Cancer.* 2007;110:326-33.

- 501 35. Schultz J, Koczan D, Schmitz U, Ibrahim SM, Pilch D, Landsberg J, et al. Tumor-promoting role of
502 signal transducer and activator of transcription (Stat) 1 in late-stage melanoma growth. *Clin Exp*
503 *Metastasis*. 2010;27:133-40.
- 504 36. Einav U, Tabach Y, Getz G, Yitzhaky A, Ozbek U, Amariglio N, et al. Gene expression analysis
505 reveals a strong signature of an interferon-induced pathway in childhood lymphoblastic leukemia as well
506 as in breast and ovarian cancer. *Oncogene*. 2005;24:6367-75.
- 507 37. Perou CM, Sørlie T, Eisen MB, van de Rijn M, Jeffrey SS, Rees CA, et al. Molecular portraits of
508 human breast tumours. *Nature*. 2000;406:747-52.
- 509 38. Perou CM, Jeffrey SS, Van De Rijn M, Rees CA, Eisen MB, Ross DT, et al. Distinctive gene
510 expression patterns in human mammary epithelial cells and breast cancers. *Proc Natl Acad Sci USA*.
511 1999;96:9212-7.
- 512 39. Fryknäs M, Dhar S, Öberg F, Rickardson L, Rydåker M, Göransson H, et al. STAT1 signaling is
513 associated with acquired crossresistance to doxorubicin and radiation in myeloma cell lines. *Int J Cancer*.
514 2007;120:189-95.
- 515 40. Tsai M-H, Cook JA, Chandramouli GV, DeGraff W, Yan H, Zhao S, et al. Gene expression profiling
516 of breast, prostate, and glioma cells following single versus fractionated doses of radiation. *Cancer Res*.
517 2007;67:3845-52.
- 518 41. Patterson S, Wei S, Chen X, Sallman D, Gilvary D, Zhong B, et al. Novel role of Stat1 in the
519 development of docetaxel resistance in prostate tumor cells. *Oncogene*. 2006;25:6113-22.
- 520 42. Luszczek W, Cheriya V, Mekhail TM, Borden EC. Combinations of DNA methyltransferase and
521 histone deacetylase inhibitors induce DNA damage in small cell lung cancer cells: correlation of
522 resistance with IFN-stimulated gene expression. *Mol Cancer Ther*. 2010;9:2309-21.
- 523 43. Alvarez-Breckenridge CA, Yu J, Price R, Wojton J, Pradarelli J, Mao H, et al. NK cells impede
524 glioblastoma virotherapy through NKp30 and NKp46 natural cytotoxicity receptors. *Nat Med*.
525 2012;18:1827-34.
- 526 44. Fulci G, Dmitrieva N, Gianni D, Fontana EJ, Pan X, Lu Y, et al. Depletion of peripheral
527 macrophages and brain microglia increases brain tumor titers of oncolytic viruses. *Cancer Res*.
528 2007;67:9398-406.
- 529 45. Workenhe ST, Simmons G, Pol JG, Lichty BD, Halford WP, Mossman KL. Immunogenic HSV-
530 mediated oncolysis shapes the antitumor immune response and contributes to therapeutic efficacy. *Mol*
531 *Ther*. 2014;22:123-31.
- 532 46. Leddon JL, Chen C-Y, Currier MA, Wang P-Y, Jung FA, Denton NL, et al. Oncolytic HSV virotherapy
533 in murine sarcomas differentially triggers an antitumor T-cell response in the absence of virus
534 permissivity. *Mol Ther Oncolytics*. 2015;1.
- 535 47. Corrales L, Gajewski TF. Molecular Pathways: Targeting the Stimulator of Interferon Genes
536 (STING) in the Immunotherapy of Cancer. *Clin Cancer Res*. 2015;clincanres. 1362.2015.
- 537 48. Wang J, Basagoudanavar SH, Wang X, Hopewell E, Albrecht R, García-Sastre A, et al. NF- κ B RelA
538 subunit is crucial for early IFN- β expression and resistance to RNA virus replication. *J Immunol*.
539 2010;185:1720-9.
- 540 49. Ng S-L, Chua MA, McWhirter SM, García-Sastre A, Maniatis T. Multiple functions of the IKK-
541 related kinase IKK ϵ in interferon-mediated antiviral immunity. *Science*. 2007;315:1274-8.
- 542 50. Nguyen H, Chatterjee-Kishore M, Jiang Z, Qing Y, Ramana CV, Bayes J, et al. IRAK-dependent
543 phosphorylation of Stat1 on serine 727 in response to interleukin-1 and effects on gene expression. *J*
544 *Interferon Cytokine Res*. 2003;23:183-92.

546 **FIGURE LEGENDS:**

547 **Figure 1: oHSV productivity and activation of the PKR response.** Human (A) and mouse (B) derived
548 MPNST cell lines were infected with R3616 (MOI=1, 24 hpi) and viral recovery measured using standard
549 titration methods. Data were collected in triplicate and the titers are reported as the average total
550 plaque forming units (PFU) with standard deviation. PKR and eIF2 α in human cell lines (C) or eIF2 α
551 alone in mouse cell lines (D) was assessed by western blot for phosphorylation in response to mock or
552 R3616 (MOI=1, 12 hpi) infection.

553 **Figure 2: STAT1 response to oHSV infection and association with viral productivity.** STAT1
554 phosphorylation in response to R3616 infection (MOI=1, 6hpi) was assessed by western blot in human
555 (A) and mouse (B) cell lines. Cell lines considered STAT1 responsive are marked with an asterisk. The
556 mean viral titers (from Fig. 1 A-B) from each cell line were sorted into STAT1 unresponsive and
557 responsive groups and tested for statistical significance using the Mann-Whitney U test with the median
558 and interquartile range plotted (C). Cell lines were assessed in a multistep infection assay (MOI=0.1, 48
559 hpi) with C101 for the percentage of cells positive for GFP (D) and the infected cell count as a
560 percentage of the mock infected cell count (E). Data were collected in triplicate and the mean reported.
561 Cell lines were sorted based on their STAT1 response and tested for statistical significance using the
562 Mann-Whitney U test with the medians and interquartile range plotted.

563 **Figure 3: PKR activation with C134 and association of productivity with STAT1 response.** PKR and
564 eIF2 α in human cell lines (A) was assessed by western blot for phosphorylation in response to mock or
565 C134 (MOI=1, 12 hpi) infection. Cell lines were assessed in a multistep infection assay (MOI=0.1, 48 hpi)
566 with C134 and M2001 for the percentage of cells positive for GFP (B and D) and the infected cell count
567 as a percentage of the mock infected cell count (C and E). Data were collected in triplicate and the

568 mean reported. Cell lines were sorted based on their STAT1 response and tested for statistical
569 significance using the Mann-Whitney U test with the medians and interquartile range plotted.

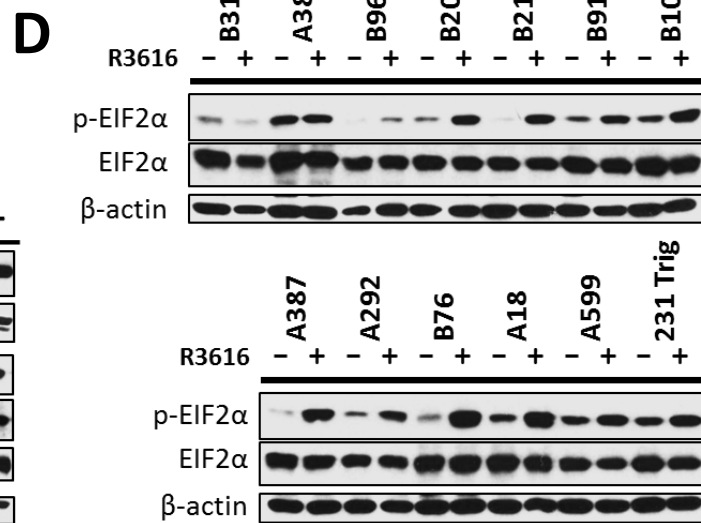
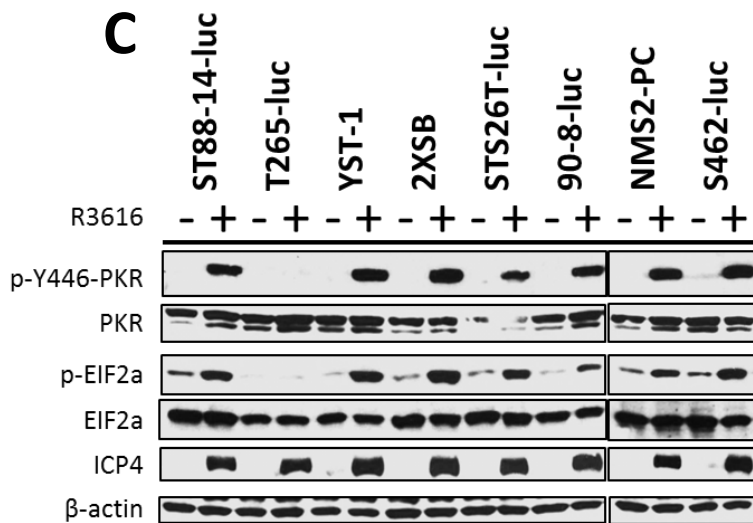
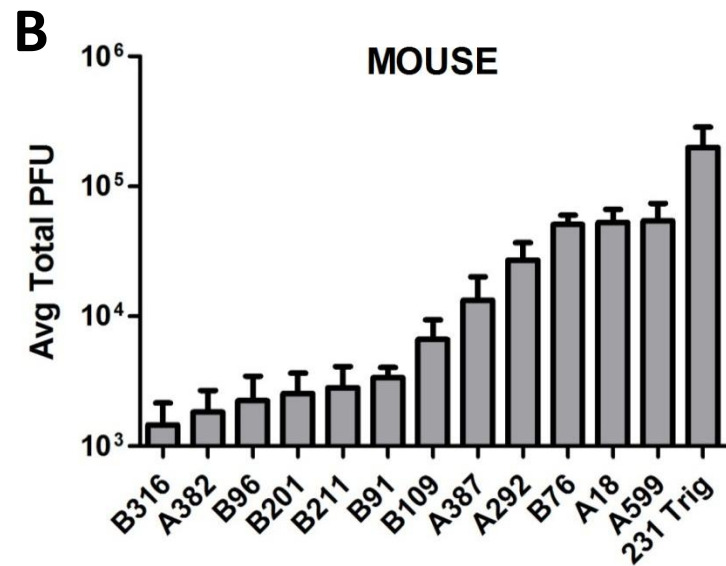
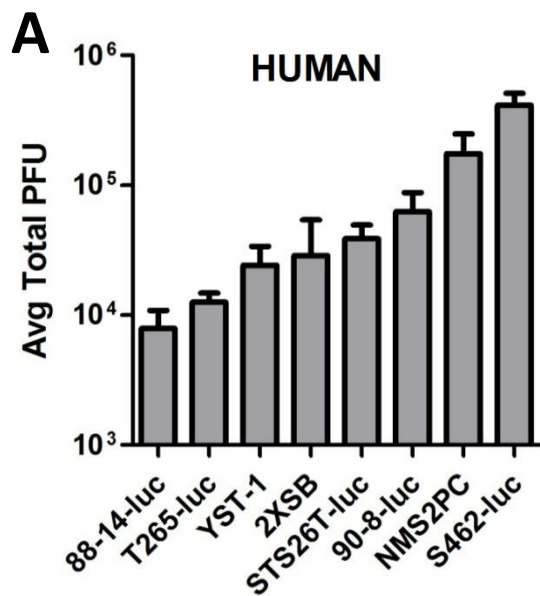
570 **Figure 4: Effect of JAK inhibitor ruxolitinib on viral productivity, basal ISRE activity, and ISG expression.**

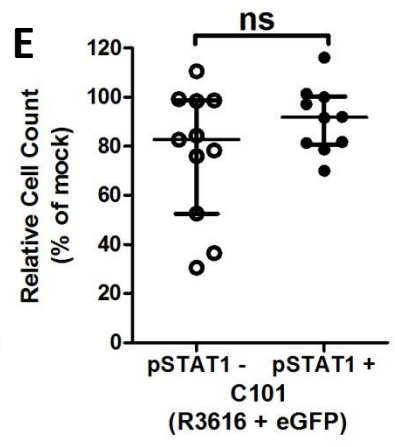
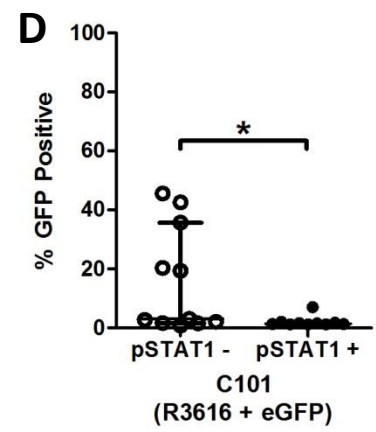
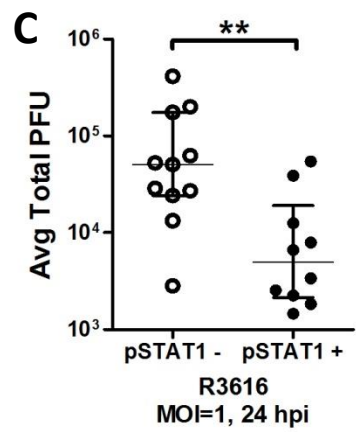
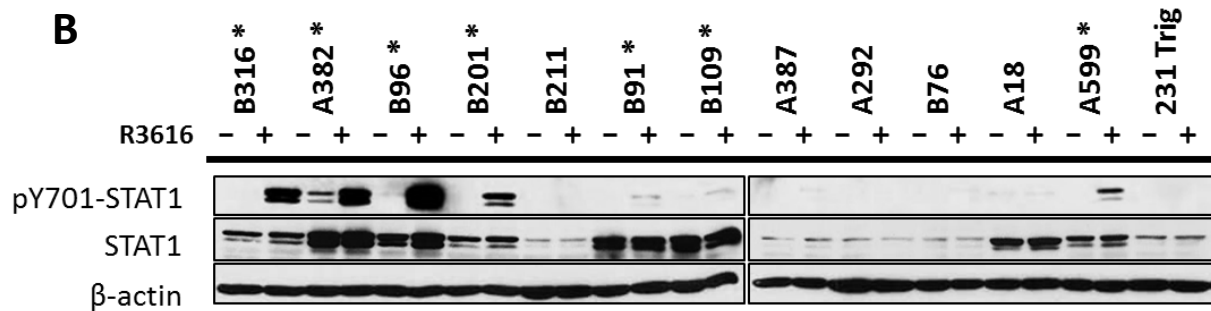
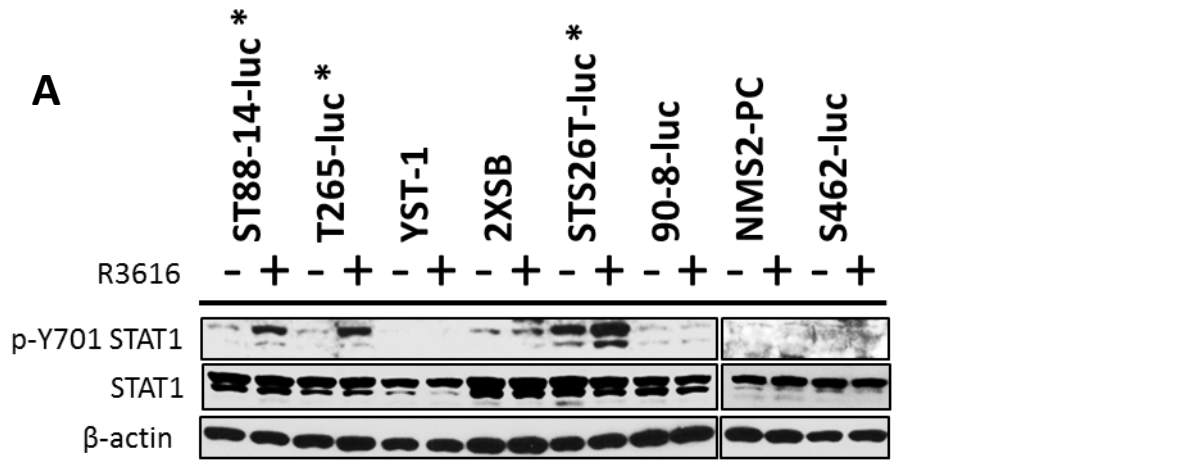
571 Cell lines were pretreated with either DMSO or 250 nM ruxolitinib (Rux) for 48 hrs prior to infection.
572 One hour after oHSV infection, each group was further co-treated with DMSO or ruxolitinib (250 nM).
573 GFP expressing virus C101 was used to assess effects on oHSV spread by multistep infection (MOI=0.1,
574 48 hpi) (A-B, E-F). Multistep (MOI=0.1, 48 hpi) (C and G) and single-step (MOI=1, 25 hpi) (D and H)
575 infection with R3616 was used to assess viral recovery. Data for spread and recovery assays were
576 collected in triplicate and the standard deviation reported. For viral recovery, the log-fold change is
577 reported under the significance indicator. Phosphorylation of STAT1 was observed by western blot in
578 ST88-14-luc treated with combinations of DMSO and ruxolitinib (I). ISRE activity was measured by dual
579 luciferase assays after 24 hr treatment with various concentrations of ruxolitinib (J). ISRE nanoluciferase
580 activity was normalized to that of firefly luciferase and final values reported as the percentage of DMSO
581 treated cells. Expression of ISGs MDA5, RIG-I, MX1, IFIT3, and OAS1 in cell lines treated with DMSO or
582 ruxolitinib (250 nM) for 48 hrs was observed by western blot (K).

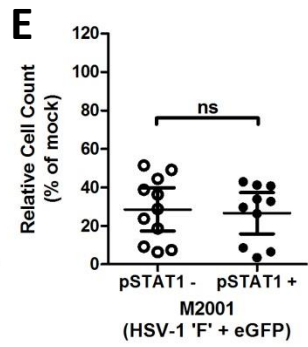
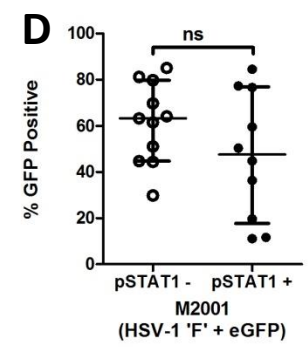
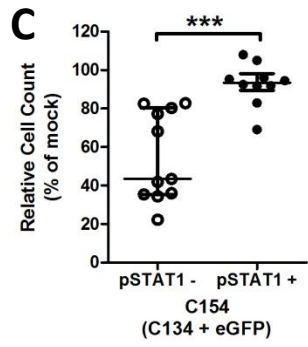
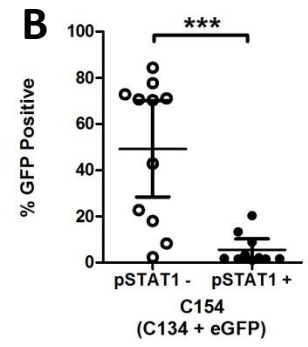
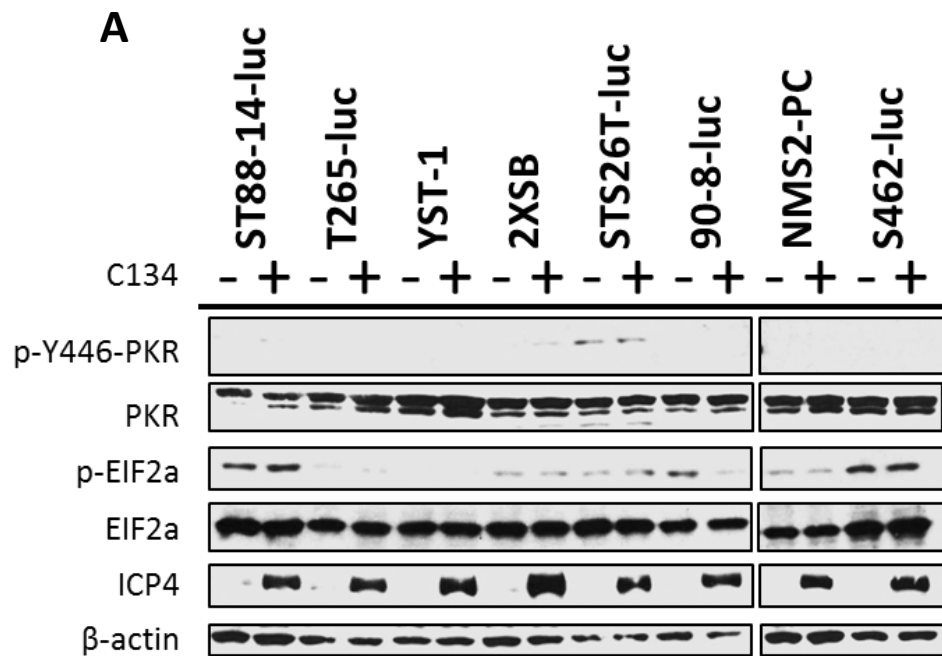
583 **Figure 5: Basal expression of ISGs in MPNST cell lines and effect of increased ISG expression on viral**

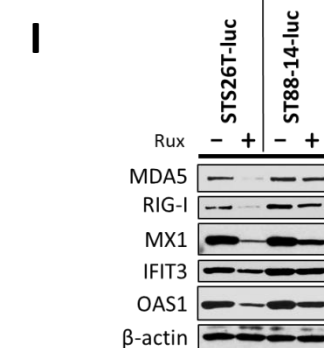
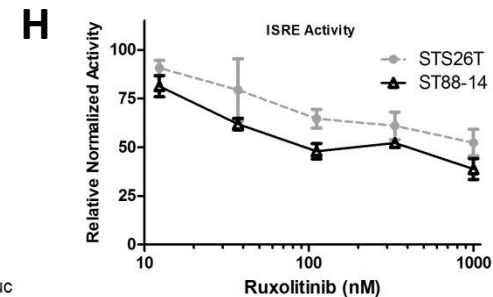
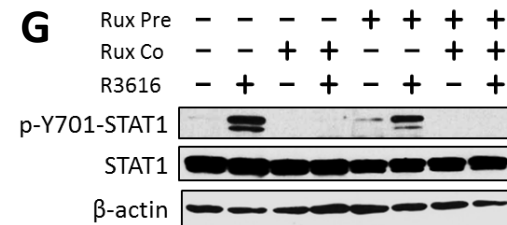
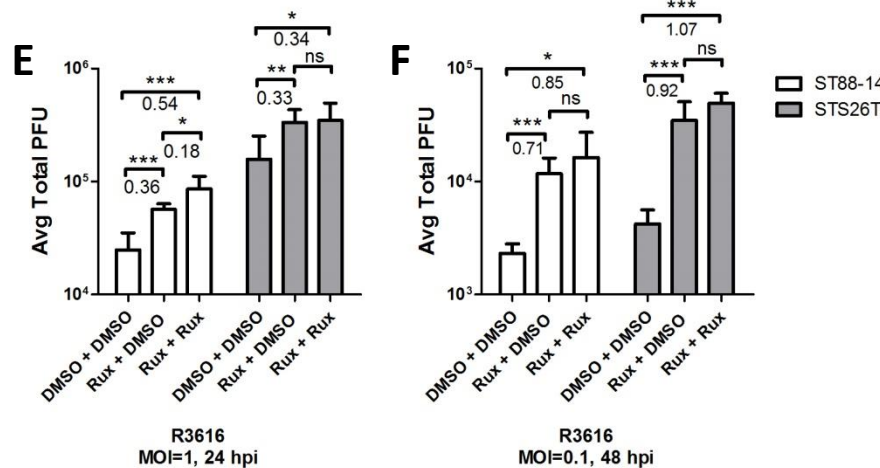
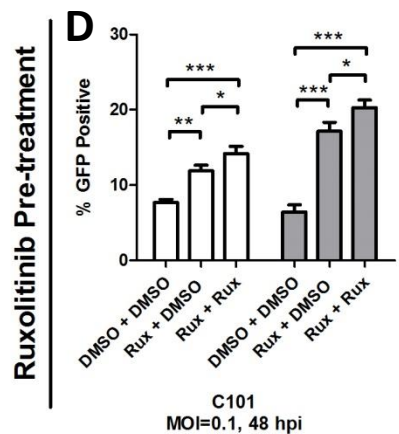
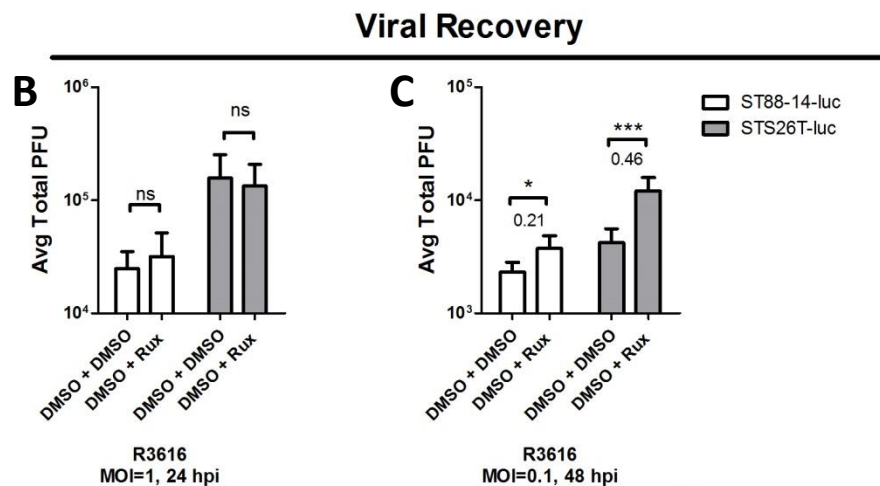
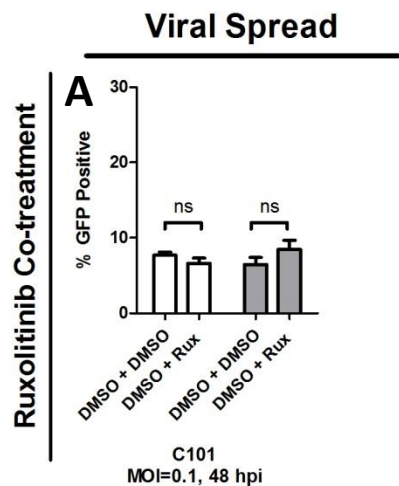
584 **productivity.** Basal expression of ISGs in all human MPNST cell lines was assessed by western blot (A).
585 Cell lines stably transduced with a control lentivirus (DsRed2) or lentiviruses encoding the transcription
586 factors STAT1-FLAG, STAT2 and IRF9 which compose the ISGF3 complex were assessed for ISG
587 expression by western blot (B). Multi-step (MOI=0.1, 48 hpi) (C) and single-step (MOI=1, 24 hpi) (D) viral
588 recovery assays with R3616 were conducted in control and ISGF3 transduced cell lines. Data were
589 collected in triplicate and the standard deviation reported. The log-fold change is reported under the
590 significance indicator.

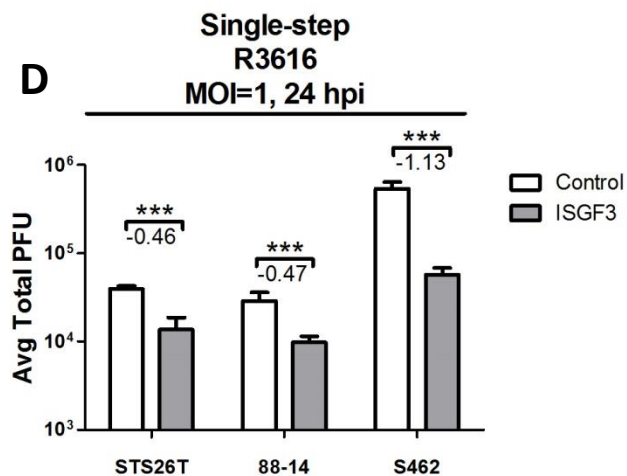
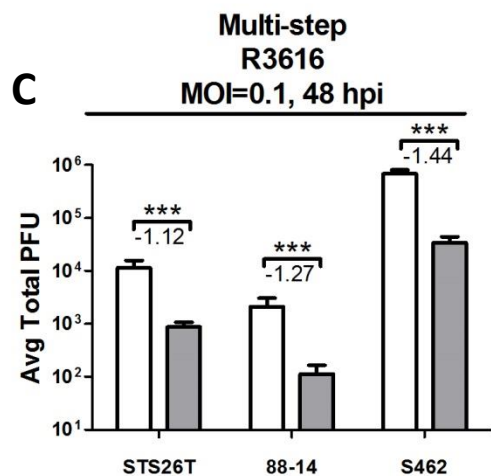
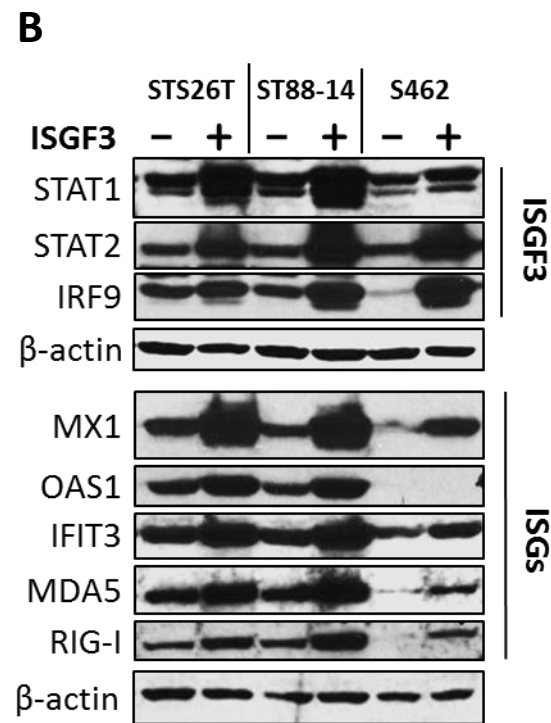
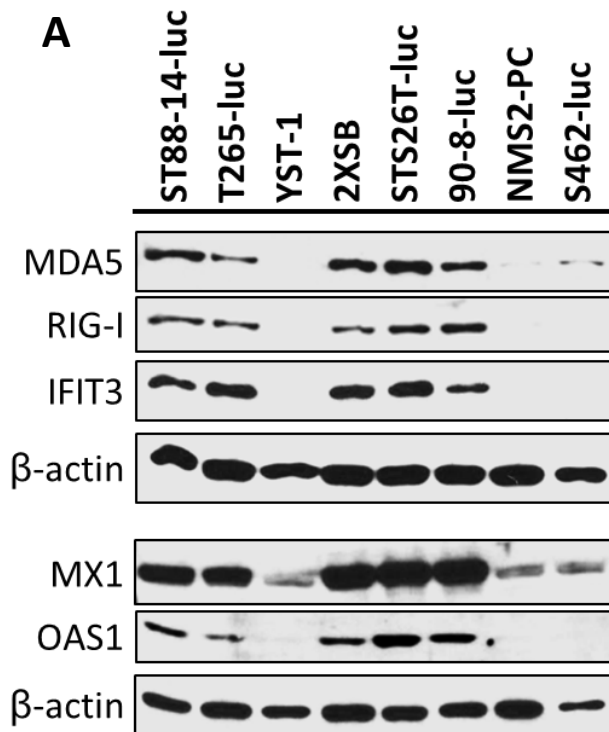
591 **Figure 6: Relationship of NFκB to basal ISG expression.** Phosphorylation of P65/RelA was assessed in
592 human cell lines by western blot (A). The cell line ST88-14-luc expressing either NFκB or ISRE luciferase
593 reporters were stably transduced with the inhibitor of κB super repressor (IκB-SR) and nano-luciferase
594 (Nluc) activity measured (B). Firefly luciferase (Fluc) normalized data were collected in quadruplicate
595 and standard deviation reported. IκB-SR transduced ST88-14-luc was probed for IκB and ISG expression
596 by western blot (C). NFκB (D) and ISRE (E) luciferase activity was measured in response to the small
597 molecule inhibitor TPCA-1. Firefly luciferase normalized data were collected in triplicate and the
598 percentage of activity relative to DMSO treatment was reported with standard deviation. Expression of
599 ISGs was probed in TPCA-1 treated cell lines (250 nM, 96 hr) by western blot (F). Cell lines were
600 pretreated with either DMSO or 250 nM TPCA-1 (Rux) for 96 hrs prior to infection. One hour after oHSV
601 infection, each group was further co-treated with DMSO or TPCA-1 (250 nM). GFP expressing viruses
602 C101 (G), M201 (H), and C134 (I) were used to assess effects on oHSV spread by multistep infection
603 (MOI=0.1, 48 hpi). Data were collected in triplicate and the standard deviation reported.

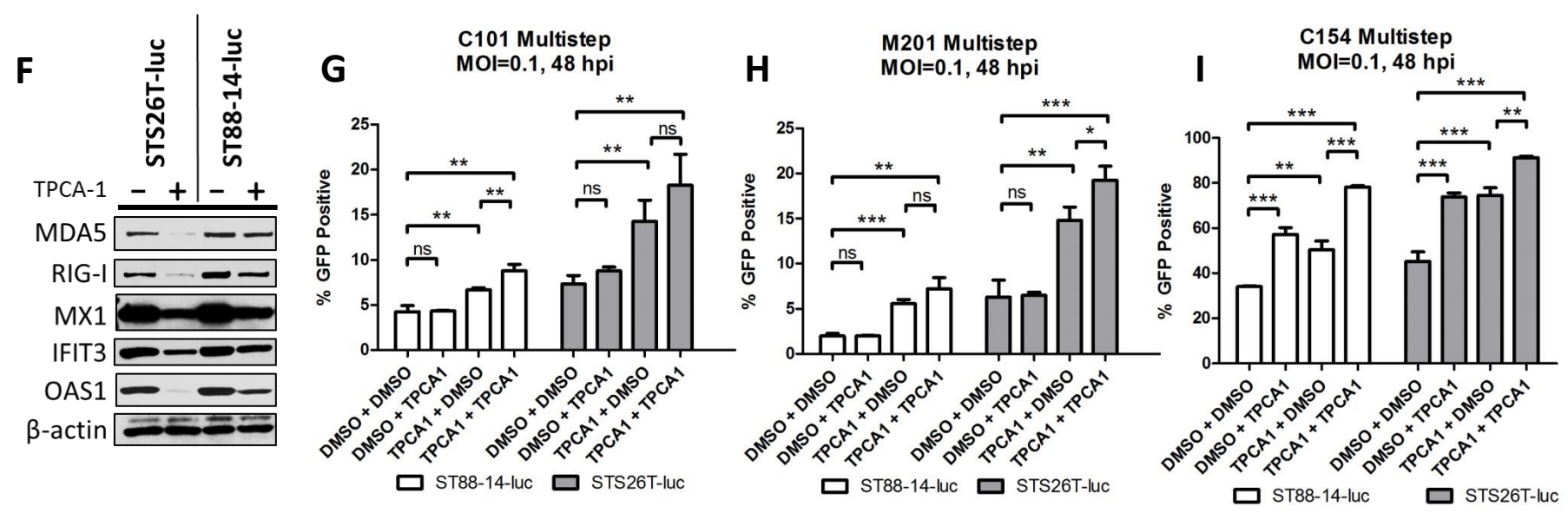
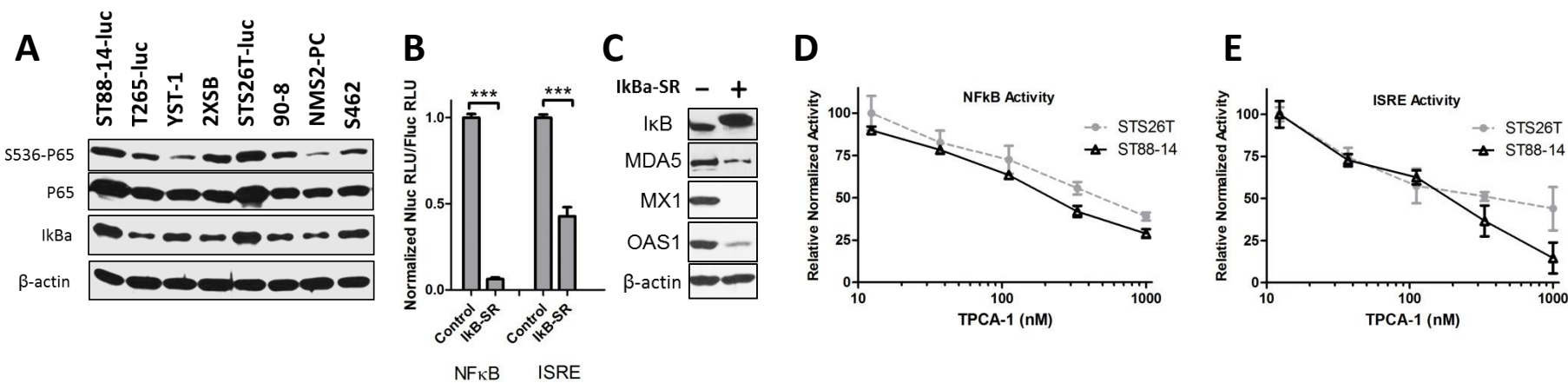












SHORT COMMUNICATION

Assessment of oncolytic HSV efficacy following increased entry-receptor expression in malignant peripheral nerve sheath tumor cell lines

JD Jackson¹, AM Morris¹, JC Roth², JM Coleman¹, RJ Whitley², GY Gillespie^{1,3}, SL Carroll^{4,5}, JM Markert^{1,2,6} and KA Cassady^{2,6}

Limited expression and distribution of nectin-1, the major herpes simplex virus (HSV) type-1 entry-receptor, within tumors has been proposed as an impediment to oncolytic HSV (oHSV) therapy. To determine whether resistance to oHSVs in malignant peripheral nerve sheath tumors (MPNSTs) was explained by this hypothesis, nectin-1 expression and oHSV viral yields were assessed in a panel of MPNST cell lines using $\gamma_134.5$ -attenuated ($\Delta\gamma_134.5$) oHSVs and a $\gamma_134.5$ wild-type (wt) virus for comparison. Although there was a correlation between nectin-1 levels and viral yields with the wt virus ($R=0.75$, $P=0.03$), there was no correlation for $\Delta\gamma_134.5$ viruses (G207, R7020 or C101) and a modest trend for the second-generation oHSV C134 ($R=0.62$, $P=0.10$). Nectin-1 overexpression in resistant MPNST cell lines did not improve $\Delta\gamma_134.5$ oHSV output. While multistep replication assays showed that nectin-1 overexpression improved $\Delta\gamma_134.5$ oHSV cell-to-cell spread, it did not confer a sensitive phenotype to resistant cells. Finally, oHSV yields were not improved with increased nectin-1 *in vivo*. We conclude that nectin-1 expression is not the primary obstacle of productive infection for $\Delta\gamma_134.5$ oHSVs in MPNST cell lines. In contrast, viruses that are competent in their ability to counter the antiviral response may derive benefit with higher nectin-1 expression.

Gene Therapy advance online publication, 14 August 2014; doi:10.1038/gt.2014.72

INTRODUCTION

Malignant peripheral nerve sheath tumors (MPNSTs) are a highly aggressive cancer of the peripheral nervous tissue believed to originate within the Schwann cell lineage¹ and are most commonly associated with the genetic condition neurofibromatosis type-1. Treatment options for MPNSTs beyond surgery are inadequate, resulting in a median survival of only 26 months.² Oncolytic virotherapy by attenuated herpes simplex type-1 viruses (oHSVs) has been proposed as an alternative to chemotherapy and radiotherapy for the treatment of MPNSTs.^{3–7} HSVs with $\gamma_134.5$ neurovirulence gene deletions are safe in humans and have been shown to selectively replicate in tumor cells.⁸ These attenuated $\Delta\gamma_134.5$ oHSVs have a clinically verified safety profile in patients with malignant glioma and have been associated with measurable antitumor responses.^{9–13} However, these patient responses have varied widely, likely due to tumor susceptibility. Therefore, we have sought to further elucidate the mechanisms of oHSV resistance.

In our initial investigation into potential oHSV resistance mechanisms within MPNSTs, we have tested the hypothesis that oHSV resistance is attributable to the insufficient expression of HSV-1 entry receptors by tumor cells.^{14–18} Four viral glycoproteins (gD, gB and gH/gL) and a cellular glycoprotein D (gD)-interacting receptor have been demonstrated as necessary and sufficient to trigger cellular entry.^{19–23} Of the three cellular HSV-1 gD-interacting

receptors, nectin-1, a cellular adhesion protein expressed in epithelial cells,²⁴ fibroblasts and neurons,²⁵ has been proposed as the major HSV-1 entry receptor.²⁶ Herpes virus entry mediator (HVEM)²⁷ and 3-O-sulfated heparan sulfate (3-OS-HS)²⁸ have also been demonstrated to facilitate HSV-1 entry. Additional cell-surface molecules that interact with other viral glycoproteins have been identified, though the broad necessity of these in permitting HSV-1 infection and spread remains to be determined and the lack of these molecules has not yet been implicated in limiting the oncolytic capacity of oHSV.

Here, we have investigated the hypothesis that HSV entry-receptor expression is a determinant of oHSV efficacy in MPNST cells and have identified whether an increase in entry-receptor expression improves the viral yield and spread of oHSVs. The influence of entry-receptor expression was examined in the context of an array of viral genotypes, including a representative wild-type (wt) $\gamma_134.5$ HSV-1, a fully attenuated $\Delta\gamma_134.5$ oHSV, and an attenuated second-generation oHSV capable of host antiviral evasion. We report the following conclusions: (1) correlation of nectin-1 expression with viral production capacity appears more important in viruses which are genetically competent to counter the intrinsic antiviral response, (2) increased expression of entry-receptor molecules modestly improves cell-cell spread of $\Delta\gamma_134.5$ oHSVs, but yields little benefit to viral production and (3) increases in entry-receptor expression do not render resistant MPNST cell lines permissive to $\Delta\gamma_134.5$ oHSV infection.

¹Department of Neurosurgery, University of Alabama at Birmingham, Birmingham, AL 35233, USA; ²Department of Pediatrics, University of Alabama at Birmingham, Birmingham, AL 35233, USA; ³Department of Microbiology, University of Alabama at Birmingham, Birmingham, AL 35233, USA; ⁴Department of Pathology, University of Alabama at Birmingham, Birmingham, AL 35233, USA; ⁵Department of Pathology and Laboratory Medicine, Medical University of South Carolina, Charleston, SC, USA and ⁶Department of Cell, Developmental and Integrative Biology, University of Alabama at Birmingham, Birmingham, AL 35233, USA. Correspondence: Dr J Markert, 510 20th Street South, FOT 1060, Birmingham, AL 35294, USA.

E-mail: markert@uab.edu

Received 17 March 2014; revised 30 May 2014; accepted 25 June 2014

RESULTS AND DISCUSSION

MPNST cell lines have been previously identified as susceptible to oHSV infection and cytotoxicity.³ To examine the correlation between viral production capacity and entry-receptor expression, human MPNST cell lines STS-26T, T265-2c, NMS2-PC, S462, YST-1, 90-8, ST88-14 and 2XSB, or their luciferase-expressing derivatives ('-luc'), were first infected at a multiplicity of infection (MOI) of 10 (single-step replication assay) with a panel of genetically modified HSV-1 and cellular lysates collected 24 h post infection (h.p.i.) for viral recovery analysis (Supplementary Figure 1). The viral yields from this assay are presented in correlation with nectin-1 expression in Figures 1a–e.

HSV-1 entry receptors have not been previously identified in MPNSTs or cells of the Schwann cell lineage. Upon examination of nectin-1 and HVEM expression in our panel of MPNST cell lines, we found detectable levels of nectin-1 in all of the lines, with population-wide (>95%) expression of nectin-1 in five of eight cell lines (Figure 1f). Population-wide expression of HVEM in MPNST cell lines was observed in only one of eight lines (Supplementary Figure 2D); therefore, HVEM was excluded as a candidate for the major entry receptor in MPNSTs. The other established entry receptor 3-OS-HS was not examined in this study due to the lack of a commercially available antibody. However, HSV-1 infection of the resistant cell lines selected for further study (STS26T-luc and T265-luc) was found to be dependent on nectin-1 expression alone by nectin-1 neutralization assays (Supplementary Figure 2).

Pearson's correlation coefficients were calculated between viral recovery data and nectin-1 expression levels. Possible positive associations were found for the wt M2001 ($R = 0.75$; $P = 0.03$) and attenuated second-generation oHSV C134 ($R = 0.62$, $P = 0.10$) viruses (Figures 1a and b). While prior studies involving thyroid cancer¹⁴ and head and neck squamous cell carcinoma¹⁵ cell lines demonstrated correlation between viral yields of oHSV NV1023 (a derivative of R7020) and nectin-1 expression, no such associations were observed for G207, C101 or R7020 oHSVs suggesting that the specific viral genotype influences the outcome of infection.

The lack of a clear association of nectin-1 expression with attenuated $\Delta\gamma_{134.5}$ oHSV viral yields led us to further evaluate the functional impact of increased entry-receptor expression on oHSV sensitivity. To assess this, the oHSV-resistant cell lines, T265-luc and STS26T-luc were transduced with full-length human nectin-1 (nectin-1a) using lentivirus LV2114CK. An mCherry expressing lentivirus was used as a control and confirmed that transduction alone did not alter viral production (data not shown).

If low entry-receptor expression diminishes the ability of oHSV to establish an initial infection, we would predict that increased nectin-1 expression would increase the initial opportunity for entry, resulting in replication within a greater number of cells and an increase in the total production of virus. To determine the impact of increased nectin-1 expression on viral yields in MPNSTs, single-step (MOI=10, 24 h.p.i.) and multistep (MOI=0.1, 24, 48, 72 h.p.i.; Supplementary Figure 3) viral recovery assays were performed using the parent and nectin-1 transduced cell lines. Because the

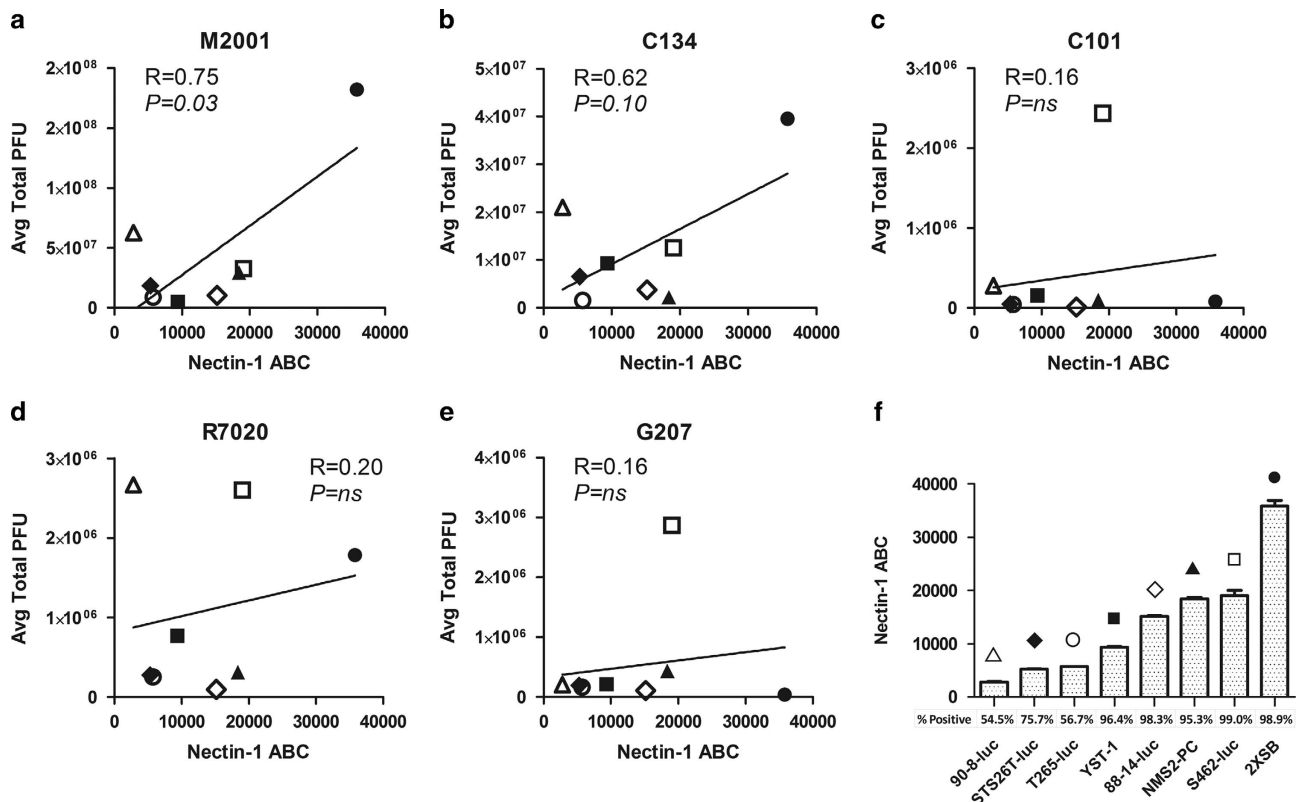


Figure 1. Correlation of nectin-1 expression with viral titers. Pearson's correlation coefficients (a–e) were calculated between the viral titering data from M2001, C134, C101, R7020, G207 (Supplementary Figure 1) and the nectin-1 expression levels (f) from cell lines 90-8-luc (open triangle), STS26T-luc (closed diamond), T265-luc (open circle), YST-1 (closed square), 88-14-luc (open diamond), NMS2-PC (closed triangle), S462-luc (open square), and 2XSB (closed circle). A strong and significant correlation was noted for M2001. Cells were infected in triplicate by a single-step replication assay (MOI=10) and the lysates collected and titered at 24 h.p.i. Nectin-1 expression was quantified by flow cytometry after incubation with phycoerythrin (PE)-conjugated mouse monoclonal antibody with subsequent quantification using antibody quantification beads. The percentage of the cell population staining above the isotype control is also reported. Receptor quantification was performed in triplicate with the standard deviation reported.

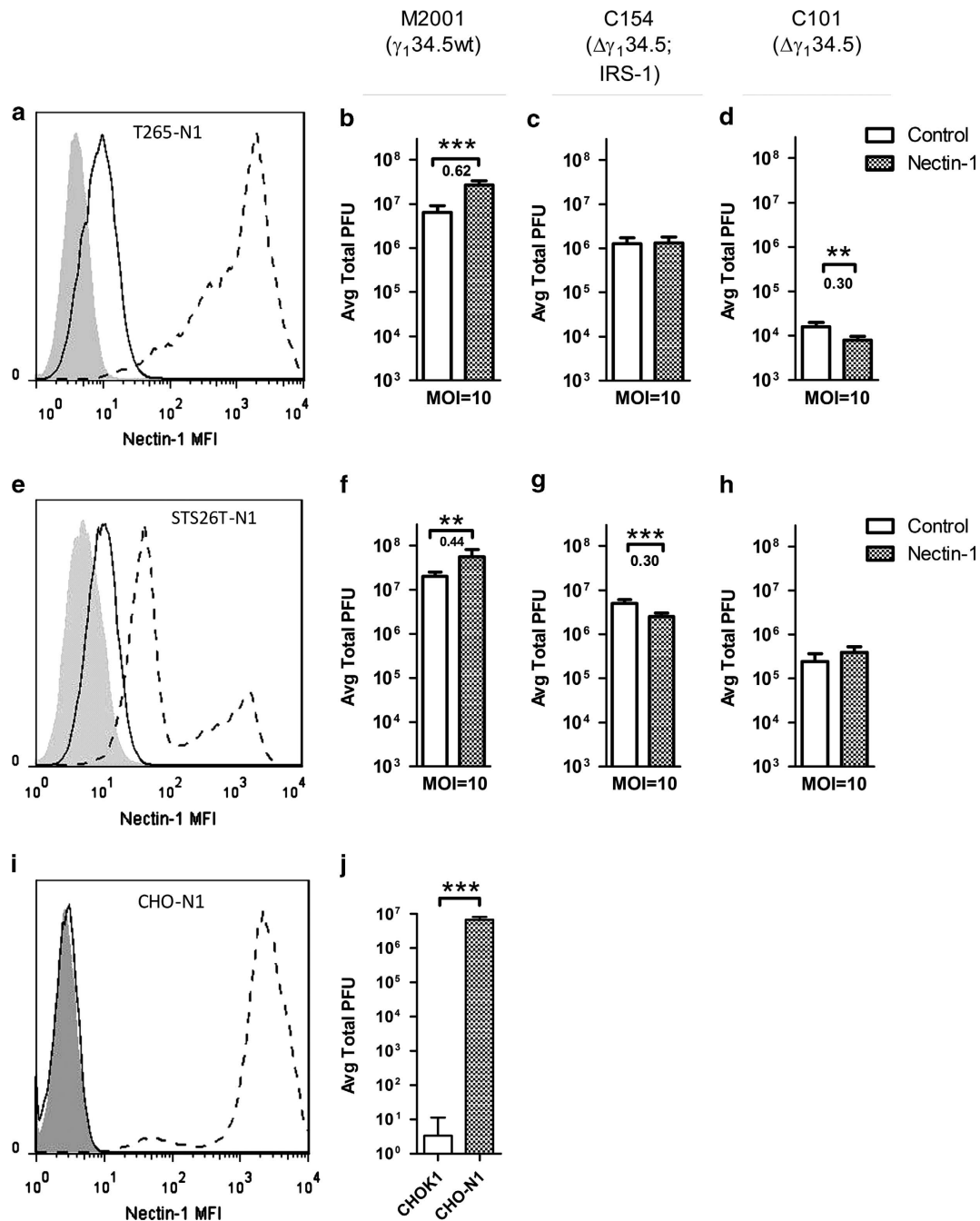


Figure 2. Overexpression of nectin-1 in resistant cells and impact on single-step replication assays. Nectin-1 was transduced via lentivirus into oHSV-resistant cell lines T265-luc (a) and STS26T-luc (e) as well as control cell line CHO-K1. Isotype control (shaded), parent (solid line) and transduced (dashed line) cell lines are shown. Transduction of the nectin-1-deficient cell line (i) demonstrated function as an entry receptor as apparent by M2001 replication (j). The impact of nectin-1 overexpression in resistant cell lines was tested by single-step (MOI=10) replication by viruses M2001 (b, f), C154 (c, g) and C101 (d, h) and compared with control cell lines. Significance was determined by two-tailed Student's *t*-test with unequal variance. Significance was set at $P < 0.05$. For cells with significant changes in titer, the logarithm of the absolute value of the increase was reported below the significance marking. Changes in titer greater than 0.5 log are considered to be biologically relevant. ** $P > 0.01$ and *** $P > 0.001$.

reliable titering repeatability of HSV is within approximately 0.5 log, only changes in titer greater than 0.5 log are considered to be biologically relevant. The nectin-1 transduction of T265-luc and STS26T-luc resulted in abundant nectin-1 expression in T265-N1 and STS26T-N1 cell lines, respectively (Figures 2a and e). While increased entry-receptor expression improved the yields of a representative wt virus (Figures 2b and f), the increased expression did not improve the titers of a next-generation oHSV C154, an EGFP

expressing variant of C134 (Figures 2c and g) or first-generation $\Delta\gamma_1 34.5$ oHSV C101 (Figures 2d and h). To demonstrate that increased nectin-1 expression would be expected to improve viral production, the HSV receptor-deficient cell line CHO-K1 was transduced with nectin-1. A significant and greater than 5 log increase in wt HSV-1 titers was observed (Figures 2i and j).

Interaction with HSV entry receptors is essential for initial HSV entry as well as the subsequent cell-to-cell spread of HSV.²⁹

To assess the effect of increased nectin-1 expression on viral spread, we measured viral GFP expression in MPNST cells over the time in multistep assays following infection with GFP expressing C101 and C154 (Figure 3) or M2001 (Supplementary Figure 4). The results show that nectin-1 overexpression improved the ability of C101 to undergo cell-to-cell spread and increased the proportion of cells infected from 3 to 27% and from 1 to 7% of the cell population in T265-N1 and STS26T-N1 in multistep replication assays (MOI=0.1, 24, 48 and 72 h.p.i.) respectively (Figures 3a and b). Despite this improved spread in resistant lines, the maximum spread was much less than that observed in the naturally permissive S462-luc and NMS-2PC MPNST cell lines, where C101 was capable of infecting >80% of the cells (Figure 3c). This suggests that endogenous levels of entry receptors are sufficient to permit infection and sustain $\Delta\gamma_1,34.5$ oHSV spread in these lines and that increased entry-receptor expression is not sufficient to render resistant cell lines with a permissive phenotype. Of note, the overexpressed nectin-1 levels far exceeded the highest

endogenous levels in the permissive lines (Supplementary Figure 5), suggesting that restricted entry is not an explanation for MPNST resistance to oHSVs. This conclusion is further supported by the fact that infection of the same cell lines with a second-generation oHSV (that is, C134 or C154) capable of evading the antiviral response³⁰ resulted in approximately 10-100 fold increase in viral titers and notably greater cell-to-cell spread as compared with C101 (Figures 3d and e).

To determine the extent to which *in vivo* studies recapitulated these results, athymic nude mice were engrafted with either parent or nectin-1 expressing cell lines. Of the resistant cell lines, only STS26T-luc and the nectin-1 overexpressing variant established flank tumors. Tumors were injected with 1×10^7 plaque forming units of C101 or C154, and viral recovery was measured on days 3 and 5 post injection. Similar to the *in vitro* results (Figure 3g and h), the next-generation virus had a >10-fold viral production advantage over the $\Delta\gamma_1,34.5$ oHSV C101, however neither virus demonstrated an increased viral titer between days 3

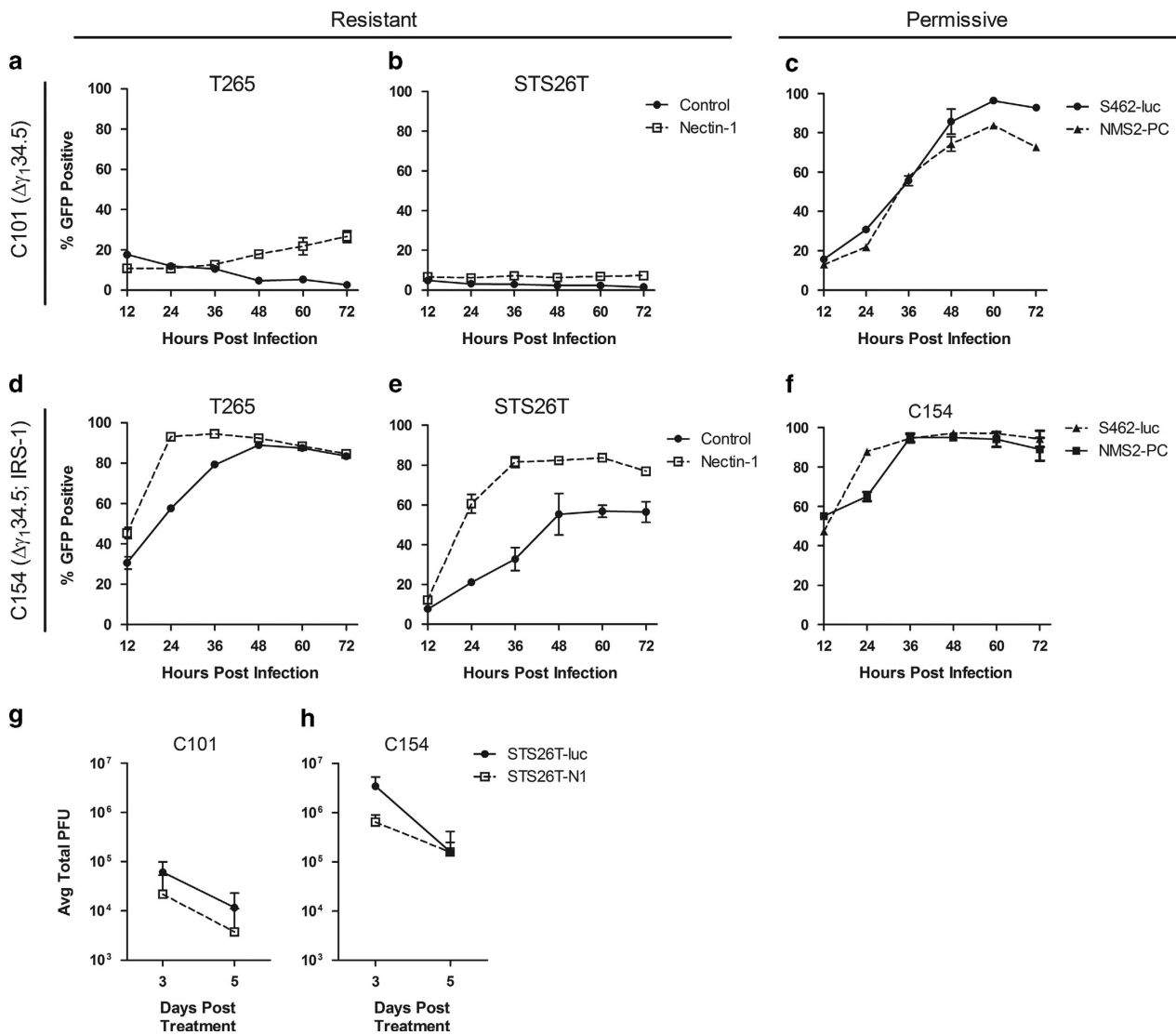


Figure 3. Impact of increased nectin-1 expression on oHSV spread *in vitro* and viral recovery *in vivo*. Resistant cell lines STS26T-luc and T265-luc and their nectin-1 transduced variants, as well as permissive cell lines S462-luc and NMS2-PC, were infected in a multistep assay (MOI=0.1) with fully attenuated oHSV C101 (a–c) or second-generation C154 expressing HCMV IRS1 (d–f) and monitored by flow cytometry over time for viral infection as evident by expression of viral GFP. STS26T-luc and STS26T-N1 cells were engrafted in the flanks of nude mice and following tumor formation were injected with 1×10^7 plaque forming units (PFU) of C101 or C154. Tumors were harvested and viral titers determined at days 3 and 5 following infection (g and h). Data are representative of four tumors with standard deviation reported.

and 5 even with increased nectin-1 expression. Tumors were also collected for immunohistochemistry and staining for HSV-1 confirmed that increased nectin-1 expression did not benefit oHSV spread between days 3 and 5 (data not shown). The *in vivo* results therefore confirmed that neither the first- nor the second-generation oHSVs derived a benefit to viral output from increased entry-receptor expression.

In summary, the work presented here provides insight into one of the proposed determinants of oHSV therapeutic efficacy. We conclude that the primary mode of MPNST resistance to $\Delta\gamma_134.5$ oHSVs is not due to limited expression of nectin-1. Despite the primary conclusions of previously published work that entry-receptor expression is predictive of a productive infection by oHSV, we suggest that the use of viruses in these previous studies which contained at least one functional copy of the $\gamma_134.5$ gene (NV1023)^{14,15,18} or $\gamma_134.5$ under a nestin promoter (rQnestin34.5)¹⁶ is in line with our conclusions that viruses which are genetically competent to counter the intrinsic antiviral response benefit the most from increased entry-receptor expression. Similarly in our work, the wt HSV-1 and C134 viruses derived greater benefit from higher entry-receptor expression than did the first-generation $\Delta\gamma_134.5$ oHSVs. Furthermore, the work of Wang *et al*¹⁶ showed that only the $\gamma_134.5$ containing virus was able to substantially benefit from increased nectin-1 expression while the $\Delta\gamma_134.5$ control virus did not. Future work should therefore include the characterization of the capacity for an intrinsic antiviral response as the major mechanism for oHSV resistance in MPNSTs.

MATERIALS AND METHODS

Cell lines

MPNST cell lines STS26T-luc, T265-luc, ST88-14-luc, S462-luc, 90-8-luc, NMS2-PC, YST-1 and 2XSB were provided by Dr Steve Carroll (University of Alabama at Birmingham). Cell lines STS26T-luc, T265-luc, and ST88-14-luc express firefly luciferase and have been previously described.³¹ S462-luc and 90-8-luc were transduced *via* lentivirus to express Renilla luciferase. HSV-1 entry receptor-deficient cell line CHO-K1 was generously provided by Dr Yancey Gillespie (University of Alabama, Birmingham). All MPNST cell lines were maintained in DMEM, 10% FBS, and 1% P/S. CHO-K1 cells were maintained in Ham's F12, 10% FBS and 1% P/S. Vero cells were obtained from American Type Culture Collection (Manassas, VA, USA) and maintained in MEM and 5% BGS. All cell lines were confirmed to be free of Mycoplasma by DAPI staining and PCR detection.

Viruses

All viruses have been previously described. Briefly, M2001 was constructed by insertion of the gene encoding EGFP under the control of the CMV immediate early promoter into the U_L3 - U_L4 intergenic region of the prototypical wt HSV-1 (F) strain.³² C101 and C134 were derived from the $\Delta\gamma_134.5$ mutant HSV-1 R3616 by insertion respectively of the *EGFP* or *HCMV IRS1* genes under the control of the CMV immediate early promoter in the U_L3 - U_L4 intergenic region.³³ C154 is derived from C134 by insertion of EGFP into the deletion loci of $\gamma_134.5$. G207 (Medigene, Inc., San Diego, CA, USA) is a clinical grade oHSV derived from R3616 with the additional insertion of *lacZ* in the U_L39 region.³⁴ R7020 (kindly provided by Bernard Roizman; University of Chicago, Chicago, IL, USA), is a clinical grade oHSV derived from HSV-1 (F) strain by insertion of a region of the HSV-2 genome encoding glycoproteins G, D, I and a portion of E into one of the internal repeat regions of HSV-1 (F) disrupting one copy of the neurovirulence gene $\gamma_134.5$.³⁵

Viral titering assays

Viral titers were determined by limiting dilution plaque formation assays as previously described.³³ MPNST cells were incubated for 2 h with virus diluted in 100 μ l infection media (DMEM + 1% FBS) and replaced with growth media after infection. An equivalent volume of sterile milk was added and the plate subjected to three cycles of freeze-thaw at -80°C . Lysate was collected, sonicated, serially diluted in Vero infection media (MEM + 1% BGS), and incubated on Vero monolayers. Infection media was replaced with growth media containing 0.01% human AB serum (Corning Cellgro, Corning, NY, USA). After 48 h, plaques were counted following May-Grunwald/methanol staining as previously described. All experiments were performed in triplicate and the average total plaque forming units reported with standard deviation.

Viral entry-receptor quantification

Expression of entry receptors was quantified by flow cytometry using either phycoerythrin-conjugated mouse monoclonal antibodies to nectin-1 (R1.302) (Biolegend, San Diego, CA, USA), HVEM (Biolegend), or isotype control (BD Biosciences, San Jose, CA, USA). Antibody concentrations used were confirmed to be saturating. Cells analyzed using a FACSCaliber flow cytometer (Becton Dickinson, Franklin Lakes, NJ, USA). Concurrently, Quantum Simply Cellular beads (Bangs Laboratories, Fisher, IN, USA) were used to determine the antibody binding capacity of each cell line. Mean fluorescence analysis was performed using FlowJo (v 7.6.1; Tree Star, Ashland, OR, USA) and the receptor-mean fluorescence intensity data converted to antibody binding capacity using a script provided with the Quantum Simply Cellular kit. All measurements were averaged from three independently seeded wells, and the final antibody binding capacity reported as the difference above the isotype control.

Correlation of nectin-1 and viral recovery

Pearson's correlation coefficients between nectin-1 expression and viral recovery were determined by analysis of the data in Prism 5 (GraphPad Software, La Jolla, CA, USA). Cutoff for statistical significance was set at $P < 0.05$.

Nectin-1 overexpression

A self-inactivating lentiviral vector was used to overexpress nectin-1 or control mCherry in oHSV-resistant cell lines. Human nectin-1 clone (Clone ID: 8322523) was obtained from Open Biosystems (Thermo Scientific, Waltham, MA, USA). Nectin-1 cDNA was PCR amplified using primers 5'-CGGATCCCGGGTTCGACCCGATGGCTC GGATGGGGCTT-3' and 5'-CCGGTCCGAGCGCGCCGCTACACGTAC CACTCCTTCTGGAA-3' (IDT, Coralville, IA, USA) in a T100 Thermal Cycler (Bio-Rad, Hercules, CA, USA). The recipient vector has been previously described.³⁶ An intermediate lenti-vector was first constructed by insertion of an IRES-puromycin *N*-acetyl-transferase cassette into the *NotI*- and *EcoRI*-digested pLVmnd lentivirus. The intermediate construct was then digested with *Sall* and *NotI* for subsequent insertion of the PCR-amplified Nectin-1 cDNA. The sequence of the coding region of the resulting lentiviral vector pCK2114 was verified. The control lentivirus (pLVmnd.CIP) was similarly constructed by insertion of mCherry upstream of the IRES-puromycin *N*-acetyl-transferase cassette in the intermediate virus. Lentiviruses were produced by co-transfection of pCK2114 or pLVmnd.CIP with pMD.G (VSFG pseudotype), and pCMV. deltaR8.91 (HIV packaging) in 293T cells using Lipofectamine 2000 and OptiMEM media (Gibco, Carlsbad, CA, USA). After 12 h, transfection media was replaced with DMEM/F12 with 10% FBS. Lentiviral-enriched supernatant was collected 48 h post transfection, filtered through a 0.22-micron filter, and mixed with polybrene (8 $\mu\text{g ml}^{-1}$). STS26T-luc and T265-luc cells were

subsequently transduced with the resulting lentiviruses enriched by puromycin selection ($5 \mu\text{g ml}^{-1}$), followed by fluorescence activated cell sorting to obtain pure populations (UAB Comprehensive Flow Cytometry Core, Birmingham, AL, USA).

HSV titers in nectin-1 overexpressing cell lines

The impact of increased nectin-1 expression on viral titers in resistant cell lines was determined as described above with the exception of replacing infection media with MPNST growth media and 0.01% human AB serum to minimize extracellular spread of the virus. Statistical significance was determined by two-tailed Student's *T*-test assuming equal variance. Star notation indicating significant differences is as follows: (*) for $P < 0.05$, (**) for $P < 0.01$ and (***) for $P < 0.001$.

HSV spread as measured by GFP expression

Cells were incubated with virus or mock infected for 2 h at MOI=0.1 in infection media. Infection media was replaced with growth media and 0.01% human AB serum following incubation. Cells were harvested at 12 h intervals and analyzed by flow cytometry. The percent GFP-positive measurement was assessed by defining the GFP (FL1) gate at 1% positive of the mock-treated cells. The percentage of the infected cell population expressing GFP was then recorded. All data points were performed in triplicate, averaged, and the standard deviation reported.

In vivo viral recovery

Six-week-old athymic nude (nu/nu) mice (NCI-Frederick, Frederick, VA, USA) were obtained and allowed to adjust for a period of 2 weeks. Bilateral, subcutaneous tumors were engrafted in the flank by injection of 5×10^6 cells suspended in 50:50 BD Matrigel (Becton Dickinson) and serum-free DMEM. Four tumors were used for each virus and timepoint. When tumors reached an average size of 300 mm^3 , 1×10^7 plaque forming units of oHSV suspended in saline-buffered solution was injected intratumorally. At days 3 and 5 following infection, mice were euthanized and tumors recovered in DMEM and kept on ice. After tumors were mechanically dissociated, an equivalent volume of sterile milk was added to the homogenate and viral titering was performed as described above. Titers are plotted with standard deviation.

CONFLICT OF INTEREST

JMM, GYG, and RJW are co-founders, stockholders and consultants for Cathexer, Inc., which holds intellectual property related to oncolytic HSV.

ACKNOWLEDGEMENTS

Funding for this research was provided through DOD-W81XWH-10-NFRP-IIRA-NF1001157, P20 CA151129-03, P01 CA71933-15 and P50 CA97247-05. Special thanks to Enid Keyser in the UAB Comprehensive Flow Cytometry Core for assistance in cell sorting and Dr Bernard Roizman for providing R7020.

REFERENCES

- Carroll SL, Ratner N. How does the Schwann cell lineage form tumors in NF1? *Glia* 2008; **56**: 1590–1605.
- Kolberg M, Høland M, Ågesen TH, Brekke HR, Liestøl K, Hall KS *et al*. Survival meta-analyses for > 1800 malignant peripheral nerve sheath tumor patients with and without neurofibromatosis type 1. *Neuro-oncology* 2013; **15**: 135–147.
- Mahller YY, Rangwala F, Ratner N, Cripe TP. Malignant peripheral nerve sheath tumors with high and low Ras-GTP are permissive for oncolytic herpes simplex virus mutants. *Pediatric Blood Cancer* 2006; **46**: 745–754.
- Mahller YY, Vaikunth SS, Currier MA, Miller SJ, Ripberger MC, Hsu Y-H *et al*. Oncolytic HSV and erlotinib inhibit tumor growth and angiogenesis in a novel malignant peripheral nerve sheath tumor xenograft model. *Mol Ther* 2007; **15**: 279–286.

- Farassati F, Pan W, Yamoutpour F, Henke S, Piedra M, Frahm S *et al*. Ras signaling influences permissiveness of malignant peripheral nerve sheath tumor cells to oncolytic herpes. *Am J Pathol* 2008; **173**: 1861–1872.
- Maldonado AR, Klanke C, Jegga AG, Aronow BJ, Mahller YY, Cripe TP *et al*. Molecular engineering and validation of an oncolytic herpes simplex virus type 1 transcriptionally targeted to midkine-positive tumors. *J Gene Med* 2010; **12**: 613–623.
- Mahller Y, Sakthivel B, Baird W, Aronow B, Hsu Y, Cripe T *et al*. Molecular analysis of human cancer cells infected by an oncolytic HSV-1 reveals multiple upregulated cellular genes and a role for SOCS1 in virus replication. *Cancer Gene Ther* 2008; **15**: 733–741.
- Chou J, Kern ER, Whitley RJ, Roizman B. Mapping of herpes simplex virus-1 neurovirulence to gamma 134.5, a gene nonessential for growth in culture. *Science* 1990; **250**: 1262–1266.
- Harrow S, Papanastassiou V, Harland J, Mabbs R, Petty R, Fraser M *et al*. HSV1716 injection into the brain adjacent to tumour following surgical resection of high-grade glioma: safety data and long-term survival. *Gene Therapy* 2004; **11**: 1648–1658.
- Markert J, Medlock M, Rabkin S, Gillespie G, Todo T, Hunter W *et al*. Conditionally replicating herpes simplex virus mutant, G207 for the treatment of malignant glioma: results of a phase I trial. *Gene Therapy* 2000; **7**: 867–874.
- Ramplung R, Cruickshank G, Papanastassiou V, Nicoll J, Hadley D, Brennan D *et al*. Toxicity evaluation of replication-competent herpes simplex virus (ICP 34.5 null mutant 1716) in patients with recurrent malignant glioma. *Gene Therapy* 2000; **7**: 859.
- Markert JM, Liechty PG, Wang W, Gaston S, Braz E, Karrasch M *et al*. Phase Ib trial of mutant herpes simplex virus G207 inoculated pre- and post-tumor resection for recurrent GBM. *Mol Ther* 2008; **17**: 199–207.
- Markert JM, Razdan SN, Kuo H-C, Cantor A, Knoll A, Karrasch M *et al*. A phase I trial of oncolytic HSV-1, G207, given in combination with radiation for recurrent GBM demonstrates safety and radiographic responses. *Mol Ther* 2014; **22**: 1048–1055.
- Huang Y-Y, Yu Z, Lin S-F, Li S, Fong Y, Wong RJ. Nectin-1 is a marker of thyroid cancer sensitivity to herpes oncolytic therapy. *J Clin Endocrinol Metab* 2007; **92**: 1965–1970.
- Yu Z, Adusumilli PS, Eisenberg DP, Darr E, Ghossein RA, Li S *et al*. Nectin-1 expression by squamous cell carcinoma is a predictor of herpes oncolytic sensitivity. *Mol Ther* 2007; **15**: 103–113.
- Wang P, Currier M, Hansford L, Kaplan D, Chioocca E, Uchida H *et al*. Expression of HSV-1 receptors in EBV-associated lymphoproliferative disease determines susceptibility to oncolytic HSV. *Gene Therapy* 2012; **20**: 761–769.
- Friedman GK, Langford CP, Coleman JM, Cassidy KA, Parker JN, Markert JM *et al*. Engineered herpes simplex viruses efficiently infect and kill CD133+ human glioma xenograft cells that express CD111. *J Neuro-oncology* 2009; **95**: 199–209.
- Chen C-h, Chen W-Y, Lin S-F, Wong RJ. Epithelial mesenchymal transition enhances response to oncolytic herpes viral therapy through nectin-1. *Human Gene Ther* 2014; **25**: 539–551.
- Forrester A, Farrell H, Wilkinson G, Kaye J, Davis-Poynter N, Minson T. Construction and properties of a mutant of herpes simplex virus type 1 with glycoprotein H coding sequences deleted. *J Virol* 1992; **66**: 341–348.
- Ligas MW, Johnson DC. A herpes simplex virus mutant in which glycoprotein D sequences are replaced by beta-galactosidase sequences binds to but is unable to penetrate into cells. *J Virol* 1988; **62**: 1486–1494.
- Cai W, Gu B, Person S. Role of glycoprotein B of herpes simplex virus type 1 in viral entry and cell fusion. *J Virol* 1988; **62**: 2596–2604.
- Pertel PE, Fridberg A, Parish ML, Spear PG. Cell fusion induced by herpes simplex virus glycoproteins gB, gD, and gH-gL requires a gD receptor but not necessarily heparan sulfate. *Virology* 2001; **279**: 313–324.
- Roop C, Hutchinson L, Johnson DC. A mutant herpes simplex virus type 1 unable to express glycoprotein L cannot enter cells, and its particles lack glycoprotein H. *J Virol* 1993; **67**: 2285–2297.
- Rikitake Y, Mandai K, Takai Y. The role of nectins in different types of cell-cell adhesion. *J Cell Sci* 2012; **125**: 3713–3722.
- Mizoguchi A, Nakanishi H, Kimura K, Matsubara K, Ozaki-Kuroda K, Katata T *et al*. Nectin an adhesion molecule involved in formation of synapses. *J Cell Biol* 2002; **156**: 555–565.
- Richart SM, Simpson SA, Krummenacher C, Whitbeck JC, Pizer LI, Cohen GH *et al*. Entry of herpes simplex virus type 1 into primary sensory neurons in vitro is mediated by nectin-1/HveC. *J Virol* 2003; **77**: 3307–3311.
- Montgomery RI, Warner MS, Lum BJ, Spear PG. Herpes simplex virus-1 entry into cells mediated by a novel member of the TNF/NGF receptor family. *Cell* 1996; **87**: 427–436.
- Shukla D, Liu J, Blaiklock P, Shworak NW, Bai X, Esko JD *et al*. A novel role for 3-O-sulfated heparan sulfate in herpes simplex virus 1 entry. *Cell* 1999; **99**: 13–22.

- 29 Even DL, Henley AM, Geraghty RJ. The requirements for herpes simplex virus type 1 cell–cell spread via nectin-1 parallel those for virus entry. *Virus Res* 2006; **119**: 195–207.
- 30 Shah A, Parker J, Gillespie G, Lakeman F, Meleth S, Markert J *et al*. Enhanced antiglioma activity of chimeric HCMV/HSV-1 oncolytic viruses. *Gene Therapy* 2007; **14**: 1045–1054.
- 31 Byer SJ, Eckert JM, Brossier NM, Clodfelder-Miller BJ, Turk AN, Carroll AJ *et al*. Tamoxifen inhibits malignant peripheral nerve sheath tumor growth in an estrogen receptor–independent manner. *Neuro-oncology* 2011; **13**: 28–41.
- 32 Friedman GK, Haas MC, Kelly VM, Markert JM, Gillespie GY, Cassady KA. Hypoxia moderates γ 134. 5-deleted herpes simplex virus oncolytic activity in human glioma xenoline primary cultures. *Transl Oncol* 2012; **5**: 200.
- 33 Cassady KA. Human cytomegalovirus TRS1 and IRS1 gene products block the double-stranded-RNA-activated host protein shutoff response induced by herpes simplex virus type 1 infection. *J Virol* 2005; **79**: 8707–8715.
- 34 Mineta T, Rabkin SD, Yazaki T, Hunter WD, Martuza RL. Attenuated multi-mutated herpes simplex virus-1 for the treatment of malignant gliomas. *Nat Med* 1995; **1**: 938–943.
- 35 Meignier B, Longnecker R, Roizman B. *In vivo* behavior of genetically engineered herpes simplex viruses R7017 and R7020: construction and evaluation in rodents. *J Infect Dis* 1988; **158**: 602–614.
- 36 Gerson SL. Cotransduction with MGMT and ubiquitous or erythroid-specific GFP lentiviruses allows enrichment of dual-positive hematopoietic progenitor cells *in vivo*. *ISRN Hematol* 2012; **2012**.

Supplementary Information accompanies this paper on Gene Therapy website (<http://www.nature.com/gt>)

Appendix iii

AWARD NUMBER: W81 XWH-11-1-0498

TITLE: Engineered Herpes Simplex Viruses for the Treatment of Malignant Peripheral Nerve Sheath Tumors

PRINCIPAL INVESTIGATOR: James M. Markert, MD

List of the personnel paid from grant over its three year duration:

1. James M. Markert, PI
2. Steve L. Carroll, Collaborator
3. Kevin A. Cassady, Co-Investigator
4. G. Yancey Gillespie, Co-Investigator
5. Stephanie J. Byer, Research Associate
6. Jennifer M. Clement, Research Associate
7. Catherine P. Langford, Research Assistant
8. Li Li, Research Associate
9. Amy Turk, Research Assistant
10. Joshua D. Jackson, Student